ROBUST CONTROL SYSTEM DESIGN WITH APPLICATION TO HIGH PERFORMANCE HELICOPTERS

Michael Stanley Tombs

St. John's College, Oxford



This is a replacement copy for the one lost in the post April 1990
Theo Dimmich
19.3.91

Submitted in partial fulfilment of the requirements for the degree of

Doctor of Philosophy at the University of Oxford, Trinity 1987

ROBUST CONTROL SYSTEM DESIGN WITH APPLICATION TO HIGH PERFORMANCE HELICOPTERS

Michael Stanley Tombs

St. John's College, Oxford

Submitted in partial fulfilment of the requirements for the degree of Doctor of Philosophy at the University of Oxford, Trinity 1987

ABSTRACT

This thesis presents one of the first applications of H^∞-optimization to the design of controllers for industrial problems. The system considered was an unstable helicopter model, obtained from a large non-linear simulation (provided by the Royal Aircraft Establishment, Bedford) configured to represent future high performance helicopters. The problem was to design a full authority flight control system, to stabilize the aircraft and decouple the controlled inputs, thus reducing pilot workload. Robustness was a primary issue because of model uncertainty, particularly due to the omission from the design model of higher order rotor dynamics.

The optimization problem was based on the minimization of sensitivity (for performance) and control output (for robustness) transfer functions. Simple weighting functions were found to be useful for examining the fundamental performance-versus-robustness trade-off, and to be more effective at shaping the closed loop transfer functions than LQG/LTR techniques. A controller designed for a 4-input, 6-output, 8-state linearized plant model was successfully implemented in a non-linear simulation with rotor dynamics. This stabilized the system and enabled good control for small variations about the design operating point. The 'standard problem', consisting of the plant augmented with weights, had 20 states; the controller had 18, which was much smaller than researchers had been predicting, and it is conjectured that all H^∞-optimal controllers will have at most the same number of states as the defining 'standard problem'.

An important improvement to the H^∞-optimization solution process was the development of a numerically reliable algorithm to perform minimal realization. This algorithm solves for a truncated balanced realization of stable state-space systems that are arbitrarily close to being either uncontrollable and/or unobservable. Depending on the choice of partitioning of the Hankel singular values, it can be used to perform minimal realization, or model reduction, with a guaranteed L^∞ error bound.

To Caroline

ACKNOWLEDGMENTS

Firstly, I would like to thank Dr Ian Postlethwaite, my supervisor, for his guidance and encouragement throughout the course of this research, and for gathering together an excellent research team; I am indebted to Siu O'Young and Da-Wei Gu for their technical expertise and tremendous programming effort, as well as for their friendly support. For their help and advice in my association with the Royal Aircraft Establishment, Bedford, I would like to thank Dr Gareth Padfield and Stuart Winter.

Thanks must also go to Jane Thorpe, D. Tyler and Paul Brinson of Westlands for their help on the helicopter control problem.

I have benefited from discussions with Professors Mike Safonov (who also introduced me to the work of Peter Thompson), Bruce Francis and John Doyle on the intricacies of H_∞-Optimization.

For creating an enjoyable working environment I acknowledge the support of fellow students Andy Yue, Mark Dunstan, Ai-Poh Loh, Yung Kuan Foo and Mi-Ching Tsai in my own research group; and for extolling the virtues of self-tuning control, Coorous Mohtadi-Haghighi.

My wife Caroline, co-editor, co-typist and fellow sufferer, has been a constant source of support and understanding, for which I am very grateful.

This research was funded by an SERC CASE award in collaboration with the RAE, Bedford.

CONTENTS

Chapter I INTRODUCTION

1.1 Motivation 1
1.2 Related work and literature review 3
1.3 Contribution and organization of this thesis 7
1.4 Notation and terminology 10

Chapter II ROBUSTNESS CHARACTERIZATION

2.1 Introduction 13
2.2 System configuration
2.2-1 Structure 14
2.2-2 Equations 15
2.3 Model uncertainty 17
2.4 Robustness tests
2.4-1 Unstructured perturbations 18
2.4-2 Lehtomaki's robustness test 20
2.4-3 Gain and phase margins 21
2.4-4 Structured uncertainty 23
2.4-5 Other methods 25
2.5 Design implications 26
2.6 Concluding remarks 29

Chapter III ROBUSTNESS OF SAMPLED DATA SYSTEMS

3.1 Introduction 30
3.2 Functional analysis
3.2-1 Functions 32
3.2-2 Function spaces .
3.2-3 Relations and operators 33
3.2-4 Gain and stability 34
3.2-5 Conic sectors 35
3.2-6 Closed-loop stability 36
3.3 Conic sectors applied to sampled data systems
3.3-1 Thompson's conic sector result 38
3.3-2 The A-scaling approach 40
3.3-3 Robustness considerations 42
3.4 Concluding remarks 46

Chapter IV THE HELICOPTER

4.1 Introduction 47
4.2 Helicopter types
4.2-1 Configuration 48
4.2-2 The rotor 49
4.3 Control inputs 50
4.3-1 Main rotor collective 51
4.3-2 Cyclic pitch controls .
4.3-3 Tail rotor collective 52
4.3-4 The throttle .
4.3-5 Extra controls .
4.3-6 Major interactions 53

4.4 The control problem
4.4-1 Control of a rigid body in space 54
4.4-2 Nomenclature 55
4.4-3 System outputs 58
4.5 Present control systems 59
4.6 Problems in controlling rates 61
4.7 Mathematical modelling
4.7-1 Equations of motion 64
4.7-2 Rotor degrees of freedom 69
4.7-3 Computer simulation .
4.7-4 Helicopter modes 70
4.7-5 Numerical results 72
4.8 Concluding remarks 75

Chapter V **H^∞ OPTIMIZATION**

5.1 Introduction 76
5.2 The standard problem 78
5.3 Theoretical solution
5.3-1 Primary constraints 81
5.3-2 Internal stability 82
5.3-3 Parameterization of all stabilizing controllers .
5.3-4 Model-matching problem 83
5.3-5 2-Block γ-iteration 86
5.3-6 Recovery of controller 87
5.4 State-space solution
5.4-1 The standard problem 88
5.4-2 Parameterization of all stabilizing controllers .
5.4-3 Model-matching problem 89
5.4-4 2-Block γ-iteration 91
5.4-5 Controller recovery and dimension .
5.4-6 Model reduction in H^∞-design 92
5.5 A specific H^∞-optimization problem
5.5-1 Problem statement 94
5.5-2 Conversion to standard problem 95
5.5-3 Textbook example 96
5.6 Concluding remarks 104
Appendix 5.1 Optimal anti-causal approximation 105
Appendix 5.2 The 2-Block γ-iteration 111

Chapter VI **APPLICATION OF H^∞ OPTIMIZATION TO THE HELICOPTER**
6.1 Introduction 115
6.2 Helicopter model 116
6.3 Design objectives 118
6.4 Scaling of the nominal model 119
6.5 Weighting function selection 121
6.6 Controller selection 124
6.7 Closed-loop frequency responses 127
6.8 Linear time-responses 129
6.9 Non-linear simulation 134
6.10 More general H^∞-optimization problems 140
6.11 Concluding remarks 141
Appendix 6.1 Computation times for the design process 142
Appendix 6.2 State-space model of the helicopter 143

Chapter VII LINEAR QUADRATIC GAUSSIAN OPTIMAL CONTROL

7.1 Introduction 144
7.2 The linear quadratic regulator
7.2-1 Specific assumptions 145
7.2-2 Problem definition .
7.2-3 Problem solution 146
7.2-4 Feedback configuration .
7.2-5 LQR properties 147
7.2-6 LQR loop shaping 148
7.2-7 Problems and restrictions 150
7.3 The linear quadratic servo
7.3-1 Reformation of the problem 150
7.3-2 Interpretation as multivariable P.I.D. 152
7.3-3 Problems and restrictions 153
7.4 The steady-state Kalman filter
7.4-1 Specific assumptions 154
7.4-2 Problem definition .
7.4-3 Problem solution .
7.4-4 Feedback configuration 155
7.4-5 Kalman filter properties .
7.4-6 Kalman filter loop shaping 156
7.4-7 Problems and restrictions .
7.5 The linear quadratic Gaussian control problem
7.5-1 Problem description 157
7.5-2 Problem solution .
7.5-3 Feedback configuration .
7.5-4 Robustness properties 158
7.5-5 Robustness recovery .
7.5-6 Problems and restrictions 160
7.6 Example of LQG/LTR 161
7.7 Concluding remarks 173

Chapter VIII TRUNCATED BALANCED REALIZATION OF A STABLE NON-MINIMAL STATE-SPACE SYSTEM

8.1 Introduction 174
8.2 Theoretical algorithm 176
8.3 Implementation details 183
8.4 Numerical examples 186
8.4-1 Example 1 187
8.4-2 Example 2 188
8.5 Concluding remarks 191
Appendix 8.1 194

Chapter IX CONCLUSIONS AND RECOMMENDATIONS FOR FURTHER RESEARCH

9.1 Summary 195
9.2 Suggestions for future research 196

References 199

CHAPTER I

INTRODUCTION

1.1 Motivation

It is important to clarify the precise meaning of robustness in the context of robust control system design. In any mathematical model of an engineering process, uncertainties - ranging from known modelling approximations to unknown parameter variation - will always be present. A feedback control system designed to have desirable properties on the basis of the nominal model, should retain these properties when the control is applied to the true plant. If this is the case, such properties are said to be robust. It is generally impractical to assess the robustness of a system by direct experimentation. Robustness analysis therefore uses mathematical techniques to determine the extent to which the design model can be perturbed without losing its desirable properties.

Stability is the most important property of a feedback control system, and so in this thesis 'robustness' generally refers to stability robustness. Robust performance, which clearly implies robust stability, is a more desirable objective, and is receiving increased attention in the research community. It can be shown that traditional control system design techniques, particularly when applied to multivariable systems, do not adequately address the problem of robustness. The aim of 'robust' control system design is therefore to modify existing techniques and to

develop new procedures that will guarantee or optimize given measures of robustness.

The helicopter is an excellent example of a difficult control problem. The dynamics of the helicopter are highly coupled, inherently unstable and vary considerably with operating point. A modern helicopter pilot has at least four control inputs with which to control a select number of variables specifying the attitudes and motion of the aircraft. Conventional helicopters are stabilized by a combination of mechanical design and simple feedback loops. Future battlefield helicopters will be designed to be faster and more agile. To enable pilots to operate the helicopters close to their limits, more complex controllers will be required. The performance objectives for such controllers are to minimize cross-coupling, to achieve improved stability margins, and to meet specifications on time-response characteristics required for good handling qualities. These are all aimed at reducing pilot workload.

Robustness is a primary concern in helicopter control system design, because of model uncertainty, sensor noise and wind-gusts. In particular it has been found that the performance of controllers designed using conventional techniques on models omitting higher order dynamics, can be severely degraded when tested on models which include these extra degrees of freedom. The problem is also complicated by rate and amplitude constraints on the actuators.

It is stressed that this thesis will only be concerned with the problem of designing fixed parameter controllers. It is expected that some form of gain scheduling will be used to cope with large known parameter variation through the flight envelope. The principal reason for not considering self-tuning control, for example, is that given a good mathematical model, the problem of finding the 'best' robust controller has yet to be fully solved. There are also doubts about the reliability

of self-tuners when used in such a dynamically fast and critical application as that presented by the helicopter.

1.2 Related work and literature review

In his historical review Dorato [DOR1] attributes the first use of the term 'robust control' to Davison [DAV1] in 1973 and Pearson and Staats [PEA1] in 1974. This does not imply that earlier designs had no concept of robustness - far from it. When Black proposed the use of high gain feedback in 1927 [BLA1], his primary concern was the uncertain nature of the vacuum tube amplifier components. This was not, of course, the first use of feedback systems for control; for a historical review of earlier work, on governors for example, see Bennet [BEN1].

In 1945 Bode published his classical book [BOD1] on the design of feedback systems. This work used the the stability theory of Nyquist [NYQ1] and, by introducing the concepts of gain and phase margin presented a robust control system design methodology. This work, together with Evans' root-locus [EVA1] and Nichol's plots [JAM1], forms what is now known as 'classical control system design' for single input, single output systems. The concepts of high gain at low frequency for good sensitivity, low gain at high frequency for stability margins, and their generalization to multivariable systems form the basis of modern robust control [DOY3].

The emphasis in the 1960s was on the development of 'optimal control'. This was initiated by Newton, Gould and Kaiser [NEW1] who applied the earlier work of Wiener [WIE1] on optimal filtering to control system design. Their approach modelled noise and disturbance signals as random processes and formulated the design as a well defined quadratic optimization problem. Thus the well known state-space design approach, linear quadratic Gaussian (LQG), reached maturity [ATH1], [AND1], [KWA1].

The major problem with this approach was that model uncertainty could not be directly considered, unless modelled as noise processes [ATH2]. It was therefore easy to ignore the robustness issues and to use the powerful state-space techniques to synthesize closed-loop systems with arbitrary pole locations (desired response) - but only for the nominal linear model. Such controllers would generally use high gain and large bandwidths inconsistent with robust control ideas.

Notable exceptions to this trend were Horowitz [HOR1], who extended the work of Bode to systems with finite plant variation, and Cruz and Perkins [CRU1], who introduced the sensitivity comparison matrix for the analysis of closed-loop versus open-loop accuracy for possibly multivariable systems.

Throughout the 1970s, while optimal control was still strongly favoured in the U.S.A., researchers in the U.K. continued to work on generalizations to multivariable systems of the classical frequency response techniques [ROS1]-[ROS4], [MAC1]-[MAC5], [POS1], [SMI1]. Unfortunately, Rosenbrock's 'inverse Nyquist array' (INA) and MacFarlane's 'characteristic loci' (CL), the most succesful of these, both fail satisfactorily to address the issue of robustness. A general criticism of these techniques is that they rely heavily on the 'skillfulness' of the user. For example, the manipulation of multivariable Nyquist diagrams or characteristic locus plots to obtain nominal stability for a 4-input, 4-output helicopter model is a daunting task. In addition, since there are no criteria for the optimality of a resulting design, it is impossible to tell whether a poor design is the result of fundamental system constraints or of designer incompetence. For these reasons CL and INA were not considered appropriate candidates for high performance helicopter control system design. (Recent research at the University of Cambridge under Professor MacFarlane [BOY1], on the

application of expert systems to aid the user, may help to alleviate these restrictions.)

The optimal control approach received increased attention in 1977 when Safonov [SAF1], [SAF2] showed that the well known gain margin of (1/2, ∞) and phase margin of 60 degrees for single input, single output systems [AND1] extended to multivariable systems. These margins are obtained in every plant input channel when a diagonal matrix is used for control weighting and where full state feedback is assumed. Unfortunately, Doyle demonstrated in 1979 [DOY1] that when a Kalman filter is combined with the optimal regulator, the system as a whole can exhibit arbitrarily small stability margins. A technique for asymptotically recovering the full state feedback stability margins was given by [DOY2] and [DOY3], using results derived by Kwakernaak [KWA1]. This technique is known as LQG loop transfer recovery (LTR) and will be considered further in Chapter VII.

The use of singular values for the analysis of multivariable feedback systems was promoted by the 1981 IEEE Transactions on Automatic Control special issue on multivariable control [DOY2], [POS3], [SAF3], [CRU2], [LEH2]. There are several reasons why singular value techniques have become so popular for robustness analysis. One is that they provide a straightforward generalization of the modulus of a complex number to the moduli of a complex matrix. Another is that they give good 'indicators' of robustness [MAC6], whereas eigenvalues, for example, cannot. This approach to robustness analysis is not without criticism - over conservatism, for example - and will be discussed in greater detail in Chapter II.

Until recently the LQG/LTR design methodology was promoted as the only systematic procedure for performing the singular value loop-shaping required for robust control system design. In 1981, however, Zames [ZAM2] motivated a new theory of feedback design: H^{∞}-optimization. (An earlier

use of H^∞ in an engineering context can be found in [HEL1].) Zames argued that the poor robustness characteristics of LQG could be blamed on the integral criterion, and he criticized the use of white noise to represent disturbances. He considered the problem of designing a feedback controller for a single-input, single-output system required to minimize the effect of a disturbance on the plant output, subject to the constraint of closed-loop stability. The disturbance was assumed to belong to a pre-specified set of signals, and the energy of the output was to be minimized for the worst disturbance in the set. The solution involved the minimization of the H^∞-norm (maximum modulus) of the sensitivity function, i.e., the transfer function from the disturbance to the output over the set of all stabilizing controllers. This minimax approach was subsequently extended to multivariable systems and to problems containing robustness optimization criteria. By 1984 the theory had become firmly established, as demonstrated by the notes from a workshop on 'Advances in multivariable control' [DOY7]. Notable contributions to the theory were made by [FRA1], [FRA2], [ZAM3], [NET1], [SAF5], [GLO1]; for a full bibliography see [FRA3]. Chapter V presents an overview of the theoretical and state-space solution to the H^∞ problem, based on the approach taken by [CHU1].

Despite the relative maturity of the theory, few practical applications of H^∞-optimization to control system design have appeared in the literature; recent examples may be found in [SAF8], [DOY8], and [LIM3].

The major application of modern multivariable control system design has been in the aerospace industry. This is because accurate models may be derived, and high performance is demanded, especially in military aircraft. A number of papers present examples based on the Chinook CH47 helicopter; [BRO1], for example, contains a complete digital design for this twin-rotor aircraft, loosely based in LQG. [DOY3] uses the same

example for a demonstration of LQG/LTR. [PAR1] considers the application of modal control theory to the single rotor helicopter. The effect of high order dynamics on helicopter flight control system bandwidth is discussed in [CHE2]. Chapter IV contains a more detailed discussion of current helicopter control systems.

1.3 Contribution and organization of this thesis

This thesis presents one of the first applications of H^{∞}-optimization to the design of controllers for industrial problems. The system considered was an unstable helicopter model, obtained from a large non-linear simulation (provided by the Royal Aircraft Establishment, Bedford) configured to be representative of future high performance helicopters. The control problem was to design a full authority flight control system which would stabilize the aircraft and decouple the controlled inputs, thus reducing pilot workload.

The optimization problem was based on the minimization of a combination of sensitivity (for performance) and controller output (for robustness) transfer functions. Simple weighting functions were found to be useful for examining the fundamental performance-versus-robustness trade-off, and to be effective at shaping the transfer functions as desired.

A controller designed for a 4-input, 6-output, 8-state linearized plant model was successfully implemented in a non-linear simulation with rotor dynamics. This stabilized the system and enabled good control for small variations from the design operating point, fulfilling the design objectives. The 'standard problem', consisting of the plant augmented with weights, had a state dimension of 20. The optimal controller, the solution to this '2-Block' problem, had a state dimension of 18. The

controller 'size' was much smaller than researchers had been predicting. On the basis of this observation, and other similar results, it is conjectured that all H^{∞}-optimal controllers will have at most the same number of states as the defining 'standard problem'.

An important improvement to the H^{∞}-optimization solution process was the development of a new algorithm to perform minimal realization of a stable state-space system. This algorithm solves for a truncated balanced realization of systems that are arbitrarily close to being either uncontrollable and/or unobservable. Depending on the choice of partitioning of the Hankel singular values, it can be used to perform minimal realization, or model reduction, with a guaranteed L^{∞} error bound. In numerical implementation the algorithm has proved to be both accurate and reliable.

A comparison was performed between the H^{∞}-design procedure and that of the linear quadratic Gaussian, loop transfer recovery (LQG/LTR) techniques. The H^{∞}-design procedure was found to be a far superior technique for shaping the closed-loop system transfer functions, and a better design was obtained, albeit at the expense of greater computational burden.

This thesis is organized into nine chapters. In **Chapter II** a review of singular value robustness tests is given. This approach to the robustness of linear multivariable systems will be a central theme throughout the thesis, and provides motivation for pursuing a class of H^{∞}-optimization problems.

Future helicopter controllers will be digitally implemented; **Chapter III** considers the robustness implications of using such controllers. The conclusion is - not surprisingly - that digital implementation will not introduce any problems of robustness, providing the sampling frequency is fast enough and appropriate filters are used. This chapter should not be

considered a major contribution to the thesis, but is included for completeness.

Chapter IV presents the helicopter control problem. The intention is to provide sufficient information about the helicopter for a control engineer to understand the problems involved. The chapter includes sections on how the helicopter is controlled and the basis of its mathematical modelling.

In **Chapter V** an overview of the H^{∞}-optimization solution process is presented. Particular attention is given to numerical difficulties that had to be overcome during software implementation. Two conjectures are offered on the properties of H^{∞}-optimal controllers. These were made after observing the solutions to a number of example problems, the largest of which was the helicopter design. A simple example is given to demonstrate the design philosophy developed.

In **Chapter VI** H^{∞}-optimization is applied to the helicopter; this example shows that, at least in simulation, H^{∞}-optimization can be used to design a control system satisfying both performance and robustness criteria for a realistic practical control problem.

Chapter VII describes an alternative approach to multivariable control system design: the state-space optimal control, LQG. Its extension LQG/LTR is applied to the helicopter, and the results compared with those in the previous chapter.

In order to overcome difficulties experienced in implementing the H^{∞}-optimization solution, a new algorithm was developed, to perform truncated balanced realization of stable state-space systems. This is detailed in **Chapter VIII.**

Chapter IX contains concluding remarks and suggestions for further research.

1.4 Notation and terminology

In general, terms will be defined where they are first used. With the exception of Chapter II, only linear time invariant systems will be considered, and unless otherwise stated these will normally be multivariable. In order to simplify notation, the dependence of such functions on an independent variable will be omitted when there is no risk of ambiguity. Capital letters will be used to define matrix valued quantities, with lower case for vector and scalar quantities.

The following symbols will be employed throughout this thesis:

$\stackrel{\Delta}{=}$	Equal to, by definition
=>	Implies
<=	Is implied by
<=>	If, and only if
Re[s]	The real part of the complex number s
Im[s]	The imaginary part of the complex number s
diag[d_1, d_2...]	Diagonal matrix with elements d_1, d_2, etc.
rank[M]	The rank of the matrix M
det[M]	The determinant of the square matrix M
M^H	The complex conjugate transpose of the matrix M; if M is real rational, then $M^H \stackrel{\Delta}{=} M(\bar{s})^T$
M^*	The adjoint of the matrix M; if M is real rational, then $M^* \stackrel{\Delta}{=} M(-s)^T$
$\lambda_i(M)$	The i^{th} eigenvalue of the square matrix M
$\sigma_i[M]$	The i^{th} singular value of the matrix M; $\sigma_i[M] = \lambda_i^{1/2}[M^H M]$

SVD	All n x m complex matrices M have a singular value decomposition $M = U\Sigma V^*$ where U and V are unitary and Σ is a diagonal matrix with non-zero elements σ_i, for i = 1, rank[M]
$\|x\|$	The magnitude of a vector or scalar x
$\bar{\sigma}[M]$	The maximum singular value of the matrix M; $= \max_{\|x\|=1} \|Mx\|$
$\underline{\sigma}[M]$	The minimum singular value of the matrix M; $= \min_{\|x\|=1} \|Mx\|$
j	Complex number such that $j^2 = -1$
R(s)	The space of real rational functions
H^∞	Hardy space of functions bounded and analytic in the open RHP
RH^∞	The space of real rational functions in H^∞
$\|\|M(s)\|\|_\infty$	The H^∞-norm of the stable transfer function matrix M(s) (or L^∞-norm if M is unstable and proper with no $j\omega$-axis poles); the supremum of the maximum singular value of M(s) for s on the imaginary axis
$\sigma_{hi}[G(s)]$	The Hankel singular values of the stable system G(s)
$\|\|G(s)\|\|_H$	The Hankel norm of G(s); the largest hankel singular value of the stable system G(s)
L_2	The space of square integrable time (vector) functions
H^2	Hardy space of functions analytic in the open RHP and square integrable on the $j\omega$-axis
$b \varepsilon A$	b is an element of the set A
LHP	Left half complex plane
RHP	Right half complex plane
CRHP	Closed right half complex plane

Poles	The poles of G(s) are defined as the zeros of the determinant det[sI-A] where A is the A-matrix of a state-space realization of G(s)
Zeros	The zeros of G(s) are defined as the zeros of the polynomial det[sI-A]·det[G(s)]
D_D	Direct Nyquist D-contour with indentations to the left of imaginary axis poles, and with a clockwise orientation
D_I	Inverse Nyquist D-contour with indentations to the left of imaginary axis zeros, and with a clockwise orientation
Ω_D	Segment of D_D for which $Re[s] \leq 0$
Ω_I	Segment of D_I for which $Re[s] \leq 0$

A rational function or matrix is said to be <u>stable</u> if it is analytic in $Re[s] \geq 0$, <u>proper</u> if it is finite at $s=\infty$, and strictly proper if it is zero at $s=\infty$.

CHAPTER II

ROBUSTNESS CHARACTERIZATION

2.1 Introduction

This chapter provides an introduction to the 'singular value'-based robustness tests that were popularized by Doyle and Stein and others in the 1981 special issue of the IEEE Transactions on Automatic Control [DOY3], [POS3], [SAF3], [CRU2], [LEH2]. This approach to the robustness of a closed-loop feedback control system will be a central theme throughout this thesis.

Shortcomings of this approach when applied to practical problems in the aerospace industry have been reported [LY1] and [CHA1]. The major concerns are the excessive conservatism of the results and the lack of design techniques to perform singular value loop-shaping. The conservatism problem is tackled by the structured perturbation analysis techniques introduced by Doyle [DOY4], [DOY5] and discussed in section 2.4-4. The design problem is considered in section 2.5 and provides motivation for pursuing H^{∞}-optimization problems, the solution of which is the subject of Chapter V.

The mathematical results in this chapter are possible because of the use of finite dimensional linear time invariant plant models. Chapter IV clearly demonstrates that the helicopter is far from linear; the results will therefore only apply to linearized models about given operating

points, and for small changes from these points. It is accepted that local stability about a number of such points is not a sufficient condition for the global stability of the system. Non-linear simulation will be used in Chapter IV to demonstrate the robustness of the helicopter design.

2.2 System configuration

2.2-1 Structure

The unity feedback structure of Figure 2.1 will be used extensively to represent a multivariable feedback system.

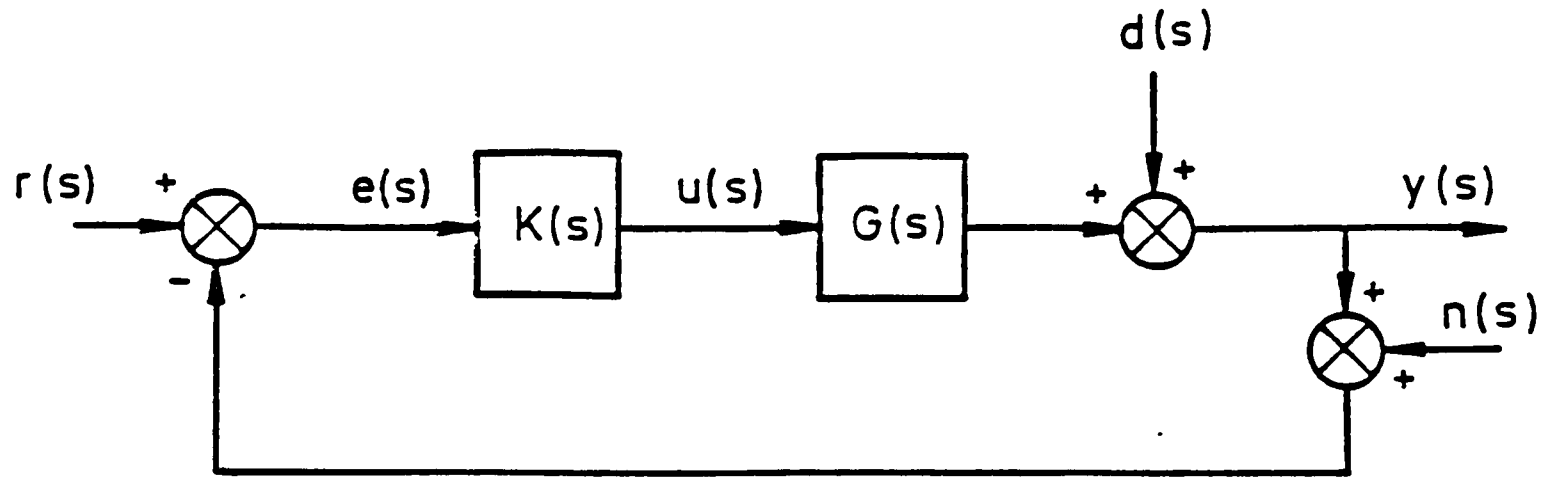


Figure 2.1 Unity feedback system

The plant G(s) is an l x m matrix-valued transfer function representing the plant; K(s) an m x l transfer function matrix representing the controller. The signal vectors r, e, u and y represent the l reference inputs, l error signals, m control signals and l output signals respectively d(s) and n(s) model plant disturbance and measurement signal vectors.

This system structure is known as a 1 degree of freedom (DOF) design since the input-output and feedback loop transfer functions cannot be changed independently.

The system shown in Figure 2.2 is a common example of a 2 DOF system.

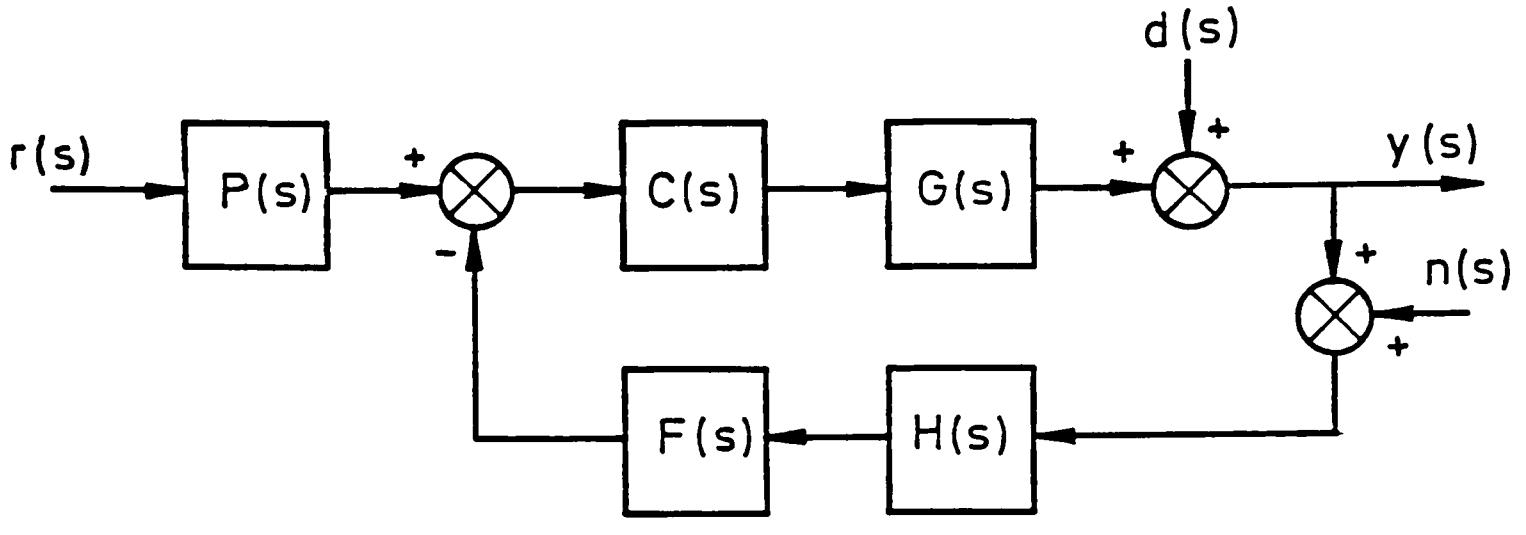


Figure 2.2 General feedback structure

In this system the controller is (over-)parameterized by a command prefilter P(s), cascade compensator C(s) and feedback compensator F(s). H(s) represents sensor dynamics. It has been proven by Pernebo [PER1] that, when prefiltering of commands is permitted, there is a complete and rigorous separation between command response and the choice of feedback loop transfer matrix.

In this thesis the system described by Figure 1 will be used predominately. This is because it is sufficient to analyze the 'feedback properties' of the system [SAF3], [MAC3] and simplifies the equations. Within the same general framework 2 D.O.F. systems can be designed by the 'standard problem' approach outlined in Chapter V or by a two-stage procedure proposed by Moore et al [MOO2]. This is a subject of current research.

2.2-2 Equations

From standard matrix algebra, the input-output behaviour of the

in Figure 2.1
system may be expressed as

$$y = (I + GK)^{-1}GK(r-n) + (I + GK)^{-1}d \qquad (2.1)$$

$$= T(r-n) + Sd \qquad (2.2)$$

after appropriately defining S(s), the sensitivity function, and T(s) the complementary sensitivity function (or closed-loop transfer function). With the same terminology the error and control signal may be written as

$$e = r - y = S(r-d) + Tn \qquad (2.3)$$

$$u = Ke \quad = KS(r-d) + KTn \qquad (2.4)$$

Equations (2.2) to (2.4) summarize the fundamental benefits and design objectives inherent in feedback loops. Specifically, the errors e are made small by making S small when reference signals and disturbances are present, and T small when noise is significant. That this cannot be achieved simultaneously at all frequencies is demonstrated by the identity:

$$S(s) + T(s) = I \qquad (2.5)$$

Equation (2.4) also states that high gain, used for example to make S small, may lead to large control signals.

These equations express the complications in designing a feedback system for a given plant description. A further complication is that this plant model may be inaccurate.

2.3 Model uncertainty

Some form of uncertainty will always be present in a finite dimensional, linear time invariant (FDLTI) model of an engineering process, whether the model is derived from test data or physical equations. The omission of high frequency dynamics or parameter uncertainty are common examples. Whenever such a model is used, it should be accompanied by some specification of the uncertainties involved. Doyle and Stein [DOY3] introduced the terms nominal model for the design model and representation of uncertainty for the error specification.

Representations of uncertainty vary in terms of the amount of structure they contain. An aircraft description may be very precise with error bounds on a large number of aerodynamic and physical coefficients. A process model derived from noisy input/output data would be less accurately described. An example of an aircraft parameterization is given in [STE1]. [EDM1] and [LOH1] consider the problem of obtaining gain and phase information, together with uncertainty bounds, from plant data.

A convenient representation of uncertainty is the unstructured perturbation characterization. In these representations the true plant model Gp(s) is assumed to be within a set defined by a nominal model transfer function G(s), together with a norm-bounded fictitious perturbation. Four such representations may be defined for all s on the direct Nyquist D-contour, D_D.

$$\left\{ Gp(s) \right\}_E \triangleq \left\{ G(s) + E(s) \mid \bar{\sigma}\,[E(s)] \leq e(s) \right\} \tag{2.6}$$

$$\left\{ Gp(s) \right\}_{\Delta_o} \triangleq \left\{ (I + \Delta_o(s))\, G(s) \mid \bar{\sigma}\,[\Delta_o(s)] \leq \delta_o(s) \right\} \tag{2.7}$$

$$\left\{ Gp(s) \right\}_{\Delta_i} \triangleq \left\{ G(s)\,(I + \Delta_i(s)) \mid \bar{\sigma}\,[\Delta_i(s)] \leq \delta_i(s) \right\} \qquad (2.8)$$

$$\left\{ Gp(s) \right\}_{\tilde{\Delta}_o} \triangleq \left\{ (I + \tilde{\Delta}_o)^{-1}\, G(s) \mid \bar{\sigma}\,[\tilde{\Delta}_o(s)] \leq \tilde{\delta}_o(s) \right\} \qquad (2.9)$$

where e, δ_o, δ_1, $\tilde{\delta}_o$ are positive scalar functions.

The adequacy of each of these representations is considered in [FOO1]. It is of particular importance to note that the input multiplicative perturbation Δ_i cannot be used to represent all possible uncertainties when the plant has more outputs than inputs. Thus, although Δ_i is useful for modelling actuator uncertainty, and is used exclusively in [LEH2], it will not be considered further.

An advantage of using unstructured perturbation models is that simple graphical robustness results can be derived. The main disadvantage is that directionality information about the uncertainty is lost, and conservative (i.e., over pessimistic) results can be obtained. Since the uncertainty is characterized by a scalar function, such as $\delta_o(s)$, it is essential that the plant inputs and outputs are appropriately scaled (normalized), so that equally important errors in each loop have equal contribution.

2.4 Robustness tests

2.4-1 Unstructured perturbations

Given that the nominal closed-loop system is stable, the robustness tests give necessary and sufficient conditions under which the system, with G replaced by any allowable Gp, will remain stable.

a) Direct Nyquist-based tests

This class of robustness tests is applicable when G and Gp share the same number of CRHP poles. The inequalities ensure that the number of origin encirclements of the image of D_D under det [I + G(s)K(s)], as G is continuously perturbed to Gp, is unchanged. This is achieved if, for all G ε {Gp}

$$\det [\, I + Gp(s)K(s)] \neq 0 \qquad (2.10)$$

$$<=> \qquad \bar{\sigma} [I + Gp(s)K(s)\,] > 0 \qquad (2.11)$$

After appropriate manipulation, the following inequalities are obtained. For Gp ε $\{Gp\}_E$, the closed-loop system will remain stable if, and only if:

$$e(s)\cdot\bar{\sigma} [\, K(s)S(s)\,] < 1 \qquad (2.12)$$

and for Gp ε $\{Gp\}_{\Delta_o}$ if, and only if

$$\delta_o(s)\cdot\bar{\sigma} [\, T(s)\,] < 1 \qquad (2.13)$$

where S(s) and T(s) are as before.

b) Inverse Nyquist-based tests [POS4]

These are applicable when G and Gp share the same number of CRHP zeros. The inequalities are derived in a similar manner to those above, but using the inverse Nyquist diagram of the image of the inverse Nyquist contour D_I under det [$I+(G(s)K(s))^{-1}$].

Thus, the closed-loop system will remain stable for Gp ε $\{Gp\}_{\tilde{\Delta}_o}$ if,

+ Equations (2.10) to (2.13) are required to hold for all s ε D_D.

and only if , for all $s \in D_I$,

$$\tilde{\delta}_o(s).\ \bar{\sigma}\ [\ S(s)\ ] < 1 \qquad (2.14)$$

c) Nyquist and inverse Nyquist combined [POS4]

By defining a more refined set {Gp(s)} it is possible to combine tests from a) and b) above, and to relax the conditions on numbers of CRHP poles and zeros. The set {Gp(s)} is assumed to be arcwise connected in the topology of unstable plants [VID1]. This ensures that there cannot be sudden changes in pole-zero structure between elements of the set.

The closed-loop system is then robustly stable if either a direct or an indirect test is satisfied over all frequencies.

2.4-2 Lehtomaki's robustness test

In [LEH2] an alternative robustness test is presented. Lehtomaki considers a unity feedback system as in Figure 2.1, but with K=I, and uses his result to prove the robustness properties of linear quadratic control system designs (cf. Chapter VII). The representation of uncertainty is defined by

$$Gp(s) = G(s)L(s) \qquad (2.15)$$

and the test may be stated as follows:

The feedback system of Figure 2.1 will remain stable when G(s) is replaced by G(s)L(s) if

(a) G(s) and $G_p(s)$ have the same number of poles in D_D

(b) $\underline{\sigma}\ [\ I + G(s)] \triangleq \alpha(s) > \bar{\sigma}\ [\ L(s)^{-1} - I\ ]$, for all $s \in \Omega_D$ (2.16)

(c) any one of the following is satisfied at each $s \in \Omega_D$

$$\text{(i)} \quad \alpha(s) \leq 1 \tag{2.17}$$

$$\text{(ii)} \quad L(s)^H + L(s) \geq 0 \tag{2.18}$$

$$\text{(iii)} \quad 4(\alpha(s)^2 - 1)\, \underline{\sigma}^2[L(s) - I] > \alpha(s)^2\, \bar{\sigma}^2\, [L(s) + L(s)^H - 2I] \tag{2.19}$$

Ω_D is the segment of D_D for which $\mathrm{Re}[s] \leq 0$.

$L(s)^H$ is the complex conjugate transpose of $L(s)$.

Condition a) is needed because Lehtomaki uses a direct Nyquist-based approach to the robustness problem. Condition b) is the same inequality that would be obtained by an inverse Nyquist-based approach. Condition c) was replaced in two later papers [CHA2] and [LEH3] by:

c) $L(s)$ has no zero or strictly negative real eigenvalues for any $s \in D_D$.

In [POS5] it is shown that the conditions in either version of c) are sufficient to ensure that the number of CRHP zeros does not change as $G(s)$ is perturbed to $G(s)L(s)$.

Lehtomaki's test is therefore a special case of an inverse Nyquist-based test where both the numbers of CRHP poles and zeros of $G(s)$ and $G(s)L(s)$ are the same.

2.4-3 Gain and phase margins

For single input, single output systems, gain and phase margins are extensively used as measures of robustness. To examine these margins in the plant input channels the uncertainty is assumed to be in the form

$$g_p = g \cdot l \quad \text{where} \quad l = \alpha \cdot e^{j\theta} \tag{2.20}$$

The gain and phase margins are determined by the values of α and θ that are separately required to cause instability. These are easily obtained from a Nyquist diagram. Systems may be conceived which have good gain and phase margins, but are arbitrarily sensitive to a simultaneous gain and phase change. Nevertheless, these margins have been found to be useful in practice.

By allowing the uncertainty to be a diagonal matrix

$$L = \text{diag}(\alpha_i e^{j\theta_i}, \ \ldots \ , \alpha_m e^{j\theta_m}) \tag{2.21}$$

phase and gain margins may be defined for multivariable systems. It is easy to show that these are not reliable measures of robustness for multivariable systems. Gain and phase margins are required for flight control systems in the USA military specification MIL-F-9490D - '... variations shall be made with all gain and phase values in the feedback paths held at nominal values except for the path under investigation.' In [SAN1] examples are given of control systems for the CH-47B helicopter that satisfy this mil-spec, but are very sensitive to small cross-feed modelling errors. A diagonal uncertainty matrix is not adequate to represent these errors.

Since the uncertainty model for gain and phase margins is multiplicative, guaranteed margins for any loop, independently or simultaneously, can be obtained from equations (2.13) and (2.14).

It should be noted that these guarantees will be conservative when compared with the classically obtained margins. This is true even for SISO systems, because the unstructured perturbation tests permit simultaneous gain and phase changes by allowing the uncertainty matrix Δ

to be complex. This is made more explicit by rearranging equation (2.14) to

$$\tilde{\delta}(s) < \underline{\sigma} [I + G(s)K(s)] \qquad (2.22)$$

Thus, for SISO a constant $\tilde{\delta}$ must be smaller than the smallest distance from the Nyquist loci of G(s)K(s) to the -1 point.

2.4-4 Structured uncertainty

The unstructured perturbation method of analyzing systems has a major drawback in many real applications: plant parameter errors, for instance, are often highly structured and conservative results are obtained. One technique for extending the usefulness of the unstructured test was proposed by [LEH1], [LEH2]. In this method a singular value decomposition is used to determine the structure of the perturbation to which the plant is most sensitive. If this perturbation is inadmissible, from physical knowledge of the plant, less conservative margins can result.

Another restriction of unstructured perturbation tests is that uncertainty is only considered at one point in the loop. It is often possible to transfer uncertainty from several different points to a single position, but this can be arbitrarily conservative. [FRE1] provides a technique for assessing the sensitivity of the singular values at one point (e.g., plant input) to uncertainty at another (e.g., plant output). The example given shows a system that has good stability margins at plant input and output, but is destabilized by small simultaneous perturbations.

This sensitivity can also be predicted by the structured singular value analysis technique of Doyle [DOY4], [DOY5]. This procedure analyzes a system with the structure given in Figure 2.3, where $\Delta(s)$ is a block diagonal matrix whose blocks are each norm-bounded $\leq \delta$. M(s) is an 'equivalent system' derived from the nominal plant G(s) and controller K(s).

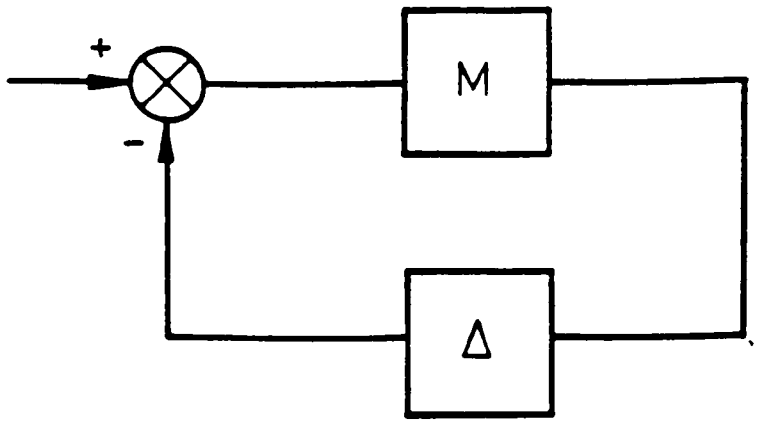


Figure 2.3 Feedback configuration

For this system stability is ensured if for all permissible Δ

$$\det (I + M\Delta) \neq 0 \tag{2.23}$$

Doyle then defines μ, the structured singular value, with the following property:

$$\mu(M) = \begin{cases} 0 \text{ if no } \Delta \in X_\infty \text{ solves } \det (I + M\Delta) = 0 \\ \left(\min_{\Delta \in X_\infty} \left\{ \bar{\sigma}(\Delta) \mid \det (I + M\Delta) \right\} \right)^{-1} \end{cases} \tag{2.24}$$

where X_∞ is the set of block diagonal matrices with no norm restriction.

Stability is then guaranteed if, and only if

$$\delta \cdot \mu(M) < 1 \tag{2.25}$$

The computation of μ is not an easy problem; various numerical procedures have been proposed and it is now possible to compute μ for most cases [KOU2], [FAN1], [DAN2].

As an example of the use of the structured singular value, consider the simultaneous input and output perturbation problem,

$$\text{i.e.,} \quad \text{let } Gp = (I + \Delta_o)\, G\, (I + \Delta_i) \tag{2.26}$$

Then, after rearranging, the problem may be cast into the form of Figure 2.3 with

$$M = \begin{bmatrix} (I + KG)^{-1}KG & (I + KG)^{-1}K \\ -(I + GK)^{-1}G & (I + GK)^{-1}GK \end{bmatrix}$$

and

$$\Delta = \begin{bmatrix} \Delta_i & 0 \\ 0 & \Delta_o \end{bmatrix}$$

It is also possible to rearrange a system with uncertainty in particular elements (e.g., a coefficient in a state-space description) into this form.

A major restriction on this problem formulation is that Δ must be stable. An extension to permit Δ to be unstable and to use different plant models is proposed in [FOO2]. This presents a generalization of the combined direct and inverse Nyquist-based tests for unstructured perturbations to the block-structured case.

2.4-5 Other methods

[WIN2] presents a method for analyzing the sensitivity of a closed-loop system to errors in the system A-matrix. In this approach the system is first manipulated into a form similar to that in Figure 2.3, with Δ the matrix of errors in the system A-matrix.
A Nyquist array of $M(s) = -(sI-A+BK(s)C)^{-1}$ can then be used, together with the small gain theorem [ZAM1], [ZAM2], to determine stability margins.

Singular value analysis can also be used to determine sets of simultaneous changes to which the system is most sensitive.

For this example, and others, larger margins can be obtained if the uncertainty is constrained to be real-valued [MOR1]. Permitting real parameter values to have a complex perturbation is not unreasonable, however, since the uncertainty may be due to unmodelled dynamic effects.

For highly structured uncertainty, the least conservative results may be obtained by experimentation on a large, probably non-linear, dynamic simulation. A major problem with this is the amount of computation required, especially with large numbers of perturbed variables. A second problem is that the results are highly dependent on the assumed structure of the uncertainty, as was found with gain and phase margins.

2.5 Design implications

The robust design problem may be summarized as one of finding a compensator K(s), such that:

a) The nominal feedback system, $(I + GK)^{-1}GK$, is stable.

b) The perturbed system, $(I + GpK)^{-1}GpK$, is stable for all possible Gp.

c) Performance objectives are satisfied for all possible Gp.

It has been established that the singular value is an important tool in the analysis of multivariable systems, and should therefore be used as an indicator of robust stability [MAC6], whatever design procedure is adopted. Nominal stability and nominal performance are not sufficient grounds for accepting a control system design.

Prior to H^{∞}-optimization the most successful multivariable design tools were the frequency domain-based inverse Nyquist array (INA) [ROS2]

and the characteristic loci (CL) [MAC2] methodologies, and the time domain optimal linear quadratic Gaussian (LQG) (see Chapter VII). Both the INA and CL are based on reducing the multivariable design problem to a set of scalar problems, to which 'classical' SISO techniques can be applied. Unfortunately, it can be shown, albeit with pathological examples, that although the scalar functions may have good feedback properties, the resulting multivariable system may not [DOY3], [POS2].

A considerable advantage of LQG is that nominal stability is guaranteed. Thus techniques were developed to choose weighting matrices in an attempt to manipulate the system singular values. The resulting design procedure is discussed further in Chapter VII. The idea behind this procedure is to shape the loop transfer function GK, and hence, indirectly, S, T, KS. Nominal performance is achieved by designing K such that

$$\underline{\sigma}\,[GK] \geq p(\omega) \text{ at low frequency} \qquad (2.27)$$

and robustness is obtained by ensuring

$$\bar{\sigma}\,[GK] < q(\omega) \text{ at high frequency.} \qquad (2.28)$$

Equation (2.27) ensures that S(s) is small at low frequency; equation (2.28) ensures that T(s) rolls off outside the bandwidth of the system. The functions p and q are derived from desired performance and uncertainty models.

A more direct approach to the design problem was provided by the advent of H^{∞}-optimization. The simplest problem to be proposed, and later solved, was that of the sensitivity minimization problem [ZAM2]: to find a stabilizing controller that would minimize the maximum δ over all frequency and all controllers of

$$\bar{\sigma}\ [\ S(s)] \tag{2.29}$$

This quantity is known as the H^∞-norm of the sensitivity function S(s), $||S(s)||_\infty$. Referring to the system in Figure 2.1, S(s) is the transfer function between disturbance d(s) and output y(s). Minimizing equation (2.29) minimizes the worst amplification of d(s) to y(s). (N.B. This is also the same transfer function from r(s) to e(s).) Generally, disturbances and errors will be more important over some frequency ranges than others, and so weighting functions are added.

The problem then becomes

$$\min_{\text{stabilizing K}} \ || W_1(s)\ S(s)\ W_i(s) \ ||_\infty \tag{2.30}$$

The robustness tests for unstructured perturbations - equations (2.12), (2.13), (2.14) - also suggest H^∞-optimization problems, i.e.,

$$\min_{\text{stabilizing K}} \ || W_2K(s)\ S(s)\ W_i ||_\infty \tag{2.31}$$

where W_2 is related to e(s). This can be regarded as an optimal robust stabilization problem [GLO2].

Clearly neither (2.30) nor (2.31) satisfy all the objectives a) to c) of a robust design methodology, and some method of combining different problems is required. The problem generated by minimizing the sum of the infinity norms of equations (2.30) and (2.31) cannot be solved. The following problem can, however, and will be used in Chapter VI.

$$\min_{\text{stabilizing K}} \left|\left| \begin{matrix} W_1(s)\ S(s)\ W_i(s) \\ W_2(s)\ KS(s)\ W_i(s) \end{matrix} \right|\right|_\infty \tag{2.32}$$

Similar problems were proposed in [KWA2], [KWA3] for polynomial systems, and in [FOO3], where sensitivity and complementary sensitivity functions are combined. Note that equation (2.32) is in fact a robust stabilization problem with nominal performance; the problem of minimizing (2.32) for the set of all possible plants is not yet completely solved [BIR1].

One approach to the complete problems of robust stabilization and robust performance is provided by [DOY8]. In this technique, performance objectives are included in the structured perturbation form of Figure 2.3. The resulting procedure, known as μ-synthesis, attempts to minimize μ over all frequency. This procedure uses a μ analysis of one design to provide weighting functions for the next H^∞-optimization. Unfortunately, although both the μ and H^∞ problems are convex, the joint problem is not, and the complete solution to this non-linear programming problem has yet to be obtained [SAF9].

2.6 Concluding remarks

This chapter has introduced the concepts involved in modern robust multivariable control system design. The use of the singular value plots as indicators of robustness provides a major motivation for pursuing H^∞-optimization techniques. This will be considered further in Chapter V, with a helicopter application in Chapter VI. The helicopter model used did not have detailed information about the uncertainty involved; the unstructured perturbation approach was therefore adopted.

The complete solution to the robust control system design for linear systems has yet to be solved.

CHAPTER III

ROBUSTNESS OF SAMPLED-DATA SYSTEMS

3.1 Introduction

A major goal of research into helicopter control systems is the implementation of multivariable controllers on digital flight control computers. The effect of the sampling on the robustness of the resulting system is therefore an important issue. This chapter presents an approach to this subject based on using non-linear mathematical tools to analyze sampled-data systems with continuous-time techniques. The 'conic sector' is used to provide a generalization of the singular value based robustness tests to these non-linear systems. The work originates from an MIT PhD thesis by Thompson [TH01] on the conic sector analysis of such systems and extensions by [WAL1], [TH02]. The principal motivation for looking at these systems with continuous time techniques, such as frequency responses, is that the physical system being controlled is continuous. Techniques that are used in the z or w planes, for example, only consider the plant at discrete points in time, and require that the plant model be first discretized. A problem in robustness analyses in these domains is that the plant uncertainty must also be discretized. It is not clear that this is valid, particularly when robustness to uncertain high frequency dynamics is considered.

When a control system is digitally implemented, three potentially damaging effects are introduced:

1) Aliasing

2) Lack of control over intersample behaviour

3) Time delay caused by data processing

The continuous-time approach deals with these effects in the following manner.

1) The effect of aliasing is quantified by the magnitude of the uncertainty associated with the compensator.

2) Intersample behaviour is due to system response at frequencies above the Nyquist frequency; the sensitivity to model uncertainty at these frequencies is quantified by the continuous-time approach.

3) Time delays, possibly a fraction of the sample time, have a known frequency response of the form $\exp(j\omega T)$ and can be included in the 'nominal' loop transfer function.

These effects are not adequately captured by either the z or w-plane analysis techniques. Other properties, notably nominal closed-loop stability and time response, can be analyzed adequately with these techniques. The conic sector frequency domain approach is not as useful in these contexts.

The main result is a characterization of the uncertainty due to sampling; this is presented in section 3.3. It relies heavily on ideas from functional analysis, and so in section 3.2 an introduction is given to this mathematics, which is often unfamiliar to engineers. The

mathematical rigour is necessary in order to capture the time varying non-linear nature of the sampling process.

3.2 Functional analysis

This section presents and defines the key ideas from functional analysis that will be used later in the chapter. A good reference is [VID2]; material is also taken from [ZAM1], [SAF1], [SAF4],[THO1], [MEE1] and [DES1].

3.2-1 Functions

A function maps one set of values into another set. Functions will be used to represent signals such as inputs and outputs of a system. The function x may be defined by

$$x: T \rightarrow V \qquad (3.1)$$

where T is a given subinterval of real numbers representing the time variable. V is a given linear space, e.g. R^n the set of n-dimensional vectors. The set of elements in a linear space must satisfy a number of axioms such as addition and multiplication, the existence of identity and zero elements, etc.

The symbol x_t denotes the truncated function $x_t : T \rightarrow V$ with the values

$$x_t(\tau) = x(\tau) \quad \text{for } \tau < t$$
$$x_t(\tau) = 0 \quad \text{elsewhere} \qquad (3.2)$$

3.2-2 Function spaces

Function spaces contain sets of functions with certain properties. A normed space is a space in which some measure of size is defined. For

example the L_p spaces are normed linear spaces, the elements $x \varepsilon L_p$ all have a finite norm denoted by $|| x ||_{L_p}$.

$$\text{For } p = [1,\infty) \quad || x ||_{L_p} \triangleq \left[\int_0^\infty || x(t) ||_E^p \, dt \right]^{1/p}$$
$$\text{for } p = \infty \quad || x ||_{L_p} \triangleq \sup_{t \geq 0} || x(t) ||_E \qquad (3.3)$$

where the Euclidean vector norm

$$|| x ||_E \triangleq \left[\sum_{1=1}^{n} | x_i |^2 \right]^{1/2} \qquad (3.4)$$

The engineering significance of L_2 is that it is the set of all signals with finite energy.

In order to incorporate signals that may have finite power or are the output of an unstable system. it is necessary to define an extension of L_2, namely L_{2e}.

L_{2e} is the space consisting of those functions whose truncations lie in L_2, this is a normed linear space with norm

$$|| x ||_\tau \triangleq \left[\int_0^\tau || x(t) ||_E^2 \, dt \right]^{1/2} \qquad (3.5)$$

3.2-3 Relations and operators

The relationships between functions are described by relations, often as a subset of a given product space; e.g. $L_2 \times L_{2e}$ which implies that the relation transforms functions from L_2 to L_{2e}.

If H is a relation, and (x,y) a pair of functions related by H, y is said to be an image of x under H. often denoted Hx (In general x can have multiple images). The range Ra(H), and the domain Do(H) are the sets of possible functions for y and x. An operator is a special class of relations whose domain is L_{2e} and is single valued.

The inverse of a relation is a set with the elements x and y arranged in the reverse order. This inverse relation always exists and may be defined by

$$H^{-1} \triangleq \{ (y,x) \in L_{2e}^{m} \times L_{2e}^{n} \mid (x,y) \in H \} \tag{3.6}$$

The inverse of an operator may be a relation.

3.2-4 Gain and stability

The gain of a relation is defined by

$$|| H ||_{L_2} \triangleq \sup \frac{|| Hx ||_\tau}{|| x ||_\tau} \tag{3.7}$$

where the supremum is taken over all non-zero $x \in Do(H)$ and all corresponding $Hx \in Ra(H)$, for all $\tau \in Rx$, i.e. all possible input-output pairs and all truncations.

A relation is said to be L_{2e} - stable if its L_2 gain is finite, in this case there will exist a constant k such that

$$|| Hx ||_\tau < k || x ||_\tau \quad \text{for all } x \in Do(H), \quad Hx \in Ra(H) \text{ and all } \tau \in Rx. \tag{3.7}$$

This is bounded input, bounded output (BIBO) stability.

For stable linear time invariant (LTI) operators the norm may be transformed to the frequency domain, and the following is well known:

$$|| H ||_{L_2} = || H(j\omega) ||_\infty \tag{3.9}$$

That is, the infinity norm of a stable transfer function matrix is equal to the L_2 gain of its time domain operator.

3.2-5 Conic sectors

If H is a relation between x and y and

$$|| y - Cx ||_\tau^2 < || Rx ||_\tau^2 \qquad (x,y)\varepsilon H,\ \tau\varepsilon R_+ \tag{3.10}$$

where C and R are operators, then H is said to be 'strictly inside a conic sector with centre C and radius R' or 'inside (C, R)'.

The conic sector is defined as a time domain inequality and as such is applicable to very general relations that are both non-linear and time-varying. The use of a conic sector is that it is possible to rigorously approximate such relations by linear time-invariant operators C and R. The conic sector may be interpreted as an approximation of the relation together with a measure of the additive error.

For the special case when (H, C, R) are linear non-anticipative operators such that H-C and R are stable, then the conic sector is merely a generalization of the usual 'additive perturbation' representation,

i.e., H is inside cone (C, R)

$$\Leftrightarrow \bar{\sigma}\left[H(j\omega) - C(j\omega) \right] < \bar{\sigma}\left[R(j\omega) \right] \text{ for all } \omega \tag{3.11}$$

For a proof see [SAF2], but note that it is not necessary to require the existence and stability of R^{-1} and that H and C do not need to be stable.

3.2-6 Closed loop stability

Consider the general feedback system of Figure 3.1.

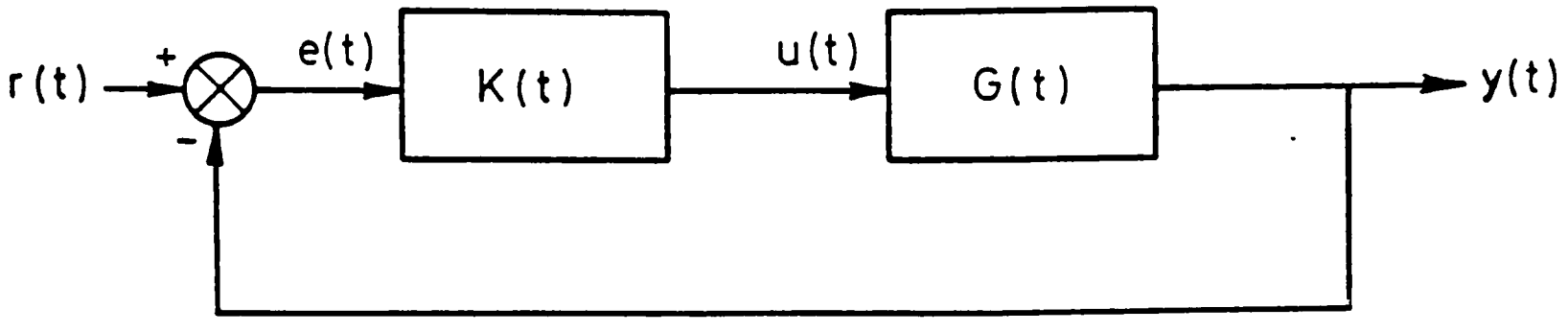


Figure 3.1 General Feedback System

K and G can be general causal time-varying operators. A useful result known as the small-gain theorem, ([ZAM1], [SAF4]) states that the closed loop system will be stable if

$$|| K ||_{L_2} \cdot || G ||_{L_2} < 1 \qquad (3.11)$$

Since we generally require the loop transfer function to be large for good control, this theorem cannot generally be applied directly. Fortunately it is often possible to first perform loop transformations, as illustrated below.

If we now assume K is described as being inside cone (C,R) where C and R are LTI, and G is also LTI. That the system is well-posed requires $(I+GK)^{-1}$ to exist and it is also required that R is stable and we may therefore write

$$K = C+E \quad \text{where} \quad ||E||_\tau < || R ||_\tau \quad \text{for all } \tau \qquad (3.12)$$

where E is a stable operator.

The system equations may then be written

$$y = G(E+C)\,(r-y)$$

$$\Leftrightarrow \quad y = (I+GC)^{-1}GCr + (I+GC)^{-1}\,GE(r-y) \tag{3.13}$$

This suggests an equivalent system as shown in Figure 3.2

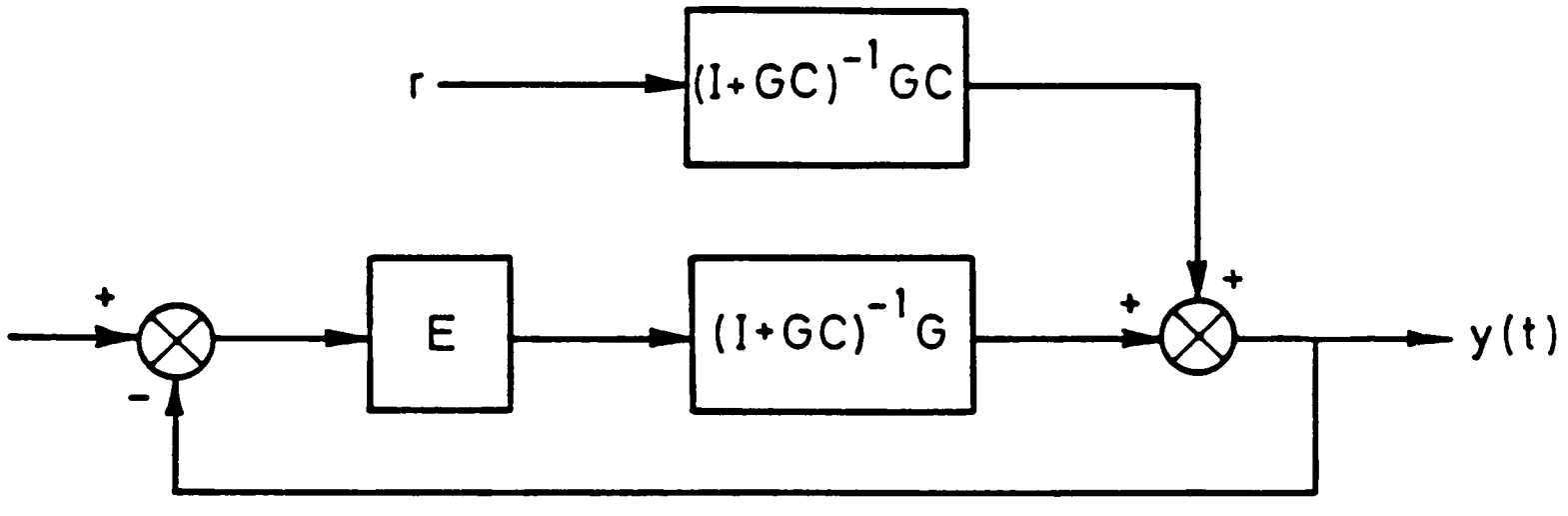


Figure 3.2 System after loop transformation

Stability of this system is then guaranteed if

(i) $(I+GC)^{-1}GC$ is stable (3.14)

(ii) $\|E\|_{L_2} \cdot \|(I+GC)^{-1}G\|_{L_2} < 1$ for all E (3.15)

$\Leftarrow$ $\|R\|_{\tau} \cdot \|(I+GC)^{-1}G\|_{\tau} < 1$ for all $\tau \varepsilon R_+$ (3.16)

(from equation 3.12)

Equation (3.14) states that the 'nominal' system must be stable. Equation (3.16) is a condition on the size of the radius of the conic sector that guarantees closed loop stability. By assuming all signals are

sinusoidal and all operators linear, we may transform (3.16) to the frequency domain to obtain

$$\bar{\sigma}\left[\, R(j\omega) \,\right] \cdot \bar{\sigma}\left[\, (I+GC)^{-1}\, G(j\omega) \,\right] < 1 \qquad (3.17)$$

which is the familiar robustness result for linear systems with an additive perturbation. The requirement that the number of right half plane poles of K does not change is implicit in the fact that R must be stable.

3.3 Conic sectors applied to sampled-data systems

3.3-1 Thompson's conic sector result

Consider the sampled-data compensator in Figure 3.3

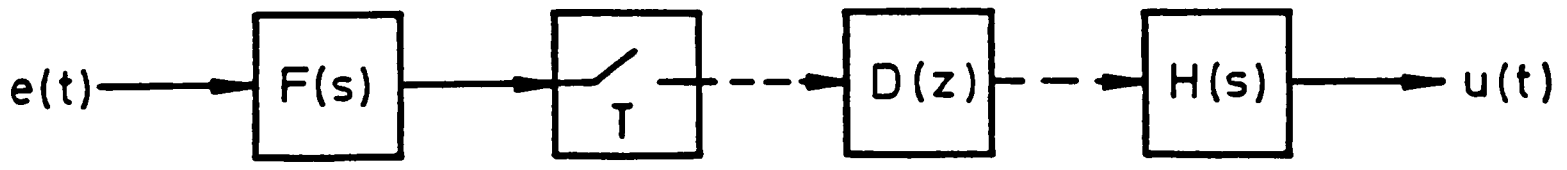


Figure 3.3 Sampled-data compensator

In this compensator an analogue output signal is produced from an analogue input signal, via conversion to and from a digital signal. A digital computer algorithm is used to perform the control. At a particular point in time, the relationship between input and output spectra is given by:

$$u(j\omega) = \frac{1}{T} \; H(s=j\omega)\; D(z=\exp(j\omega T)) \left\{ \sum_{k=-\infty}^{\infty} F(j\omega - j\omega_s k)\; e(j\omega - j\omega_s k) \right\} \qquad (3.18)$$

where T is the sample time, $\omega_s = \frac{2\pi}{T}$ the sampling frequency (rad/s))

The summation in equation (3.18) appears because the output at a particular frequency includes contributions from other frequencies by the aliasing effect. The relationship between e(jω) and u(jω) is described as linear time-varying.

Thompson's main result [TH01] is that this time-varying operator can be rigorously approximated by a conic sector with LTI operators C and R.

Thus with:

$F_k = F(j\omega - j\omega_s k)$, $D^* = D(z=\exp(j\omega T))$ and Σ_k = summation from k = $-\infty$ to ∞. The sampled-data compensator K is inside cone (C,R) with LTI C and R if

$$\underline{\sigma}\,[R] > \surd \left[\frac{1}{T} \Sigma_k \sum_{n \neq k} \bar{\sigma}^2 \,[H_k D^* F_n] + \Sigma_k \,\bar{\sigma}^2 \,[\, \frac{1}{T} H_k D^* F_k - C_k] \right] \qquad (3.19)$$

The choice of $C(j\omega) = \frac{1}{T} HD^*F$ minimizes the radius, although equation (3.18) is sufficiently general to allow any choice of centre.

Major shortcomings of this approximation technique are:

(i) The sampled-data compensator must be stable, in order to give a finite radius.

(ii) When the results are used for robustness analysis conservative results are obtained. This is because no account is taken of the structure and bandwidth of the error signal. For multivariable systems conservatism is introduced because only the maximum singular value of D(z) is used.

3.3-2 The A-scaling approach

This approach was introduced by [WAL1] and later by [THO2]. The problem of conservatism is tackled by introducing a new cone containing just the sampler, surrounded by fictitious operators, as in Figure 3.4.

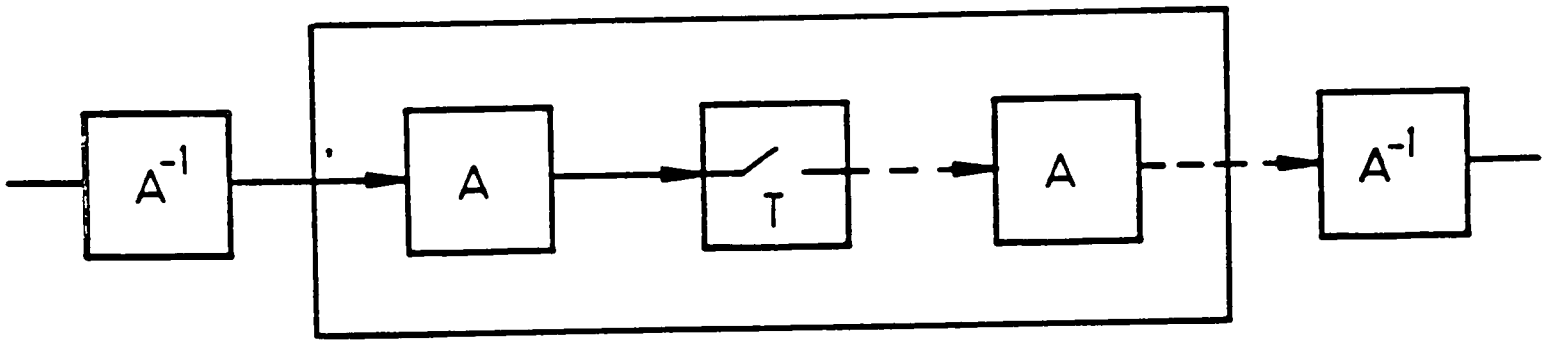


Figure 3.4 New conic sector

By introducing the inverse operators A^{-1} this cone can be used to generate a conic sector representation of the sampled-data compensator. This approach does not require the digital compensator to be stable and the flexibility in the choice of the operator A can be used to reduce conservatism.

The choice of A is not trivial, however, and must depend on the system being considered. The problem is defined below:

If we denote the sampling operator by S, then the operator ASA is in the cone $(\frac{1}{T} A^2, R)$ if

$$\underline{\sigma}\,[R(j\omega)] > \frac{1}{T} \sqrt{\left[\Sigma_m \Sigma_{n \neq m} \left|\left|A(j\omega + j\omega_s m)\, A(j\omega + j\omega_s n \right|\right|_2^2 \right]} \qquad (3.20)$$

where A is LTI, has no poles or zeros in the CRHP and is diagonal with equal elements. The closed loop system is then stable if the nominal closed loop system is stable and

$$|| \, RTA^{-2} \, ||_2 \; || \, I + (\tfrac{1}{T} \; GHD^{*}F)^{-1} \, ||_2^{-1} \; < 1 \qquad (3.21)$$

(obtained from equation (3.16) using above properties of A)

Since all operators are LTI this may be written as:

$$\bar{\sigma} \left[RTA^{-2} \right] . \; \bar{\sigma} \left[(I + (\tfrac{1}{T} \; GHD^{*}F)^{-1})^{-1} \right] < 1 \quad \text{for all } \omega \qquad (3.22)$$

Thus the problem is to choose A such that R given by equation (3.20) ensures that equation (3.22) is met with the greatest margin over all frequency.

Note:

(1) For the radius computation (equation (3.20)) to converge A must have at least a one-pole roll off.

(2) R is periodic with frequency ω_s. To minimize R, A(jω) should be as small as possible outside the fundamental frequency band

$$\frac{-\omega_s}{2} < \omega < \frac{\omega_s}{2}$$

(3) The maximum roll off rate of A(jω) is that which ensures that equation (3.21) holds at high frequency. Thus the maximum pole excess of A^2 is equal to that of FGH.

(4) The presence and magnitude of modelling errors should be taken into account.

In [WAL1] a suggested candidate for A is

$$\lim_{\partial \to 0} \quad \frac{1}{s + \partial} \qquad (3.23)$$

For this operator an analytic solution to the infinite summation may be obtained when $\omega_s = 1$, $T = 2\pi$.

$$RTA^{-2} = \pi^2 \sqrt{(2/3)} \frac{\omega^2}{|\sin(\pi\omega)|} \qquad (3.24)$$

In [TH02] it is shown that this is still useful, despite the infinite peaks at integer ω, because if H(s) is a zero-order hold $H(j\omega)$ will be zero at these frequencies. More useful choices were found to be Butterworth filters with the maximum allowable roll-off, as illustrated in the next section.

3.3-3 Robustness considerations

The quantity RTA^{-2} may be loosely interpreted as a multiplicative type of perturbation representing uncertainty in the controller due to the sampling operation. Thus define δ_s, a frequency dependent variable bounding this uncertainty.

$$\delta_s = \bar{\sigma} \left[RTA^{-2} \right] \quad \text{for all } \omega. \qquad (3.25)$$

A preferred method to analyze systems with uncertainty at more than one point would be to use a form of Doyle's structured perturbation theory as in [WAL1]. It is instructive, however, to examine equation (3.22) when G is assumed to be LTI with uncertainty represented by unstructured perturbations. By singular value inequality manipulation we obtain the following results for unstructured perturbations

a) Output multiplicative perturbation model

$$G_p = (I + \Delta)\, G, \qquad \bar{\sigma}[\Delta] < \delta \quad \text{for all } \omega.$$

The closed loop sampled-data system will remain stable if, for all ω:

$$\delta < \frac{\underline{\sigma}\left[I + \left(\frac{1}{T} GHD^* F \right)^{-1} \right] - \delta_s}{1 + \delta_s} \qquad (3.26)$$

and

b) Output inverse multiplicative error

$$G_p = (I + \tilde{\Delta})^{-1}G, \qquad \bar{\sigma}[\ \tilde{\Delta}\ ] < \tilde{\delta} \quad \text{for all } \omega.$$

The closed loop sampled-data system will be stable if, for all ω:

$$\tilde{\delta} < \left(1 - \delta_s\ \bar{\sigma}\ [\ (I + \frac{1}{T}\ GHD^*F)^{-1})^{-1}\ ]\right) .\ \underline{\sigma}\ [\ I + \frac{1}{T}\ GHD^*F] \qquad (3.27)$$

It should be clear that equations (3.26) and (3.27) tend to the equivalent results for continuous systems when $\delta_s \to 0$. Equation (3.27) is similar to one presented in [F005].

Figure 3.5 shows an example of δ_s when A(s) is a 5th order Butterworth filter with cut-off frequency ω_o = 1, 5, 10, 50, 100 with ω_s = 200 rad/s. The effect of changing the cut-off frequency is to reduce the magnitude of δ_s at either low or high frequency. It is interesting that they all pass through the same point at ω = 100 rad/s. It is to be expected that at this frequency ($\omega_s/2$) the uncertainty is > 1 because there is 100% uncertainty when sampling a sinusoidal signal at its Nyquist frequency.

The function $(I + (\frac{1}{T}\ GHD^*F)^{-1})$ is the inverse of the nominal closed loop transfer function. Figure 3.6 is a graphical illustration of equation (3.22) when

$$f(s) = \frac{2500}{s^2 + 70s + 2500}\ ,\ g(s) = \frac{150}{(s+1)(s+3)}\ ,\ h(s) = \frac{1 - \exp(-sT)}{s}$$

$$d(z) = \frac{0.805\ (z - 0.910)^2}{(z - 0.98)(z - 0.48)}\ , \qquad T = \frac{\pi}{100} \quad \text{sec.} \qquad (3.28)$$

(see [TH01] section 5.2 for more information on this example).

The function used for A(s) is as in Figure 3.5 with ω_o = 1 rad/s. This was used because it maximizes the minimum value of δ given by equation (3.26).

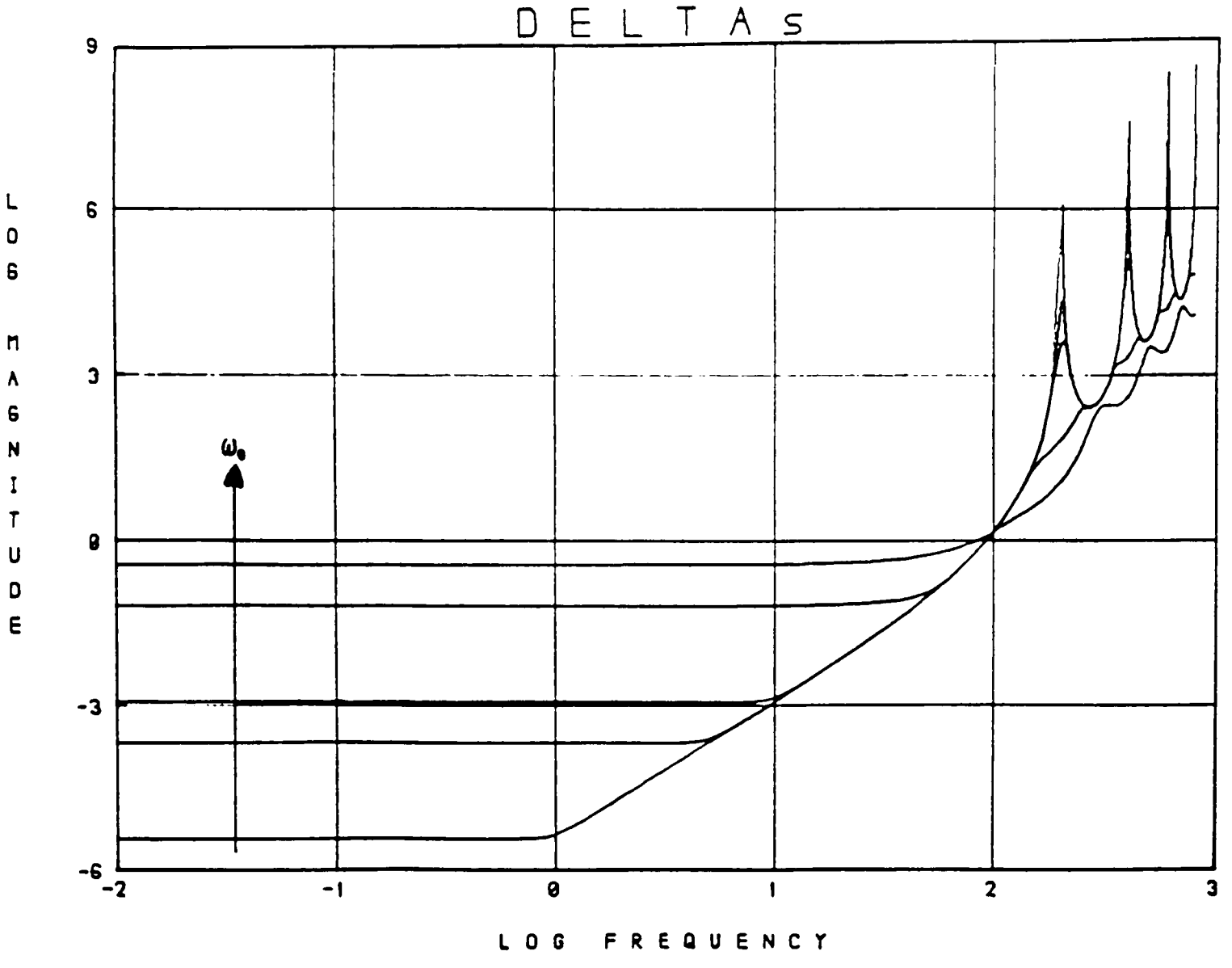


Figure 3.5

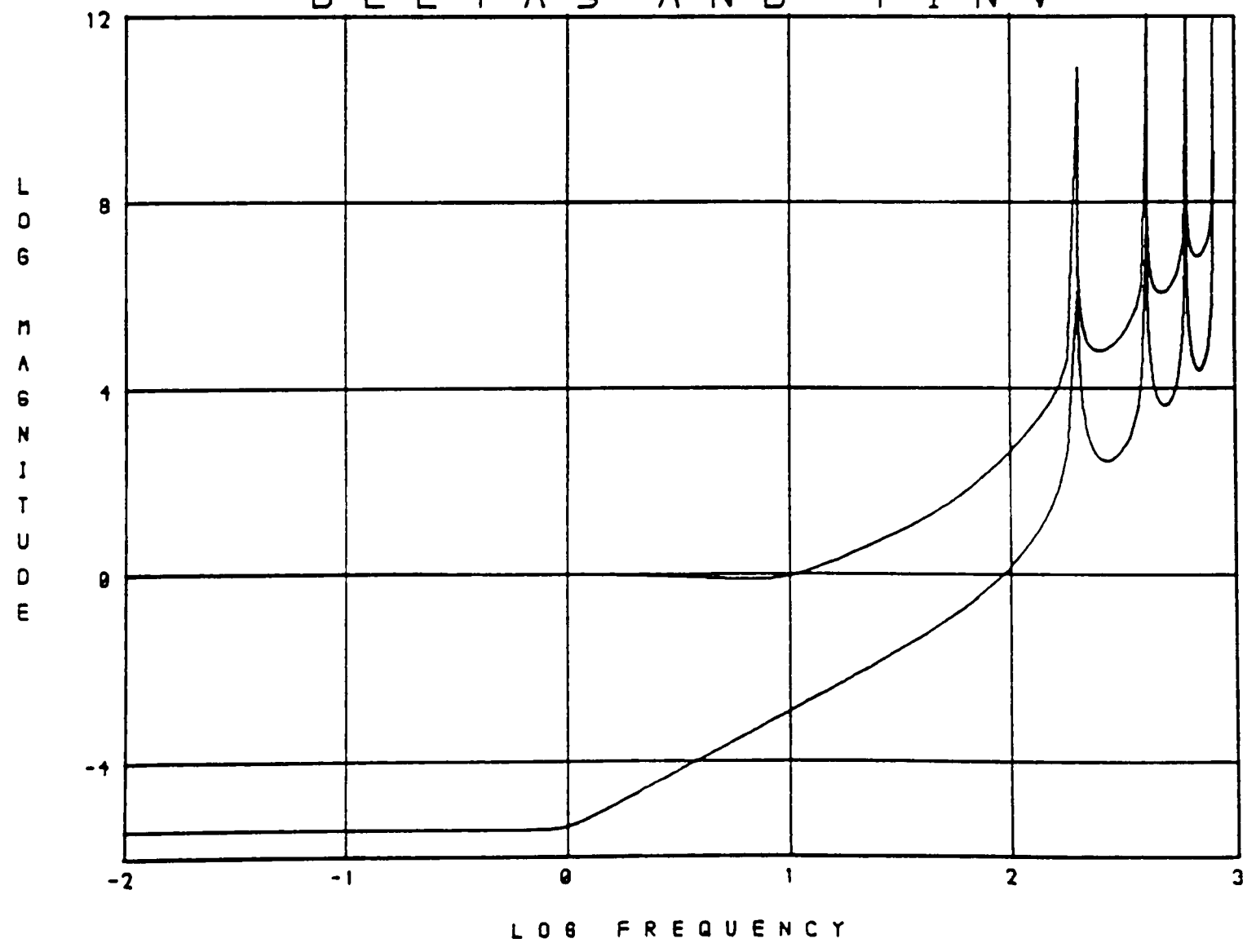


Figure 3.6

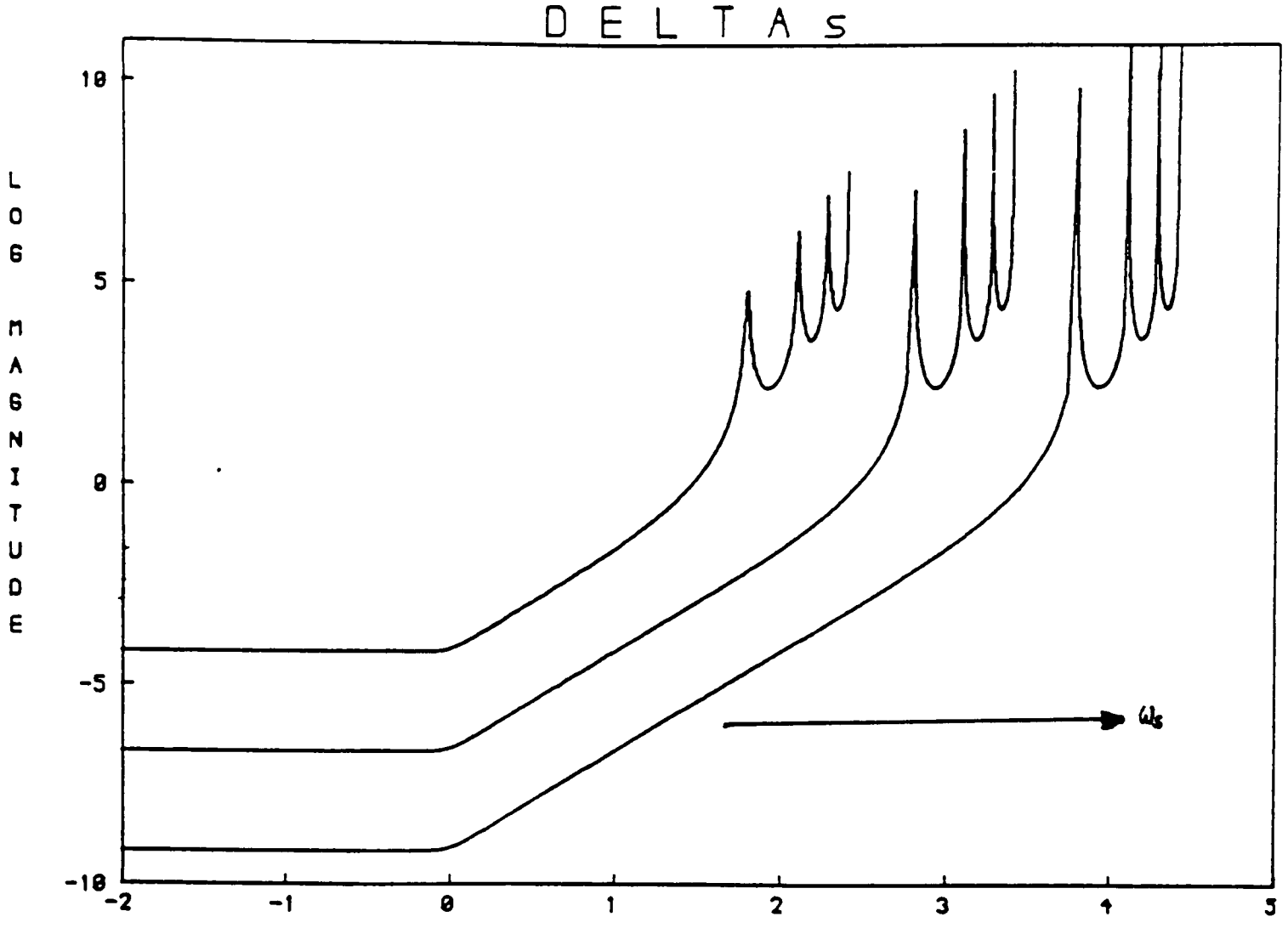


Figure 3.7

Figure 3.7 demonstrates the effect on δ_s of changing the sample frequency from ω_s = 200 to 20 and 2000 rad/s. It should be clear that if the sample frequency is significantly greater than the nominal system bandwidth δ_s will be negligible. If the controller tends to its continuous counterpart as the sample rate is increased the sampled-data system will therefore asymptotically recover the robustness margins of the continuous system.

3.4 Concluding remarks

This chapter has presented an approach to the problem of quantifying the effect of digital implementation on the robustness of control systems. The results tend to give justifications to the common assumption that a sampled-data system will behave in a similar way to the corresponding continuous system provided the sampling is fast enough. The robustness results might be useful to a designer in the selection of the sampling rate and filtering required for a particular application.

It is straightforward to extend this work to analyze systems with multivariable sampling, but in this case the more powerful structured perturbation results would be required to analyze the robustness.

CHAPTER IV

THE HELICOPTER

4.1 Introduction

This chapter is devoted to a study of the helicopter. The original aim of this work was to provide a good understanding of the control problem from which sensible and practically usable design procedures would result. With hindsight this could be stated much more strongly - it is impossible to create a good design without a thorough understanding of the problem. The H^{∞}-design approach proved to be very good at highlighting gaps in this understanding; in particular the problems associated with controlling the aircraft angular rates were revealed.

The material presented in this chapter is intended to provide background information for a study of the helicopter by control engineers, and consequently from the point of view of flight mechanics and aerodynamics, it will be far from complete. For further information on these topics the standard references include Bramwell [BRA1], Johnson [JOH1], Gessow and Myers [GES1] and Saunders [SAU1]. Good introductions to aircraft stability and control are given by Babister [BAB1] and Pallett [PAL1], and for lighter reading on 'How to fly helicopters', see Collier [COL1].

4.2 Helicopter types

4.2-1 Configuration

Helicopters are characterized by the use of rotating wings (the rotor) to produce lift, propulsive power and control. The consequent versatility of flight envelope - from vertical take-off/hovering to high-speed manoeuvring flight - explains their widespread use and the continuing study to improve performance.

Two main methods are used to balance the torque which results when a shaft-driven rotor is producing power, giving rise to the familiar appearance of helicopters:

(i) Single main rotor and tail rotor.

(ii) Multiple contra-rotating rotors.

Other methods have been suggested; for example, single main rotor with large vane in the rotor downwash, or jet thrust in the tail. However, these are less widely used. In this study only the first type is considered, with particular reference to the Lynx and Puma helicopters.

A common example of the second type is the Chinook CH47 which has a rotor at either end of the fuselage. This has appeared in the control literature as an example for multivariable control system design methods eg., Doyle and Stein [DOY3]. It has the advantage for analysis that the control problem can be split into two parts, namely longitudinal and lateral. It is assumed that some form of control is implemented to balance the rotors laterally, and so control of longitudinal motion only is considered. This simplifies the analysis by halving the number of inputs, outputs and states in the design models. This partitioning of the model is common in fixed-wing aircraft, but the single main rotor/tail rotor helicopter has considerable coupling between the two sub-systems.

4.2-2 The Rotor

Helicopter types may be further sub-divided by the design of the main rotor into three broad classes, as follows:

(i) Teetering rotor

In this design the blades are connected together rigidly by the hub, but the hub is free to tilt with respect to the shaft. This type is common among light two-bladed helicopters (Bell, etc.), where the blades move in a 'see-saw' motion about the shaft.

(ii) Articulated rotor

The blades are attached to the hub by hinges, free to flap up and down and to swing back and forth (lead and lag) in the plane of the rotor disc. The hinges are offset by a small amount from the shaft. This is important for its ability to generate moments. This is the rotor system used in the Puma and in many other helicopters.

(iii) Rigid rotor

The blades are connected rigidly to the shaft. Flapping and lead-lagging motion is only possible by bending of the hub. This is the system used in the Lynx, the hub being manufactured from Titanium. Many recent designs may be classed as semi-rigid. They have no hinges, but use elastomeric composite elements which deform, more like the rigid rotor.

The main rotor produces both the lifting forces required to fly and also the forces and moments required for forward and turning flight. The positions of the blades are determined by the lift, drag, centrifugal and coriolis forces acting on them. Individual control is obtained by varying the pitch of the blade, as described in section 4.3.

In all three systems, force control is obtained by tilting the thrust vector. This force is essentially perpendicular to the rotor disc plane (for the articulated rotor, this is the tip-path plane).

The rotors differ, however, in their ability to produce moments. All three types produce a moment by the thrust tilting, but the articulated rotor, with offset flapping hinges, is also able to produce a moment about the hub.

It can be shown that due to the flexing of the blades used, the rigid rotor can be considered as having a large effective hinge offset. A typical value of the hinge offset in a helicopter such as the Puma is 4% of the rotor radius. The effective hinge offset in the Lynx is about 12% which gives the Lynx about three times the moment generating capability. This explains the greater manoeuvrability of the Lynx over that of the Puma and is particularly marked in the roll-rate command response [BRO2].

4.3 Control inputs

A helicopter pilot has control over the following variables, which are later to be used as control inputs in the mathematical model of the helicopter:

(i) Collective pitch of main rotor θ_{o_e}

(ii) Longitudinal cyclic pitch θ_{1_s}

(iii) Lateral cyclic pitch θ_{1_c}

(iv) Tail rotor collective pitch θ_{tre}

(v) Throttle control of engines.

Ignoring any mechanical interlinks which would be present in a conventional helicopter, in order to reduce interaction, we may associate each of the pilot's control devices with these variables.

4.3-1 Main rotor collective

This control is usually a lever to the left of the pilot's seat, which controls the average pitch of all the main rotor blades. When moved it changes the pitch of all the blades by equal amounts in the same direction. Combined with a means of keeping the rotor speed constant, this provides a method of controlling the total rotor thrust and power.

4.3-2 Cyclic pitch controls

These are operated by a stick in front of the pilot. Its purpose is to tilt the rotor disc in the direction of movement of the stick. The lift/thrust produced by the rotor is perpendicular to the disc and so the helicopter will move in the direction of stick movement. The cyclic control has little effect on the magnitude of total lift/thrust force, but changes the direction of this force.

The cyclic pitch control system tilts the rotor by changing the pitch of the rotor blades individually during the cycle of rotation. For instance, for forward flight the blade which is moving round to the rear of the disc (retreating) must be made to ride up to be at its highest position at the rear of the disc; conversely, the blade which is advancing must be made to be at its lowest position when at the front of the disc.

When an increase in pitch is given to a blade, the blade does not rise immediately but does so approximately 90 degrees later. This can be explained by considering the response to be of second order. When driven at the natural frequency the output will lag the input by 90 degrees. A centrally hinged rotor would have this lag, but the presence of the offset hinge increases the natural frequency and hence reduces the phase lag.

4.3-3 Tail rotor collective

As previously mentioned, the main purpose of the tail rotor is to counteract the main rotor torque. This control is operated by foot-pedals, such that pushing the right pedal will tend to yaw the helicopter to the right.

This control is used differently between the hover and forward flight. When hovering, it is used to rotate the helicopter and control heading. In forward flight it is used to ensure coordinated flight ie., prevent sideslip (cyclic pitch control is used to turn). The transition between these modes is usually taken to be at about 40 knots.

4.3-4 The throttle

When provided, this appears as a twist-grip on the collective lever. This control is usually implemented by an automatic governor, which senses rotor speed and collective pitch demand. The present mathematical model does not include engine/rotor speed dynamics although a proportional reduction in speed with torque may be specified. The engine/rotor/gearbox are usually assumed to be working at their design speed.

Work is in progress at the RAE, Bedford and Glasgow University to remove this restriction by including the additional engine dynamics.

4.3-5 Extra controls

Research has been done at Glasgow University to provide an extra control input by adding an active tailplane, equivalent to an elevator on fixed-wing aircraft. Simulation studies have shown that using optimal control theory, this pilot-independent control can lead to an improvement in performance, though results are difficult to quantify [HOU1]. It is evident from the design work performed for this thesis that the control over the longitudinal motion of the helicopter is a major problem in its

control system design and an extra control in this direction would seem useful.

Individual blade control is another active research topic (see, for instance, the six papers in the 36th Annual Forum of the American Helicopter Society, 1980). Higher harmonic control (more than once per revolution) of the rotor blades, implemented using adaptive control techniques, can be used to reduce helicopter vibration levels.

4.3-6 Major interactions

In almost all flight conditions the uncompensated helicopter is unstable, so the pilot is required to make continual small adjustments to maintain stability, even in a 'trimmed' state. In addition, as clearly demonstrated in the control signal time responses of the helicopter in closed-loop (Chapter VI), the following interactions are present:

(i) Main rotor collective - tail rotor (and throttle)

A change in main rotor collective always requires a change in the tail rotor collective to balance the extra torque, and more power is required to maintain rotor speed. The amount of tail rotor compensation required varies with flight speed.

(ii) Cyclic - collective, etc.

When longitudinal or lateral cyclic is applied, to push the helicopter nose-down, to increase speed, or in rolling, to initiate a turn, the pilot must increase collective to maintain height. This is because tilting of the thrust vector reduces its vertical component. Important for control purposes is the fact that this interaction is highly non-linear. For example, it requires increased collective for whatever direction lateral cyclic is applied, and the magnitude required is a

trigonometric function of attitude angles. The range of validity of linear models is an important question introduced by this characteristic.

(iii) Longitudinal cyclic - lateral cyclic

The second moment of inertia of a helicopter when pitching longitudinally is about four times that in rolling laterally; consequently, the effect of a small interaction requires significant correction with the lateral cyclic. The amount of interaction is speed-dependent, the variation being caused in part by the asymmetric lift generated by forward flight.

(iv) Longitudinal cyclic - longitudinal cyclic

Although not a true interaction between channels, this mode requires considerable control activity to overcome its effect. The initial response to a positive step in longitudinal cyclic is to push the helicopter nose down; this leads to an increase in speed, which increases lift on the advancing blades and tends to lift the nose back up, requiring more longitudinal cyclic, etc. In simulation it has been found that it can take up to twenty seconds for the helicopter to reach a new trim state with constant control inputs, after a step demand in pitch attitude, presumably due to this effect. In linear transfer functions this motion appears to be characterized by poles and zeros close to the origin.

4.4 The control problem

4.4-1 Control of a rigid body in space

The complete control of the position and orientation of a rigid body in space requires the ability to control the forces and moments about all three axes. Thus for total control six inputs are necessary. In practice

a pilot is only provided with four controls and consequently there exist different control strategies in which some compromise is made.

In terms of the forces and moments, it is possible to produce moments about all three axes, but not without producing an accompanying force. Thus for a specified body attitude (moment equilibrium), the direction of motion (or acceleration) cannot be specified, whilst in hovering (force equilibrium), the attitude cannot be additionally specified. This problem will be discussed further after defining the necessary variables to be used.

4.4-2 Nomenclature

The variables necessary to describe the motion of the helicopter can be defined in terms of two major coordinate systems, namely body-fixed and earth-fixed axes. Other axis-systems that are used in studying aerodynamics of the rotor, etc., include hub/wind or rotor-plane axes.

(i) Body-fixed axes

This is the set of axes passing through the centre of mass of the helicopter, with (x,y,z) being forward, right, down, as shown in Figure 4.1.

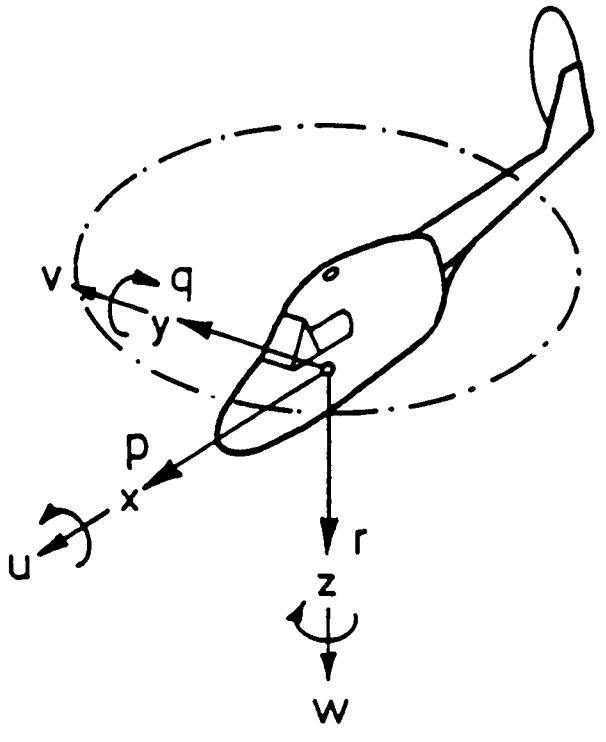


Figure 4.1 Body-fixed axes

This is the most useful set of axes in analyzing the dynamics of the helicopter, because the moments of inertia do not change with body attitude. Also defined in the diagram are (u,v,w) the components of the helicopter total velocity along each of the axes, and (p,q,r) the roll, pitch, and yaw angular rates about each axis. For control purposes this is the coordinate system in which measurements of these variables are made.

(ii) Earth-fixed axes

This is the set of axes passing through the centre of mass of the helicopter with the z_o direction pointing vertically down, x_o pointing north and y_o, east.

The three rotations necessary to define the position of the body-fixed axes relative to this fixed set are θ, ϕ, ψ, the angle of bank, pitch, and heading, as shown in Figure 4.2, commonly known as the Euler angles. The standard order of the angular rotations is: yaw through angle ψ about Oz_o, pitch through angle θ about the new position of Oy_o, roll through angle ϕ about Ox, the new position of Ox_o.

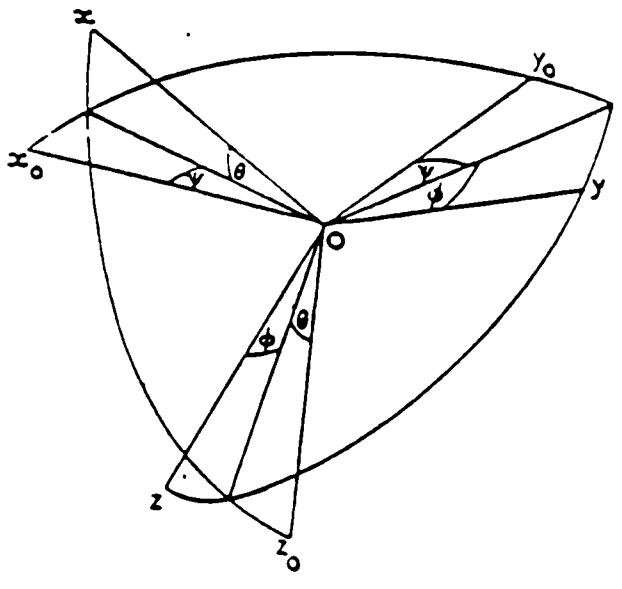


Figure 4.2 The Euler angles

The rotation matrix relating the two sets of axes is given by

$$\begin{bmatrix} x_o \\ y_o \\ z_o \end{bmatrix} = \begin{bmatrix} T \end{bmatrix} \begin{bmatrix} x \\ y \\ z \end{bmatrix} \qquad (4.1)$$

where

$$\begin{bmatrix} T \end{bmatrix} = \begin{bmatrix} \cos\theta\cos\psi & \sin\phi\sin\theta\cos\psi-\cos\phi\sin\psi & \cos\phi\sin\theta\cos\psi+\sin\phi\sin\psi \\ \cos\theta\sin\psi & \sin\phi\sin\theta\sin\psi+\cos\phi\cos\psi & \cos\phi\sin\theta\sin\psi-\sin\phi\cos\psi \\ -\sin\theta & \sin\phi\cos\theta & \cos\phi\cos\theta \end{bmatrix} \qquad (4.2)$$

obtained by multiplying the appropriate rotation matrices.

The earth-fixed axes are useful in defining the position and motion of the helicopter with respect to the ground. The velocity vector in these axes $(V_N \; V_E \; V_D)^T$ is given by a product of the rotation matrix $\begin{bmatrix} T \end{bmatrix}$ and the vector in body-fixed axes $(u \; v \; w)^T$. The position is usually given by the geographical latitude, longitude and height above sea-level.

In manoeuvring flight the helicopter motion is commonly expressed in terms of the aircraft total speed V_T, the turn-rate $\dot{\psi}$ and the descent angle γ, where:

$$V_T \triangleq \sqrt{(u^2 + v^2 + w^2)} = \sqrt{(V_N^2 + V_E^2 + V_D^2)} \qquad (4.3)$$

and

$$\gamma = \tan^{-1}\left[\frac{-V_D}{V_G} \right], \quad V_G, \text{ the ground speed, } = \sqrt{(V_N^2 + V_E^2)} \qquad (4.4)$$

Two other angles are also useful to describe the orientation of the helicopter body relative to its direction of motion:

The angle of attack, $\alpha = \tan^{-1}\left[\frac{w}{u} \right]$ (4.5)

The angle of sideslip, $\beta = \sin^{-1}\left[\frac{v}{V_T} \right]$ (4.6)

4.4-3 System outputs

We now have the following list of variables, all of which we would like to control. Fortunately they are not linearly independent, since the problem only has six degrees of freedom.

u, v, w } Components of velocity in body-fixed axes

V_T Total speed

p, q, r } Angular rates

θ, ϕ, ψ } Euler angles

α, β, γ } Incidence angles

North, East, H } Geographical position

Two possible control strategies will be considered:

(i) Flight path controller

This strategy is intended to be used in conjunction with a small side-arm controller. The inputs are treated as desired values for:

1) Flight path angle
2) Total velocity V_T
3) Bank angle ϕ (or turn rate $\dot{\psi}$)
4) Sideslip angle β

(ii) Angular rate controller

The second scheme is based on current helicopter control inputs, but automatic control will be used to reduce interaction between controls and improve performance.

1) Height rate $\dot{h}$
2) Pitch rate q
3) Roll rate p
4) Yaw rate r

The two control strategies have been simulated at the RAE, Bedford, with ideal closed-loop responses being modelled on a piloted simulation facility [BUC1]. The first is preferred by non-pilots, as it makes the helicopter easier to fly. For manoeuvring flight, however, pilots prefer to have direct control over the body of the helicopter, rather than over where it is going. The second scheme is therefore preferred by pilots, since it is closest to the conventional helicopter. Although the rate control scheme seems to be best for fast manoeuvring flight, it could become very tiresome for the pilot at other times, and for this reason the rate controller is often used in conjunction with an attitude/height hold function. The two controllers may be integrated so that the attitude hold function operates when the control sticks are centred, in order to permit 'hands off' level or constant turning flight.

4.5 Present control systems

Both the Puma and the Lynx, in common with other helicopters, have an automatic flight controller, which takes the form of a limited authority analogue stability augmentation system. The Lynx system [PAD1] is based

on an angular rate control strategy, the measured variables being pitch rate q, pitch attitude θ, roll rate p, bank angle ϕ, yaw rate r, heading angle ψ and normal acceleration a_z, obtained from rate gyros, vertical gyros and a normal accelerometer. The control system has several modes, switchable by the pilot, including speed and attitude hold functions. Additional measurements available for future control systems may include airspeed V_T, flight path angle γ or height h, sideslip angle β or lateral velocity v, and the other linear accelerations.

There are few references available for the design of such control systems. This may be due to their confidential nature, or to the fact that they are simply carefully tuned, essentially single-loop controllers. The limited authority - usually $\pm$10% of the available control power - ensures that the pilot is able to override them in the case of failure, and it is interesting to note that the British Army Gazelle helicopters do not have the autostab fitted, because it restricts performance.

Due to their complex nature, helicopter mathematical models have, until recently, been considerably more inaccurate than their fixed-wing counterparts. The current helicopter autostabs were therefore designed using poor mathematical models and limited computer simulation. They consist of mainly proportional gains (some varying with flight conditions) and phase-lead, phase-lag networks. Considerable effort has been spent in the UK on improving this modelling, both by theoretical investigation and a research helicopter at the RAE, Bedford. Westland helicopters [TYL1] and the RAE are developing control laws for an active control demonstrator helicopter, and the RAE has extensive piloted simulation facilities.

There are currently very few digital fly-by-wire helicopters in existence. These include a Bell 205 at Canada's National Aeronautical Establishment, NAE, an MBB BO105 at West Germany's DFVLR, and NASA, USA, have a Bell UH-1 and a Boeing-Vertol CH-47. They are all being used as flying control system test-beds, and typically they have two pilots - one

flying the helicopter with a full authority digital flight control system, and the second 'safety pilot' shadowing the control stick movements on a back-up conventional mechanical control system.

The NAE Canadian Bell 205 is of this form, and this normally docile helicopter has had its mechanical stabilizers removed to reduce stability. The control laws are written in ASSEMBLER using much integer arithmetic, and are implemented using three LSI 11/23 computers with 1/64 sec. sampling. The control laws are basically single-loop proportional plus integral control, with feedforward to reduce interaction. The control law gains can be manipulated on-line in flight, and many different configurations and side-arm controllers have been evaluated.

4.6 Problems in controlling rates

The physical arguments presented in this section are an attempt to explain the difficulties encountered when applying the H^{∞} optimization theory to the design of a rate control system for the helicopter.

It is well known that right half plane transmission zeros impose tight restrictions on closed loop and achievable sensitivity functions [FRE2], [OYO1], [OYO2]. The problem in controlling rates is that the associated transfer functions have transmission zeros at the origin. It is first demonstrated that this generally occurs in rate control problems.

Consider the response of an angular position θ, to an applied moment M. Including stiffness and viscous damping terms we expect a transfer function of the form

$$\frac{\theta(s)}{M(s)} = \frac{\omega_o^2}{s^2 + 2\xi\omega_o s + \omega_o^2} \qquad (4.7)$$

which is a second order transfer function with damping ξ and natural frequency ω_o. By differentiating once we obtain an expression for the rate transfer function which has a zero at the origin.

$$\frac{\dot{\theta}(s)}{M(s)} = \frac{\omega_o^2 s}{s^2 + 2\xi\omega_o s + \omega_o^2} \qquad (4.8)$$

Therefore we can expect to find zeros at the origin in a very general rate control system, assuming the presence of non-zero stiffness.

In a stable fixed-wing aircraft it is clear that this phenomenon will occur when an elevator is used to produce a small nose-up moment on the aircraft. The aircraft will pitch nose up until the increase in drag on the tailplane provides an equal opposing moment. The aircraft will assume new attitude and incidence angles and the pitch rate will decay to zero, illustrating the zero d.c. gain of applied moment to pitch rate.

If the original transfer function was unstable (negative damping) the zero d.c. gain would not be noticed in the open-loop system. However, since transmission zeros are invariant under feedback, the closed loop system must have the zero at the origin.

Consider the unity feedback system of Figure 1.1, and assume K(s) remains finite for all frequency. This implies:

$$\begin{aligned} & GK(s) = 0 \quad \text{at } s = 0 \\ \Rightarrow \quad & S(s) = 1 \\ \& \quad & T(s) = 0. \text{ at } s = 0. \end{aligned} \qquad (4.9)$$

which shows that it is impossible to achieve good tracking or disturbance rejection at d.c., with a finite gain controller.

One attempt to achieve good tracking would be for the controller to have an integrator (or even two!) in the controller, for example

proportional plus integral (P+I) control. Although this may result in acceptable input-output behaviour in theory for the system, the closed loop system must have a pole at the origin. This pole is unobservable from the output of the system, but will be present in KS(s), the transfer function from reference input (or disturbance or sensor noise!) to the control signal. The problem encountered in the design process is that this form of controller is not possible, because the closed-loop system would not be internally stable. It is therefore not possible to get the sensitivity function small at low frequency, which was the design objective.

The problem with internal stability of the system is that the steady state response of the actuator signal is unbounded to a constant disturbance or a sensor bias, for example, when the controller contains an integrator. It may be argued that a perfect integrator does not exist, but the closed loop sensitivity function must then be zero at the origin!

In the helicopter model, at different operating points transmission zeros occur either very close to, or exactly at the origin (calculated using the QZ algorithm in [LAU1]) when a rate control set of outputs is selected. The 'zero directions' are not directly aligned with any particular input-output pair due to the high levels of interaction. The performance implications are that it is impossible to get 'perfect' step responses in rate. But would a pilot really want step responses in rate? The answer, we believe, is no; a pilot might want an apparent step for a short period of time, before requiring a step in the opposite direction resulting in a doublet demand. In which case it does not matter what the d.c. gain is like, provided the short term response is acceptable. Exactly what the pilot requires is a very difficult problem, and falls into the problem of converting 'Handling Qualities Criteria' into time or frequency domain specifications [YUE1].

The solution adopted in this thesis is to design an 'attitude command' control system, which does not suffer from the problems of zeros at the origin, while still limiting the amplitude and coupling of the rate responses. Thus, rather than a pilot demanding a roll rate for a short period of time in order to obtain a new bank angle, the pilot demands the bank angle, and the control system generates an appropriate rate profile. An attitude command system is not an unheard of proposal and is mentioned in [PAU1] and [LEW1]. It is accepted that such a control system appears to be less valid at high bank angles, when pitch attitude demand requires yaw rate, etc., due to the definitions of the Euler angles. Controlling the integral of p and the integral of q might be a better alternative.

It is noted here that it may be that the integrator control approach is required, and the stability problem carefully allowed for in implementation. In which case procedures such as 'jω-axis shifting' may be employed to move the offending zeros before the design is undertaken, this will be left as a topic for future research.

4.7 Mathematical modelling

4.7-3 Equations of motion

First a derivation of the equations of motion of a rigid body in space, about body fixed axes.

Applying Newton's second law for linear and rotational motion yields equations (4.11) to (4.16).

$$\underline{F} = m \frac{d}{dt}(\underline{v}) \quad , \quad \underline{H} = \frac{d}{dt}(\left[I \right] \underline{\omega})$$

$$\text{where } \underline{v} = \begin{bmatrix} u \\ v \\ w \end{bmatrix}, \quad [I] = \begin{bmatrix} Ixx & -Ixy & -Ixz \\ -Iyx & Iyy & -Iyz \\ -Izx & -Izy & Izz \end{bmatrix}, \quad \underline{\omega} = \begin{bmatrix} p \\ q \\ r \end{bmatrix} \qquad (4.10)$$

Linearly,

$$\frac{1}{m}\begin{bmatrix} X \\ Y \\ Z \end{bmatrix} = \begin{bmatrix} \dot{u} \\ \dot{v} \\ \dot{w} \end{bmatrix} + \begin{bmatrix} p \\ q \\ r \end{bmatrix} \times \begin{bmatrix} u \\ v \\ w \end{bmatrix} = \begin{bmatrix} \dot{u}+qw-vr \\ \dot{v}+ru-pw \\ \dot{w}+pv-qu \end{bmatrix} \qquad \begin{matrix} (4.11) \\ (4.12) \\ (4.13) \end{matrix}$$

$(X\ Y\ Z)^T$ is the vector of forces acting on the helicopter in body axes

Rotationally,

$$\begin{bmatrix} L \\ M \\ N \end{bmatrix} = [I]\begin{bmatrix} \dot{p} \\ \dot{q} \\ \dot{r} \end{bmatrix} + \begin{bmatrix} p \\ q \\ r \end{bmatrix} \times [I]\begin{bmatrix} p \\ q \\ r \end{bmatrix} \qquad \begin{matrix} (4.14) \\ (4.15) \\ (4.16) \end{matrix}$$

$(L\ M\ N)^T$ is the vector of moments acting on the helicopter in body axes

We also have the kinematic relationships between $\dot{\phi}$, $\dot{\theta}$, $\dot{\psi}$ and p, q, r.

$$\begin{bmatrix} \dot{\phi} \\ \dot{\theta} \\ \dot{\psi} \end{bmatrix} = \begin{bmatrix} 1 & \sin\phi\tan\theta & \cos\phi\tan\theta \\ 0 & \cos\phi & -\sin\phi \\ 0 & \sin\phi\sec\theta & \cos\phi\sec\theta \end{bmatrix}\begin{bmatrix} p \\ q \\ r \end{bmatrix} \qquad \begin{matrix} (4.17) \\ (4.18) \\ (4.19) \end{matrix}$$

(The inverse relationship is also useful

$$\begin{bmatrix} p \\ q \\ r \end{bmatrix} = \begin{bmatrix} 1 & 0 & -\sin\theta \\ 0 & \cos\phi & \sin\phi\cos\theta \\ 0 & -\sin\phi & \cos\phi\cos\theta \end{bmatrix}\begin{bmatrix} \dot{\phi} \\ \dot{\theta} \\ \dot{\psi} \end{bmatrix} \quad)$$

To complete the set we also have three equations which fix the position of the body in space. (North, East, Down)

$$\frac{d}{dt}\begin{bmatrix} \text{North} \\ \text{East} \\ \text{Down} \end{bmatrix} = [T]\begin{bmatrix} u \\ v \\ w \end{bmatrix} \qquad \begin{matrix} (4.20) \\ (4.21) \\ (4.22) \end{matrix}$$

where $[T]$ is the matrix rotating the body axes into the earth axes, as defined by equation (4.2).

The forces and moments in the above equations are equal to the sum of the following components.

(i) Gravitational

$$\begin{bmatrix} X \\ Y \\ Z \\ L \\ M \\ N \end{bmatrix} = mg \begin{bmatrix} -\sin\theta \\ \cos\theta\sin\phi \\ \cos\theta\cos\phi \\ 0 \\ 0 \\ 0 \end{bmatrix} \qquad (4.23)$$

(ii) Rotor Components

The rotor produces forces and moments about all axes, complex functions of control inputs, speeds, angular rates, attitudes, etc.

(iii) Fuselage components

Forces and moments generated by lift and drag are usually modelled with polynomial functions of speed, and angles of attack and sideslip.

(iv) Tailplane components

Usually assumed to produce a force in the z-direction and a moment in the y-direction. The coefficients are modelled as polynomial functions of the angles of attack and sideslip of the tailplane.

(v) Fin components

(vi) Tail rotor components

These produce forces in the y-direction and moments about x and z axes.

(vii) Other components

These include contributions from additional wings (used to offload the main rotor in forward flight) or devices to produce horizontal thrust for greater speed, etc.

The 12 equations (4.11) to (4.22) above, together with the force and moment calculations are sufficient to determine the position and velocity of the helicopter as a function of time.

Before linearizing, we note that the states ψ, North, East, Down are functions only of the other states. Their inclusion then, only produces extra poles at the origin, and will not effect the modes of the overall system.

Making the usual simplifying assumptions that Ixy=Izy=0 (the helicopter would be symmetrical looking from the front or above if the tail rotor is ignored!), we obtain the state-space description of the helicopter for small perturbations about an operating point of steady turning flight, in the form:

$$\dot{\underline{x}} = A\underline{x} + B\underline{u} \ , \tag{4.24}$$

where

$$\underline{x} = (\ \delta u, \ \delta w, \ \delta q, \ \delta\theta, \ \delta v, \ \delta p, \ \delta\phi, \ \delta r \ )^T \tag{4.25}$$

and

$$\underline{u} = (\ \delta\theta_{o_e}, \ \delta\theta_{1_s}, \ \delta\theta_{1_c}, \ \delta\theta_{tre} \ )^T \tag{4.26}$$

The elements of the state matrices, as in [CHE1], are given overleaf.

The A-matrix is given by:

$$\begin{array}{cccccccc}
x_u & x_w-q_o & x_w-w_o & -g\cos\theta_o & x_v+r_o & x_p & 0 & x_r+v_o \\
z_u+q_o & z_w & z_q+u_o & -g\cos\theta_o\sin\theta_o & z_v-v_o & z_p-v_o & -g\sin\phi_o\cos\theta_o & z_r \\
m_u & m_w & m_q & 0 & m_v & \begin{matrix} m_p-2p_o\frac{Ixz}{Iy} \\ -r_o\frac{(Ix-Iz)}{Iy} \end{matrix} & 0 & \begin{matrix} m_r+2r_o\frac{Ixz}{Iy} \\ -p_o\frac{(Ix-Iz)}{Iy} \end{matrix} \\
0 & 0 & \cos\theta_o & 0 & 0 & 0 & \dot{\psi}\cos\theta_o & -\sin\phi \\
y_u-r_o & y_w+p_o & y_q & -g\sin\phi_o\sin\theta_o & y_v & y_p+w_o & g\sin\phi_o\sin\theta_o & y_r-u_o \\
l'_u & l'_w & l'_q+t_1p_o+t_2r_o & 0 & l'_v & l'_p+t_1q_o & 0 & l'_r-t_2q_o \\
0 & 0 & \sin\theta_o\tan\theta_o & \psi_o\sec\theta_o & 0 & 1 & 0 & \cos\phi_o\tan\theta_o \\
n'_u & n'_w & n'_q-t_3p_o-t_1r_o & 0 & n'_v & n'_p-t_3q_o & 0 & n'_r-t_1q_o
\end{array}$$

The B-matrix is given by:

$$\begin{array}{ccccc}
x_{\theta_{o_e}} & .. & .. & .. \\
z_{\theta_{o_e}} & .. & .. & .. \\
m_{\theta_{o_e}} & .. & .. & .. \\
0 & 0 & 0 & 0 \\
y_{\theta_{o_e}} & .. & .. & .. \\
l'_{\theta_{o_e}} & .. & .. & .. \\
0 & 0 & 0 & 0 \\
n'_{\theta_{o_e}} & .. & .. & ..
\end{array}$$

where

$$x_i = \frac{X_i}{m};\ y_i = \frac{Y_i}{m};\ z_i = \frac{Z_i}{m};\ m_i = \frac{M_i}{Iy}$$

$$l'_i = \frac{Iz}{IxIz-I^2xz}L_i + \frac{Ixz}{IxIz-I^2xz}N_i\ ,\ n'_i = \frac{Ixz}{IxIz-I^2xz}L_i + \frac{Ix}{IxIz-I^2xz}N_i$$

$$t_1 = \frac{Ixz(Iz+Ix-Iy)}{IxIz-I^2xz}\ ;\ t_2 = \frac{Iz(Iz-Iy)+I^2xz}{IxIz-I^2xz}\ ;\ t_3 = \frac{Ix(Iy-Ix)+I^2xz}{IxIz-I^2xz}\ ;$$

and $X_i = \frac{\partial X}{\partial i}$, computed for i=u, v, w, p, q, r, θ_{o_e}, θ_{1_s}, θ_{1_c}, θ_{tre} (4.27)

4.7-2 Rotor degrees of freedom

The eight state description of the helicopter given above assumes a quasi-steady model of the rotor which is non-dynamical and does not increase the state dimension. This is of course only an approximation, and a more detailed model includes the blade flapping angles, and their derivatives, as states. These extra main rotor variables when included, are:

BTA0	Coning angle.
B1CW	fore/aft disc tilt, wind axes.
B1SW	lateral disc tilt.
BTA0DT	rate of change of BTA0
B1CWDT	rate of change of B1CW
B1SWDT	rate of change of B1SW

4.7-3 Computer simulation

Two major pieces of software were provided by the RAE, Bedford, containing a non-linear helicopter model. The first, HELISTAB, [SMI2], is primarily a tool for studying the dynamics of the open-loop helicopter. It has the facility to trim the model about a set of given operating points, defined by the flight-path variables, and to generate a variety of plots showing variations of any components of the linearized model. It should be noted that because the model is of the form

$$\dot{x} = f(x, \dot{x}, u) \tag{4.28}$$

the solution has to be iterative. Recent software developments have greatly improved the selection of initial values and iteration control variables, and convergence to the solution is readily obtained.

The second software package, HELISIM, uses essentially the same non-linear model of the helicopter as that used in HELISTAB, but has been written to be used in conjunction with the TSIM [WIN1], [CAM1], nonlinear simulation facility. This is the package used for the nonlinear closed-loop simulations in Chapter VI. All the initial design work was performed on a version without the rotor dynamics, and it was very satisfying that the addition of the rotor dynamics had very little effect on the closed-loop responses.

Additional software was written at Oxford to interface these packages and the control package CLADP [EDM2], and the Oxford H^{∞}-design package. The control system for the non-linear helicopter was written within the TSIM/HELISIM package and could accept a state-space controller, of arbitrary state dimension, directly from the H^{∞}-design package.

4.7-4 Helicopter modes

The natural modes of fixed-wing aircraft are well known, and are described first. These can be obtained from the eigenvector decomposition of the system A-matrix. The natural modes of the helicopter are often given the same names but as can be observed by numerical experimentation, the distinction between modes is not as clear as in fixed-wing aircraft. This is due to the large amounts of cross-coupling, and is especially noticeable at high bank angle.

(i) Longitudinal (u, w, q, θ)

a) Short period oscillation:

Consider the response of a stable aircraft to a sudden up-gust (symmetrical to both wings). The angle of incidence will soon return to its original value. There is a small change in forward speed, but this is usually small compared with the changes in incidence and pitch. Analysis

shows that this response is oscillatory with a period that is approximately inversely proportional to the forward speed of the aircraft.

b) Phugoid (long period) oscillation:

With the same disturbance as before, a much slower oscillation may result. This motion consists principally of slow sinusoidal motion, in which the height and forward speed of the aircraft vary, while the angle of incidence remains practically unchanged. Analysis shows that the period increases with forward speed and is usually lightly damped.

(ii) Lateral (v, p, ϕ, r)

a) Roll damping (subsidence):

This is the response of the aircraft to a roll-rate disturbance (or control input). It is characterized by a large negative real root. Usually, a good estimate of its value is obtained from its single degree-of-freedom value L_p (the coefficient relating $\dot{p}$ to p in the A-matrix of the state-space description) i.e.

$$\frac{dp}{dt} = L_p + L_{\theta 12}\theta_{1c} \qquad (L_p \text{ is negative}) \qquad (4.29)$$

b) Spiral mode:

This is the tendency of the airplane to recover slowly or diverge slowly from a bank angle disturbance (if unstable this leads to an ever steepening 'spiral dive'). This is characterized by a small modulus real root. A common method of stabilizing this mode is the use of wing dihedral, the asymmetric lift from a disturbance then tends to right the aircraft. It can be shown that the stability depends on the inequality

$$l_v n_r - l_r n_v > 0. \qquad (4.30)$$

c) Dutch Roll

This is a complex motion of coupled banking, sideslipping and yawing motion, noticeably oscillatory. The motion can be described as being on the surface of a cylinder.

4.7-5 Numerical results

This section provides some examples of the information that can be obtained by using the HELISTAB package. The package was configured to model a Lynx helicopter in 80 knots level turning flight. A set of 11 bank angles from -70 to +70 degrees was used to evaluate the effect of turning flight on the linearized model. HELISTAB has the ability to plot the variation of any parameter in the linear model against turn rate; Figure 4.3 is a locus of the open-loop poles of the linear model without rotor dynamics. The roll damping pole at ≈ -10 is not shown on this figure. As expected the linear model changes rapidly at large turn rates (the min and max points are labelled with an x or o). This is partly due to the fact that at high bank angle the rotor thrust increases rapidly and because the gravitational force vector rotates into the lateral plane. Figure 4.4 is a similar locus for the model with rotor dynamics, only the slowest rotor mode is included. When plotted on the same scale as Figure 4.3 the loci are indistinguishable. This shows that the version without rotor dynamics is a good low order approximation of the version with.

The pole positions for the nominal straight and level models are given after Figure 4.4

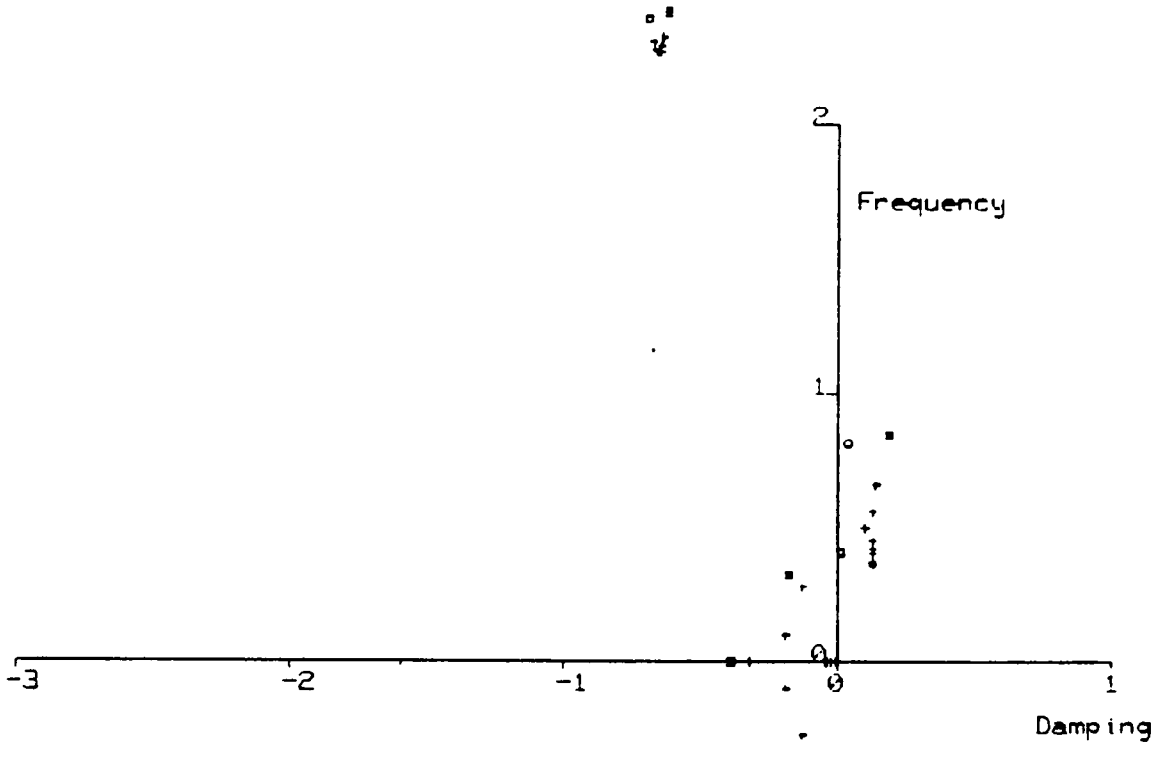


Figure 4.3 Pole locus for helicopter without rotor dynamics

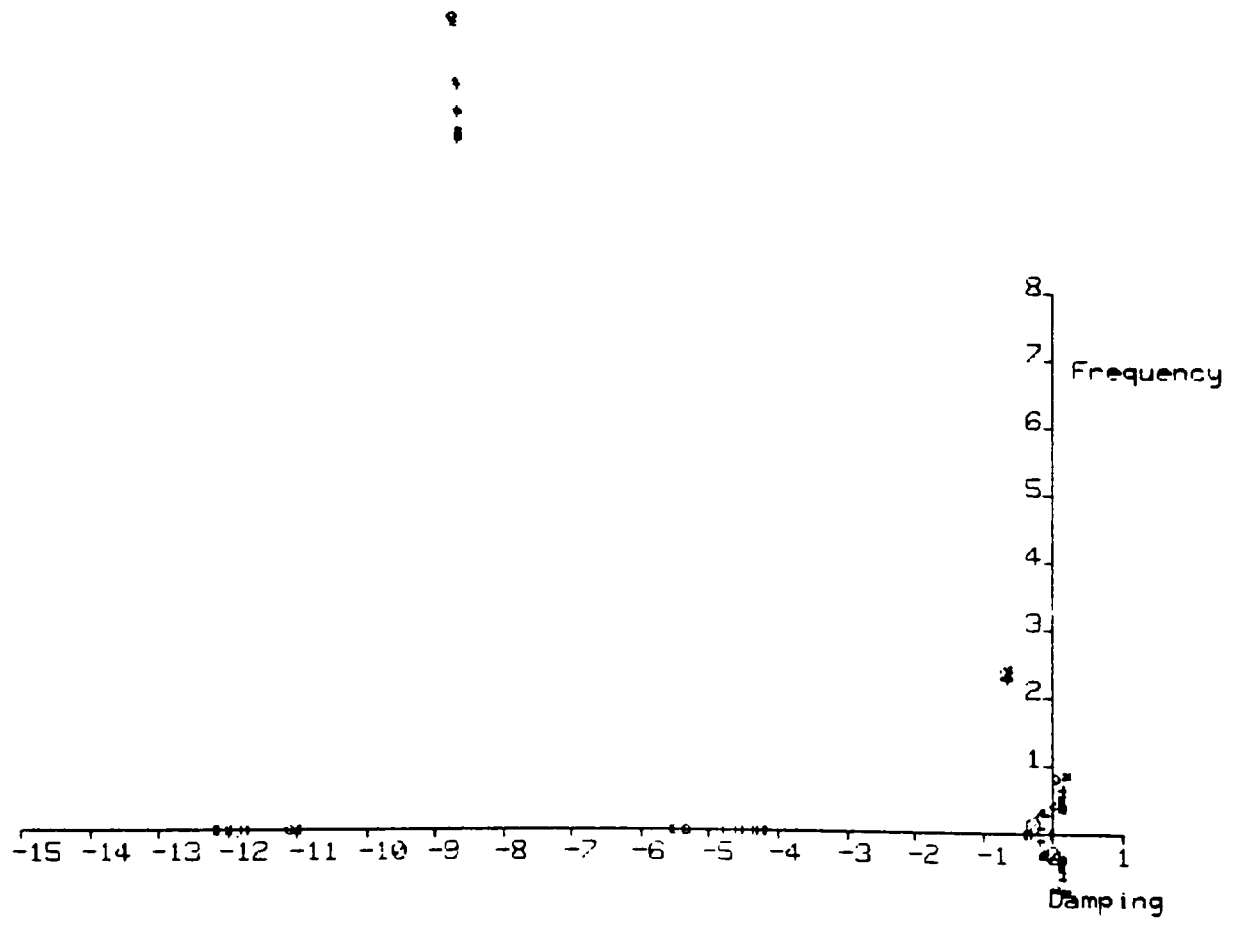


Figure 4.4 Pole locus for helicopter with rotor dynamics

Open loop POLE positions

No	(including rotor dynamics) Real and Imaginary		(without rotor dynamics) Real and Imaginary	
1	-15.5	69.6		
2	-15.5	-69.6		
3	-15.9	35.4		
4	-15.9	-35.4		
5	-8.71	10.2		
6	-8.71	-10.2		
7	-12.2		-10.5	
8	-4.19		-3.20	
9	-0.651	2.26	-0.654	2.26
10	-0.651	-2.26	-0.654	-2.26
11	0.134	0.372	0.134	0.376
12	0.134	-0.372	0.134	-0.376
13	-0.401		-0.406	
14	-0.0305		-0.0305	

Multivariable systems with more outputs than inputs generically have no multivariable zeros. The system transmission zeros for the models with output C-matrices chosen for the flight path and rate control schemes are given below.

Open loop finite transmission ZERO positions

a) Flight path controller

No	(including rotor dynamics) Real and Imaginary		(without rotor dynamics) Real and Imaginary	
1	-107.		-107.42	
2	-16.0	35.5		
3	-16.0	-35.5		
4	-0.24	5.41	-0.24	5.42
5	-0.24	-5.41	-0.24	-5.42

b) Rate command controller

1	-108.		-108.	
2	-16.0	35.5		
3	-16.0	-35.5		
4	-0.024		-0.024	
5	0.004		0.004	
6	0.000		0.000	

Note that with these outputs it appears that the rotor mode at $(-16, \pm 36)$ is not observable.

4.8 Concluding remarks

This chapter has introduced the physical system to be used as an example of a difficult multivariable system in the design sections of this thesis. Since the helicopter has been shown to be a complex, non-linear multivariable plant, care must be taken when attempting to design a control system on the basis of the linear model alone. The design model should be accompanied by a complete set of design objectives and constraints. Similarly any design technique must be flexible enough to accept the design data in whatever form is sensible in the physical system. Unfortunately, as illustrated in this chapter, the desired objectives are usually fairly incomplete and the physical constraints difficult to translate into bounds on the linear model. It is a subject of current research to determine precisely how these specifications should be presented.

CHAPTER V

H^{∞}-OPTIMIZATION

5.1 Introduction

This chapter presents an overview of the synthesis procedure used to design H^{∞}-optimal feedback controllers. Such controllers minimize the maximum singular value over all frequency of a given stable transfer function matrix, a quantity known as the H^{∞}-norm. The transfer function matrix being minimized is usually a function of the closed-loop system formed by the interconnection of the plant and the controller, augmented with suitable weighting functions. The engineering importance of the use of the infinity norm is that the optimization minimizes the 'worst-case' over all frequency. Optimization methods based on a quadratic integral criterion minimize a root-mean-square (R.M.S.) value and cannot therefore exclude local peaks at all frequencies. This observation suggests that such a design may be arbitrarily sensitive to both signal and model uncertainty at these frequencies - a major motivation for developing H^{∞}-norm based design methods [ZAM2]. Robustness recovery techniques for improving the robustness of linear quadratic Gaussian optimal controllers will be considered in Chapter VII. Although computationally much easier to implement than the H^{∞}-design procedure, these techniques only indirectly shape the closed-loop frequency responses and proved difficult to use.

Originating from the seminal work of Zames [ZAM2] in 1981, H^∞-optimization has attracted considerable interest from researchers in control theory. Notable contributions in this field were made by Francis, Helton and Zames [FRA1], [FRA2]. Major steps towards an implementable solution process were made by Nett et al [NET1] who gave a state-space technique for performing coprime factorization. Safonov and Verma [SAF5] demonstrated the link between H^∞-optimization and the Hankel-norm approximation problem, solved in state-space form by Glover [GL01].

The 'standard problem' approach, introduced by Doyle in 1984 [DOY7], [CHU1] will form the basis of this chapter. This approach enables a solution of very general H^∞-optimization problems using only standard matrix and linear algebra procedures. There are still, however, a number of numerical problems that arise when this procedure is implemented; these are considered further in this chapter. A new algorithm to obtain minimal realizations was developed to overcome some of these difficulties and is described in Chapter VIII.

The organization of this chapter is as follows. Section 5.2 will describe the standard problem and section 5.3, its theoretical solution. Section 5.4 reviews the state-space solution, and section 5.5 presents a specific H^∞-optimization problem and a simple example to illustrate the choice of weighting functions used in the helicopter example in Chapter VI. A review of Glover's optimal anti-causal approximation procedure [GL01] and further properties of the solutions are given in Appendix 5.1. Appendix 5.2 considers the computation of bounds and sensitivity to the stopping criterion of the γ-iteration.

5.2 The standard problem

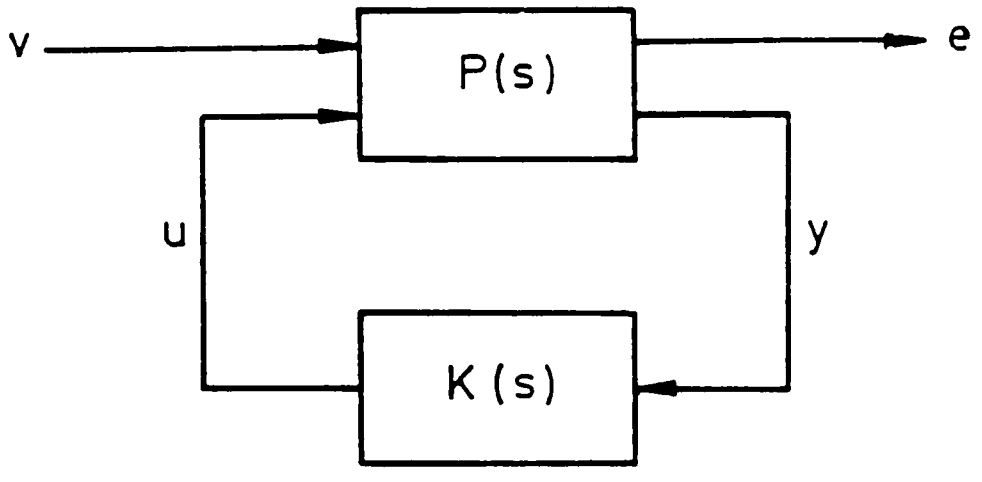


Figure 5.1 The standard problem

Figure 5.1 presents the general framework for linear time-invariant filtering and control problems introduced by Doyle [DOY7]. The advantage of considering this system is that most problems, including two-degree-of-freedom control problems, can be recast into this form. For any specific problem, however, more insight may be gained by a direct approach, as used in [GLO2] and [KWA2].

The objective is to design a controller K(s), such that the closed-loop system formed by P(s) and K(s) is internally stable, and the H^{∞}-norm of the transfer function T(s) between the inputs v and errors e is minimized.

That is,

$$\min_{\text{stabilizing } K} \; || \, T(s) \, ||_{\infty} \qquad (5.1)$$

Assume P(s) is appropriately partitioned as $P_{ij}(s)$:

$$P(s) = \begin{bmatrix} P_{11} & P_{12} \\ P_{21} & P_{22} \end{bmatrix} \qquad (5.2)$$

Then, $$T(s) = P_{11} + P_{12}K(I - P_{22}K)^{-1}P_{21} \qquad (5.3)$$

which is called a linear fractional transformation of P and K, and denoted LFT (P,K).

Depending on the number of signals in the vectors v,e,u,y, the problem may be subdivided into three classes, as described below. Their names derive from the nature of the 'model-matching problem', see section 5.3-4. It is instructive to examine why these classes of problem should arise. In order of increasing complexity they are:

(i) 1-Block problems

These arise when the number of external inputs n_v is equal to the number of measurements n_y used by the controller, and when the number of penalized variables n_e is equal to the number of control inputs to the plant n_u. That is

$$n_v = n_y \text{ and } n_e = n_u \qquad (5.4)$$

(Note that we do not require $n_y = n_u$.)

Examples of problems that fall into this category are the sensitivity minimization problem [ZAM3]

$$\min_{\text{stabilizing } K} \; ||W_1 S\, W_2||_\infty \qquad (5.5)$$

and the robust stabilization problem [GL02]

$$\min_{\text{stabilizing } K} \; ||W_1 KS\, W_2||_\infty \qquad (5.6)$$

(ii) 2-Block problems

These arise when <u>either</u> the number of external inputs is greater than the number of measured signals <u>or</u> the number of penalized variables is greater than the number of control inputs to the plant. That is

$$\begin{aligned} & n_v > n_y \text{ and } n_e = n_u \\ \text{or} \quad & n_v = n_y \text{ and } n_e > n_y \end{aligned} \tag{5.7}$$

Examples of 2-Block problems are those with a combination of sensitivity and complementary sensitivity functions [KWA2], [F003],

$$\text{i.e.,} \quad \min_{\text{stabilizing } K} \left\| \begin{matrix} W_1 S\, W_i \\ W_2 T\, W_i \end{matrix} \right\|_\infty \tag{5.8}$$

or a combination of sensitivity and robust stabilization (see section 5.5).

(iii) 4-Block problems

These occur when <u>both</u> the number of external inputs is greater than the number of measured signals <u>and</u> the number of penalized variables is greater than the number of control inputs to the plant,

$$\text{i.e.,} \quad n_v > n_y \text{ and } n_e > n_u \tag{5.9}$$

It may be argued that all realistic control problems fall into this category, since the numbers of plant inputs and measurements (+ reference inputs) are usually fixed, and less than the corresponding numbers of external inputs (references + noise + disturbances, etc) and penalized variables (errors, actuator amplitudes and rates, etc).

The problems arising from other combinations of inputs and outputs cannot yet be solved efficiently. In any case, we could add extra specifications to properly define the solution. It should be noted that these rules only apply when the elements of the signal vectors are not linearly dependent, otherwise the problem may revert to one that is easier to solve, i.e., from 4-Block to 2-Block.

5.3 Theoretical solution

5.3-1 Primary constraints

The system given in section 5.2 is said to be well posed if the closed-loop transfer function T(s), equation (5.3), exists and is proper. A system is proper when its magnitude is finite at $s = \infty$, and strictly proper when it is zero at $s = \infty$. A necessary and sufficient condition for the system in Figure 5.1 to be well posed, is

$$I - P_{22}(\infty)\, K(\infty) \text{ is invertible.} \qquad (5.10)$$

A system is said to be stabilizable and detectable if all of its unstable modes are both controllable and observable. This is clearly a necessary requirement for the existence of a stabilizing controller.

The basic assumptions, then, are that the system is well posed and that all the unstable modes of P(s) are contained in $P_{22}(s)$, which is stabilizable and detectable.

A further requirement for the existence of a solution to the problem is that $P_{12}(s)$ and $P_{21}(s)$ do not lose rank on the imaginary axis. For the existence of a proper controller, as required in the state-space solution, this must be extended to infinity, and we require $P_{12}(s)$ and $P_{21}(s)$ to have state-space realizations with full row and/or column rank D-matrices.

5.3-2 Internal stability

It is obviously a requirement that the closed-loop system contain no 'hidden' unstable modes; then all of the possible closed-loop transfer functions will be stable. This is of paramount importance in H^{∞}-design, since a purely numerical optimization approach may be tempted to permit solutions with right half plane cancellations of poles and zeros between the controller K and P_{22}. In the state-space approach a necessary and sufficient condition for internal stability of the closed-loop system is that the A-matrix of the interconnection of P and K has all of its eigenvalues with negative real parts. It is important to realize that this does not guarantee that the controller itself is stable. It is well known that some unstable plants can only be stabilized by an unstable controller (the interlacing property [YOU3]). Therefore, restricting the set of controllers to those that are stable, reduces the size of the set of achievable closed-loop transfer functions. The arguments against using unstable controllers are basically ones of integrity; what happens if a sensor fails, etc? Unstable controllers require careful 'jacketing' software on implementation. (Integral limiting / desaturation is a common example.) Fortunately, it appears that sensibly weighted problems do not result in unstable controllers when these are not needed. Further research would be necessary if this proved to be a problem.

5.3-3 Parameterization of all stabilizing controllers

The first major step in the solution is the characterization of all possible stabilizing controllers, usually referred to as 'Youla's parameterization' [YOU1], [DES2]. In addition to solving the problem of internal stability, it translates the design problem from one that is non-linear in K(s), to one that is essentially linear (affine) in a stable parameter Q(s).

First it is required to obtain left and right coprime factorizations of the system, in terms of the stable functions N, M, $\tilde{N}$, $\tilde{M}$, which also satisfy a Bezout identity with X, Y, $\tilde{X}$, $\tilde{Y}$.

That is, $$P_{22}(s) = NM^{-1} = \tilde{M}^{-1}\tilde{N}$$

and $$\begin{bmatrix} \tilde{X} & -\tilde{Y} \\ -\tilde{N} & \tilde{M} \end{bmatrix} \begin{bmatrix} M & Y \\ N & X \end{bmatrix} = \begin{bmatrix} I & 0 \\ 0 & I \end{bmatrix} \qquad (5.11)$$

Then all stabilizing controllers are given by

$$K = (Y - MQ)(X - NQ)^{-1}$$

or $$(\tilde{X} - Q\tilde{N})^{-1}(\tilde{Y} - Q\tilde{M}) \qquad (5.12)$$

Substitution of (5.12) into (5.3) results in the following parameterization of all internally stable closed-loop transfer functions T(s).

$$T(s) = T_{11} + T_{12} Q T_{21} \text{ where } Q \varepsilon RH^{\infty},$$
$$I + P_{22}(\infty)Q(\infty) \text{ invertible.} \qquad (5.13)$$

5.3-4 Model-matching problem

The factorizations in (5.11) and (5.12) are not unique, and it so happens that it is possible to construct T_{12} and T_{21} that are inner and co-inner respectively [DOY7], [CHU1].

That is,

$$T_{12}^{*} T_{12} = I \text{ and } T_{21}T_{21}^{*} = I \qquad (5.14)$$

For the 2- and 4-Block cases it is necessary to introduce complementary inner factors T' and $\tilde{T}'$, such that $\begin{bmatrix} T_{12} & T' \end{bmatrix}$ and $\begin{bmatrix} T_{21} \\ \tilde{T}' \end{bmatrix}$ are both square and inner.

In this case the optimization problem can be translated from

$$\min_{Q \in RH^{\infty}} \left\| T_{11} + \begin{bmatrix} T_{12} & T' \end{bmatrix} \begin{bmatrix} Q & 0 \\ 0 & 0 \end{bmatrix} \begin{bmatrix} T_{21} \\ \tilde{T}' \end{bmatrix} \right\|_{\infty} \tag{5.15}$$

to

$$\min_{Q \in RH^{\infty}} \left\| \begin{matrix} R_{11} - Q & R_{12} \\ R_{21} & R_{22} \end{matrix} \right\|_{\infty} \tag{5.16}$$

where $R_{11} = T_{12}{}^{*} T_{11} T_{21}{}^{*}$, etc.

This is possible because the infinity norm is invariant under multiplication by unitary functions. Equation (5.16) is a model-matching problem, in the sense that it is required to find a stable function Q that is the best approximation to R (which can be made to be completely unstable by construction).

It has been verified that a real rational solution to this problem exists when R is itself real rational [CHU1].

The 1-Block problem, when R_{12}, R_{21}, R_{22} are zero, is also known as the Hankel approximation problem, for which all solutions may be characterized [GLO1].

The solution to the 2- and 4-Block problems cannot be computed directly, but via an iterative scheme, known as the 'γ-iteration', its solution can be reached by employing a sequence of Hankel approximations [DOY7], [CHU1]. The procedure for the 2-Block case is given in the next sub-section.

Some properties of the Hankel approximation are now given below with more detail in Appendix 5.1.

Fact:

$$\inf_{Q \in RH^{\infty}} \| R_{11} - Q \|_{\infty} = \| R_{11} \|_{H} = \sigma_h \qquad (5.17)$$

where σ_h is the largest Hankel singular value of $R_{11}(-s)$, which is stable. For problems with $n_y = n_u = 1$ (Q will have the same dimension as the controller K), then the optimal solution Q is unique = Qopt, and the error function $E(s) \triangleq R_{11} - Qopt$ is all-pass form,

$$\text{i.e.,} \qquad n_y = n_u = 1 \qquad E^{*}E = \sigma_h^{2} \qquad (5.18)$$

For multivariable problems the bound in (5.17) can be achieved by a continuum of Q(s). As shown in Appendix 5.1, using Glover's algorithm [GL01] a class of solutions may be constructed with

$$\bar{\sigma} [E(s)] = \sigma_h \text{ for all } s=j\omega \qquad (5.19)$$

It is not clear that this class contains all possible solutions, but the following conjecture seems plausible.

Conjecture:

All optimal Q = Qopt that achieve the bound in (5.17) have the following property:

$$\bar{\sigma} \left[E(s=j\omega) \right] = \sigma_h \qquad (5.20)$$

That is, the maximum value of the error is constant over all frequency. It is possible that this may be formally proven using abstract operator theory, e.g. [HEL2], but a constructive proof is not currently available.+

+A proof for scalar systems that may be generalized to multivariable systems is given in [FRA4].

5.3-5 2-Block γ-iteration

Although there exists elegant mathematical theory to verify the existence of a solution to the problem

$$\gamma_o = \min_{Q \varepsilon RH_\infty} \left\| \begin{matrix} R_1 - Q \\ R_2 \end{matrix} \right\|_\infty \tag{5.21}$$

there does not exist a practicable way to directly compute the value of the optimal $\gamma = \gamma_o$, since this would involve finding the largest eigenvalue of an infinite dimensional full rank matrix. (A finite polynomial algorithm is proposed in [JON1], but this is not practically useful).

An iterative scheme is available based on the fact that if

$\gamma > \gamma_o > \| R_2 \|_\infty$, then for all Q, s=j$\omega$

$$\det \left| \gamma^2 - (R_1 - Q)^* (R_1 - Q) - R_2^* R_2 \right| > 0 \tag{5.22}$$

Thus, if we define $M^*M = \gamma^2 - R_2^* R_2$ (5.23)

$$\det \left| M^*M - (R_1 - Q)^* (R_1 - Q) \right| > 0 \tag{5.24}$$

$$\Leftrightarrow \quad \| (R_1 - Q) M^{-1} \|_\infty < 1 \tag{5.25}$$

$$+ \Leftrightarrow \quad f(\gamma) \stackrel{\Delta}{=} \| [R_1 M^{-1}]^+ \|_H < 1 \tag{5.26}$$

Similarly, if $\|R_2\|_\infty < \gamma < \gamma_o$

$$f(\gamma) > 1 \tag{5.27}$$

+The argument in the reverse direction should be read as 'If (5.26), then there exists Q such that (5.25)'.

We can therefore iterate on γ to get as close as required to γ_o, when $f(\gamma_o) = 1$. The special case $\gamma_o = ||R_2||_\infty$ results in $f(\gamma_o) < 1$, and the spectral factorization in (5.23) has zeros on the imaginary axis. In this case the γ-iteration can fail, continuing with a $\gamma=\gamma_o+\delta$, where δ is small, is a possible solution. For more information on the selection of bounds and the sensitivity of the 2-Block solution to the iteration, refer to Appendix 5.2.

When the optimal γ has been selected, $\tilde{Q}$ can be found from the Hankel approximation of the unstable part of R_1M^{-1},

$$\text{i.e., } \tilde{Q}: \qquad ||[R_1M^{-1}]^+ - \tilde{Q}||_\infty = 1 \tag{5.28}$$

and the solution Q to (5.21) is obtained as

$$Q = (\tilde{Q} + [R_1M^{-1}]^-)M \tag{5.29}$$

5.3-6 Recovery of controller

The optimal controller is simply obtained by substituting for Q in equation (5.13). There are two features which the optimal controller should possess, and this provides a check on the optimality of the controller. The first is that the controller is stabilizing. The second is that the maximum singular value of the cost function is equal to the infinity norm of the error in the model-matching problem (optimal γ in the case of the γ-iteration). For multivariable problems the number of singular values of the cost function that are flat and equal to the infinity norm, is given by the technique used to perform the Hankel approximation.

5.4 State-space solution

5.4-1 The standard problem

The first step in the solution process is to transform the particular problem to the standard form as in Figure 5.1. Then P(s) can be expressed in state-space form as

$$\left[\begin{array}{c|cc} A & B_1 & B_2 \\ \hline C_1 & D_{11} & D_{12} \\ C_2 & D_{21} & D_{22} \end{array}\right] \qquad (5.30)$$

Provided that (A, B_2, C_2) is stabilizable and detectable, and D_{12} and D_{21} are full rank, then the solution process can continue. It should be obvious that it is desirable for this state-space description to be minimal, and this can usually be guaranteed, by careful construction, when the original plant description is minimal. If the original plant is unstable it is easy to generate a state-space description that is unnecessarily unstabilizable and/or undetectable.

5.4-2 Parameterization of all stabilizing controllers

That the coprime factorizations in equations (5.11) to (5.13) could be performed in state-space, was first discovered by Nett et al [NET1]. It could then be seen that the parameterization of all stabilizing controllers could be performed by <u>any</u> stabilizing state observer/state feedback controller augmented with stable dynamics.

If $\left[\begin{array}{c|c} A & B_2 \\ \hline C_2 & 0 \end{array}\right]$ is a state-space realization

of $G_{22}(s)$, and F and H are feedback and observer gains, such that $A + HC_2$ and $A + B_2F$ are both stable, then Figure 5.2 represents this parameterization of all stabilizing controllers.

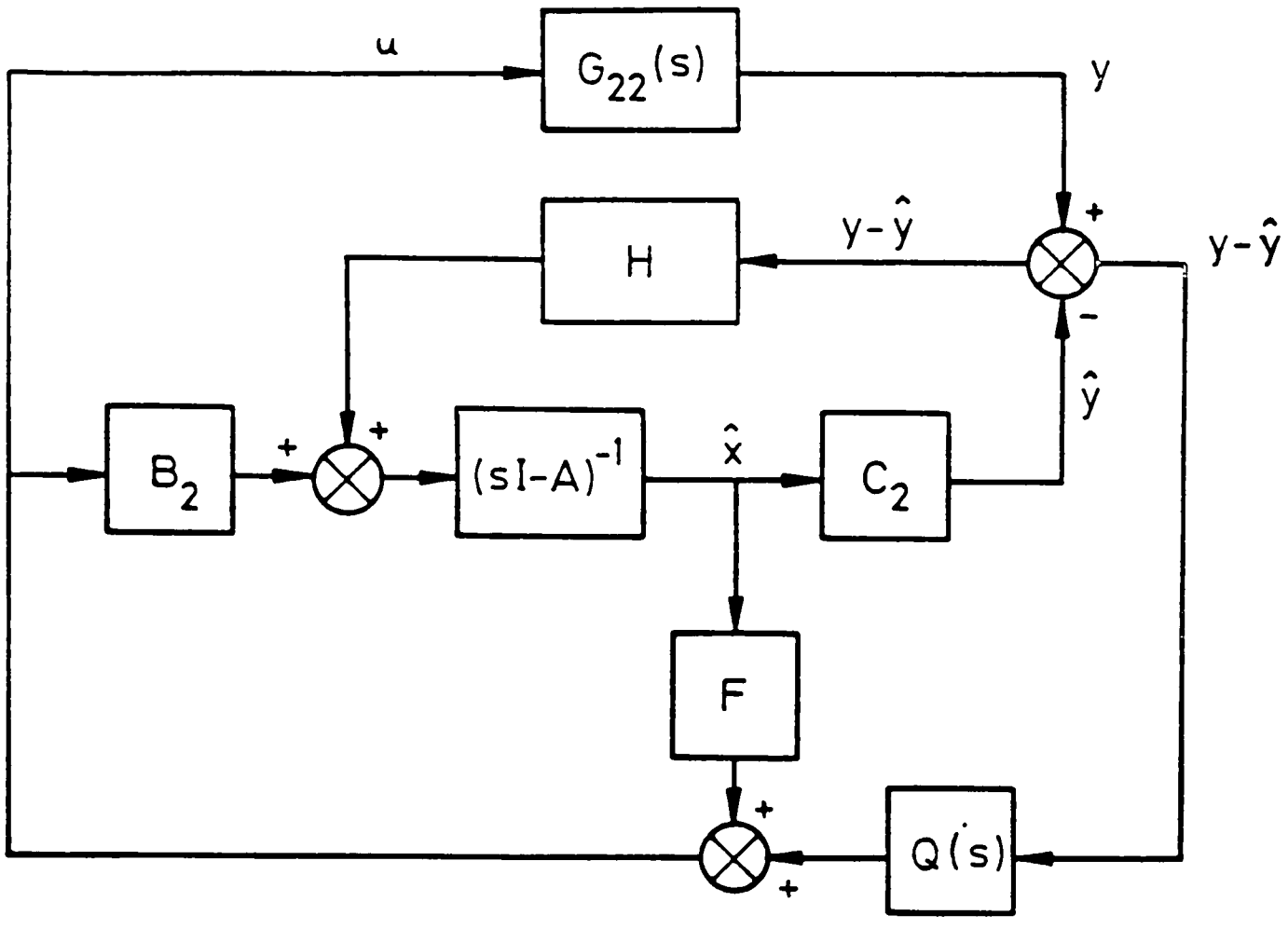


Figure 5.2 Parameterization of all stabilizing controllers

Furthermore, this parameterization is easily expressed as an LFT(J,Q), where J is given by

$$J = \left[\begin{array}{c|cc} A + B_2F + HC_2 & -H & B_2 \\ \hline F & 0 & I \\ -C_2 & I & 0 \end{array}\right] \tag{5.31}$$

N.B. For simplicity it has been assumed that $D_{22} = 0$, but this is not a necessary assumption.

5.4-3 Model-matching problem

Chu [CHU1] and Doyle [DOY7] both give state-space descriptions for R(s) in the model-matching problem

$$\min_{Q} \; || \, R - Q \, ||_{\infty} \tag{5.32}$$

in terms of the state-space description of P(s) and the solutions to two Riccati equations which define the gain matrices in equation (5.31). These Riccati equations cannot be solved when either $P_{22}(s)$ is not stabilizable or detectable, or $P_{21}(s)$ or $P_{12}(s)$ have zeros on the imaginary axis. This means that in finite precision arithmetic, the solutions may be ill-conditioned when the problem is close to one of these cases. This is not just a numerical problem; it means that the optimization problem, as posed, is close to one that cannot be solved. The best solution, then, is to pose a more sensible problem.

A major problem with the state-space model of R is that, in general, it is not minimal. By construction it has a state dimension of 2n, where n is the state dimension of the standard problem in (5.30). In particular, for the 1-Block case both [LIM1] and [POS6] prove that the McMillan degree of R is less than the sum of the numbers of right half plane zeros of P_{12} and P_{21}, which can clearly be less than 2n. This was the cause of a number of numerical problems in implementing the solution; subsequent procedures require minimal realizations of R (where indicated), and these proved much more sensitive to the non-minimality than available 'minimal realization' routines. These problems led to the development of the routine described in Chapter VIII, which finds the truncated balanced realization of a non-minimal stable state-space system (R(-s) in this case). Using this algorithm, it is clearly observed that the minimal dimension of both $R_1(-s)$ and $R_2(-s)$ for the specific 2-Block problems so far considered, is $\leq$ n (usually n). The conditions under which this will always occur have yet to be derived.

5.4-4 2-Block γ-iteration

The 2-Block γ-iteration requires the following computational steps:

(i) Left-coprime factorization with inner denominator. This is required because the spectral factorization requires a stable function. It effectively flips the poles of R_2 into the left half plane without changing the zeros:

$$R_2 = \tilde{M}^{-1}\tilde{N}$$

$\tilde{N}$ is found by solving a Riccati equation which requires R_2 to be detectable (observable, since R_2 is completely unstable).

(ii) Spectral factorization of $\gamma^2 - R_2^* R_2$. Note that since $\tilde{M}$ is inner, $R_2^* R_2 = \tilde{N}^* \tilde{N}$. This step is performed by solving a Riccati equation, which requires the realization of $\tilde{M}$ to be minimal, and have no zeros on the imaginary axis (this occurs when $\gamma \leq ||R_2||_\infty$).

(iii) Spectral decomposition of $R_1 M^{-1}$. This requires the solution of a Sylvester equation ($AX + XB = C$).

(iv) Hankel norm calculation. This requires the solutions to two Lyapunov equations to be found, then an eigenvalue (or singular value) computation.

(v) Optimal anti-causal approximation. As in Appendix 5.1 using Glover's algorithm. A minimal, balanced realization is required.

5.4-5 Controller recovery and dimension

When the (sub) optimal Q is found, the controller K is formed by substitution in the LFT defined by J in equation (5.31) and Q. Thus, the controller K will have a state dimension equal to that of J plus that of

Q. By following the computational steps in [CHU1], the bounds on this size are as follows:

1-Block	3n - 1
2-Block	6n - 1
4-Block	13n - 1

where n is the state dimension of the original standard problem, and no minimal realizations are considered. The resulting controller, however, tends not to be minimal. When R_1 and R_2 each have a minimal dimension of n, the 2-Block 'optimal controller' has a state dimension of 3n-1, and using the minimal realization algorithm in Chapter VIII, typically has a minimal dimension of n-1. This 'minimal' controller is generally indistinguishable from the 3n-1 state controller, especially when a very small tolerance is used in the γ-iteration.

It has been shown that the controller for a specific 1-Block problem requires only n-1 states [GL02]. It is claimed in [LIM1] that this bound extends to all 1-Block 'standard problems'. It therefore seems reasonable to propose the following.

Conjecture:

All H^∞-optimal controllers have at most n states.

A constructive proof of this would be very useful, since it would significantly reduce the computational problems associated with the present matrix size inflation.

In [LIM2] it was suggested that the bound for the 2-Block problems was 2n-1; this has since been revised (personal communication) to n-1.

5.4-6 Model reduction in H^∞-design

The dimension of systems within the design procedure is a limiting factor in the performance of software, in terms of both memory requirement

and computational speed. In [CHU1] it is shown that it is possible to reduce R(s) and Q(s) in the design procedure, with a bound on the degradation of the resulting cost. It has been shown by example [LIM1] that reducing the size of Q(s) can increase the controller dimension, by destroying the natural pole-zero cancellations that occur when the controller is recovered from Q(s). It is proposed in this thesis to use a model-reduction-like algorithm to obtain a minimal realization of R, but it is stressed that this is used only to remove states that in exact arithmetic should not be necessary. The non-minimality of Q causes no problems and need not be checked, since we can apply the minimal realization algorithm of Chapter VIII directly to the full controller (or more accurately, its stable part).

In the final reduction of the controller there is generally a clear number of states that are significant ($\leq$ n-1). Attempting to use model reduction to reduce the size beyond this does change the cost function and closed-loop performance. Such a reduction is very difficult because it is necessary to check that the original design specifications are still met, and the choice of further weighting functions in the reduction seems difficult. In any case it is not clear that a k'th order reduction of an optimal controller is the solution to a problem such as

$$\min_{\text{stabilizing } K \text{ with dimension} \leq k} \| T(s) \|_\infty \qquad (5.33)$$

although it may be expected to be a good starting point for a 'brute force' numerical optimization technique.

In summary, the use of true model reduction on the controller has not been considered in this work, since controller size was not considered to be a particular problem. It is suggested that such techniques should either be applied to the original problem (by approximating the plant model and using low order weighting functions), or to the final controller

(with due regard to original design specifications). The design calculations should be made as accurate as possible, since this seems to enhance the number of cancellations that occur in the controller, thus reducing its size.

5.5 A specific H^∞-optimization problem

5.5-1 Problem statement

The objective is to design a controller K, as shown in Figure 5.3, that stabilizes the closed-loop system and minimizes the cost function.

$$\min_{\text{stabilizing } K} \left\| \begin{matrix} W_1 S \, W_i \\ W_2 K S W_i \end{matrix} \right\|_\infty \qquad (5.34)$$

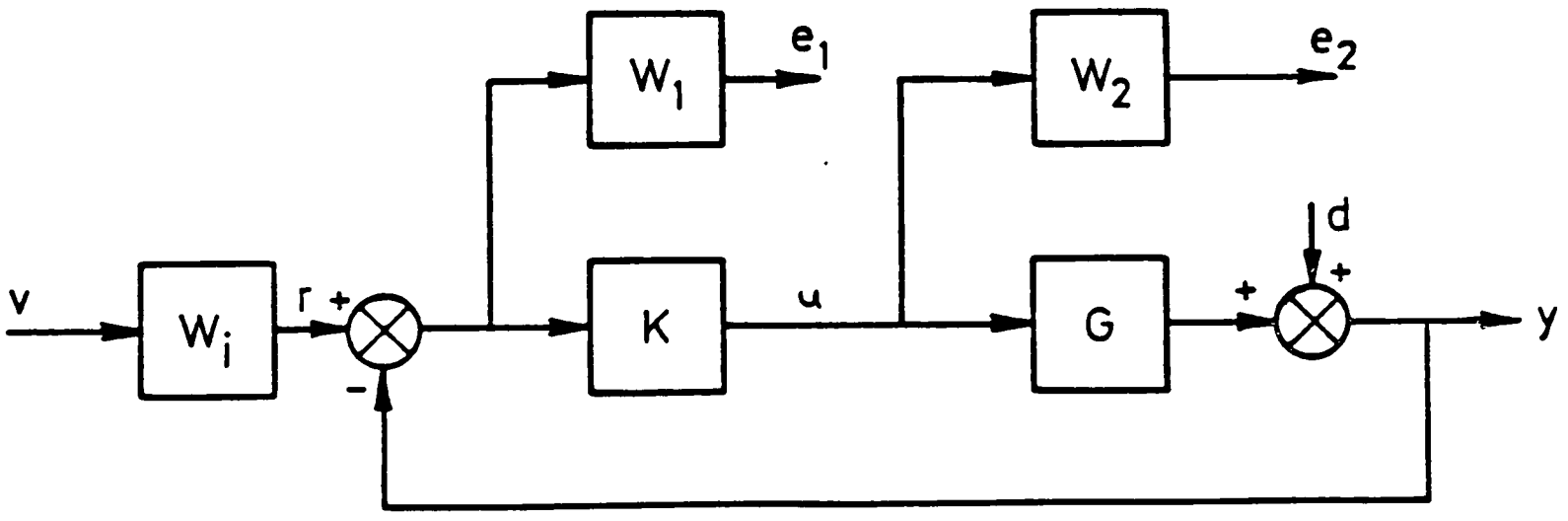


Figure 5.3 System configuration

This is probably the simplest cost function in H^∞ design that can be used to produce sensible controllers, because it is possible to penalize both performance and robustness/disturbance rejection. Therefore the inherent trade-offs can be explored by suitable choice of weighting

functions. This would not be possible if either of the elements of the cost function were treated separately.

S(s) is the transfer function from reference input r to tracking error e, which we would like to be small, especially at low frequency. It is also the transfer function from disturbance d to output y, with compatible requirements.

KS(s) is the transfer function from reference input r or disturbance d to control signal u. In order to prevent excessive actuator demands we should keep this transfer function small, particularly at high frequency. This is also the quantity we would like to minimize in the presence of additive uncertainty in the plant.

5.5-2 Conversion to standard problem

With $\left[\begin{array}{c|c} A & B \\ \hline C & D \end{array}\right]$ as a minimal realization of the plant G, we may write

$$\begin{aligned} \dot{x} &= Ax + Bu \\ y &= Cx + Dy \\ e &= r-y \\ u &= Ke \end{aligned} \qquad (5.35)$$

$$\Rightarrow \qquad \dot{x} = Ax + \begin{bmatrix} 0 & B \end{bmatrix} \begin{bmatrix} r \\ u \end{bmatrix}$$

$$\begin{bmatrix} e \\ u \\ e \end{bmatrix} = \begin{bmatrix} -C \\ 0 \\ -C \end{bmatrix} x + \begin{bmatrix} I & -D \\ 0 & I \\ I & -D \end{bmatrix} \begin{bmatrix} r \\ u \end{bmatrix} \qquad (5.36)$$

which, when augmented with the weighting functions (W_1, W_2, W_i),. leads to a minimal realization of P(s) in the standard problem. Note that because the number of reference inputs is equal to the number of controller inputs this forms a 2-Block problem.

Sufficient conditions for this problem to be solvable are:

(i) The plant is stabilizable and detectable.

(ii) The plant has no poles on the jω-axis (prevents zeros in P_{12}or P_{21}).

(iii) W_1 and W_2 have no poles or zeros on the jω-axis, including infinity (conditions on P_{12} and P_{21}).

Note: The above constraints restrict the controller as follows:

(i) It is not possible to force the controller to have integral action.

(ii) It is not possible to specify the controller to be strictly proper.

These occur because of the specific problem set-up and should not be regarded as being general properties of H^∞-optimal controllers.

5.5-3 Textbook example

This chapter is concluded with a simple design example for a single input, single output, non-minimum phase plant.

$$G(s) = \frac{0.5\ (1 - s)}{(s + 2)(s + 0.5)} \qquad (5.37)$$

The presence of the right half plane zero imposes hard constraints on the achievable performance [OY01], [OY02], [FRE1].

Nominal design specifications are:

(1) Good performance and disturbance rejection at low frequency: steady state error less than 2%.

(2) Minimize amplitude and rate of control signal demands. In particular the maximum instantaneous demand to a step should be less than the necessary steady state value.

(3) Undershoot (due to non-minimum phase zero) should be no greater than the open-loop response to an equivalent step demand.

(4) The closed-loop transfer function T should be strictly proper to prevent noise being transmitted to the output.

In choosing the weighting functions, it is convenient to assume the problem is normalized to a value of 1. Thus the weighting functions can be chosen such that, provided the final cost is less than or equal to 1, the specifications are met. General guidelines for the selection of weighting functions are then:

W_1: $|W_1(0)| = 50$ to force $|S(0)| \leq 0.02$ to satisfy specification (1). $|W_1(j\omega)| > 1$ for as large a bandwidth as possible to achieve good tracking. The non-minimum phase zero actually prevents this being achieved at frequencies approaching 1 rad/s. Also, in order to satisfy specification (3) a finite penalty on S(s) is required to restrict the 'peak' in S(s) which typically occurs in non-minimum phase systems.

W_2: W_2 is required to be non-zero for all frequencies, this ensures that specification (4) is met since the plant is strictly proper and T(s) = GKS(s). To force a greater pole excess in the closed-loop systems would require the weighting on KS to be improper, which is difficult in state space. A simple alternative would be to augment the plant with an appropriate low pass filter, later to be included in the controller.

W_i: Without loss of generality for SISO systems, W_i can be assumed to be 1. In multivariable systems W_i is useful for weighting particular inputs more heavily than others.

The open-loop system step response is shown in Figure 5.4; the weighting functions chosen for a particular design which gives a cost of 1.003 are shown in Figures 5.5 an 5.6. The cost function is shown in Figure 5.7; this is constant as expected. The results of the design are given in Figures 5.8 to 5.13.

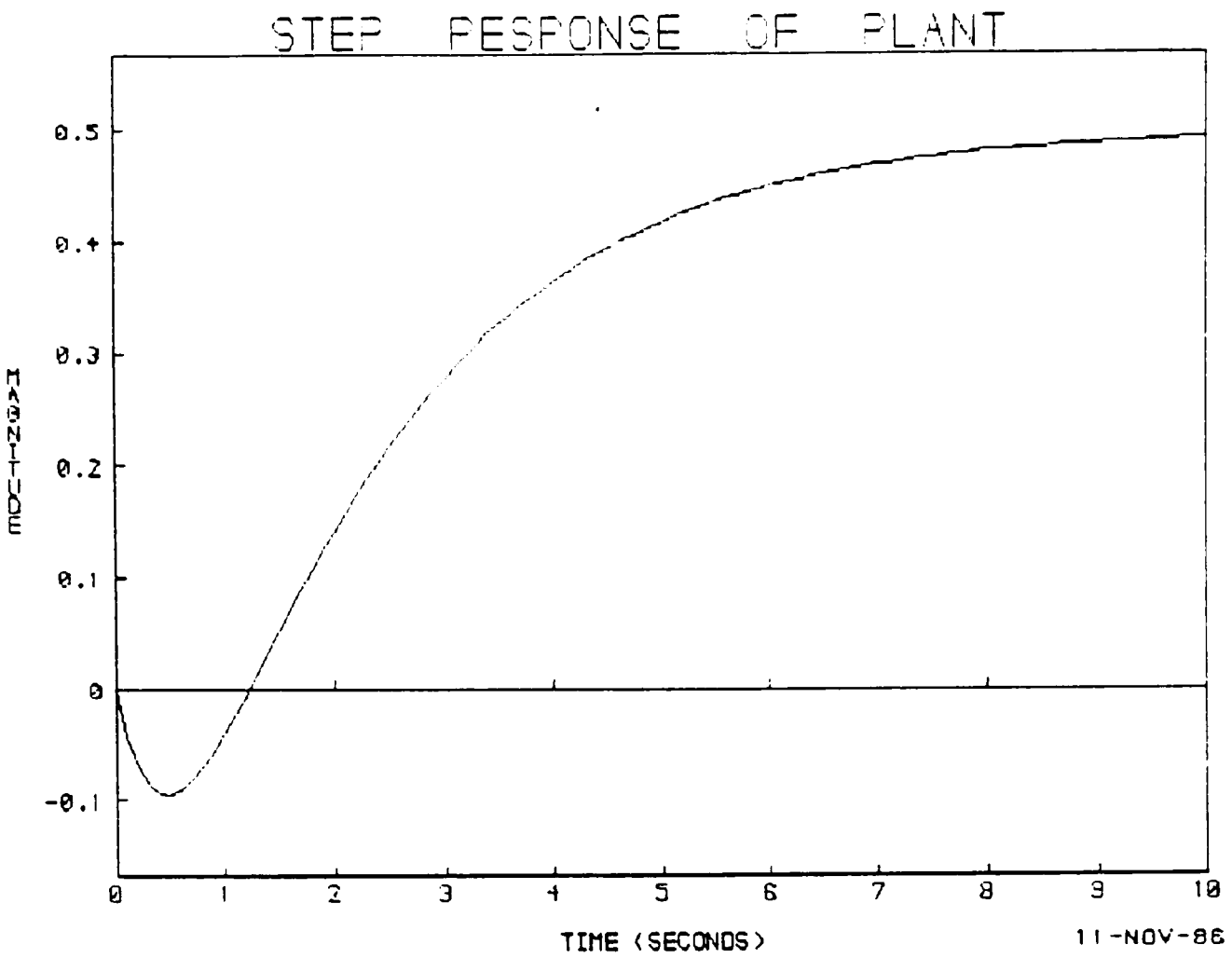


Figure 5.4

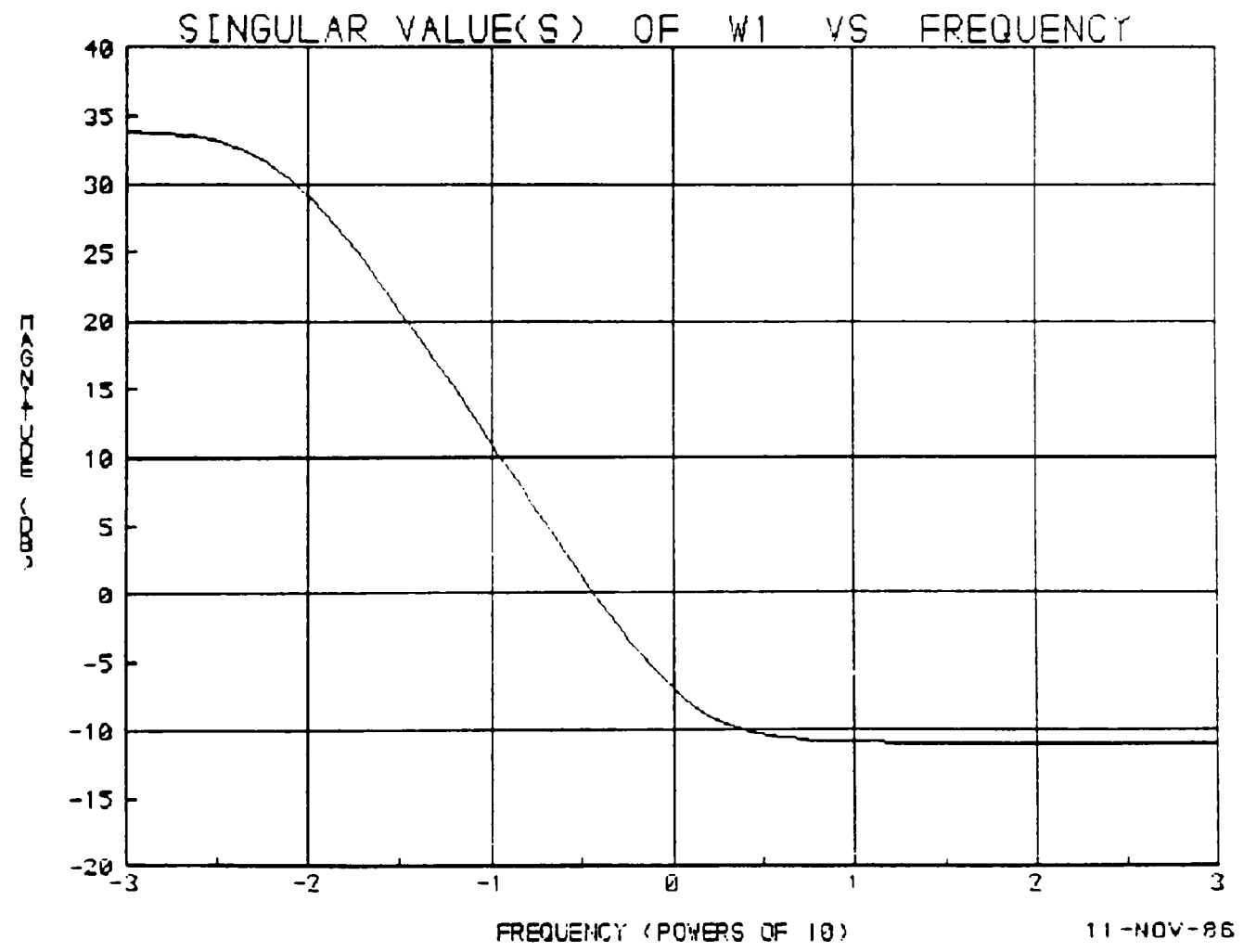


Figure 5.5

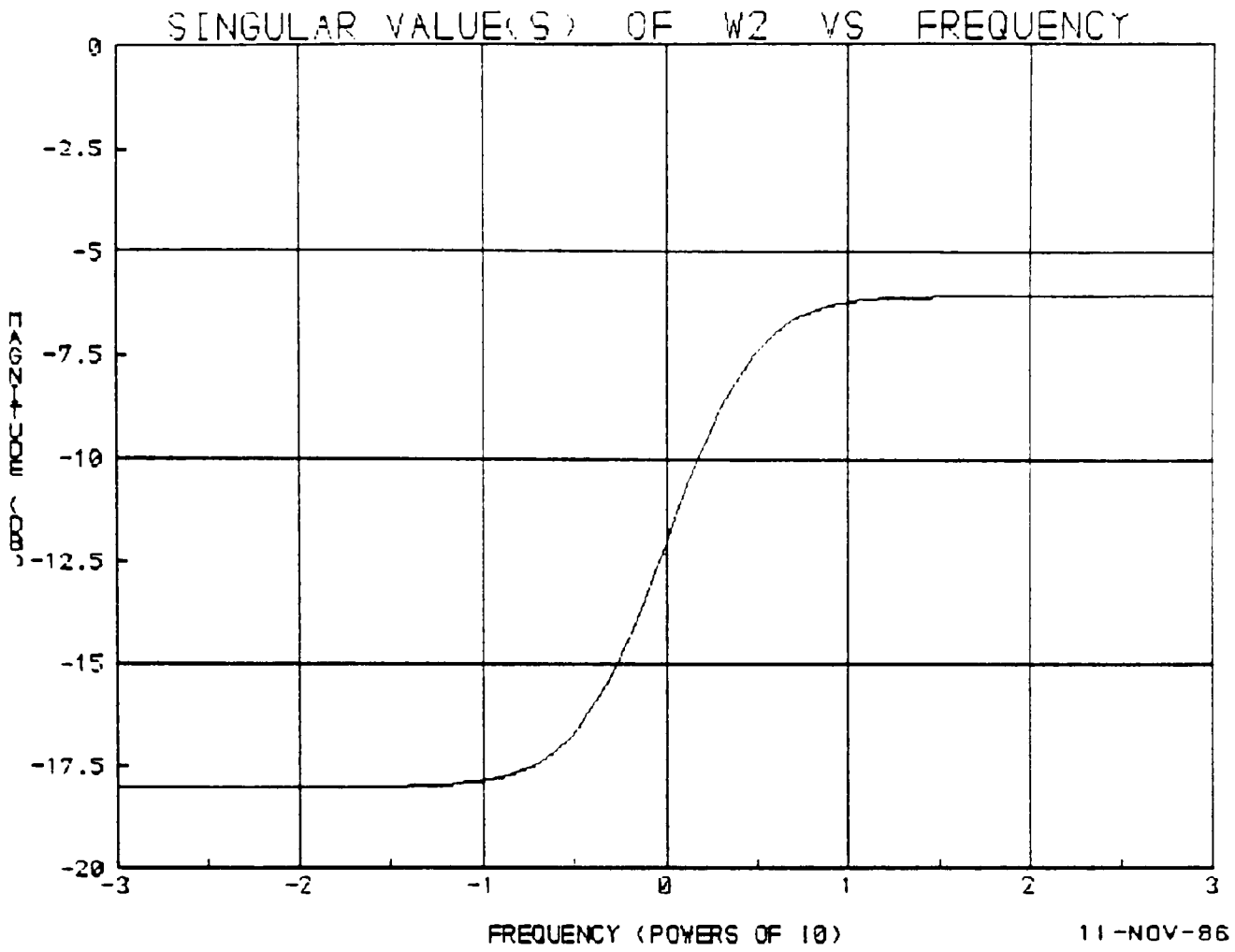


Figure 5.6

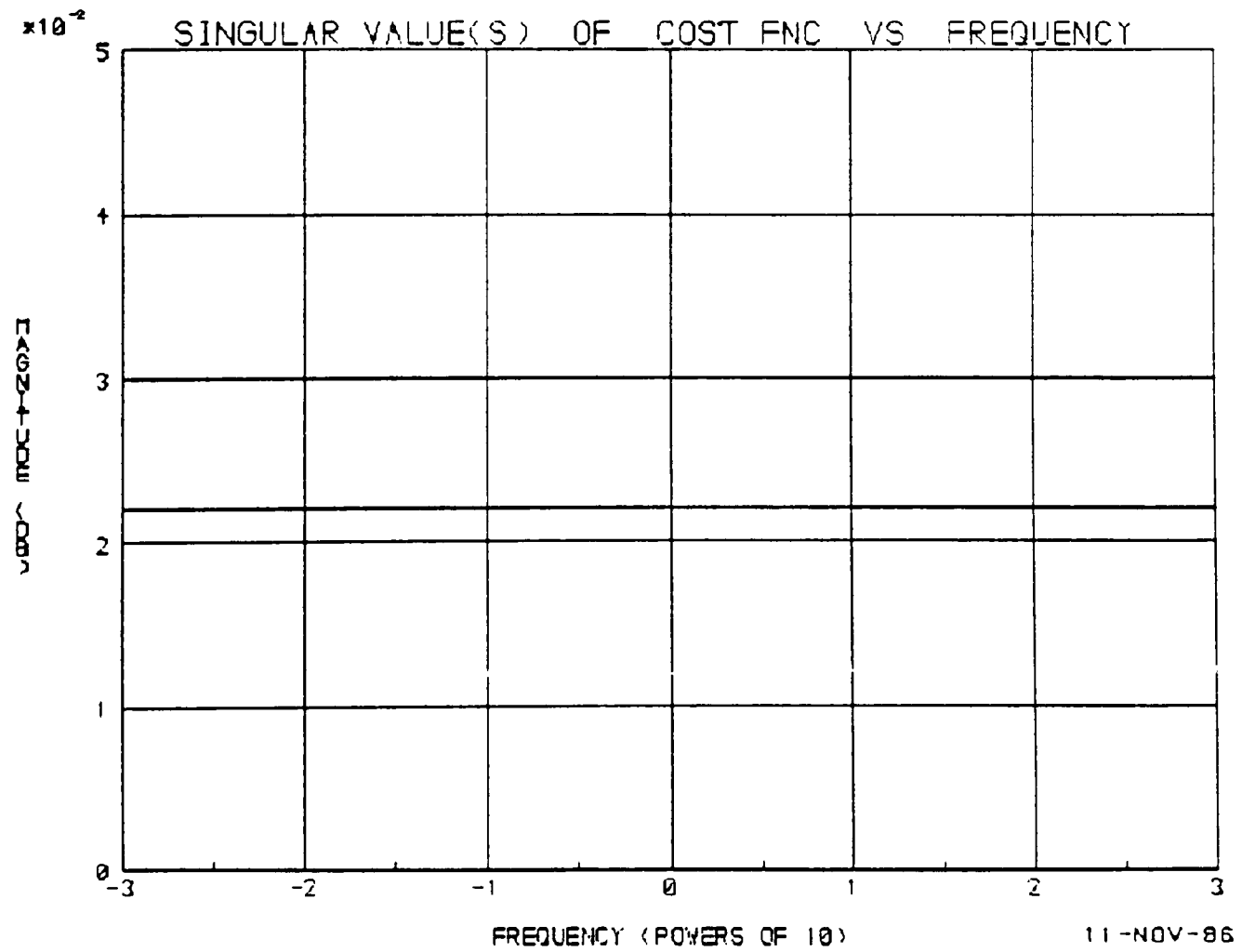


Figure 5.7

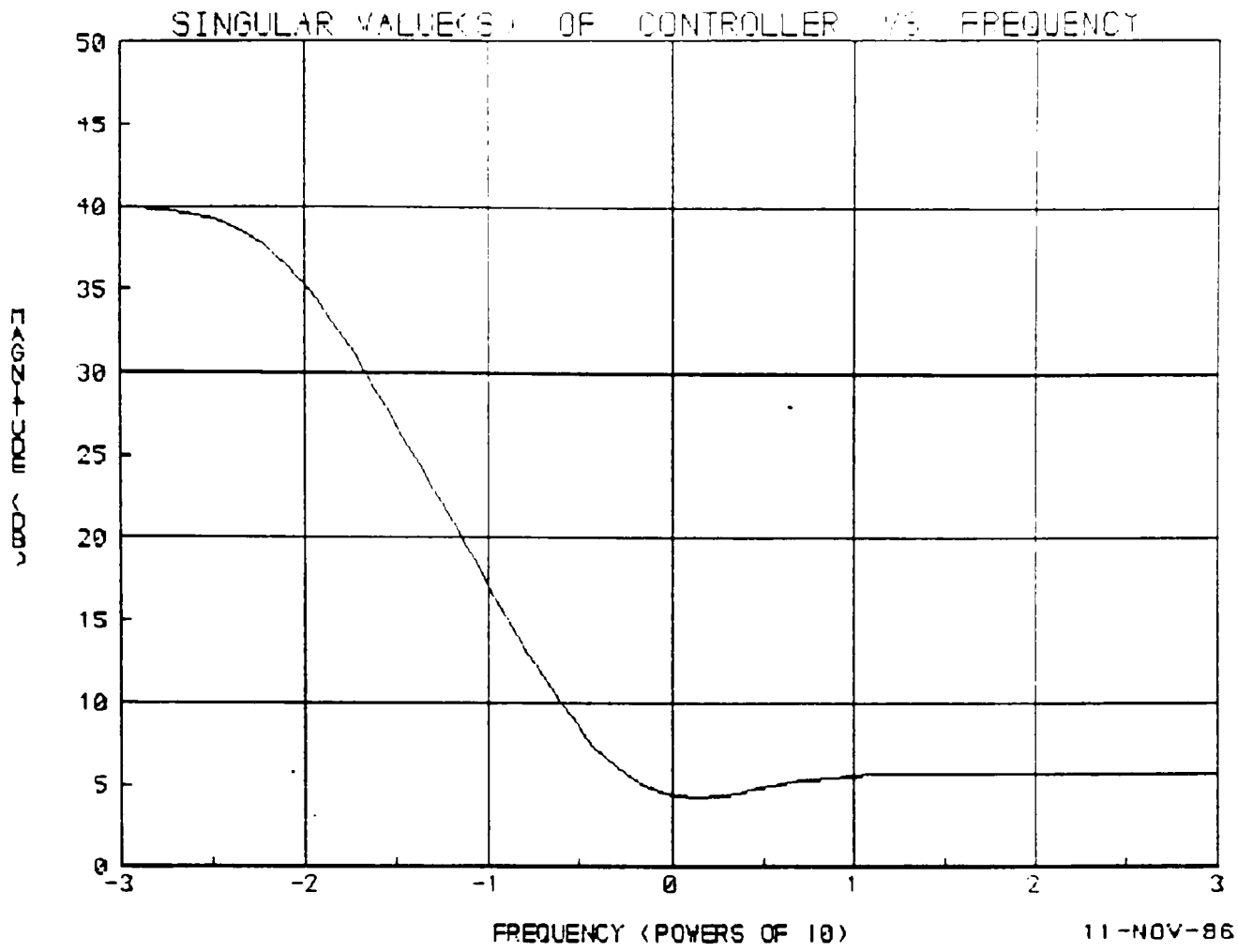


Figure 5.8

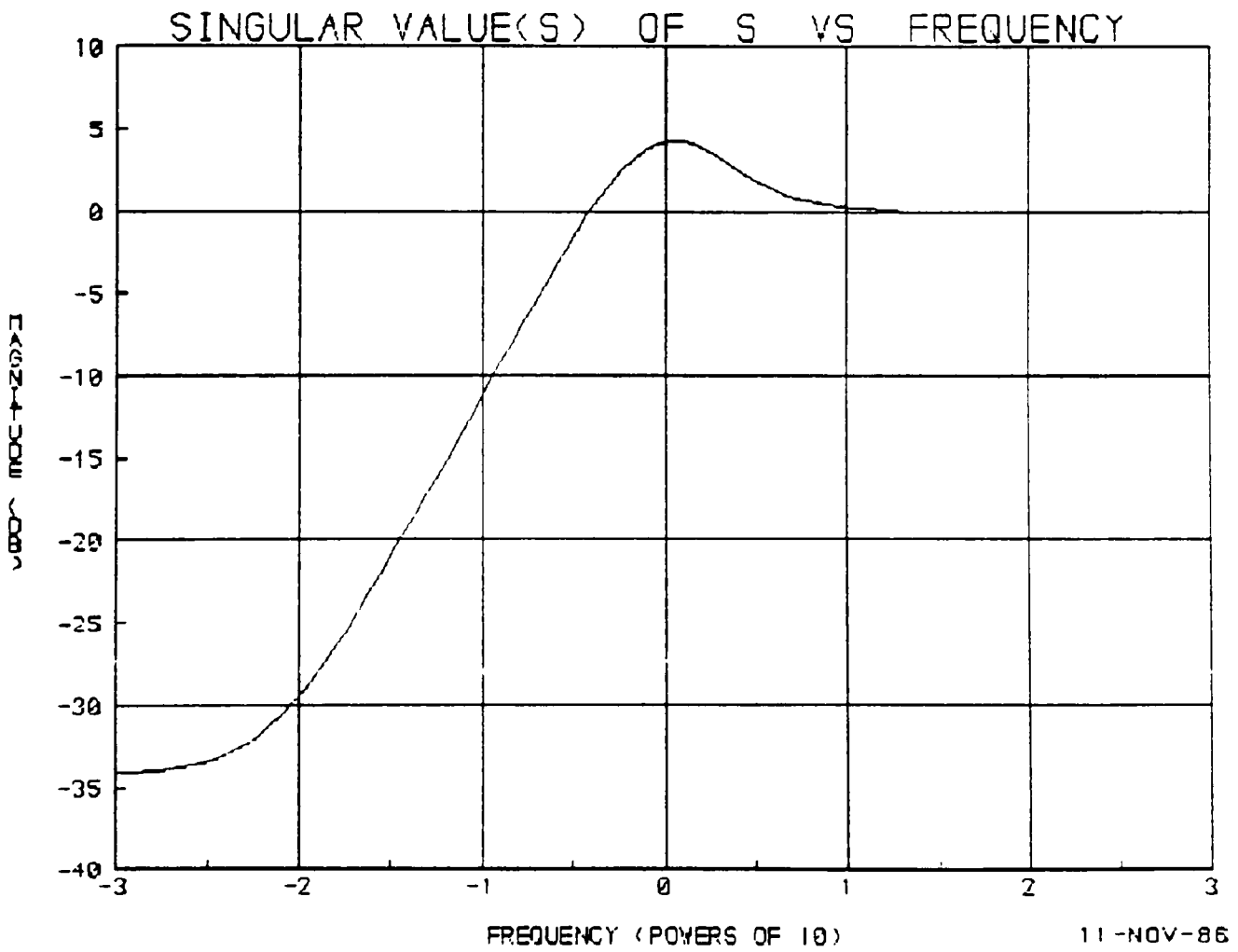


Figure 5.9

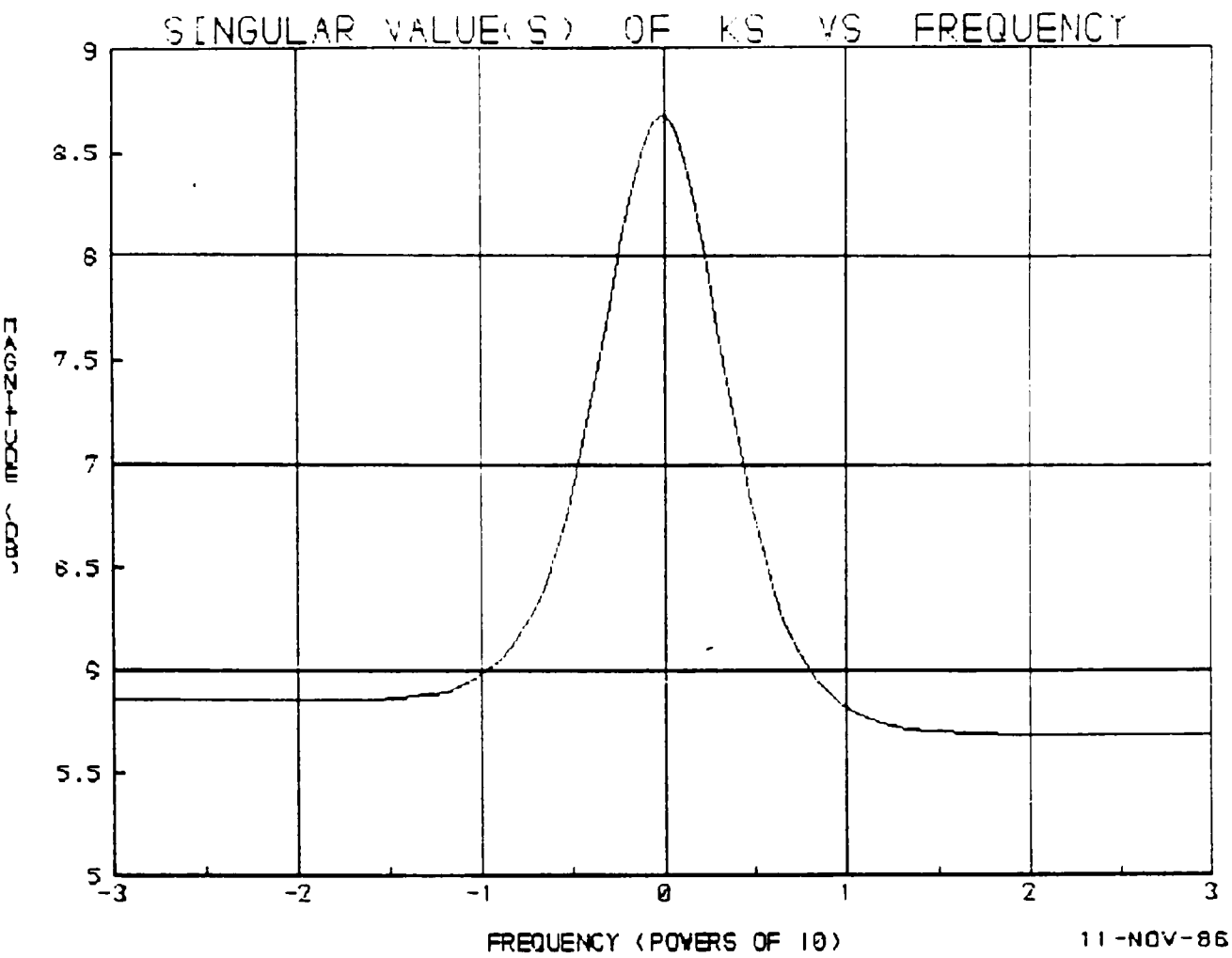


Figure 5.10

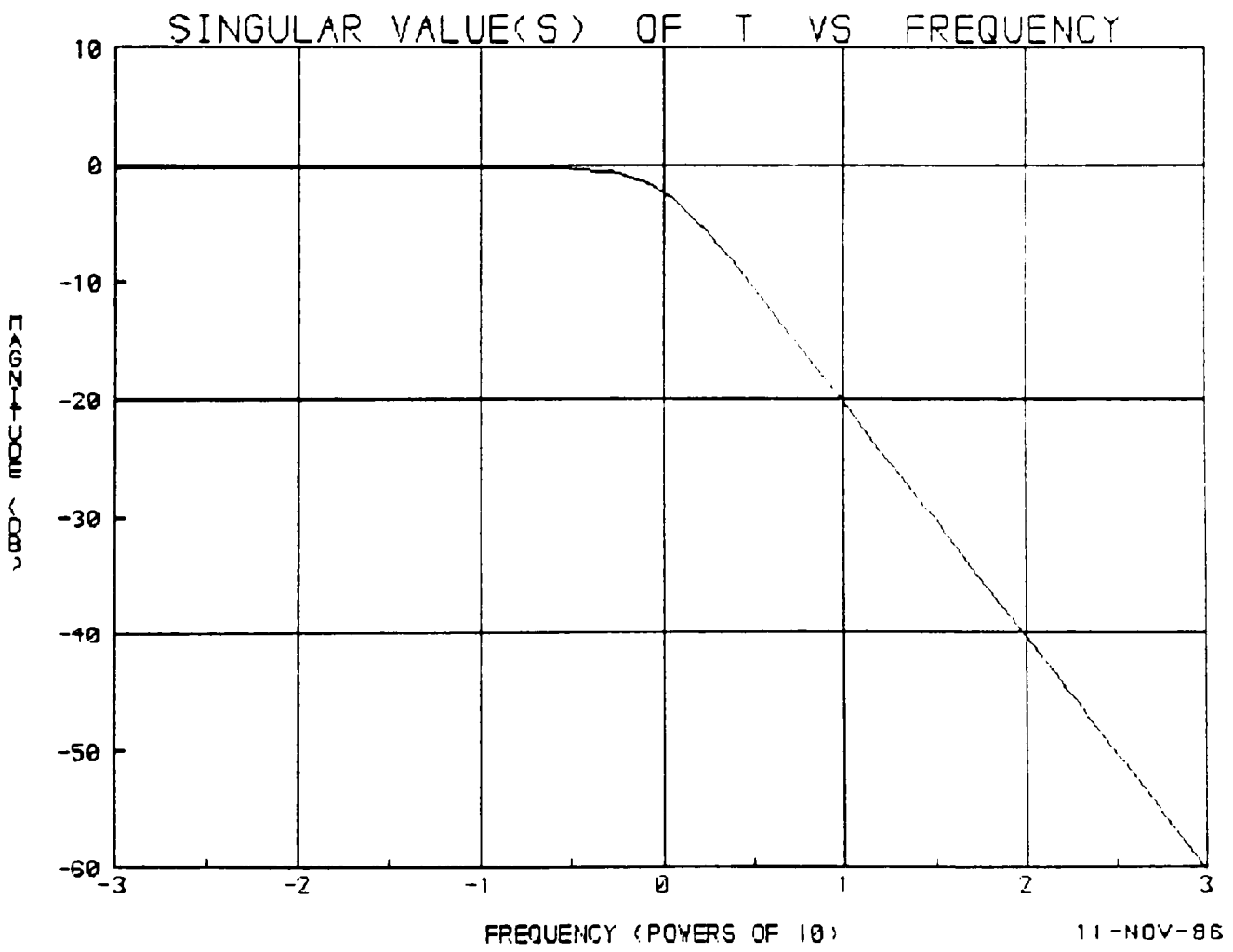


Figure 5.11

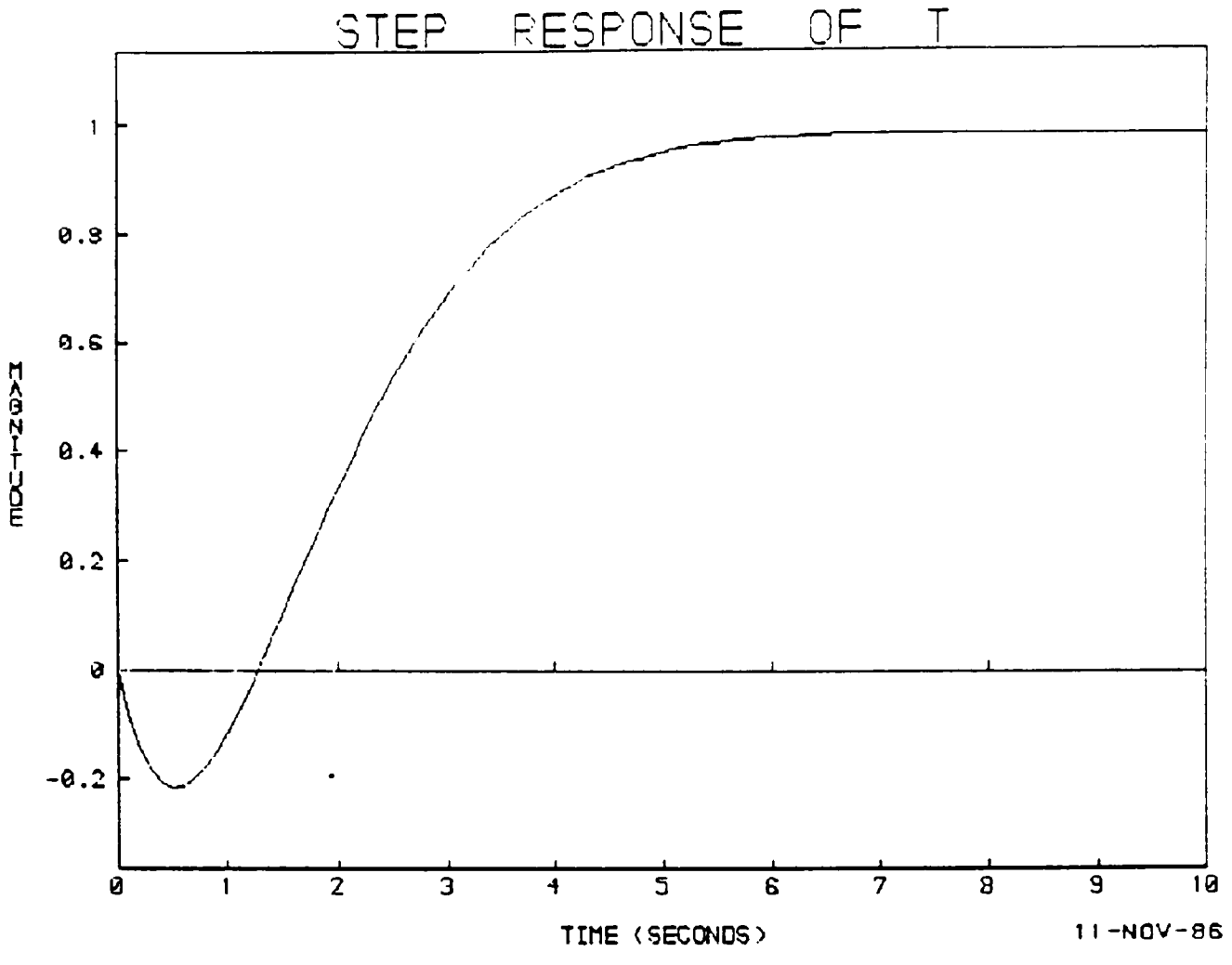


Figure 5.12

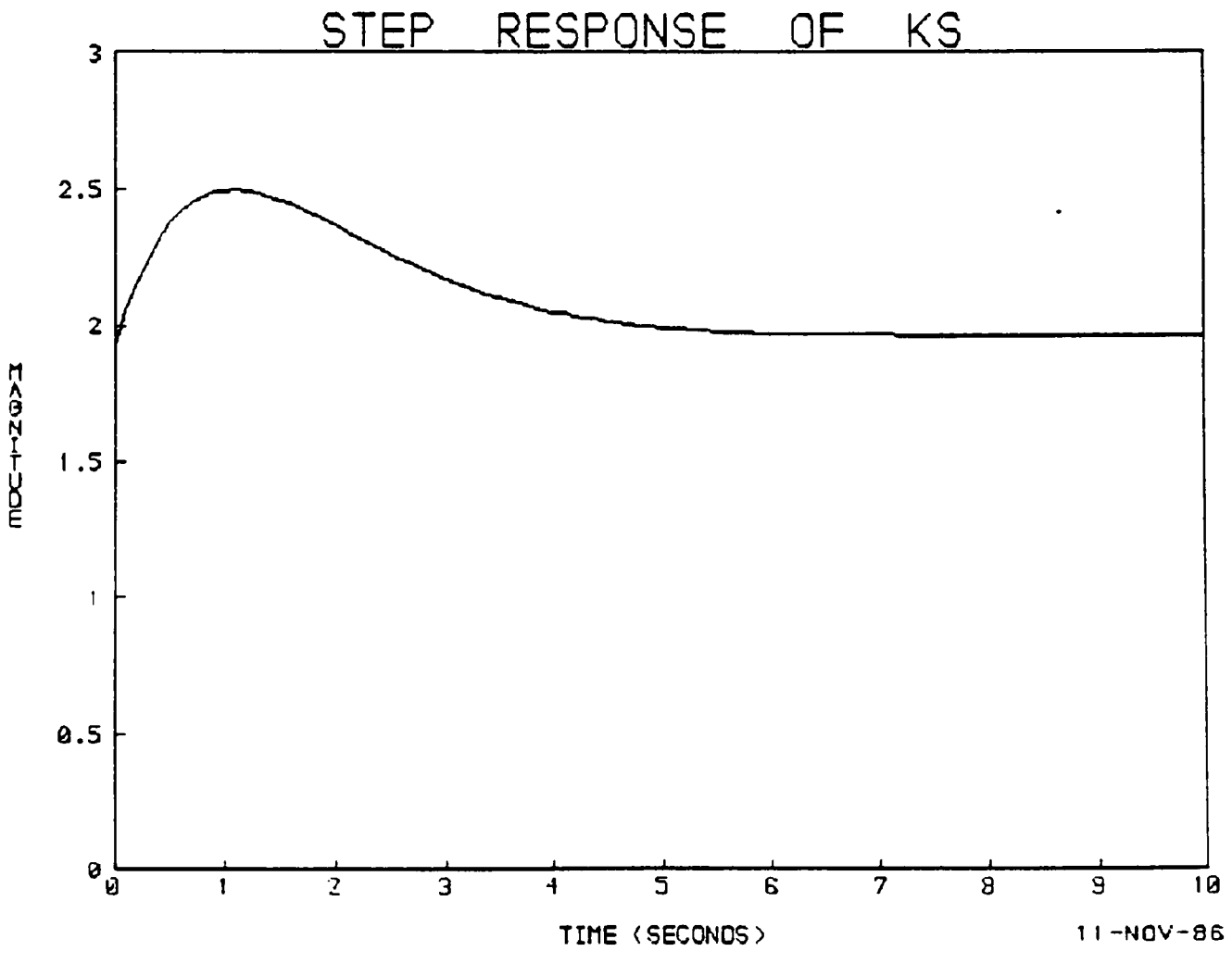


Figure 5.13

Summary of Design:

$$\text{Plant } G(s) = 0.5\ \frac{(1 - s)}{(1 + s/2)(1 + s/0.5)}$$

$$W_1(s) = 50\ \frac{(1 + s/1.245)}{(1 + s/0.007)}, \qquad W_2(s) = 0.5\ \frac{(1 + s/0.502)}{(1 + s/2)}$$

$$K(s) = 101\ \frac{(1 + s/2)(1 + s/0.5)}{(1 + s/2.725)(1+s/.007)} \tag{5.38}$$

Note that the controller is stable and has 2 states compared to 4 in the standard problem. The fact that this is n-2 rather than n-1, as previously suggested, is due to the fact that there is a fortuitous cancellation between $W_2(s)$ and $G(s)$. If the pole of $W_2(s)$ is moved from $s = -2$, then the controller does, in general, have n-1 states.

5.6 Concluding remarks

This chapter has presented the framework of the mathematical and practical solution to the 'standard problem' in H^{∞}-optimization.

Two conjectures about the properties of the optimal controller have been given. The first, which states that the maximum value of the cost function is constant over all frequency, appears to be widely assumed, though no formal proof can be quoted. The second suggests that the state dimension of the controller is always less than or equal to the dimension of the standard problem. If this is true, a significant improvement in the computational burden can be expected. Note that researchers have previously been predicting that the state dimension of the controller might be as large as six times the dimension of the problem.

The chapter was concluded with an example which demonstrates that a sensible H^{∞}-optimization problem can be posed with simple weighting functions, to give a controller consisting of two lead-lag functions.

Appendix 5.1 Optimal anti-causal approximation

Let $\left[\begin{array}{cc|c} A_{11} & A_{12} & B_1 \\ A_{21} & A_{22} & B_2 \\ \hline C_1 & C_2 & 0 \end{array}\right]$ be a balanced state-space description

of the stable transfer function G(s), with n states, m inputs and 1 outputs. The gramians are given by diag (σ_h, Σ), where σ_h is the largest Hankel singular value, with multiplicity r. Assume the state-space description to be partitioned conformally with these gramians (dim A_{11} = r x r).

Now define $\hat{G}(s)$ by the following state-space description:

$$\left[\begin{array}{c|c} \hat{A} & \hat{B} \\ \hline \hat{C} & \hat{D} \end{array}\right] = \left[\begin{array}{c|c} \Gamma^{-1}\left(\sigma_h^2 A_{22}^T + \Sigma A_{22}\Sigma - \sigma_h C_2^T U B_2^T\right) & \Gamma^{-1}\left(\Sigma B_2 + \sigma_h C_2^T U\right) \\ \hline C_2 \Sigma + \sigma_h U B_2^T & -\sigma_h U \end{array}\right] \tag{5.39}$$

U is a matrix satisfying

$$B_1 = C_1^T U \text{ and } U^T U \leq 1 \tag{5.40}$$

and

$$\Gamma \triangleq \Sigma^2 - \sigma_h^2 I_{n-r} \tag{5.41}$$

Also define the error system

$$E(s) = G(s) - \hat{G}(s) \tag{5.42}$$

Theorem 5.1

$\hat{G}(s)$ is an optimal anti-causal approximation to G(s), that is, $||E(s)||_\infty = \sigma_h$, and if

(i) l = m and $U^T U = I$, then,

(a) $E(s)^* E(s) = E(s)\, E(s)^* = \sigma_h^2 I$

(b) $\hat{G}(s)$ is minimal with degree n - r

or

(ii) $l \neq m$ and U satisfies equation (5.40)

(a) $\bar{\sigma}\,[E(j\omega)] \leq \sigma_h$ and equality must hold for some ω.

(b) $\hat{G}(s)$ is not necessarily minimal.

Proof:

Part (i) may be regarded as a restricted part of Glover's Theorem 6.3 [GL01]. That $\hat{G}(s)$ is also an optimal anti-causal approximation, under the conditions of Part (ii), follows from Corollary 7.3 in [GL01], hence (ii)a must hold. In fact, by taking this proof further, we may make the properties of E(s) more explicit, as in Theorem 5.2. Part (ii)b will be shown by example at the end of this appendix.

Theorem 5.2

For all U that satisfy equation (5.40),

$$\bar{\sigma}\,[E(s)] = \sigma_h, \text{ for all } s = j\omega \tag{5.43}$$

and

(a) If $l \leq m$ and $U^T U = I_m$, $E(s)^* E(s) = \sigma_h^2 I_m$

(b) If $m \leq l$ and $UU^T = I_l$, $E(s)E(s)^* = \sigma_h^2 I_l$

Proof:

Following [GL01] (proof of Corollary 7.3), consider an (l+m) x (l+m) system $G_a(s)$ with state-space description.

$$\left[\begin{array}{c|c} A_a & B_a \\ \hline C_a & 0 \end{array}\right] = \left[\begin{array}{cc|cc} A_{11} & A_{12} & B_1 & 0 \\ A_{21} & A_{22} & B_2 & 0 \\ \hline C_1 & C_2 & 0 & 0 \\ 0 & 0 & 0 & 0 \end{array}\right] \tag{5.44}$$

Note that because we have simply augmented the original system with zeros, the Hankel singular values are unchanged. We can now construct an orthogonal matrix V satisfying

$$\begin{bmatrix} C \\ 0 \end{bmatrix} = - V \begin{bmatrix} B_1^T \\ 0 \end{bmatrix} \tag{5.45}$$

where

$$V = \begin{bmatrix} U & (I_1 - UU^T)^{1/2} \\ (I_m - U^TU)^{1/2} & -U^T \end{bmatrix} = \begin{bmatrix} U & V_{12} \\ V_{21} & -U^T \end{bmatrix}, \text{ say} \tag{5.46}$$

Now, using equation (5.39), a state-space description of $\hat{G}_a(s)$ is given by:

$$\left[\begin{array}{c|c} \hat{A}_a & \hat{B}_a \\ \hline \hat{C}_a & \hat{D}_a \end{array}\right] = \left[\begin{array}{c|cc} \hat{A} & \hat{B} & \Gamma^{-1}C_2^T V_{12} \\ \hline C & \hat{D} & -\sigma_h V_{12} \\ V_{21}B_2^T & -\sigma_h V_{21} & \hat{D}^T \end{array}\right] \tag{5.47}$$

Then,
$$E_a(s) = \begin{bmatrix} E(s) & \Theta_1(s)V_{12} \\ V_{21}\Theta_2(s) & \Theta_3(s) \end{bmatrix} \tag{5.48}$$

where $\Theta_i(s)$ have been used to simplify notation.

Theorem 5.1 (i)a now implies

$$E_a(s)^* E_a(s) = E_a(s)E_a^*(s) = \sigma_h^2 I_{l+m} \tag{5.49}$$

Since the norm of a submatrix must be less than or equal to the norm of the full matrix, and the infinity norm of E(s) cannot be less than σ_h we have now proved Theorem 5.1 (ii)a.

Now assume that $l \geq m$, equations (5.49) and (5.48) lead to

$$E(s)^{*}E(s) + \Theta_2^{*}(s)V_{21}^{T}\, V_{21}\Theta_2(s) = \sigma_h^2\, I_m \qquad (5.50)$$

Also since U satisfies equation (5.40) and

$$B_1 B_1^{T} = C_1^{T} C_1 \qquad (5.51)$$

U must have at least rank $(C_1) = r_1$ singular values at 1 and have a singular value decomposition:

$$U = X \begin{bmatrix} I_{r_1} & 0 \\ 0 & S \\ 0 & 0 \end{bmatrix} Y^{T} \qquad (5.52)$$

where S is a diagonal matrix with elements ≤ 1.

Then, $$V_{21} = Y \begin{bmatrix} 0 & 0 \\ 0 & (I_{m-r} - S)^{1/2} \end{bmatrix} Y^{T} \qquad (5.52)$$

which shows that V_{21} is rank deficient. This implies that for every value of $s = j\omega_o$ there must exist an orthonormal vector x such that

$$V_{21}\Theta_2(j\omega_o)x = 0 \qquad (5.53)$$

and from (5.50)

$$x^{*}\, E(s)^{*}\, E(s)x = \sigma_h^{\,2} \qquad (5.54)$$

$$\Rightarrow \qquad \sigma_i\, [E(j\omega_o)] = \sigma_h \quad \text{for some } i \qquad (5.55)$$

But $$\sigma_i\, [E(j\omega)] \leq \sigma_h \text{ from equation (5.49)} \qquad (5.56)$$

Hence we may conclude that for $l \geq m$

$$\bar{\sigma}\,[E(s)] = \sigma_h \text{ for all } s = j\omega \tag{5.57}$$

It is a straightforward exercise to show that this also holds for $m \leq 1$.

Q.E.D.

A construction for an orthogonal matrix U in Theorem 5.1(i) is given below, for the case $= m > r$.

(i) Find the singular value decomposition of C_1^T

$$C_1^T = \begin{bmatrix} \tilde{U}_1 & \tilde{U}_2 \end{bmatrix} \begin{bmatrix} \tilde{\Sigma} & 0 \\ 0 & 0 \end{bmatrix} \tilde{V}^T \tag{5.58}$$

where the dimension of C_1^T is $r \times 1$, and rank $(C_1^T) = r_1$

(ii) Form $R = \tilde{\Sigma}^{-1} U_1^T B_1$ (5.59)

R has dimension $r_1 \times 1$ and has the property that $RR^* = I_{r_1}$

(iii) Find R′ such that $\begin{bmatrix} R \\ R' \end{bmatrix}$ is orthogonal.

(iv) $U = -\tilde{V} \begin{bmatrix} R \\ R' \end{bmatrix}$ and is orthogonal (5.60)

A suitable choice for U when it is only required that $\bar{\sigma}[E(s)] = 1$, is that given by

$U = (C_1^T)^+ B_1$ where $(C_1^T)^+$ is the pseudo inverse of C_1^T. This is in fact the same as that above if we were to substitute $R' = 0$.

Example:

That the realization of $\hat{G}(s)$ is not necessarily minimal in this case may be demonstrated by a simple example:

$$\text{Let } G(s) = \begin{bmatrix} \frac{1}{s+1} & 0 \\ 0 & \frac{1}{s+2} \end{bmatrix} \tag{5.61}$$

which has the state-space description

$$\left[\begin{array}{cc|cc} -1 & 0 & 1 & 0 \\ 0 & -2 & 0 & 1 \\ \hline 1 & 0 & 0 & 0 \\ 0 & 1 & 0 & 0 \end{array}\right] \tag{5.62}$$

This realization is balanced, with Hankel singular values 0.5 and 0.25. Using the above construction we get to the following state-space realization for $\hat{G}(s)$, in terms of a free parameter a, $|a| \leq 1$, in the matrix U.

$$U = \begin{bmatrix} -1 & 0 \\ 0 & a \end{bmatrix}, \quad \hat{G} = \left[\begin{array}{c|cc} (5 + 4a)/3 & 0 & (2 + 4a)/3 \\ \hline 0 & 1/2 & 0 \\ 1/4 + a/2 & 0 & -a/2 \end{array}\right] \tag{5.63}$$

The choice a = -1/2 makes $\hat{G}$ uncontrollable and unobservable. The solution is then the same as if we had treated this diagonal system as two single-input, single-output systems, and is in fact the 'super-optimal' solution [YOU3], [YOU4], [FOO3].

Appendix 5.2 The 2-Block γ-iteration

(i) Calculation of bounds

The problem is to find $\gamma_o = \min_{Q \in H^\infty} \left|\left| \begin{matrix} R_1 \\ R_2 \end{matrix} \quad Q \right|\right|_\infty$ (5.64)

Let Q be an optimal Hankel approximation to R_1, i.e.,

$$||R_1 - Q||_\infty = ||R_1||_H \tag{5.65}$$

Then, from well known singular value inequalities we may give expressions for γ_l and γ_u, such that $\gamma_l \leq \gamma_o \leq \gamma_u$ as follows

$$\gamma_u = \sqrt{(||R_1||_H^2 + ||R_2||_\infty^2)} \tag{5.66}$$

and

$$\gamma_l = \max \{||R_1||_H, ||R_2||_\infty\} \tag{5.67}$$

It may be shown that ([CHU1])

$$\frac{1}{\sqrt{2}} \gamma_o \leq \gamma_l \leq \gamma_o \leq \gamma_u \leq \sqrt{2}\, \gamma_o \tag{5.68}$$

Unfortunately, these bounds are not very useful from a computational point of view since $||R_2||_\infty$ is not easy to calculate. We can, however, bound its magnitude in terms of directly calculable terms, as follows:

$$\max \{||R_2||_H, \bar{\sigma}[R_2(s=0)], \bar{\sigma}[R_2(s=\infty)]\} \leq ||R_2||_\infty \tag{5.69}$$

$$||R_2||_\infty \leq 2 \sum_{i=1,n} \sigma_{hi}[R_2] + \bar{\sigma}[R_2(s=\infty)] \tag{5.70}$$

The upper bound given here turns out to be excessively conservative and will not be used. To see how this might happen, imagine that R_2 is all-pass form. Then,

$$2 \sum_{i=1,n} \sigma_{hi}[R_2] + \bar{\sigma}[R_2(s=\infty)] = (2n + 1) \, ||R_2||_\infty \tag{5.71}$$

since in this case $||R_2||_H = ||R_2||_\infty$ (5.72)

Another important feature of the infinity norm is given by the following lemma.

lemma:

If $\gamma_1 = \bar{\sigma} [R_2(j\omega)]$ for some ω, then for all γ, such that

$$\gamma_1 \leq \gamma \leq ||R_2||_\infty$$

$$\underline{\sigma} [\gamma^2 I - R_2^* R_2] = 0 \text{ for some } \omega \tag{5.73}$$

Proof:

For all γ in the above range, there must be at least one value of ω, such that

$$\bar{\sigma} [R_2(j\omega)] = \gamma \tag{5.74}$$

at which frequency

$$\underline{\sigma} [\gamma^2 I - R_2^* R_2] = 0 \tag{5.75}$$

Corollary:

If $\gamma > \bar{\sigma} [R_2(j\omega)]$ for some ω and $\underline{\sigma} [\gamma^2 I - R_2^* R_2] \neq 0$ for all ω, then $\gamma > ||R_2||_\infty$.

Now the spectral factorization $M^* M = \gamma^2 I - R_2^* R_2$ can only be performed when $\gamma^2 I - R_2^* R_2$ has no zeros on the imaginary axis. The implication of this lemma and corollary is that if the factorization succeeds, $\gamma > ||R_2||_\infty$.

The proposed procedure for finding bounds is then as follows.

1) $\gamma_1' = \max\left(||R_1||_H,\ ||R_2||_H,\ \bar{\sigma}\,[R_2(s=o)],\ \bar{\sigma}\,[R_2(s=\infty)]\right)$ (5.77)

Note that the Hankel norms are available from the truncated balanced realization (Chapter VIII) used to find a minimal realization of R_1 and R_2.

2) Choose $\gamma = (1 + \delta)\gamma_1'$

3) Attempt the spectral factorization with this γ

4) If successful set $\gamma_u' = \sqrt{\left(||R_1||_H^2 + \gamma^2\right)}$ and continue with the iteration. If not, increase γ and return to step 3.

Experience has shown that the optimal γ is usually within a few percent of this γ_1', and $\delta = 0.15$ almost always ensures that a binary search will converge to 1% of γ_o in 4 iterations; this is generally 'good enough' to evaluate the design.

(ii) Sensitivity of cost function in the γ-iteration

In this section an expression for the deviation of the sub-optimal cost function from an optimal cost function is derived in terms of the accuracy in the γ-iteration.

First assume M is chosen for the final γ as

$$M^*M = \gamma^2 I - R_2{}^*R_2 \tag{5.78}$$

and for this M

$$||R_1 M^{-1}||_H = \alpha \text{ where } \alpha \simeq 1 \tag{5.79}$$

Therefore $\hat{Q}$ is chosen so that

$$||(R_1 - \hat{Q})\ M^{-1}||_\infty = \alpha \tag{5.80}$$

$$\Rightarrow \qquad M^{-1*}(R_1 - \hat{Q})^*(R_1 - \hat{Q})M^{-1} \leq \alpha^2 I \tag{5.81}$$

$$\Rightarrow \qquad (R_1 - \hat{Q})^*(R_1 - \hat{Q}) \leq \alpha^2 M^* M \leq \alpha^2(\gamma^2 I - R_2{}^* R_2) \qquad (5.82)$$

Now consider the maximum singular value of the model-matching error

$$\bar{\sigma}\begin{bmatrix} R_1 - \hat{Q} \\ R_2 \end{bmatrix} = \sqrt{\left(\bar{\lambda}\,[(R_1 - \hat{Q})^*(R_1 - \hat{Q}) + R_2{}^* R_2] \right)} \qquad (5.83)$$

$$\leq \sqrt{\left(\bar{\lambda}\,[\,\alpha^2\gamma^2 I + (1 - \alpha^2)\, R_2{}^* R_2] \right)} \qquad (5.84)$$

$$\Rightarrow \qquad \bar{\sigma}\begin{bmatrix} R_1 - \hat{Q} \\ R_2 \end{bmatrix} \leq \sqrt{\left(\alpha^2\gamma^2 + (1 - \alpha^2)\, \bar{\sigma}^2[R_2] \right)} \qquad (5.85)$$

It can now be seen that the maximum deviation of this cost function from the optimal is a function of the tolerance used in the iteration and the size of R_2, $||R_2||_\infty$; this may be useful in automatically setting the tolerance in the iteration, although the infinity norm is not directly calculated.

CHAPTER VI

APPLICATION OF H^∞-OPTIMIZATION TO THE HELICOPTER

6.1 Introduction

This chapter presents a complete application of H^∞-optimization to the design of a control system for the helicopter. The design is complete in the sense that a linear model was taken from a large non-linear simulation of the helicopter, without rotor dynamics and ignoring actuator dynamics. A linear controller was then designed from this model and the design assessed by implementing the controller in a full non-linear simulation of the helicopter, including both rotor and actuator dynamics. This example establishes that, at least in simulation, H^∞-optimization can now be used to design control systems satisfying both performance and robustness criteria for realistic control problems.

As often occurs in practical situations, the achievable performance criteria were not well known a priori. Sections 6.3 and 6.4 outline the design specification used. It is hoped that criticisms of the final design (e.g., speeds of response, etc) will be seen as criticisms of these original assumptions, and not of the design procedure itself. In section 6.5 these specifications are translated into simple weighting functions in an H^∞-optimization problem.

The remainder of the chapter contains an analysis of the resulting controller and closed-loop performance. Appendix 6.1 contains an analysis

of the computation time required for this design. Appendix 6.2 contains the state-space matrices, scaled as used in this design.

6.2 Helicopter model

The non-linear simulation HELISIM, provided by the RAE, Bedford, was used as the helicopter model throughout this chapter. This was configured to represent a high performance battlefield helicopter, typical of future Army and Air Force requirements. The basis of the mathematical model was given in Chapter IV, and the design process used only the version without rotor dynamics. Information about the effect of the extra rotor degrees of freedom was obtained from the package HELISTAB. A number of differences exist between these two models, which meant that it was not feasible to implement controllers derived from HELISTAB models in HELISIM; so this information could only be used qualitatively.

The design model was taken to be a linearization of the non-linear helicopter at 80 knots, 100 ft above the ground and in straight and level flight. With hindsight it might have been better to start with a flight condition in turning flight, and to consider only turns in the chosen direction, in order to model the non-linearities more closely.

The linear model then had eight states, with the four inputs:

(1) Collective pitch θ_{o_e}

(2) Longitudinal cyclic pitch θ_{1_s}

(3) Lateral cyclic pitch θ_{1_c}

(4) Tail rotor collective pitch θ_{tre}

(All were input signals to the respective actuators.)

The six outputs selected for control were:

(1)	Flight path angle	γ
(2)	Roll rate	p
(3)	Pitch rate	q
(4)	Lateral velocity	v
(5)	Pitch altitude	θ
(6)	Bank angle	ϕ

(All outputs of appropriate sensors.)

For the non-linear simulation it was necessary to include the actuator dynamics, modelled as first order lags with the following time-constants:

(1)	0.0795	secs
(2)	0.0795	secs
(3)	0.0795	secs
(4)	0.04	secs

The simulations considered were not noticeably affected by these dynamics, since relatively small, low bandwidth central signals were used. The option to include sensor dynamics was included in the non-linear model. These proved significant when the time-constants of the filters were of similar magnitude to the desired closed-loop responses. It was assumed that in these cases the sensor dynamics would have to be included in the design model in order to achieve 'good control'. As there was no wish to increase the complexity of the design model, sensor dynamics were not considered further.

6.3 Design objectives

The major control objective was to significantly reduce pilot workload by stabilizing the aircraft and permitting fast decoupled control of selected outputs. For the reasons previously discussed in Chapter IV the selected outputs to be independently controlled were γ, v, θ, and ϕ. Also, the couplings into the rates p and q were required to be constrained both in terms of magnitude and derivative.

The desired speed of response to pilot demand was loosely determined by the assumed bandwidth of the available measurements. Since γ and v both require velocity measurements, which are poor, a nominal bandwidth of 1 rad/s was selected. Rate gyros were assumed to be good up to 5 rad/s, which gave a desired speed of response for p and q. A compatible objective for the attitude responses was found to be 1 rad/s. These bandwidth requirements were roughly translated into the time domain by requiring the closed-loop responses to have a 'similar' response to that of a first-order lag with the same time-constant. Note that it is not necessary for all the controlled outputs to have the same bandwidth. The lack of precise requirements meant, however, that there was no particular benefit in doing otherwise. Also, in a highly coupled multivariable system the 'quality' of the closed-loop response is determined by its slowest component.

It had previously been found that the non-linear model tended to exhibit increased overshoot when compared with an equivalent linear model. For this reason a design objective was to keep any overshoot in the linear model responses to a minimum.

Robustness of the resulting closed-loop system was a primary issue in the design process, due both to the 'known' unmodelled dynamics - principally actuator and rotor - and also to unknown modelling errors (e.g., engine dynamics, flexible body modes). The rotor dynamics were

found to be significant at frequencies greater than 10 rad/s and this was used as an upper bound for the bandwidth of T, the closed-loop transfer function. This bandwidth requirement was assumed to be compatible with sensor noise-rejection properties, which were not additionally included in this design (but would be in a two-degree-of-freedom design).

Disturbances present in this application included wind gusts. These enter the model by changing the local wind velocities and, therefore, the aircraft incidence angles. For simplicity, the wind gusts were assumed to result in disturbances at low frequency (0 to 1 rad/s) in the controlled outputs and over a frequency band (1 to 2.5 rad/s) in the rates. Small sensitivity, S, over these ranges then ensures good wind gust rejection. Due to lack of precise data on the wind gusts the non-linear simulation of the final design did not test for the achieved rejection properties. Actuator amplitude and rate limits were included in the non-linear model, but were not found to be a limiting factor in this design. This was because the desired responses were well within the helicopter's operational capabilities at this flight condition. This would not be true when flying close to the edges of the flight envelope.

The subsequent sections in this chapter will explain how these many desirable closed-loop features can be obtained by suitable selection of weighting functions in an H^{∞}-optimization problem.

6.4 Scaling of the nominal model

Input-output scaling of the nominal model proved to be a very important stage in the design process. This scaling cannot be performed automatically, based on the mathematical model alone; it has to be based on a sound understanding of the physical quantities involved. It must be present in any multivariable problem, and is performed by a combination of

normalization and choice of units. It proved to be especially important in H^{∞}-optimization since it defines the 'worst-case-direction'.

There is a complex interaction between this initial scaling and the subsequent selection of weighting functions. In simple problems it is possible to include the scaling in the weighting functions. It is recommended, however, that the scaling is performed first on the plant model, since then the weighting function selection is simplified.

To illustrate the need for scaling, consider the following sensitivity transfer function matrix with elements $S_{ij}(s)$

$$\begin{bmatrix} S_{11} & S_{12} & \cdot & \cdot \\ S_{21} & S_{22} & \cdot & \cdot \\ \vdots & \vdots & \vdots & \vdots \end{bmatrix} \qquad (6.1)$$

Each element may be regarded as the error introduced in the i-th channel by a change in the j-th. The diagonal elements are then non-dimensional and invariant with scaling. The off diagonal terms have a dimension given by the units of the i-th channel divided by those of the j-th. The magnitude of these terms will be affected by scaling. In problems that attempt to minimize the sensitivity function, the system outputs should be scaled so that equal magnitude errors in each channel are considered equally important. This ensures that the cost function will not be dominated, unnecessarily, by any particular interaction.

Similarly, when the control inputs to a plant are penalized it is important to ensure that equal magnitudes in each channel have a similar effect on the plant. This must also include knowledge of the available actuator signal amplitude limits.

An additional benefit of scaling the plant model is that this should improve the numerical conditioning of the design process, and the

resultant controller. The controller will in fact be appropriately scaled for Hankel and infinity norm based model reduction procedures.

The following choice of units was made for the design in this chapter. These should not be considered to be optimal in any sense, although a considerable number of iterations were used in order to find a reasonable set.

Outputs:	(1)	γ	5 degrees
	(2)	p	0.5 rad/s
	(3)	q	0.2 rad/s
	(4)	v	20 ft/s
	(5)	θ	0.2 rad
	(6)	ϕ	0.5 rad

Inputs: All in degrees

The units chosen for the rates were such that, with the desired response, a step demand in θ, say, required an equal magnitude peak response in q.

Note that this scaling involves only simple multiples of the units used in the non-linear model. Different selections were used on the plant inputs but were not found to be necessary in this example.

6.5 Weighting function selection

Problem:

$$\min_{\text{stabilizing } K} \left\| \begin{matrix} W_1 \, S \, W_i \\ W_2 K S \, W_i \end{matrix} \right\|_\infty \qquad (6.2)$$

It is proposed to find a controller satisfying the control objectives in section 6.3 by appropriate choices of W_1, W_2 and W_i. In earlier attempts to solve this problem an additional term $W_3 T W_i$ was appended to the cost function to penalize the closed-loop transfer function, particularly at high frequency [POS8]. This unfortunately tended to introduce very fast modes into the controller which were undesirable for implementation. Fortunately it was found that, since $T = GKS$, an appropriate penalty on KS was sufficient to control T.

As in the example in Chapter V, it will be assumed that the design is successful when the cost function is $\simeq 1$. This is useful in choosing the weighting functions.

W_1: The performance and disturbance rejection objectives require the sensitivity function S to be small, particularly at low frequency. The weighting functions used for W_1 are therefore generally low-pass in nature, and greater than 1 over a range of low frequencies. For this design it was decided to let W_1 have a modulus of 40 at low frequency and be > 1 for $\omega < 1$ rad/s. This ensures that the resulting closed-loop system has a d-c error of less than 2.5%. It was found that this d-c error could be reduced further without increasing the cost function, provided that the unity gain cross-over was not changed. Unfortunately it was not possible, with the available software, to force the controller to contain integral action. The value of 40 in the weight was obtained from earlier examples in which larger values tended to cause numerical problems.

Band-pass filters were used on the rate channels p and q to provide disturbance and cross-coupling rejection at frequencies between 1 and 2.5 rad/s. It was not possible to obtain good sensitivity in all channels over the same frequency range, because of the non-square controller.

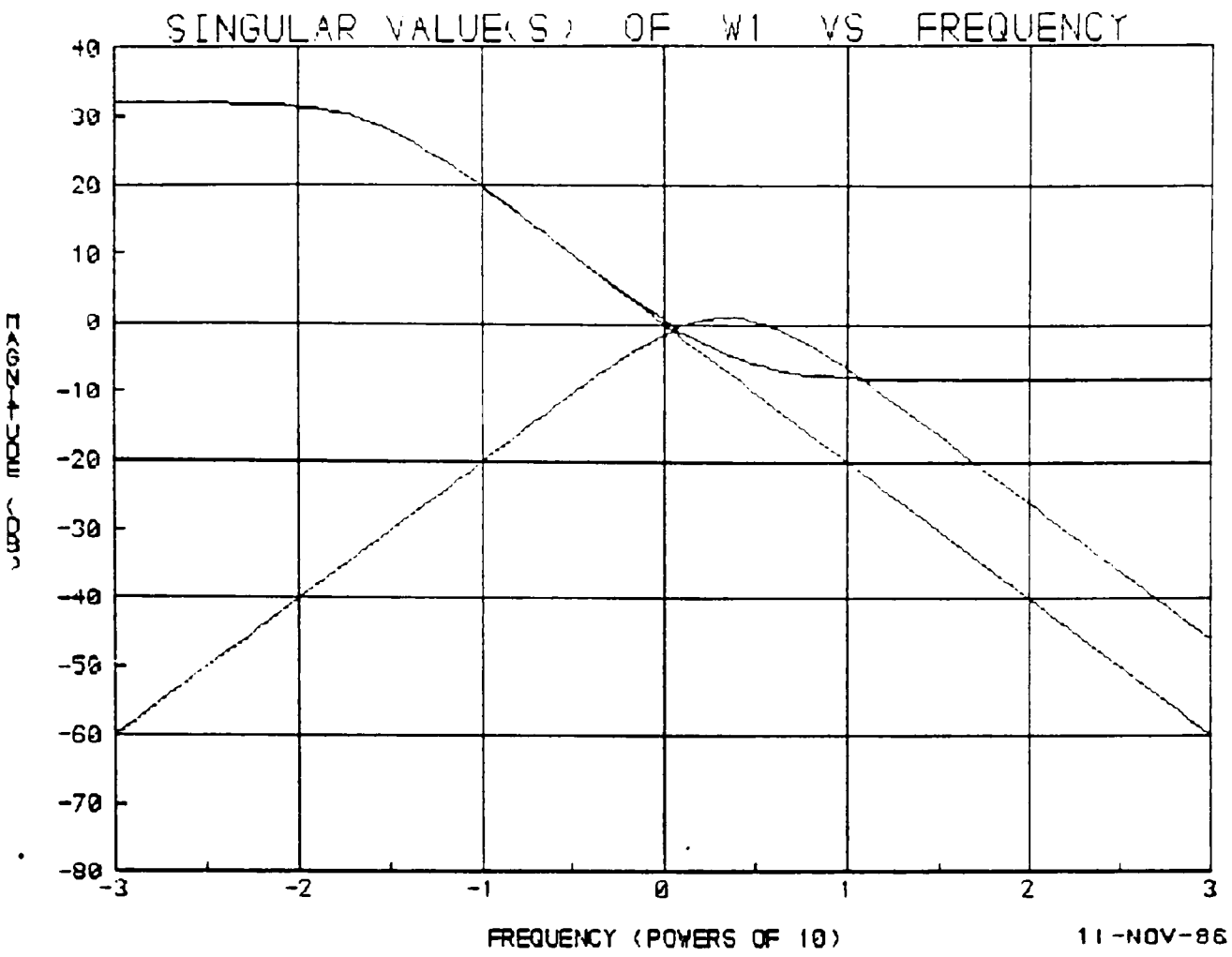


Figure 6.1

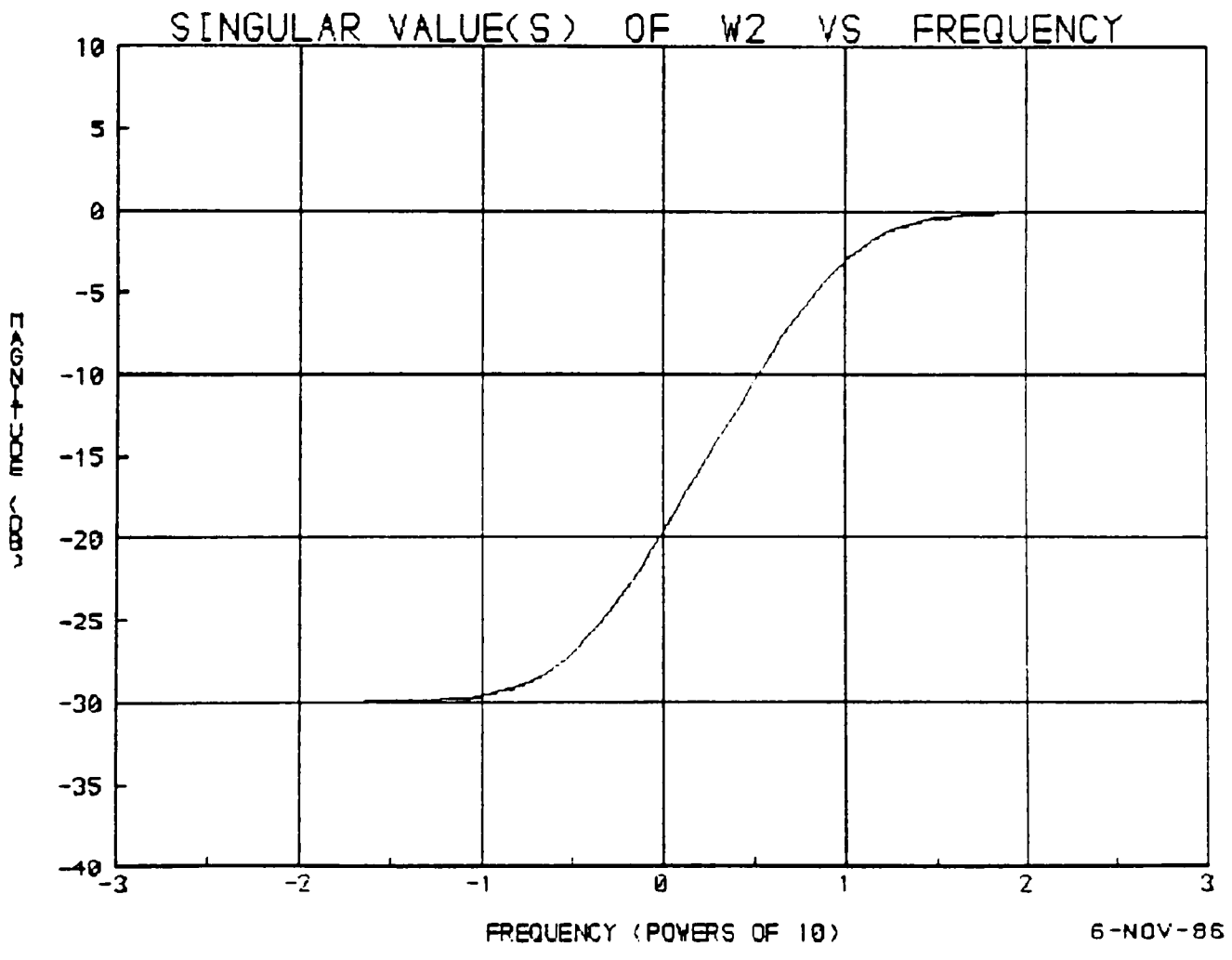


Figure 6.2

In tuning the weighting functions it was found that a finite attenuation of W_1 in the γ and v channels was useful to reduce overshoot in step responses. A magnitude plot of the final W_1 is given in Figure 6.1. Note that the band-pass filters are second order, the rest are first order.

W_2: The primary robustness requirement was that the system should roll off before 10 rad/s. This was ensured by using first order highpass filters with a cut off frequency of 10 rad/s. A low frequency gain of 30dB was used so that W_1 S W_i clearly dominates the cost function at low frequency (Figure 6.2). This weighting function was also found to effectively constrain the magnitudes of the poles in the controller.

W_i: This is used to reflect magnitudes of command or disturbance signals in each channel. A value of 0.1 was used on the rates and 1 on each of the other channels. The value of 0.1 on the rates (which are not directly controlled) was chosen, so that some disturbance rejection is obtained on these outputs without significantly affecting the cost.

6.6 Controller selection

As discussed in Chapter V, the optimal controller is not unique; different controllers may be generated by the technique used to solve the anti-causal approximation problem. From earlier design work it became clear that the most satisfactory results (judged by closed-loop time responses) were obtained when only the maximum singular value of the cost function was constant and equal to the H^∞-norm. The singular value plot of the cost function, with the controller to be used in the rest of this chapter, is given in Figure 6.3. To illustrate the freedom in controller selection, Figure 6.4 has four of the singular values constant equal to the maximum.

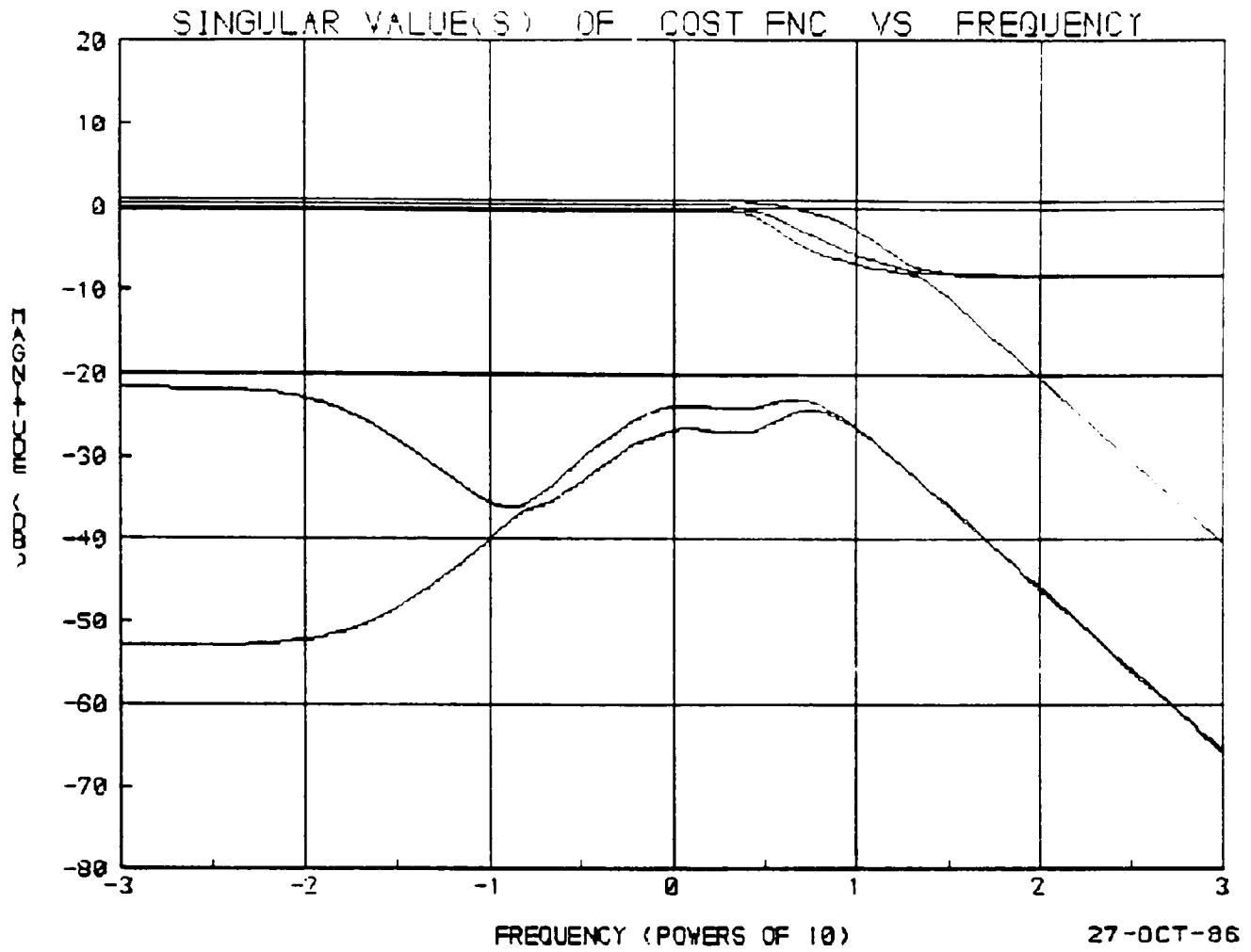


Figure 6.3

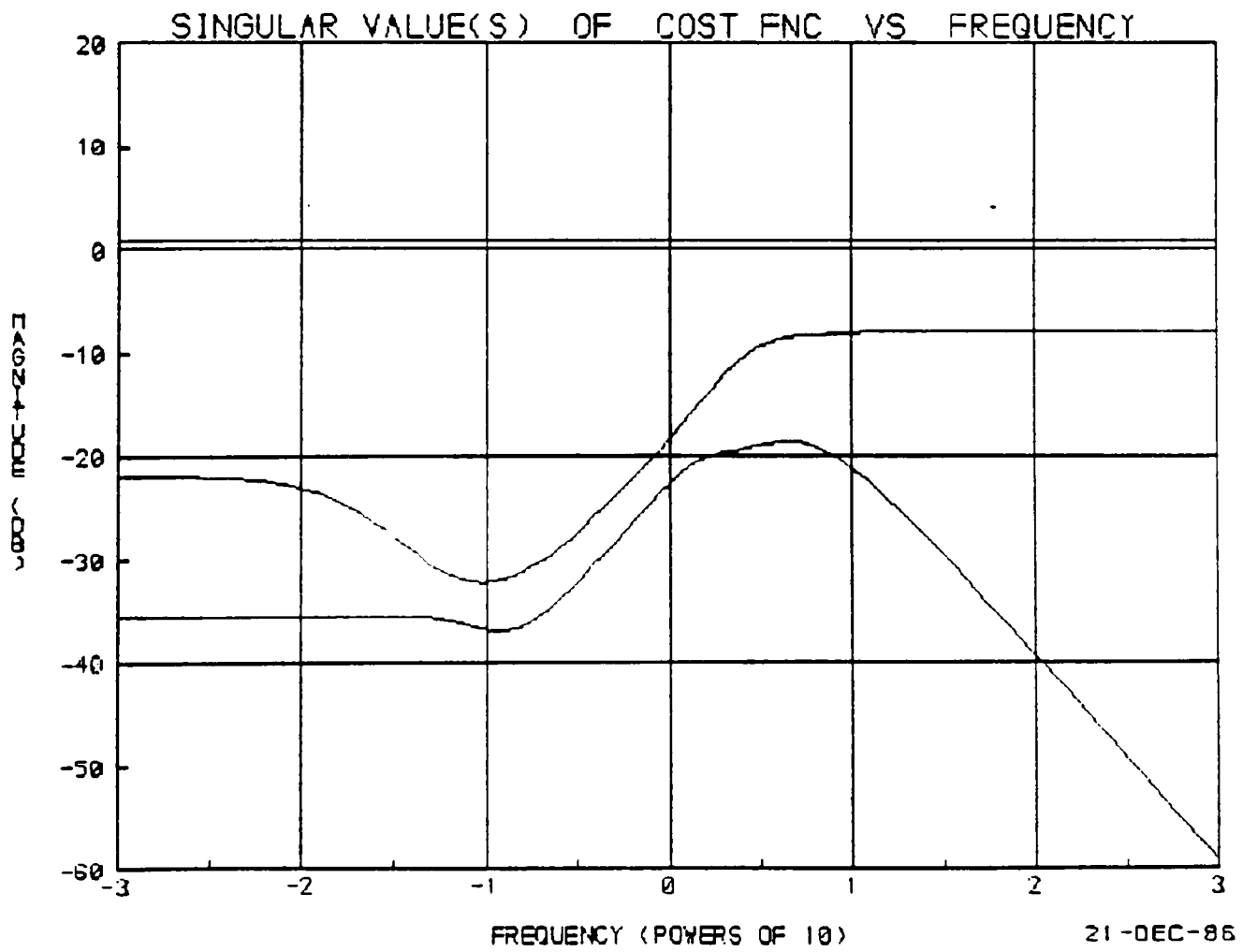


Figure 6.4

On output from the design procedure both controllers had a state dimension of 59. The first is used as an example in Chapter VIII, where it is clear that a 'minimal' dimension is 18. The second controller was unstable, but after decomposition and 'minimal realization' of the stable part, this controller also had a state dimension of 18. The maximum singular values of the cost function for this controller are given in Figure 6.5 (note use of dB scale on the magnitude).

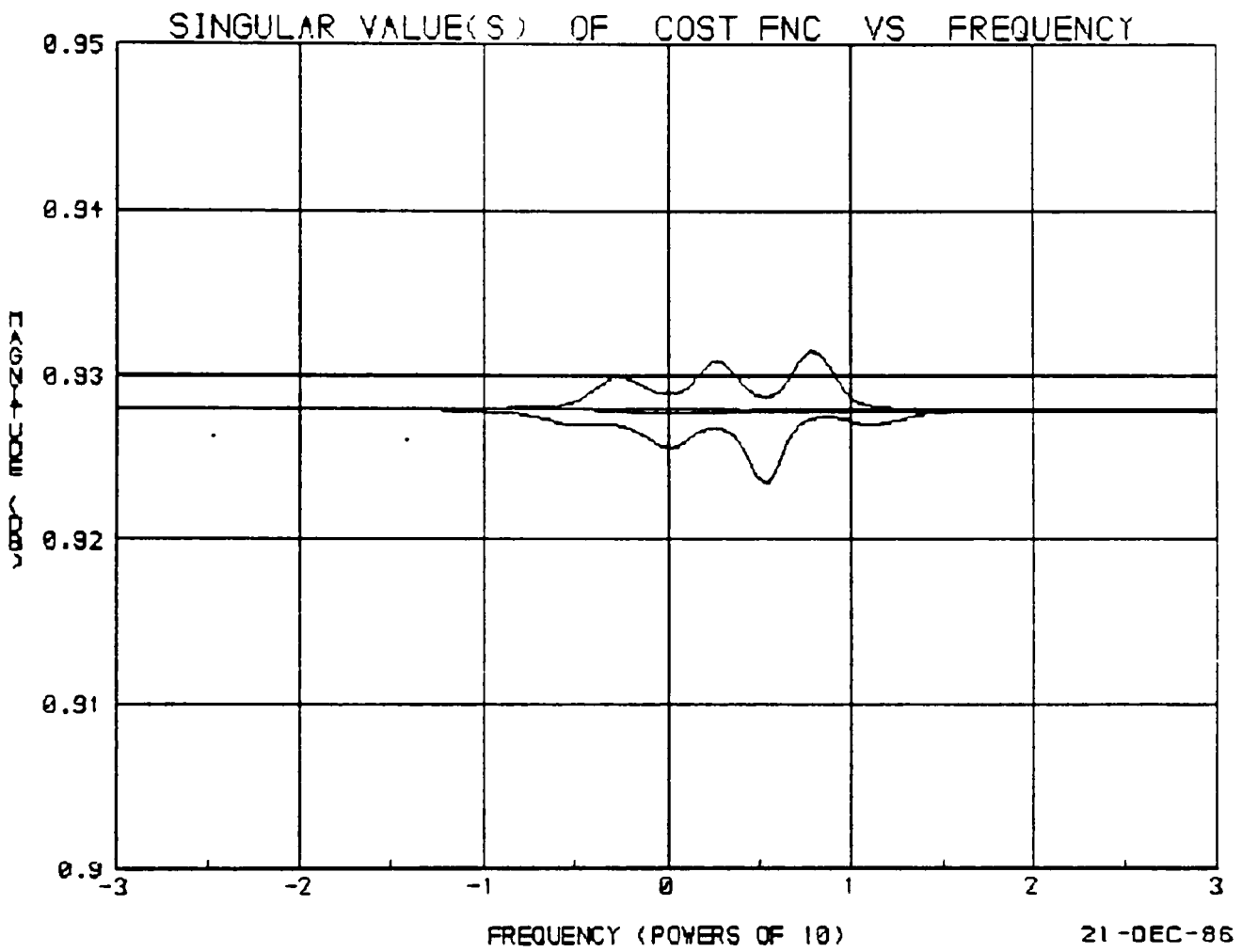


Figure 6.5

The poles of the controllers are given in the table below. The second controller would be undesirable from implementation issues, and its time response characteristics were in any case not as good as those presented in the remainder of this chapter.

No.	Controller poles		Alternative controller poles	
	Real	Imag.	Real	Imag.
1	-6.68	1.35	-29.4	
2	-6.68	-1.35	-10.0	
3	-4.59		-5.65	
4	-4.31		-2.67	
5	-3.70		-2.50	
6	-3.36	2.85	-2.00	
7	-3.36	-2.85	-1.96	3.99
8	-2.51		-1.96	-3.99
9	-2.50		-1.89	
10	-2.00		-1.32	0.740
11	-2.00		-1.32	-0.740
12	-1.64	3.25	-0.025	
13	-1.64	-3.25	-0.025	
14	-0.025		-0.025	
15	-0.025		-0.025	
16	-0.025		-0.017	
17	-0.025		1.44	
18	-0.017		19.3	

6.7 Closed-loop frequency responses

The singular value plots of the closed-loop frequency response functions S, KS and T are given in Figures 6.6 to 6.8. For comparison purposes a singular value plot of the open-loop scaled plant is given in Figure 6.25, and the controller in Figure 6.26. These diagrams are not easy to interpret because the plant and controller are both non-square. By examining these figures in the light of the robustness inequalities given by equations (2.12)-(2.14) in Chapter II, it is possible to assess the achieved robustness properties of the closed-loop system.

S(s):

The sensitivity transfer function matrix S(s) has 6 inputs and 6 outputs (e.g. reference and error signal vectors). Since the plant has only 4 control inputs it is not possible to achieve good tracking error response in every direction at the same frequency. This results in S(s) having 2 eigenvalues = 1.0 and in Figure 6.6, 2 singular values $\geq$ 1.0 at every frequency. The 4 singular values that are small at low frequency must correspond to the controlled outputs which were weighted in the problem definition. The other 2 are a result of the inherent interaction between the aircraft attitudes and angular rates. (A singular value decomposition of S(s) could be used to verify this.)

The maximum singular value of S(s) determines the size of the smallest unstructured output inverse multiplicative perturbation $\tilde{\delta}_o$ that could destabilize the system. Clearly the peak in Figure 6.6 of $\simeq$ 10 dB causes the greatest concern. From equation (2.14) this requires $\tilde{\delta}_o(\omega=0.25\text{rad/s}) < 0.3$. If the smallest value of $\tilde{\delta}_o(s)$ over all frequency = α, then, using the formulae in [LEH2], this measure of robustness guarantees a gain margin of $\left(\frac{1}{1+\alpha}, \frac{1}{1-\alpha}\right)$ and a phase margin of $\pm 2\sin^{-1}(\alpha/2)$. For this example there is a therefore a guaranteed gain margin of (0.77,3.3) and a phase margin of $\pm$ 17^o in every output channel. These values will, in most cases, be conservative since the system appears to be this sensitive only in one direction.

KS(s):

The transfer function KS(s) has 6 inputs and 4 outputs (the control signals) and therefore has 4 singular values. The closed-loop transfer function T(s) is equal to the product G(s)KS(s), and for good tracking at low frequency we require T(s) $\simeq$ I. The magnitude plot of KS(s) is therefore expected to be the inverse of that of the plant G(s) (Figure

6.8a) at low frequency. At high frequency |KS(s)| tends to 3dB (2.0), which is the inverse of the magnitude of W_2 in this range, as expected.

The maximum singular value in Figure 6.7 can be used to determine the smallest unstructured additive perturbation that will destabilize the system. From equation (2.12) at low frequency this size of e(s) is only -17dB (0.14) when some components of the plant frequency response G(s) are +24dB (16). This result demonstrates that the unstructured additive representation of uncertainty is not informative when the elements of the plant transfer function differ significantly in size. That the plant is not overly sensitive to uncertainty at low frequency may be obtained from equation (2.13) and T(s), from which it is clear that the system must be s3nsitive to this small perturbation in a direction in which its magnitude is small.

T(s):

The closed-loop transfer function T(s) has 6 inputs and 6 outputs (reference signal to output signal vectors). Since both the controller and plant are non-square this transfer function has 2 eigenvalues and therefore 2 singular values at zero over all frequency. The plant is strictly proper which results in T(s) strictly proper with all the singular values tending to zero at high frequency.

Figure 6.8 and equation (2.13) suggest that the closed-loop system is not destabilized by an output unstructured multiplicative uncertainty $\delta_o(s) < 0.3$ over all frequency. At low frequency $\delta_o(s)$ must be < 1.0 and at high frequency $\delta_o(s)$ can be very large. The assumed $\delta_o(s)$ corresponding to the omission of rotor dynamics from the nominal model was that $\delta_o(s) > 1$ for $\omega \geq 10.0$ rad/s. The H^∞-controller has therefore resulted in a closed-loop system that is robustly stable to this uncertainty, satisfying one of the major design objectives.

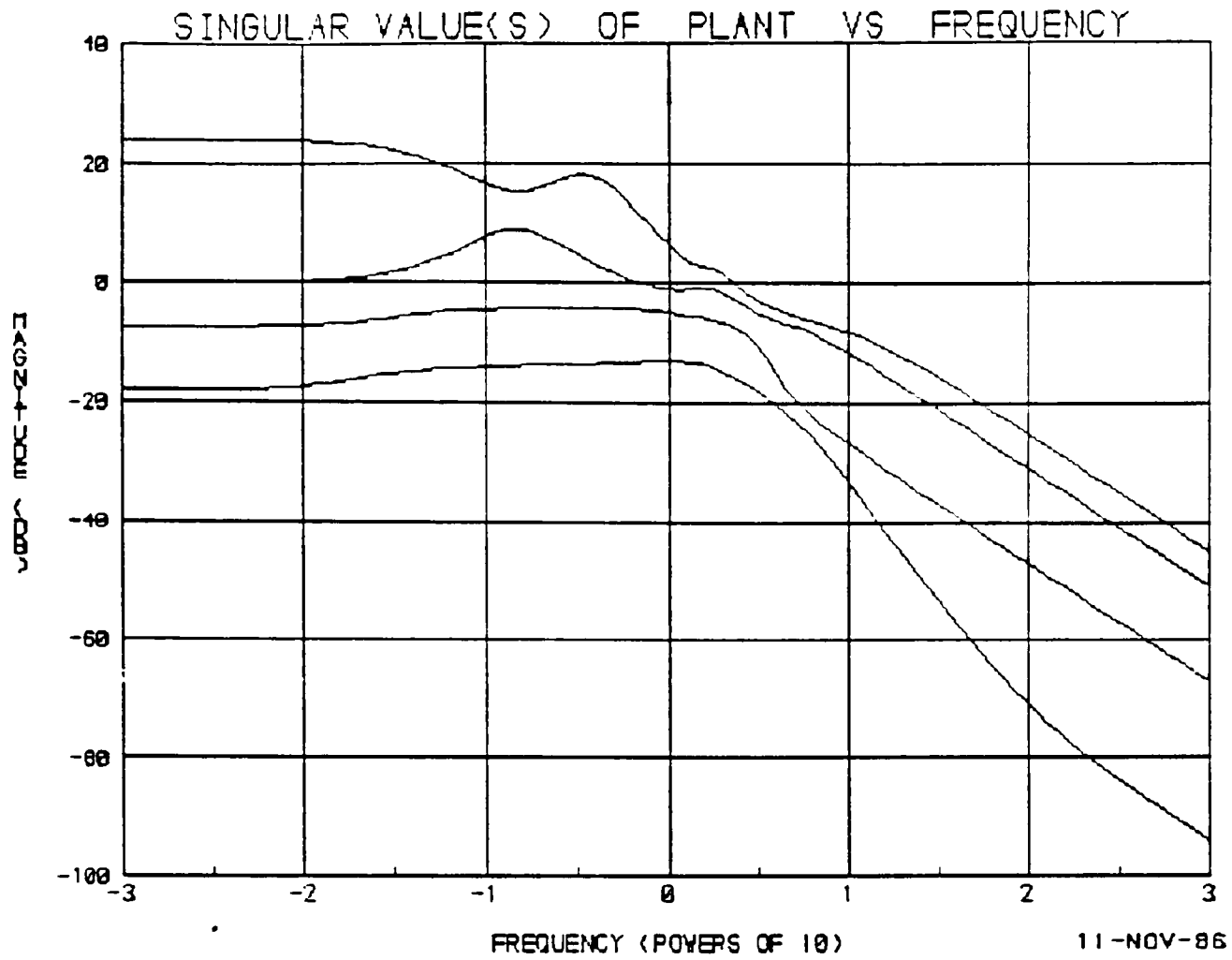


Figure 6.25

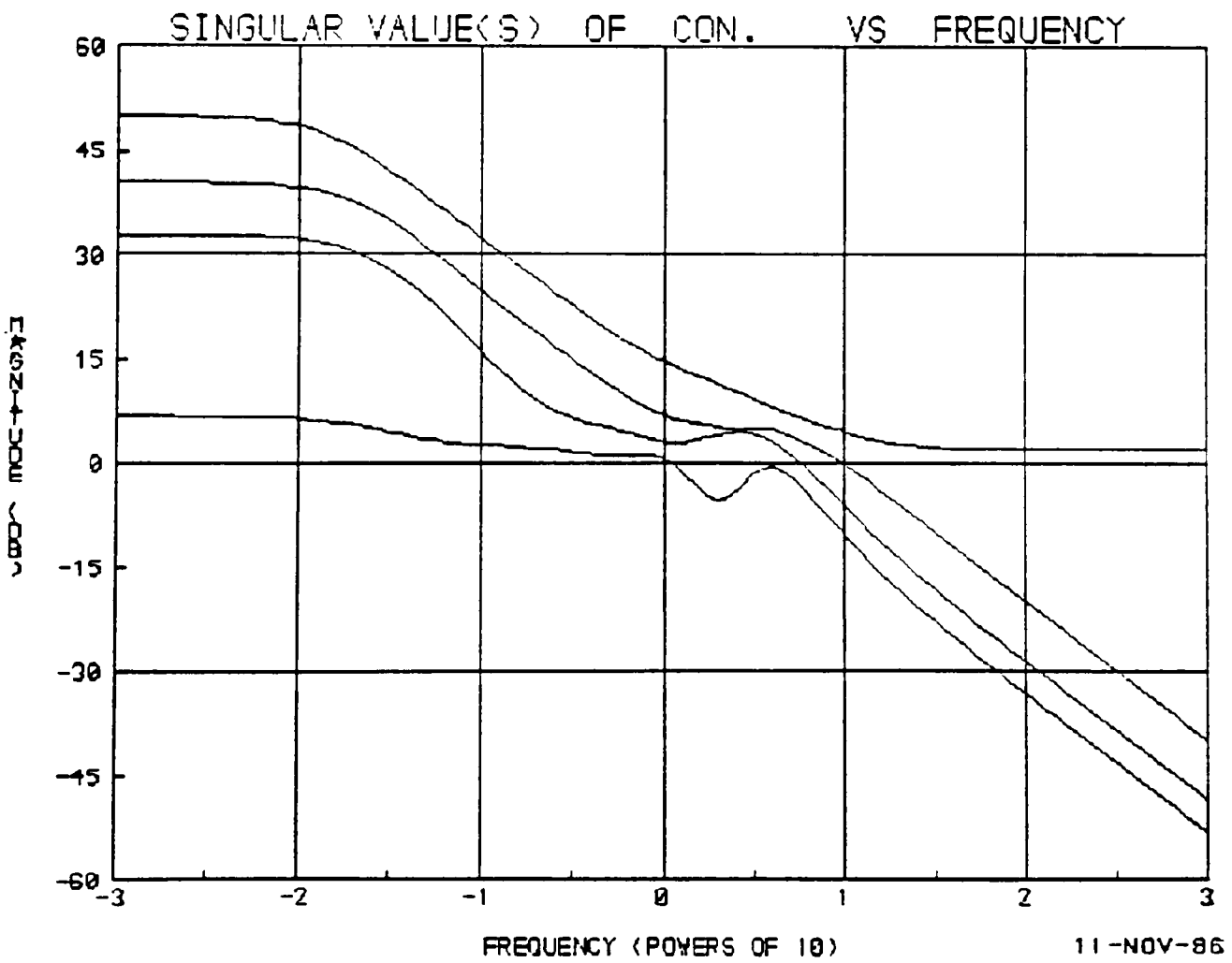


Figure 6.26

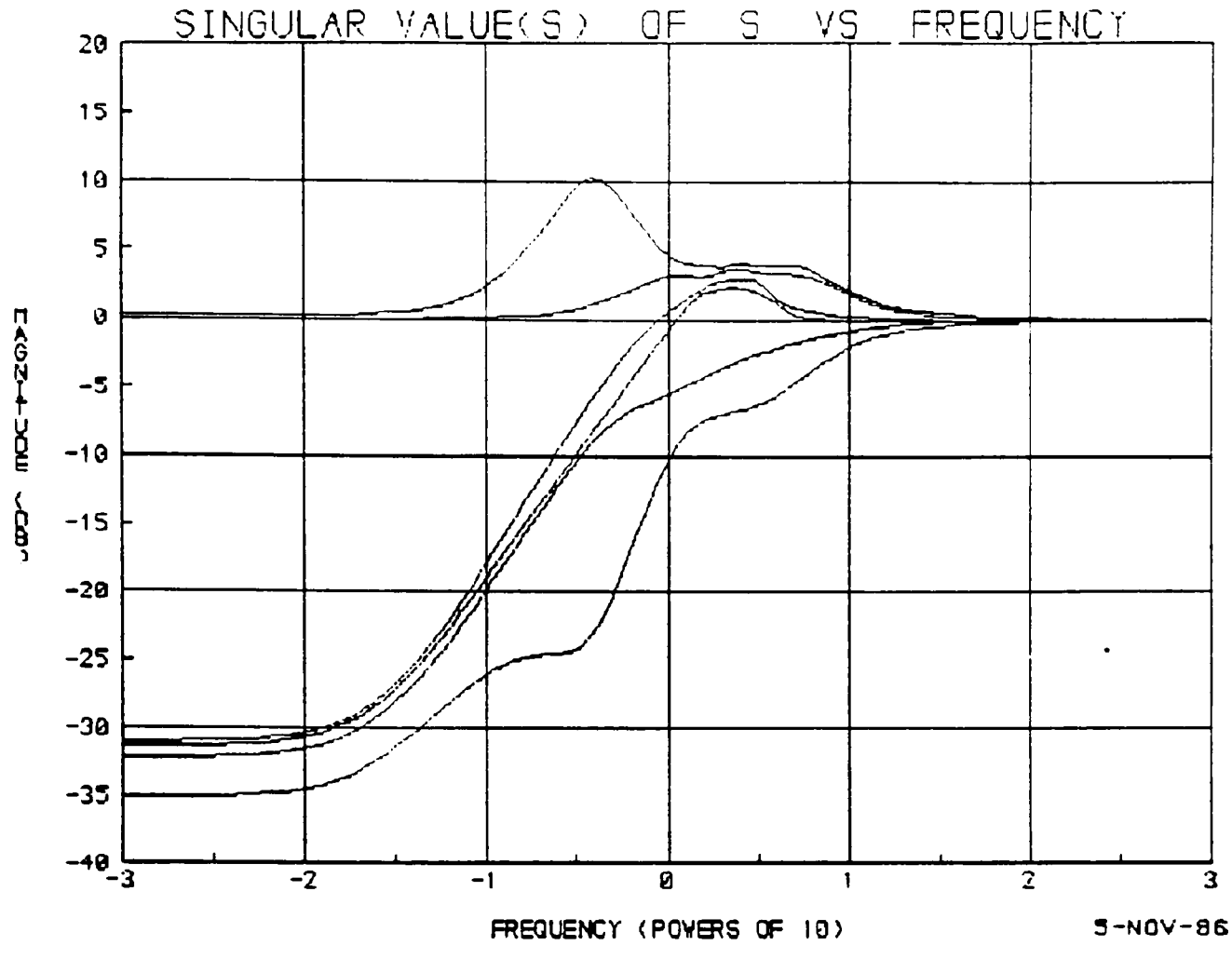


Figure 6.6

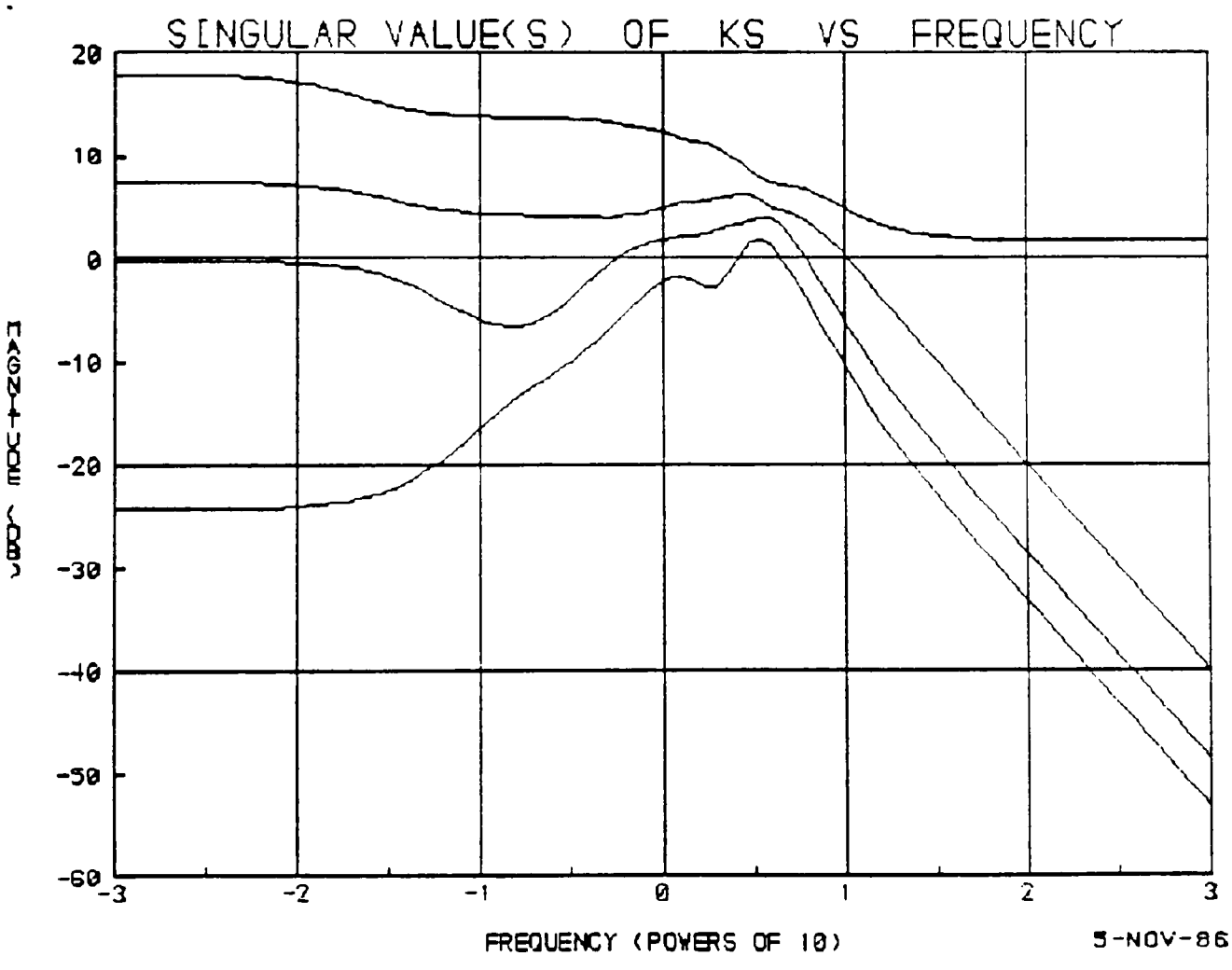


Figure 6.7

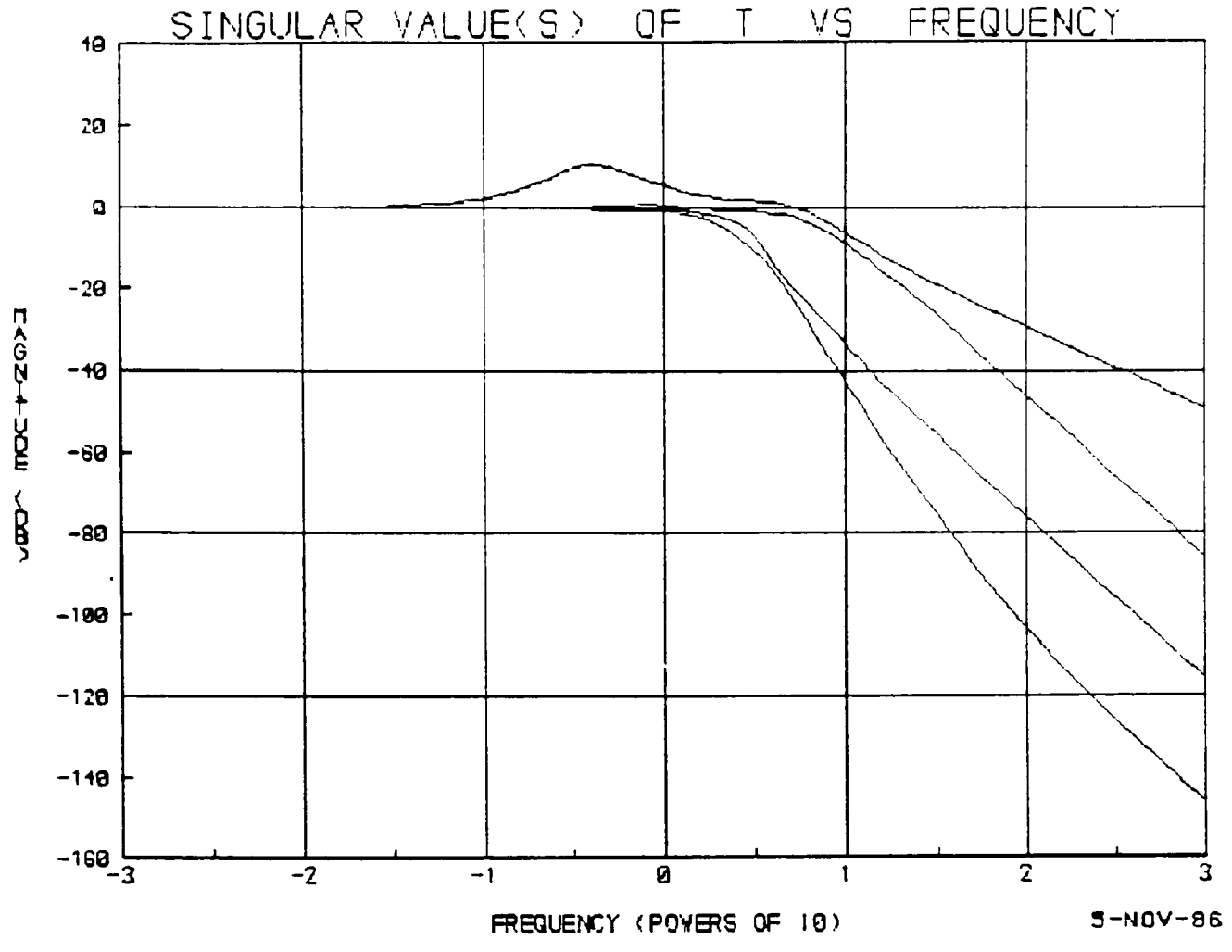


Figure 6.8

6.8 Linear time-responses

The closed-loop linear time-responses were used as the major indicator of the success of the design process. With the general guidelines on weighting function selection given in this and the previous chapter, it was found that a reasonable design could be obtained after only a few iterations. In order to improve on this initial design many further iterations were needed, particularly in the choice of scaling, in order to obtain equally 'good' responses in each loop. At each iteration it was important to appreciate that an increase in penalty on one term required a decrease on another, in order not to change the overall cost function. In this way it was possible to explore the inherent trade-offs in the design of a feedback controller for the plant.

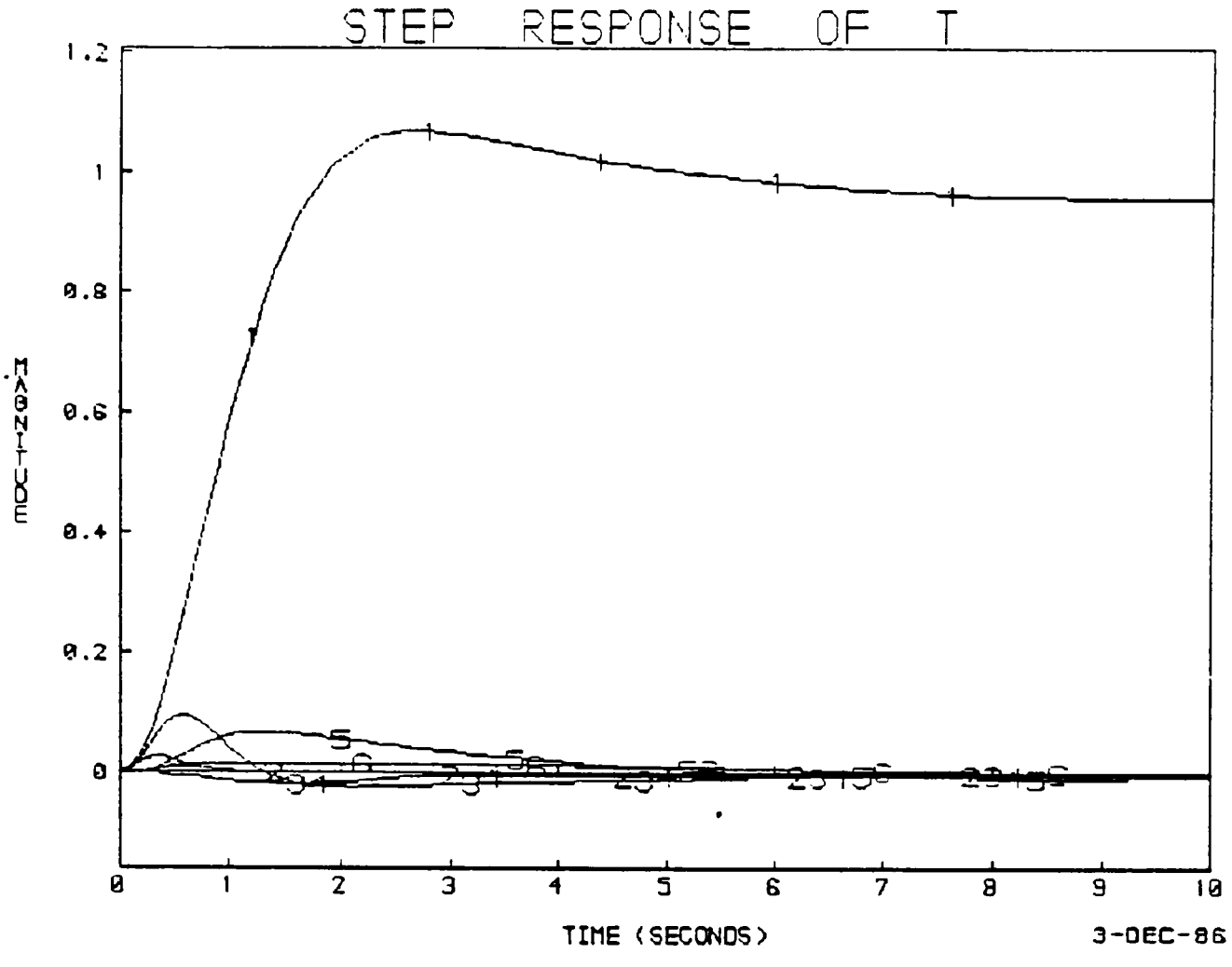


Figure 6.9 Output response to a step demand in channel 1

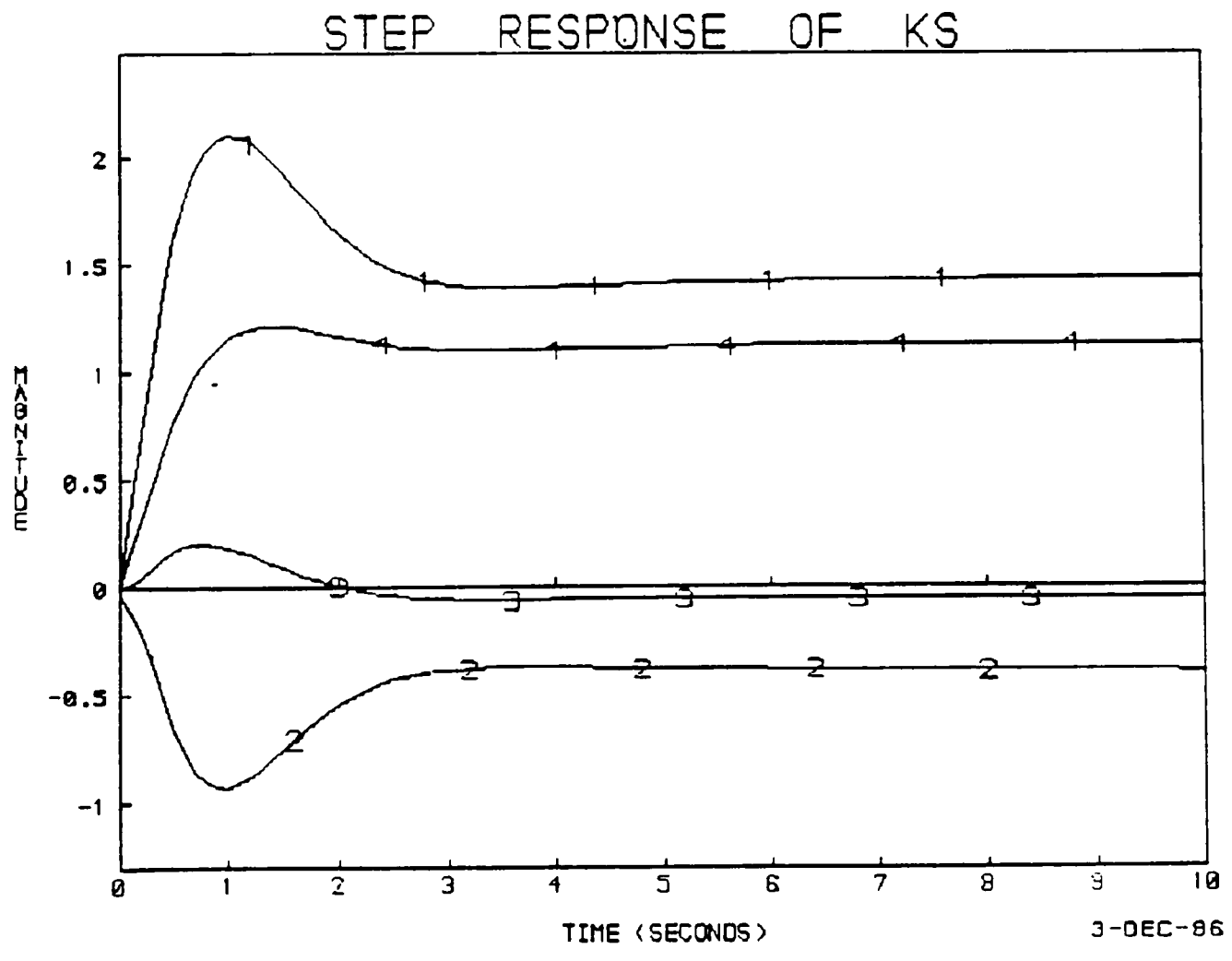


Figure 6.10 Control signal response to a step demand in channel 1

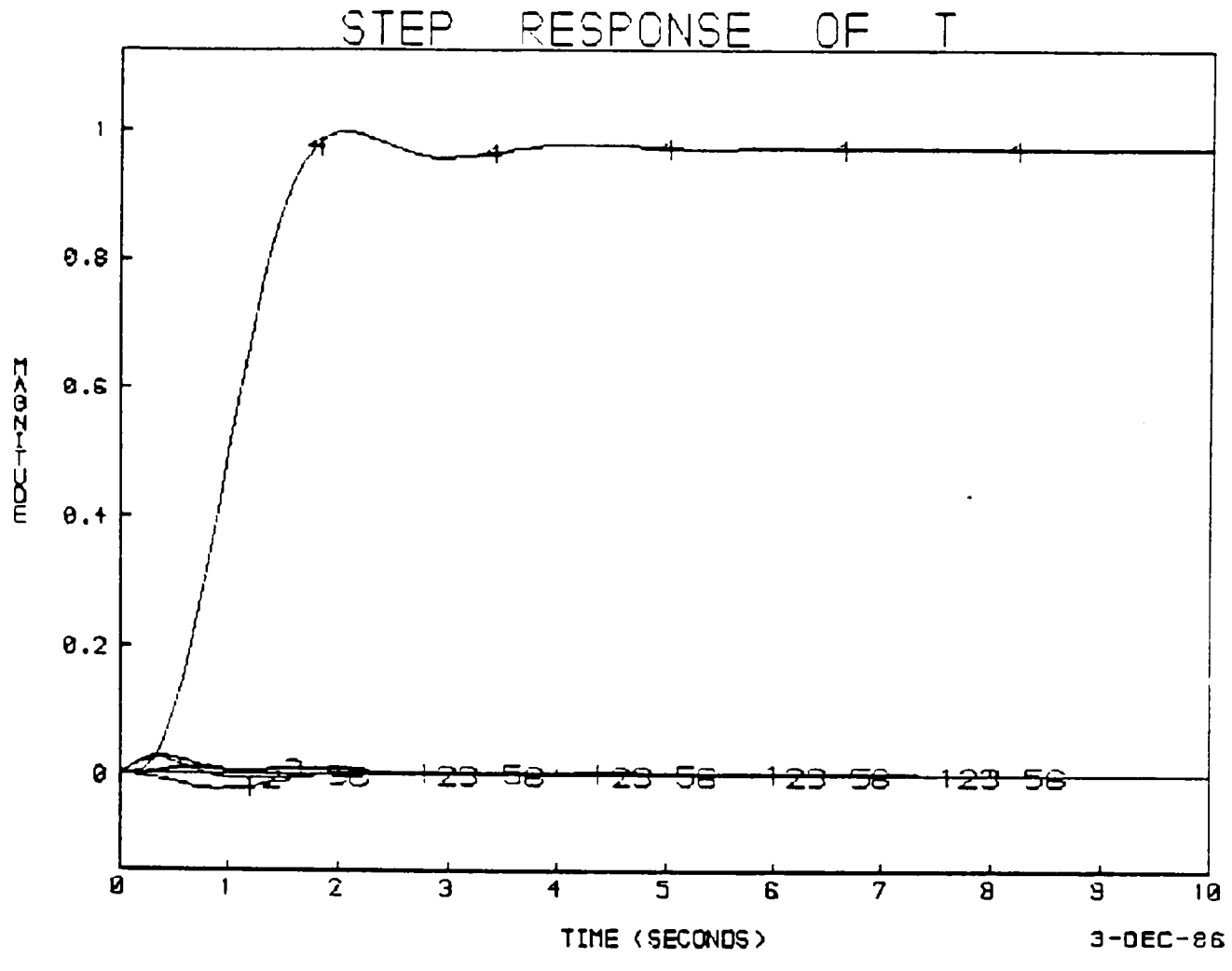


Figure 6.11 Output response to a step demand in channel 4

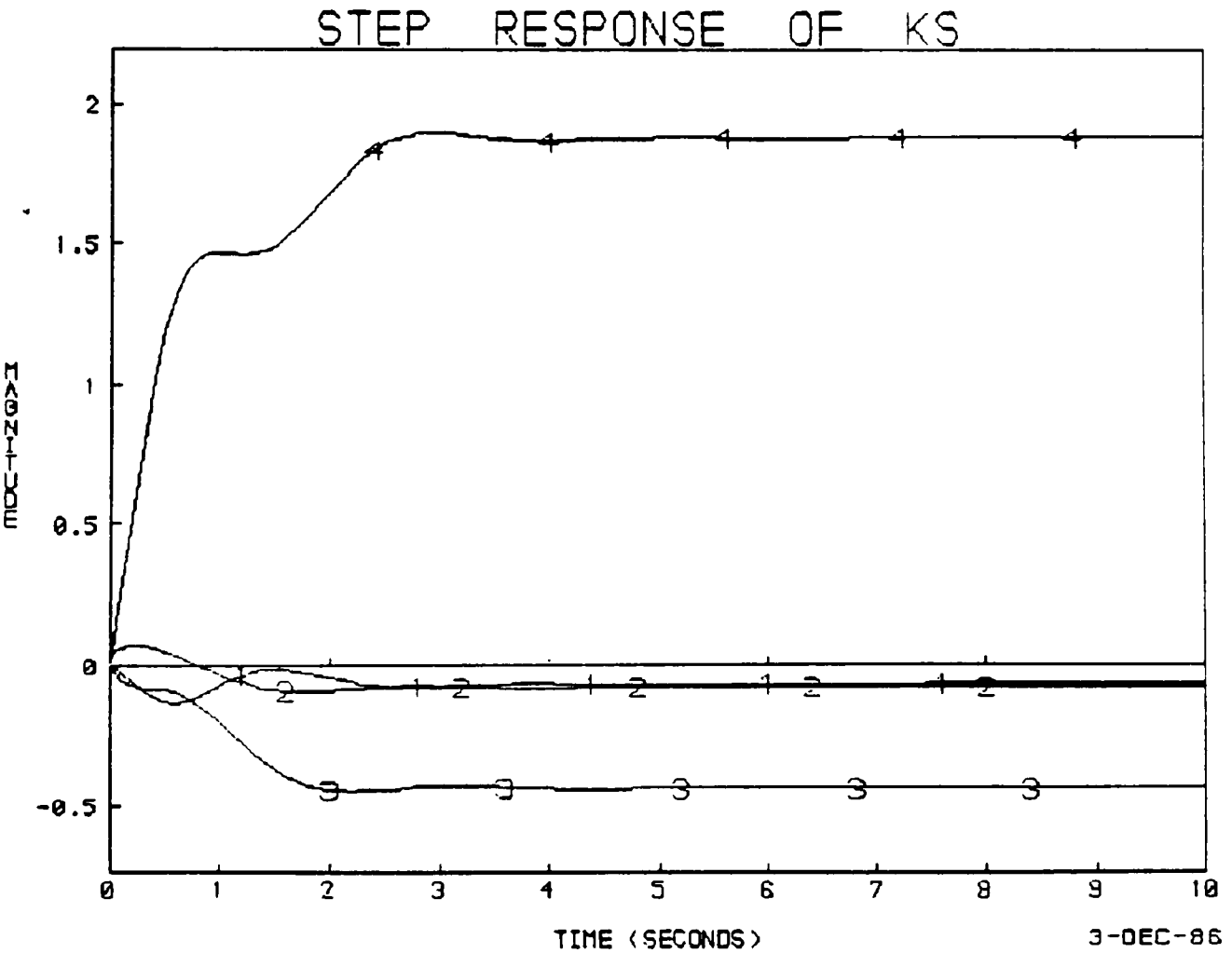


Figure 6.12 Control signal response to a step demand in channel 4

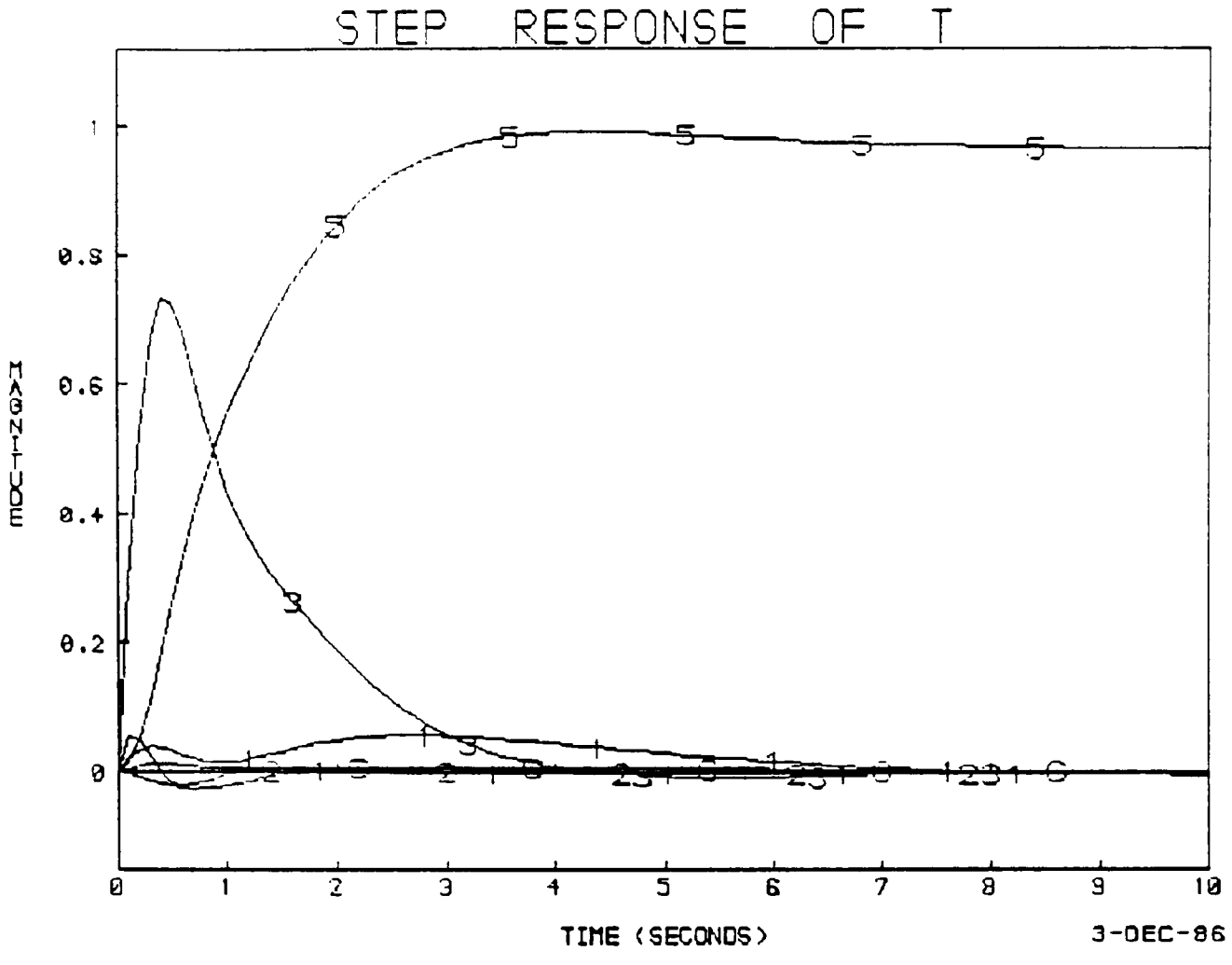


Figure 6.13 Output response to a step demand in channel 5

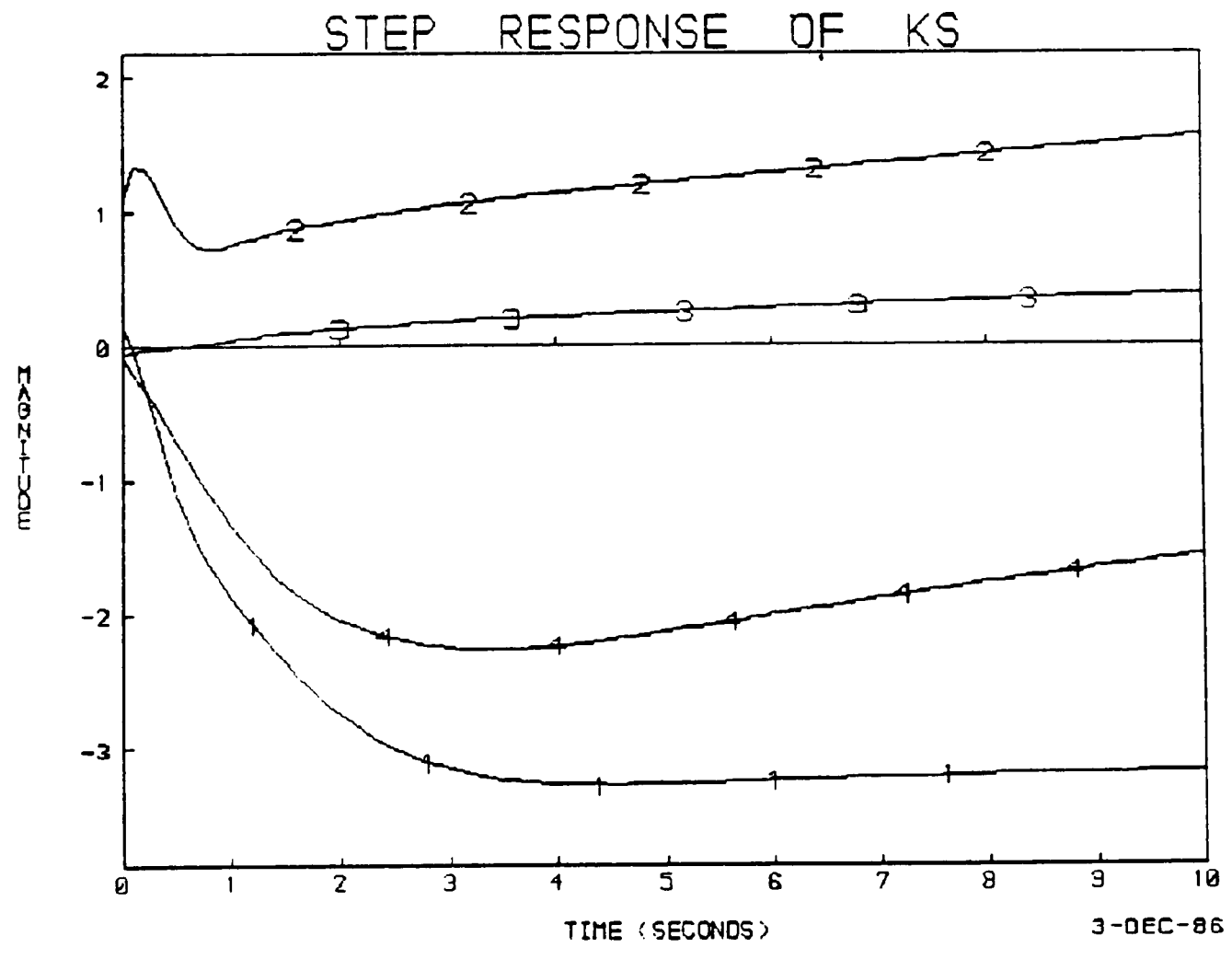


Figure 6.14 Control signal response to a step demand in channel 5

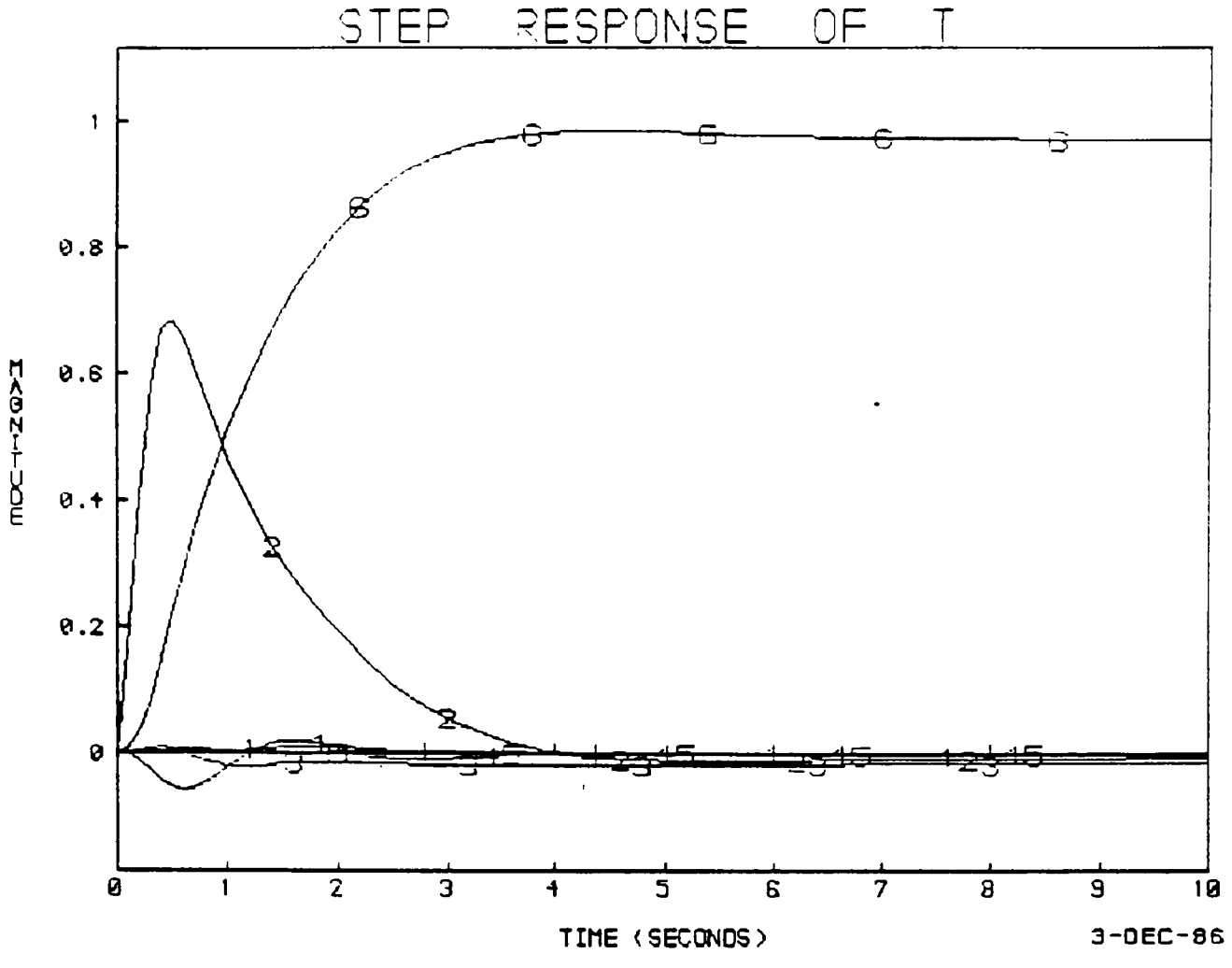


Figure 6.15 Output response to a step demand in channel 6

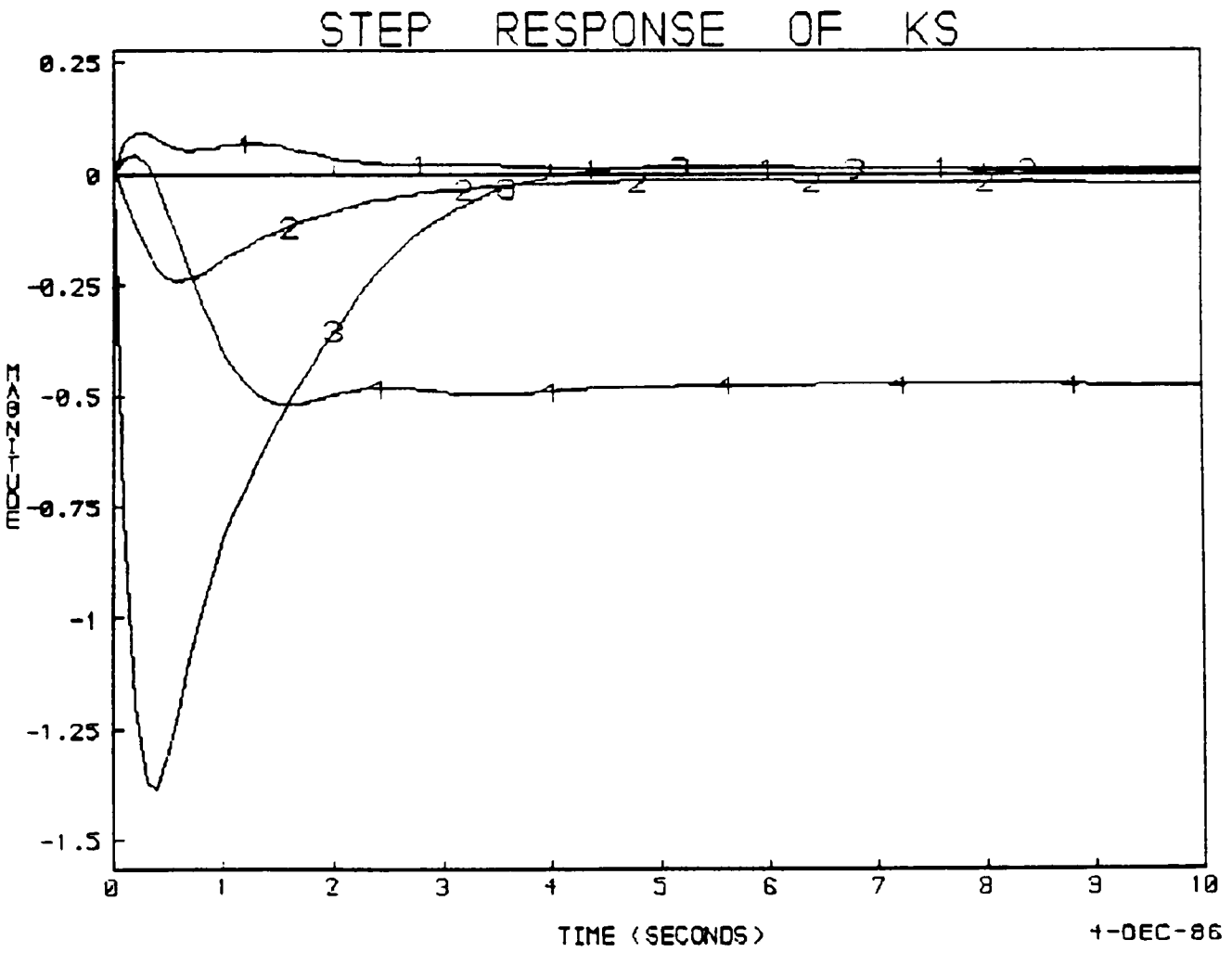


Figure 6.16 Control signal response to a step demand in channel 6

The closed-loop time-response of the outputs and control signals for unit step demands in each of the reference channels are given in Figures 6.9 to 6.16. The co-ordinated use of all the control inputs to perform each action illustrates the truly multivariable nature of the problem. Control over the pitch attitude (output 5) and its coupling with flight-path angle (output 1) proved to be most difficult. The control signal responses for a step demand in pitch (Figure 6.14) are stable, but take about 20 secs to settle.

These results were found to be sufficiently encouraging to proceed with the non-linear simulation.

6.9 Non-linear simulation

The linear controller was implemented in the non-linear simulation in an incremental manner. This enables the controller states to be initialized to zero at the start of a time-response, and they therefore do not need to be 'trimmed' to work about any particular operating point. Let (A,B,C,D) represent the controller state matrices; (x,r,y,u), the controller state, reference input, measurement signal and actuator input signal vectors; y_o and u_o , initial values. The control laws may then be written

$$\dot{x} = Ax + B\,(r-(y-y_o)) \qquad (6.3)$$

$$u = u_o + Cx + D\,(r-(y-y_o)) \qquad (6.4)$$

Although this is easy to implement, a big disadvantage of this 'black box' multivariable controller is that its loop structure is difficult to interpret. Further work on this would be required before such a controller structure could be used other than in simulation.

Airworthiness recognition for these controllers is an important area of future research.

Without modifying the helicopter simulation, it was not possible to 'ignore' the actuator dynamics, so all the non-linear time-responses include these. The non-linear response compared well with the linear ones in most respects. The most noticeable difference was the interaction between bank angle (PHIE, output 6) and flight path angle (GAMMA, output 1), not predicted in the linear model. Some improvement was obtained by reducing the size of units used to scale the flight path angle in the nominal linear model, but it was assumed that a more representative linear model or feedforward terms would be necessary in a more complete design.

The controller design was not changed when a version of the non-linear helicopter simulation with the rotor dynamics became available. The resulting time-responses are shown in Figures 6.17 to 6.24. These are not significantly different from the non-linear time-responses without rotor dynamics, (some interactions are worse), demonstrating the robustness of the design.

The non-linear time-response plots include a few extra variables which are part of the simulation. These are:

(1)	H (ft)	Height above ground
(2)	VTKT (knots)	Total air-speed
(3)	AZCG (g)	Normal acceleration at centre of gravity
(4)	PSIR (rads)	Heading angle
(5)	B1CW	rotor dynamics states
(6)	B1SW	rotor dynamics states

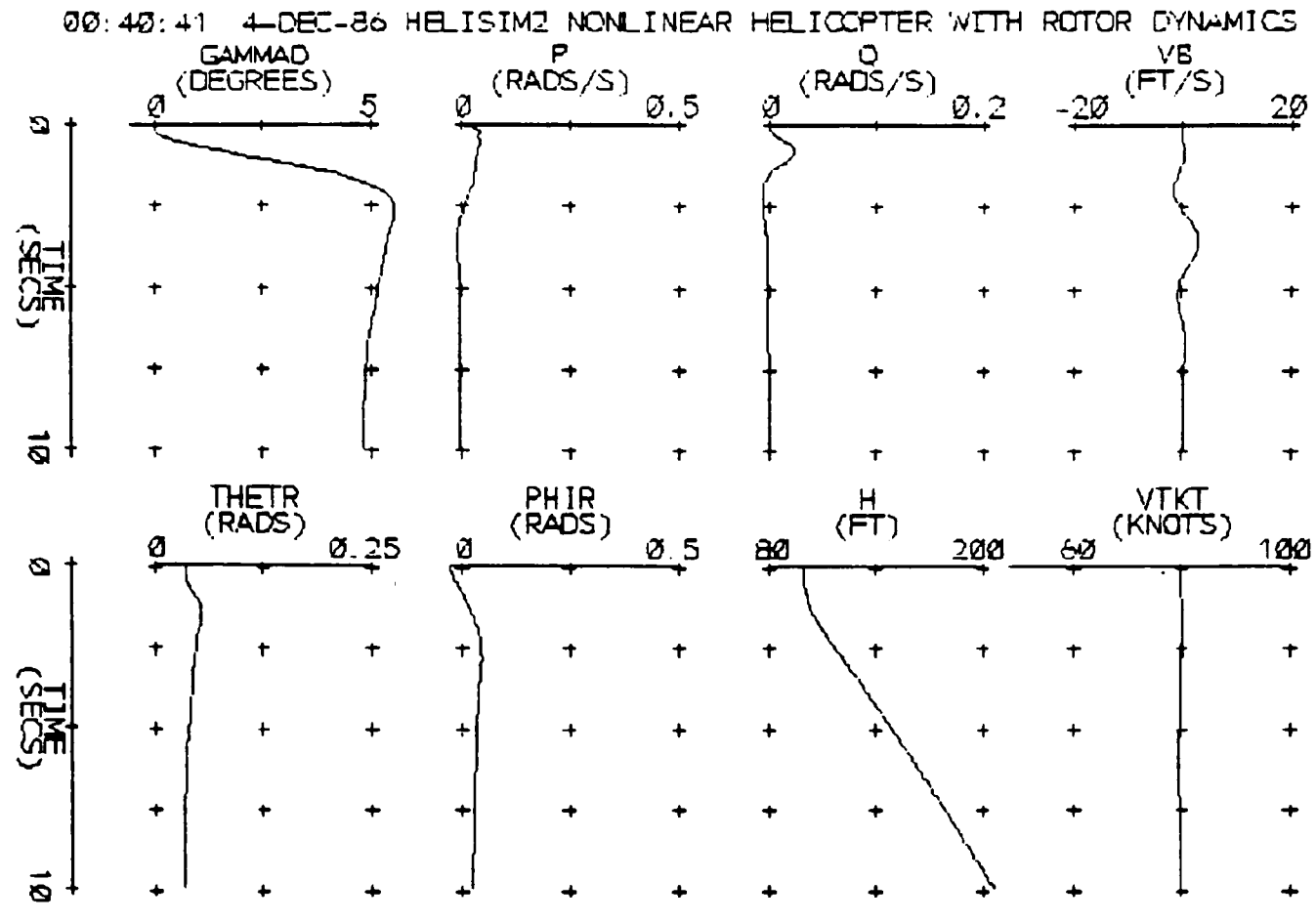


Figure 6.17 Response to a step demand in flight-path angle

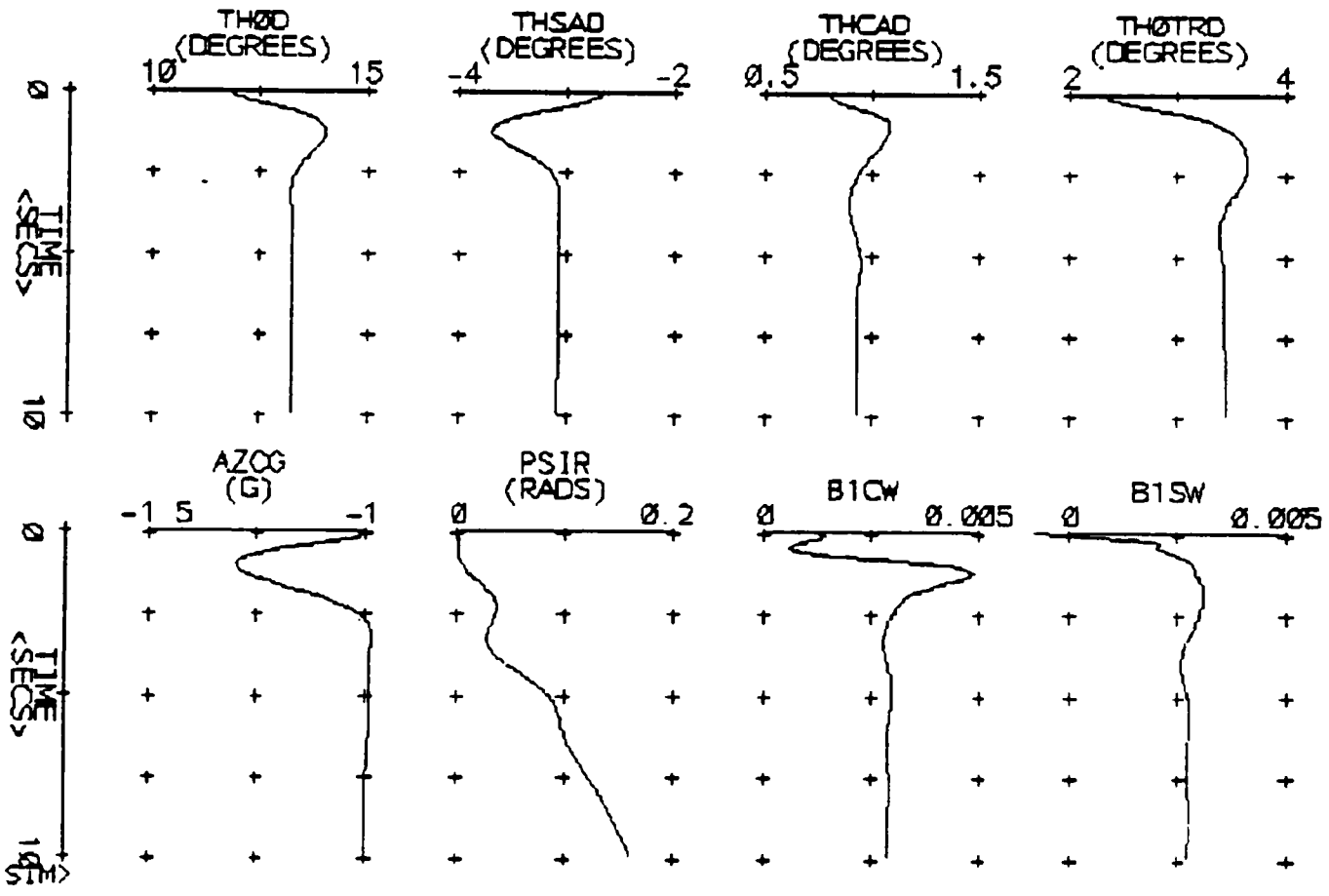


Figure 6.18 Response to a step demand in flight-path angle

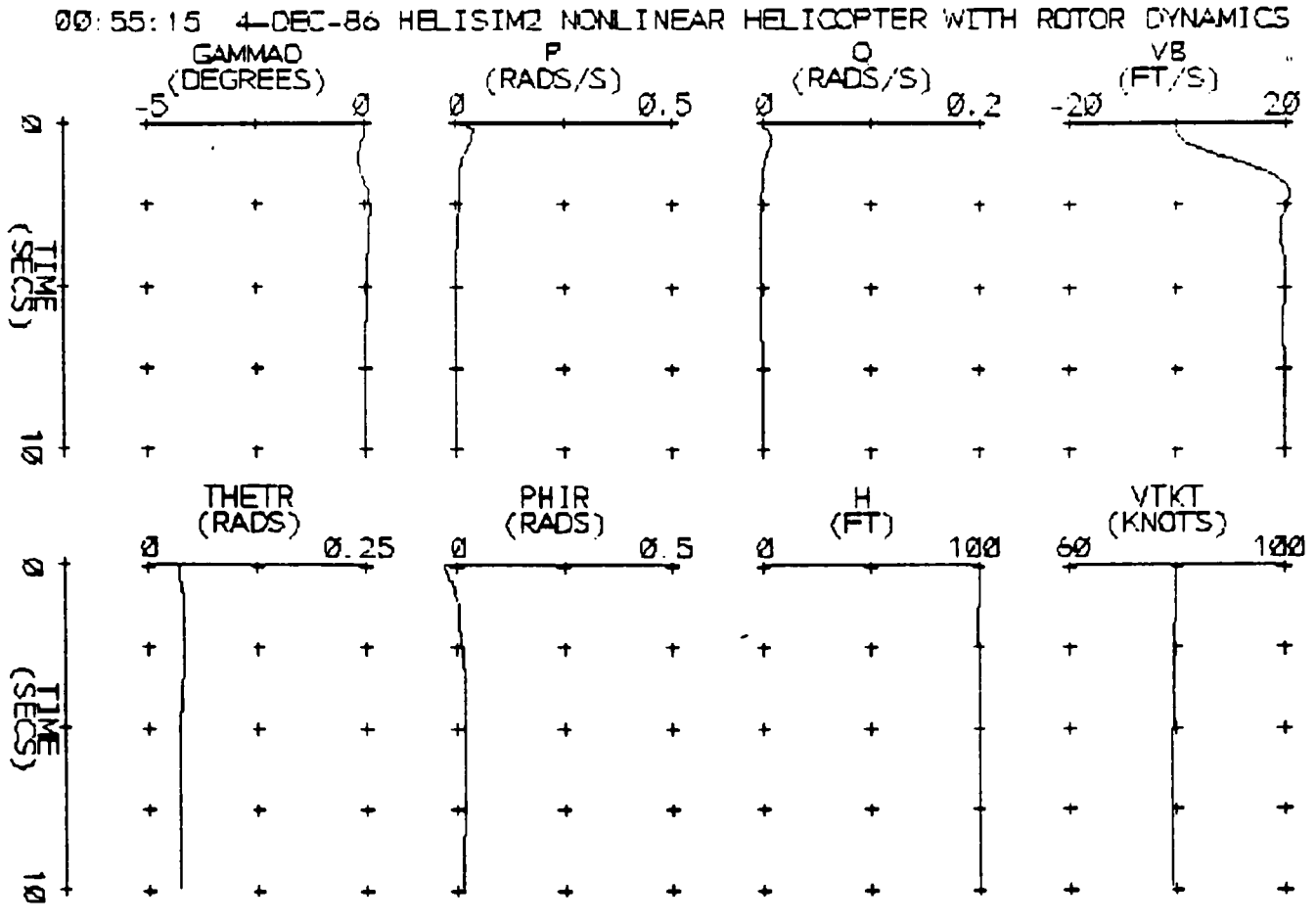


Figure 6.19 Response to a step demand in side-slip

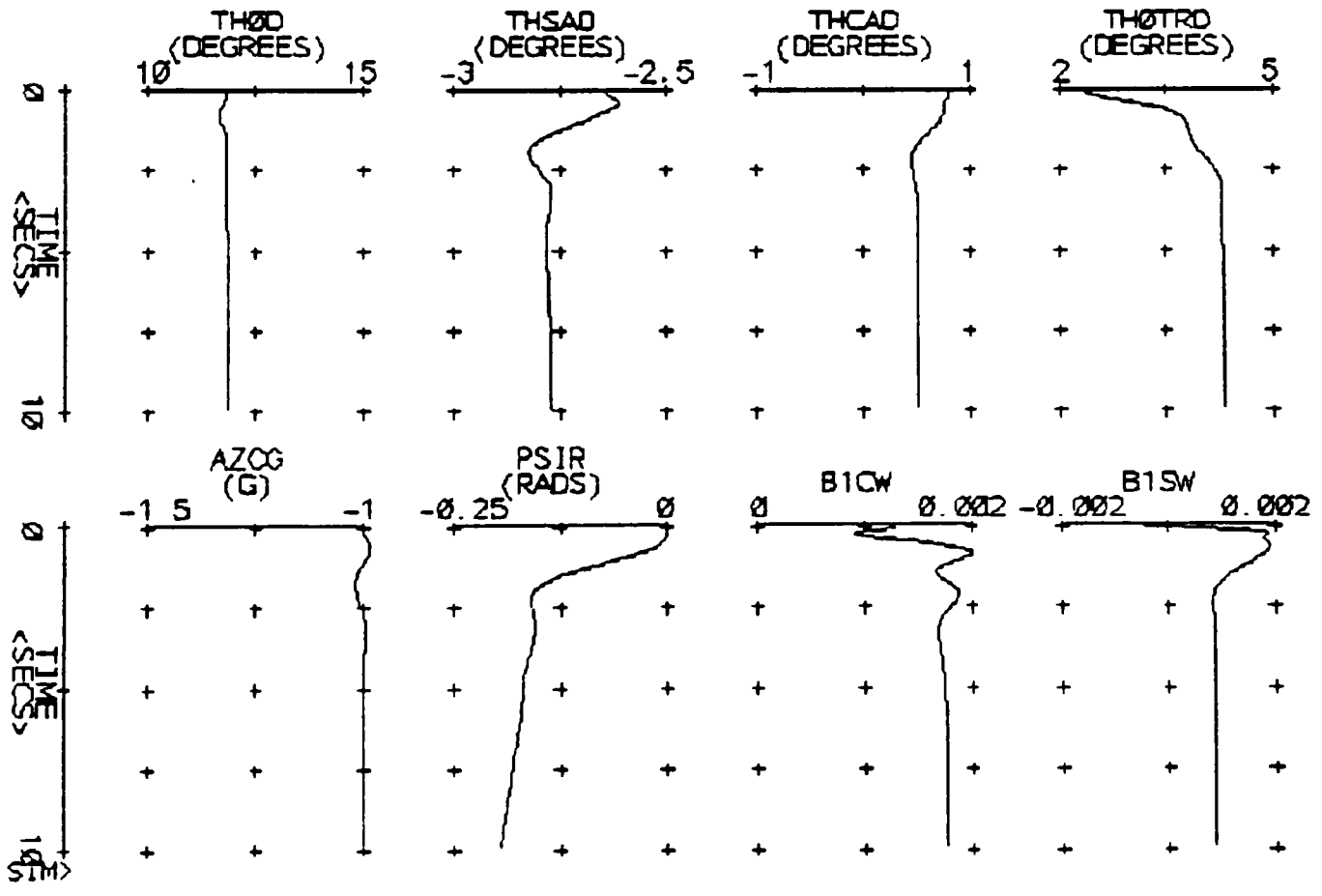


Figure 6.20 Response to a step demand in side-slip

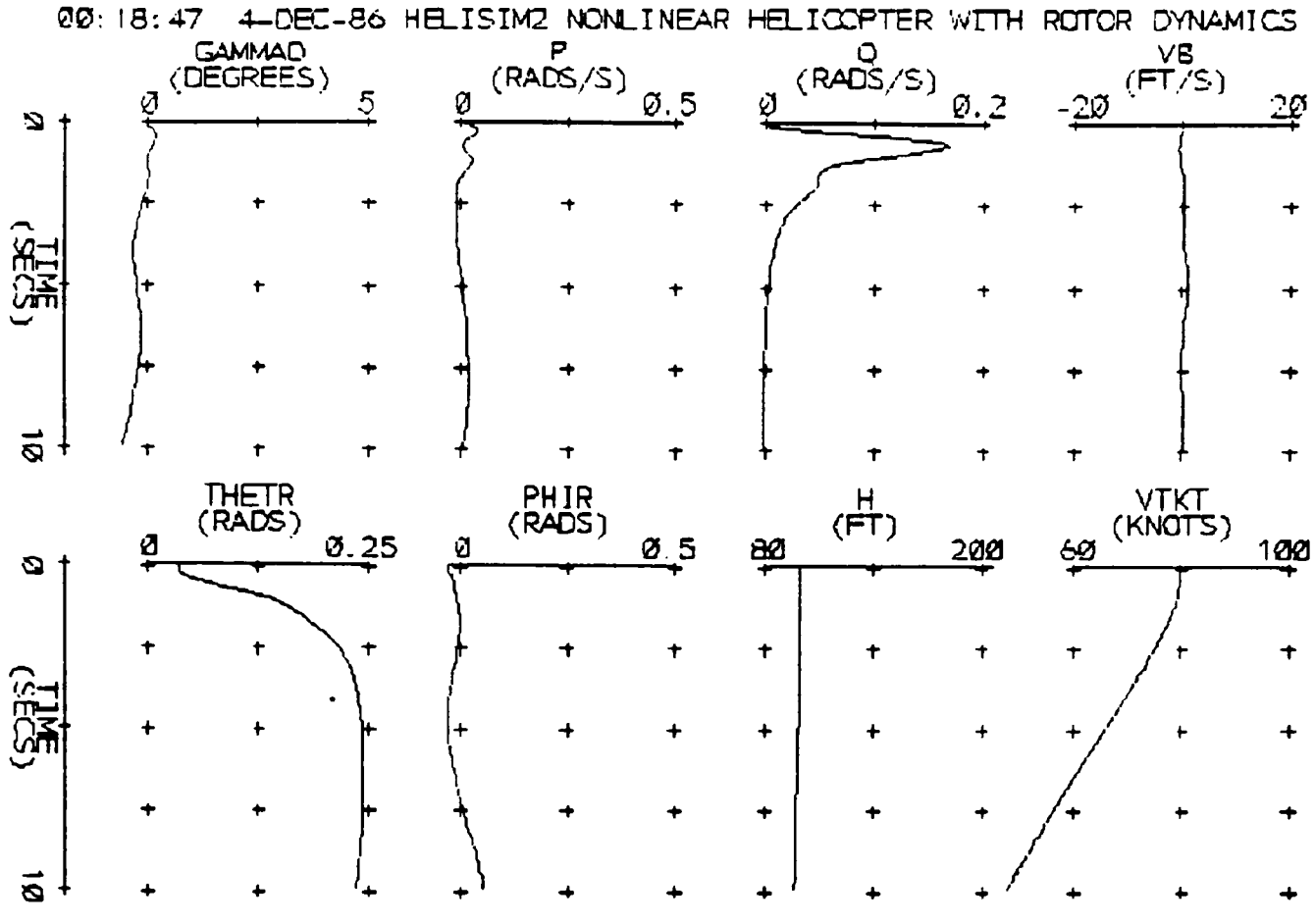


Figure 6.21 Response to a step demand in pitch attitude

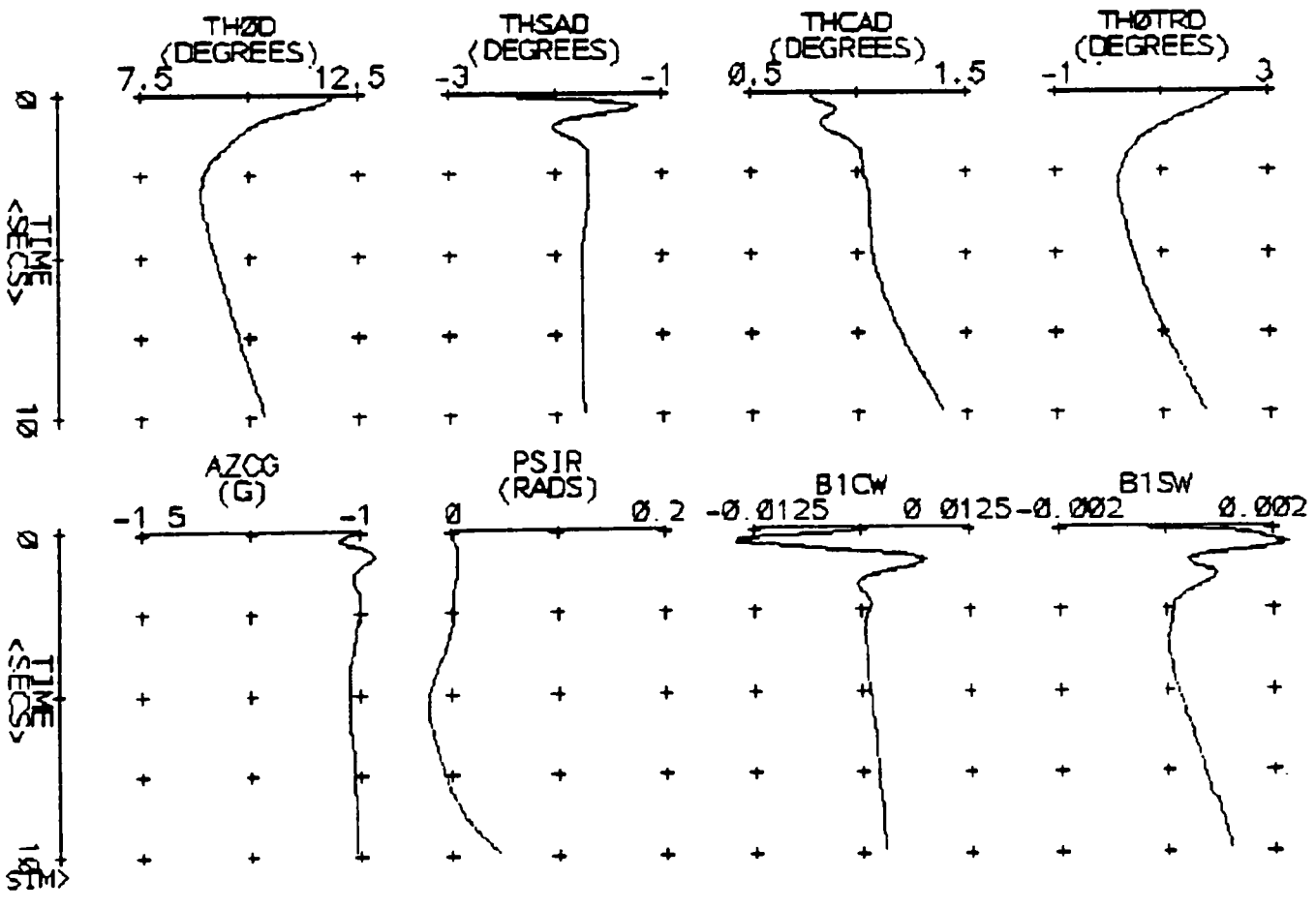


Figure 6.22 Response to a step demand in pitch attitude

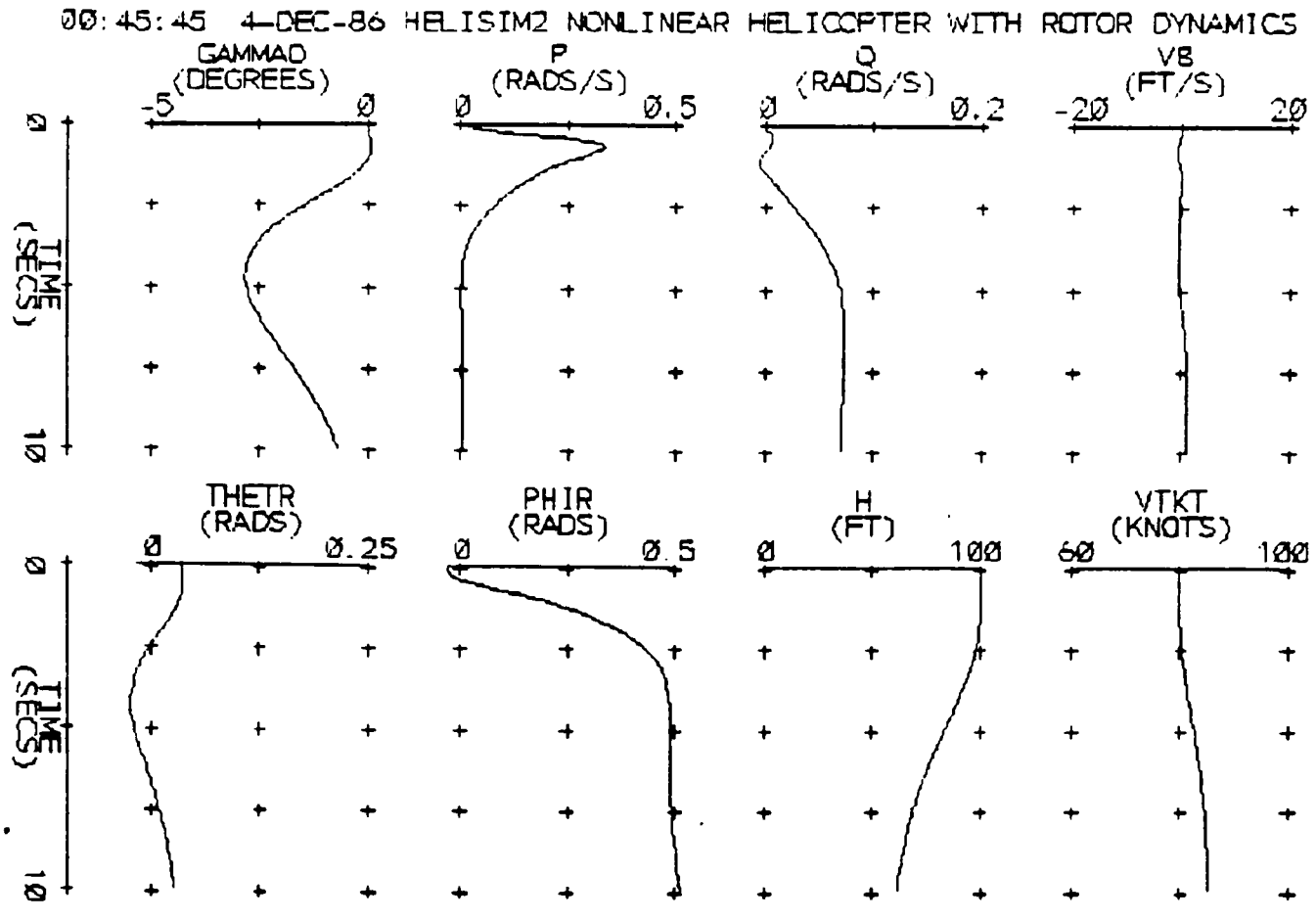


Figure 6.23 Response to a step demand in bank-angle

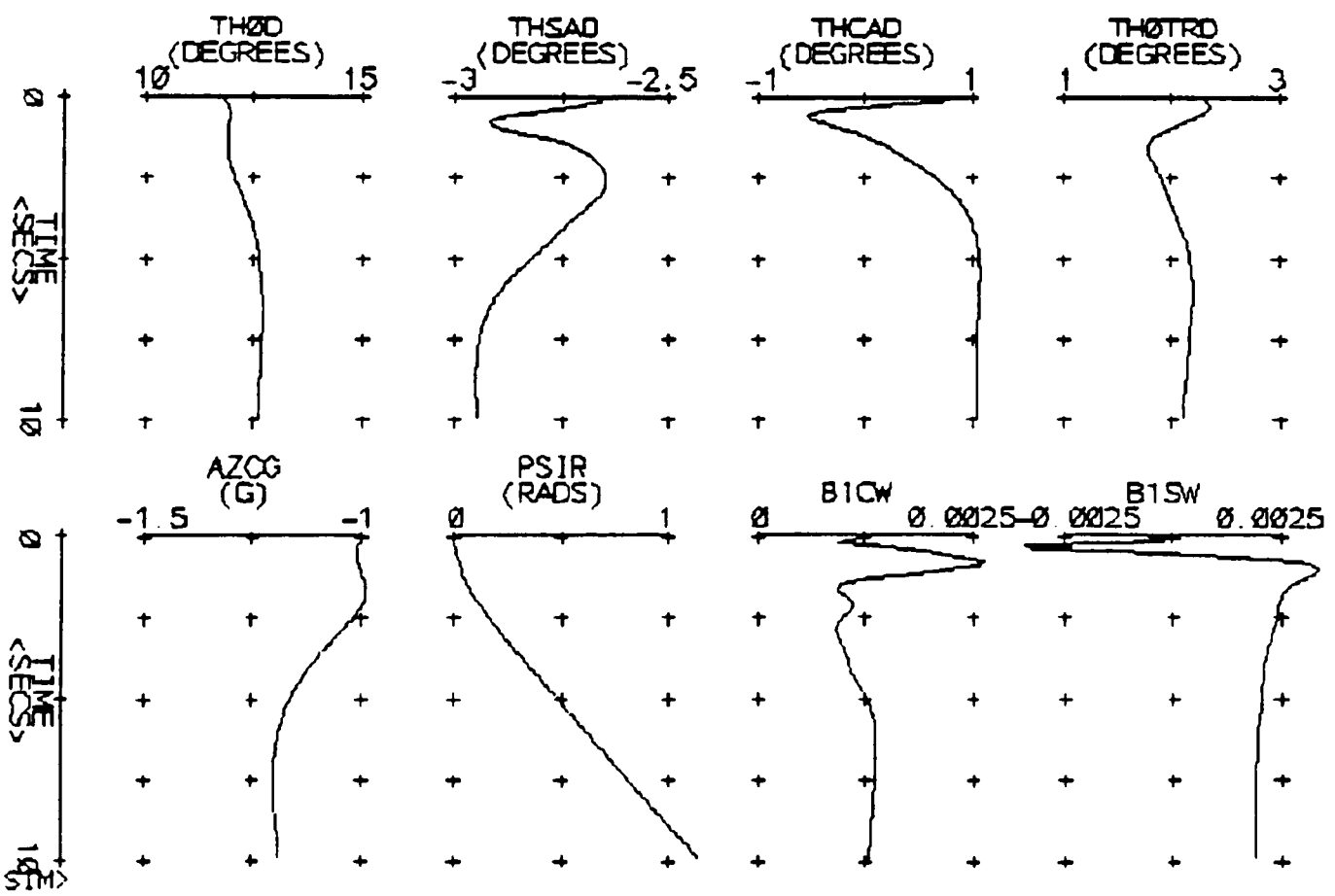


Figure 6.24 Response to a step demand in bank-angle

6.10 More general H^{∞}-optimization problems

Within the general framework of the 'standard problem' a large number of feedback control problems can be proposed. Unfortunately these will tend to be '4-block' problems with a large number of inputs, outputs and states, and will require large amounts of computational power. For the helicopter such a problem could be constructed from

Inputs:	Reference signals
	Disturbances, i.e., wind gusts
	Measurement noise
	Actuator noise
Outputs:	Tracking errors (including mode following errors)
	Actuator amplitudes and rates
	Sensor amplitudes and rates
Controller inputs:	Sensor outputs and reference signals
Controller outputs:	Actuator inputs

The plant would include models of actuators, sensors, disturbance processes and reference models. In addition, if the plant is subject to structured uncertainty Doyle's μ-synthesis procedure [DOY4], [DOY5] generates weighting functions for an additional set of inputs and outputs characterizing the uncertainty.

It is not clear that control problems are sufficiently well specified to warrant such a complex linear system problem description.

6.11 Concluding remarks

This chapter has demonstrated that H^{∞}-optimization can be used in the design of a control system for the helicopter. This is known to be a non-trivial control problem, and the addition of the rotor dynamics had proved to be a problem to control systems designed using more conventional techniques.

Of particular benefit was the ability to manipulate the closed-loop responses without worrying about the controller structure, or closed-loop stability.

The minimal state dimension of the optimal controller was 18, when that of the 'standard problem' was 20. This was much less than researchers had been predicting.

The non-linear time-responses have been shown to engineers familiar with the helicopter, who verified that the characteristics obtained are representative of helicopter motion. One criticism was that the helicopter is able to respond faster, indicating that the desired responses for this 'robust design' may have been too conservative.

Further work on the helicopter control problem should include demonstration of compliance with military specifications and should examine the usefulness of two-degree-of-freedom controllers. A problem not yet addressed is how to combine controllers designed at different operating points; and to find what criteria should be used to perform this 'gain-scheduling'. Some form of non-linear feedforward, for example from bank angle to collective, may help to reduce the effect of known non-linearities. A future goal will be the implementation of a controller, designed using H^{∞}-optimization, on the piloted simulation facility at the RAE, Bedford.

Appendix 6.1 Computation times for the design process

The following computation times, expressed as CPU seconds on a VAX 11/780, were obtained with the Oxford University H^{∞}-Design package for the design presented in this chapter.

Note: Plant has 4 inputs, 8 states and 6 outputs.

Standard problem had 6 inputs, 20 states, and 10 outputs.

Forming standard problem from weights and plant	< 1s
Transforming to model-matching problem (including a minimal realization of R)	60s
Solving model-matching using γ-iteration (1% accuracy)	95s
Recovery of controller (including stability check)	10s
Minimal realization of controller (59 to 18 states)	50s
Total	3 min 36s

(The equivalent total for the SISO example in Chapter V is 4s.)

Although this computation time is significantly greater than that of other design procedures, e.g., LQG, assessment of the design with linear frequency and time-responses can still be a greater burden. For example. a singular value magnitude plot of the cost function (with 18 state controller) over 100 frequency points, takes 95s.

A-matrix

0.000000E+00	0.000000E+00	0.000000E+00	0.999529	0.306860E-01	0.000000E+00	0.000000E+00	0.000000E+00
0.000000E+00	0.000000E+00	1.00000	-0.106264E-02	0.346130E-01	0.000000E+00	0.000000E+00	0.000000E+00
0.000000E+00	0.000000E+00	-10.5345	-1.99329	-0.303414	-0.113740E-01	-0.576577E-01	0.715008E-01
0.000000E+00	0.000000E+00	0.411235	-2.22594	0.133953E-02	0.648667E-02	0.325435E-02	0.137139E-01
0.000000E+00	0.000000E+00	-1.76440	-0.745595E-01	-1.34379	-0.769567E-02	0.192930E-01	-0.100381E-02
-32.1413	0.000000E+00	-0.365615	-2.48967	-0.745059E-03	-0.241725E-01	-0.235303E-02	0.381101E-01
0.341535E-01	32.1262	2.36172	-0.436444	-133.443	0.400672E-02	-0.166305	0.147473E-01
-1.11252	0.986290	-1.47705	134.934	-0.101090E-01	-0.855789E-02	-0.188561E-01	-0.781583

B-matrix

0.000000E+00	0.000000E+00	0.000000E+00	0.000000E+00
0.000000E+00	0.000000E+00	0.000000E+00	0.000000E+00
0.558752	0.269609	-2.69914	-0.233903E-01
0.249315	0.508953	0.304036E-01	-0.595137E-05
0.229884	0.167568E-01	-0.480247	-0.315118
0.219482	-0.463742	-0.127556E-02	0.178814E-04
0.884712E-01	0.544399E-01	-0.541970	0.383523
-6.73676	-1.67904	-0.449944	0.000000E+00

C-matrix

11.4591	-0.121633E-01	0.000000E+00	0.000000E+00	0.000000E+00	0.293928E-02	0.259922E-02	-0.846836E-01
0.000000E+00	0.000000E+00	2.00000	0.000000E+00	0.000000E+00	0.000000E+00	0.000000E+00	0.000000E+00
0.000000E+00	0.000000E+00	0.000000E+00	5.00000	0.000000E+00	0.000000E+00	0.000000E+00	0.000000E+00
0.000000E+00	0.000000E+00	0.000000E+00	0.000000E+00	0.000000E+00	0.000000E+00	0.500000E-01	0.000000E+00
5.00000	0.000000E+00	0.000000E+00	0.000000E+00	0.000000E+00	0.000000E+00	0.000000E+00	0.000000E+00
0.000000E+00	2.00000	0.000000E+00	0.000000E+00	0.000000E+00	0.000000E+00	0.000000E+00	0.000000E+00

CHAPTER VII

LINEAR QUADRATIC GAUSSIAN OPTIMAL CONTROL

7.1 Introduction

This chapter describes the state-space linear quadratic Gaussian (LQG) optimal control system design procedures. The time-domain optimal control theory was developed in the 1960s by Kalman and Bucy [KAL1], [KAL2]. The mathematical results had previously been derived by Wiener [WIE1], in the 1940s, in solving optimal filtering problems, with signals contaminated by noise modelled as random processes. Despite the fact that the problem formulations do not directly address robustness with respect to model errors, the linear quadratic regulator (LQR) can be shown to have certain guaranteed robustness properties [SAF2]. When full state feedback is not available, and an observer is used [LUE1], [LUE2] the LQG controller has no such guarantees; but techniques known as loop transfer recovery (LTR) [DOY2], [DOY3], [STE2], [STE3], can be used to asymptotically recover the LQR robustness margins. The intention of this chapter is to clearly define the conditions under which such controllers are optimal, and to present the results that enable LQG/LTR to be used as a tool for designing systems with required frequency domain characteristics.

Until recently the LQG/LTR methodology was promoted as being the only systematic procedure for performing singular value loop shaping. This

design technique was applied to the helicopter problem before the H^{∞}-optimization became available. The results, presented in [TOM2], were not very satisfactory, so the example in this chapter was performed using the same design model as in the previous chapter. This control system design problem was known to be sensibly posed, and the linear model scalings used in the previous chapter were retained. The resulting closed-loop time and frequency responses are presented in section 7.6. These were not considered sufficiently good to attempt non-linear simulation. The numerical results are believed to be correct, and the software used was able to reproduce the examples given in [DOY3], for the CH47.

7.2 The linear quadratic regulator

7.2-1 Specific assumptions

A linear model of the system about a given operating point is assumed to be available in the form

$$\dot{x} = Ax + Bu \tag{7.1}$$

where x and u are deviations from their operating point values.

It is assumed that all of the states are measurable. The system is then clearly observable, and it is also assumed to be stabilizable.

7.2-2 Problem definition

Given $x = x_o$ at time $t = 0$, find the control signal u(t) that minimizes the cost function

$$J = \int_o^{\infty} \left(x^T(t)\, Qx(t) + u^T(t)\, Ru(t)\right)dt \tag{7.2}$$

where Q is a symmetric non-negative definite weighting matrix on the states, i.e.

$$Q = Q^T \geq 0 \tag{7.3}$$

and may be factored as

$$Q = N^T N \tag{7.4}$$

R is a symmetric positive definite weighting matrix on the control inputs.

$$R = R^T > 0 \tag{7.5}$$

7.2-3 Problem solution

It is well known that the optimal control solution exists and is unique, provided that the state-space system formed by (A,B,N) is both stabilizable and detectable. It is generated by full state feedback of the form

$$u(t) = -K\, x(t) \tag{7.6}$$

where

$$K = R^{-1}B^T P \tag{7.7}$$

and P is the unique non-negative definite solution of the algebraic Riccati equation:

$$A^T P + PA + Q - PBR^{-1}B^T P = 0 \tag{7.8}$$

$$P = P^T \geq 0 \tag{7.9}$$

7.2-4 Feedback configuration

The optimal regulator structure is given in Figure 7.1. Note that, as its name suggests, the linear quadratic regulator is designed solely to regulate the system for an initial position with non-zero states. There is therefore no provision for an external input, this is considered in section 7.3.

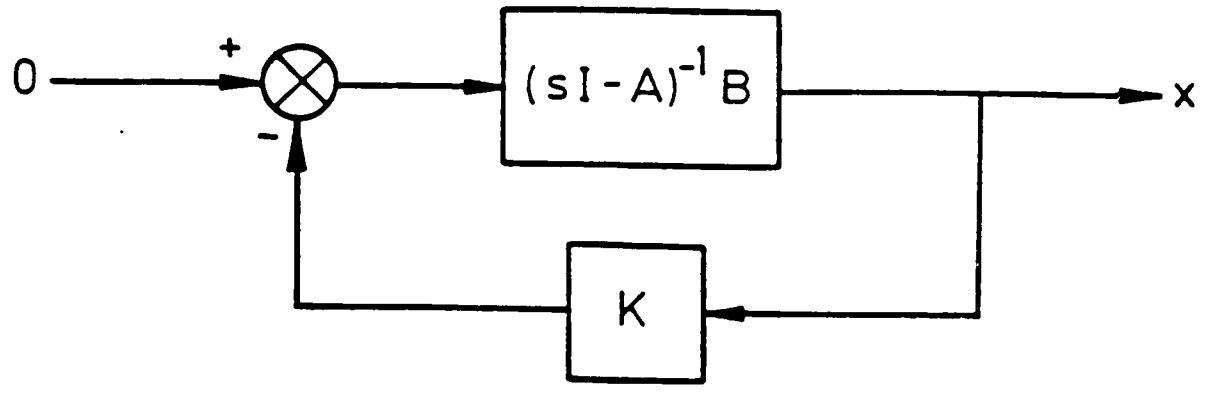


Figure 7.1 Regulator structure

7.2-5 LQR properties

(i) Stability

The closed-loop system is asymptotically stable. That is

$$\text{Re } \lambda_i \ (A - BK) < 0 \text{ for all } i = 1,n \qquad (7.10)$$

It can be shown that all stabilizing feedback gain matrices can be constructed by suitable choice of Q and R. It therefore follows from state-space pole placement theory that if [A,B] is completely controllable, these closed-loop pole positions can be anywhere in the left-half plane (subject to complex poles appearing in conjugate pairs).

(ii) Frequency domain properties

$$\text{If,} \qquad \emptyset(s) = (sI - A)^{-1} \qquad (7.11)$$

then the following identity can be obtained by routine algebra, starting with the Riccati equation (7.8), for $s = j\omega$.

$$(I + K\emptyset B)^{*} \ R \ (I + K\emptyset B) = R + (N\emptyset B)^{*} \ (N\emptyset B) \qquad (7.12)$$

then if $R = \rho I$

$$(I + K\emptyset B)^*(I + K\emptyset B) = I + \frac{1}{\rho}(N\emptyset B)^*(N\emptyset B) \qquad (7.13)$$

$$\Rightarrow \qquad \underline{\sigma}\,[I + K\emptyset B] \geq 1 \quad \text{for all } \omega \qquad (7.14)$$

and $$\underline{\sigma}\,[I + (K\emptyset B)^{-1}] \geq \frac{1}{2} \quad \text{for all } \omega \qquad (7.15)$$

(It may be shown that equations 7.14 and 7.15 also hold when R is only restricted to be diagonal.)

(iii) Robustness implications

The transfer function KØB is the loop transfer function with the loop broken at input to the plant. By considering multiplicative perturbations at this point, the celebrated LQR stability margins either of $\pm 60^o$ phase margin <u>or</u> $(\frac{1}{2}, \infty)$ gain margin, may be obtained simultaneously in each channel.

Thus, using LQR state-feedback the resulting closed-loop system is guaranteed to exhibit desirable features, both in nominal stability and robustness, when measured at the plant input.

7.2-6 LQR loop shaping

Motivated by the frequency domain equation (7.13), it is proposed to forget the time domain significance of Q and R in the cost function (7.2) and to choose N and ρ to shape the transfer function KØB. Thus, equation (7.13) may be rewritten as

$$\sigma_i\,[I + K\emptyset B] = \sqrt{\left(1 + \frac{1}{\rho}\,\sigma^2\,[N\emptyset B]\right)} \qquad \text{for } s=j\omega \qquad (7.16)$$

Away from the cross-over frequency ($\sigma_i[K\emptyset B] = 1$), we may make the gross assumption

$$\sigma_i\ [K\emptyset B] \simeq \frac{1}{\sqrt{\rho}}\ \sigma_i\ [N\emptyset B] \tag{7.17}$$

Then N may be chosen to 'balance' the singular values at a given frequency, and ρ used to make σ_i [KØB] large at low frequency, limited by the desired value of system bandwidth.

A possible algorithm for approximately matching the singular values at $s=j\omega_o$ is

(i) Find SVD of $\emptyset(j\omega_o)B = [U_1\ U_2] \begin{bmatrix} \Sigma \\ 0 \end{bmatrix} [V^*]$ (7.18)

(ii) Let $N = \Sigma^{-1}\ \mathrm{Re}\ [U_1^*]$ (7.19)

Procedures for approximately matching (or separating) the singular values at DC or HF are also possible. Unfortunately, these procedures are indirect and only approximate, and as the example in section 7.6 will show, not valid for the helicopter model.

It is quite likely impossible to achieve the desired loop shape by manipulating these constant weighting matrices. Dynamic weighting functions are most conveniently incorporated by augmenting the original system with stable additional dynamics. Integral action, to increase the gain at low frequency, is a common requirement, but all the additional integrator states must be penalized in the cost function.

7.2-7 Problems and restrictions

(i) The assumption that it is possible to measure the deviations of all the state variables from their operating point values is unlikely to be valid.

(ii) The optimal control problem does not directly address command following or disturbance rejection.

(iii) When used to perform frequency response loop shaping:

(a) The relationship between the weights and the resultant loop transfer function is not explicit.

(b) Manipulation of the singular values is difficult to perform at more than one frequency simultaneously, and is in no sense optimal.

(c) A state weighting matrix chosen to align the singular values of the loop transfer function at high frequency, for example, may lead to arbitrarily poor time response behaviour. This is because the physical significance of the terms in the cost function can be lost.

7.3 The linear quadratic servo

7.3-1 Reformation of the problem

In a servo system a given combination of the system states, $Cx(t) = y(t)$ is required to track a reference input $r(t)$ in the presence of output disturbances $d(t)$, i.e.

$$\begin{aligned} \dot{x}(t) &= Ax(t) + Bu(t) \\ y(t) &= Cx(t) + d(t) \\ e(t) &= r(t) - y(t) \end{aligned} \tag{7.20}$$

It is therefore tempting to propose a linear quadratic cost function

$$J = \int_o^\infty \left(e^T(t)\, Pe(t) + u^T(t)\, Ru(t) \right) dt \qquad (7.21)$$

Unfortunately the solution to this problem would be of the form

$$u(t) = -Kx(t) + u_c(t) \qquad (7.22)$$

where $u_c(t)$ would depend on future command inputs and future disturbances. Thus, unless specific assumptions about r and d are made, no useful solution to this problem can be found.

In the special case with future reference input constant and zero disturbance, the optimal solution is a linear quadratic regulator, with u_c used to change the operating point to the new set point.

That is:

$$x_1 \text{ such that } Cx_1 = r \qquad (7.23)$$

$$u_c \text{ such that } (A-BK)x_1 + Bu_c = 0 \qquad (7.24)$$

$$\Rightarrow \quad u_c = -[C(A-BK)^{-1}B]^{-1}r \qquad (7.25)$$

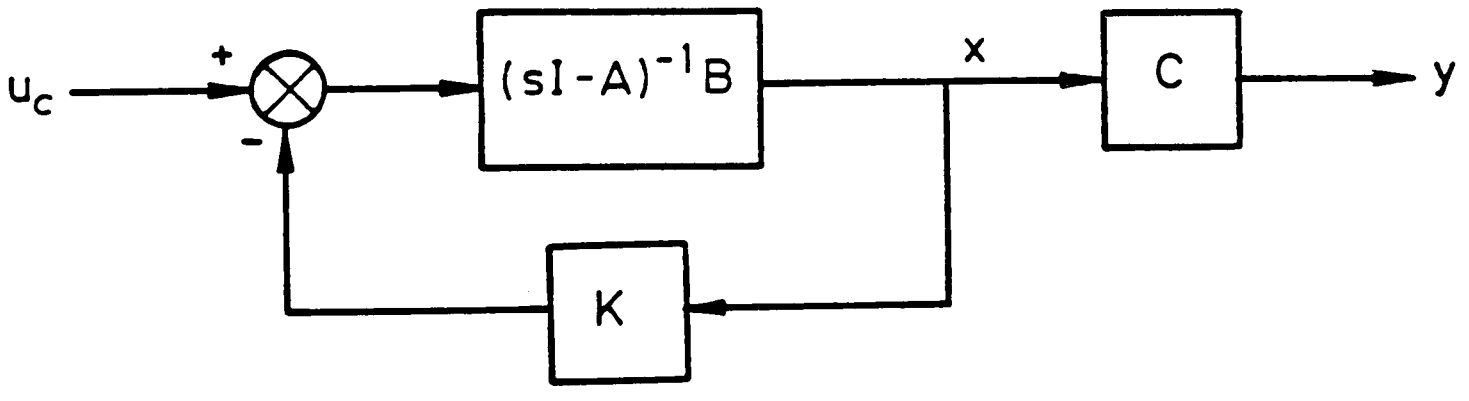


Figure 7.2 Set point following regulator

Note that because disturbances have been ignored the solution has no feedback of the error.

The remainder of this section will therefore consider sub-optimal servo systems that attempt to retain some of the properties of the linear quadratic regulator. The feedback gain matrix will be found by posing a fictitious LQR problem.

7.3-2 Interpretation as multivariable P.I.D.

Assuming that it is possible to partition the state vector in the form

$$\begin{pmatrix} x_y \\ x_d \end{pmatrix} \quad \text{where } x_y \text{ is the output vector and } x_d = f(\dot{x}_y) \tag{7.26}$$

the linear quadratic regulator can be used to determine the gains in a control system whose structure is that of a multivariable proportional plus integral plus derivative controller. The importance of being able to partition the state vector in this manner is that it is possible to implement the regulator as in Figure 7.3

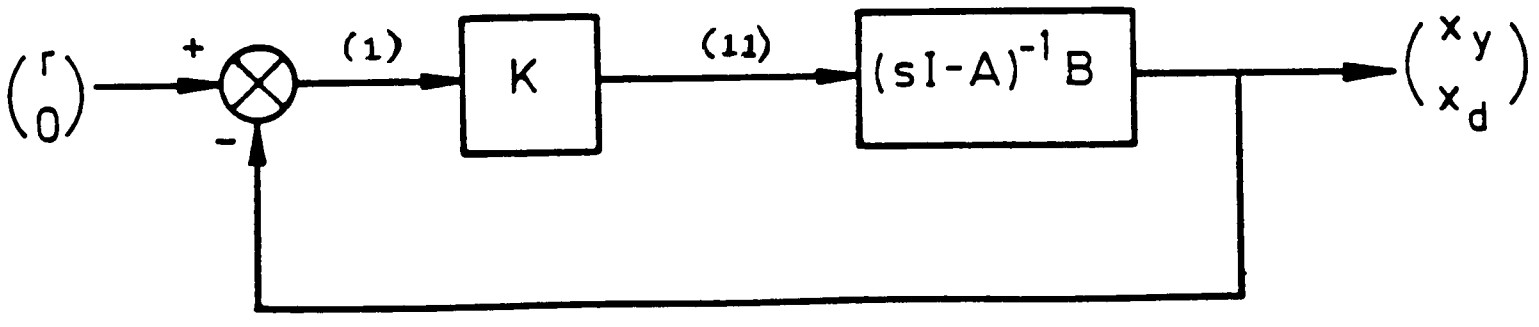


Figure 7.3 Servo feedback configuration

If it is not possible to perform the partition into reference outputs and higher derivatives, as is the case in a rate control system, it is necessary to construct a 'set point observer' [KWA1], [AND1] to calculate the (non-zero) additional elements in the reference state vector.

The loop transfer function, when the loop is broken at the plant input (11), is the LQR loop transfer function. Servo performance must be evaluated by considering the loop broken at (1). The LQR theory cannot guarantee good properties here. To complete the interpretation as multivariable P.I.D., it is necessary to augment the state vector with integral states x_i such that

$$\dot{x}_i = x_y \tag{7.27}$$

and then to partition the resultant gain vector as

$$K = [\ K_i\ K_y\ K_d\ ] \tag{7.28}$$

The controller may now be implemented as in Figure 7.4.

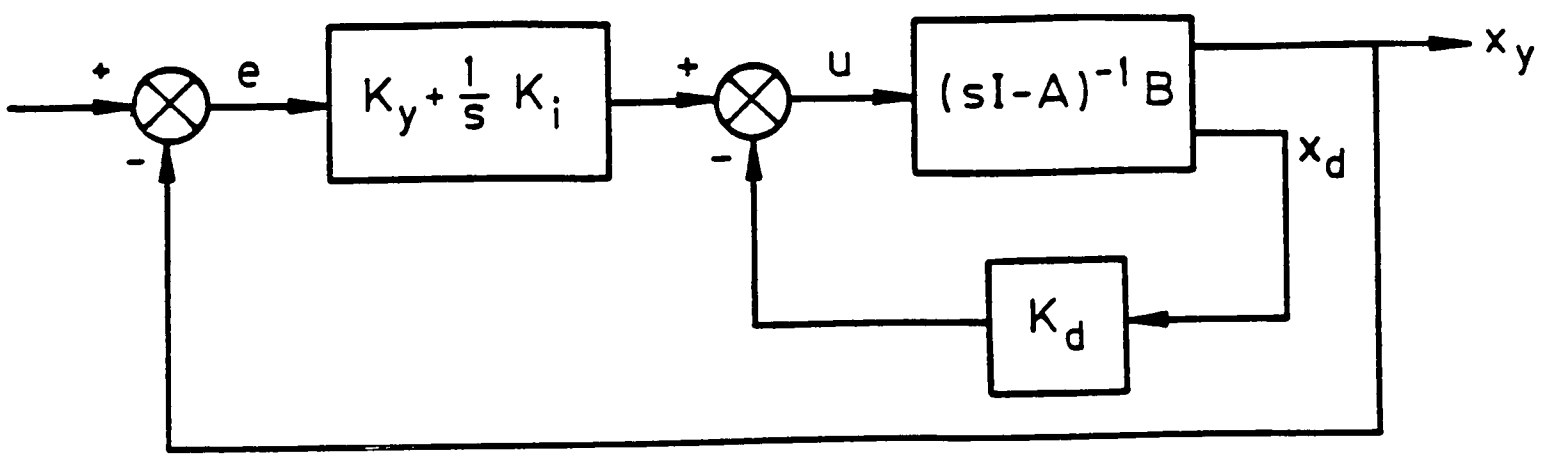


Figure 7.4 Multivariable P.I.D. servo

7.3-3 Problems and restrictions

(i) All states are assumed measurable.

(ii) Servo performance is not 'optimal'.

(iii) LQR loop transfer function properties at plant input only.

7.4 The steady-state Kalman filter

7.4-1 Specific assumptions

It is assumed that a linear model of the system in the form

$$\dot{x} = Ax + Bu + v$$
$$y = Cx + w \qquad (7.29)$$

is available. The signals v and w are independent Gaussian noise processes with zero mean and power spectral density matrices V and W. It is assumed that all the output measurements are corrupted with noise so that W is positive definite and W^{-1} exists. The system is assumed to be stabilizable and detectable.

This system models disturbances as $d(s) = C(sI-A)^{-1}v(s)$.

7.4-2 Problem definition

The system in equation (7.29) represents the common practical situation where the state vector cannot be directly measured. The Kalman filter is a model-reference observer that optimally reconstructs estimates $\hat{x}$ of the system states. The filter is designed to minimize the cost function.

$$J = \lim_{t\to\infty} E\left[(x(t) - \hat{x}(t))^T (x(t) - \hat{x}(t)) \right] \qquad (7.30)$$

7.4-3 Problem solution

The Kalman filter is defined by the following equations.

$$\dot{\hat{x}} = A\hat{x} + Bu + F\,[y - C\hat{x}] \qquad (7.31)$$

The filter gain is given by $F = PC^T W^{-1}$ (7.32)

where P is the solution to the Riccati equation

$$AP + PA^T + V - PC^T W^{-1} CP = 0 \tag{7.33}$$

7.4-4 Feedback configuration

The system and filter are shown in Figure 7.5.

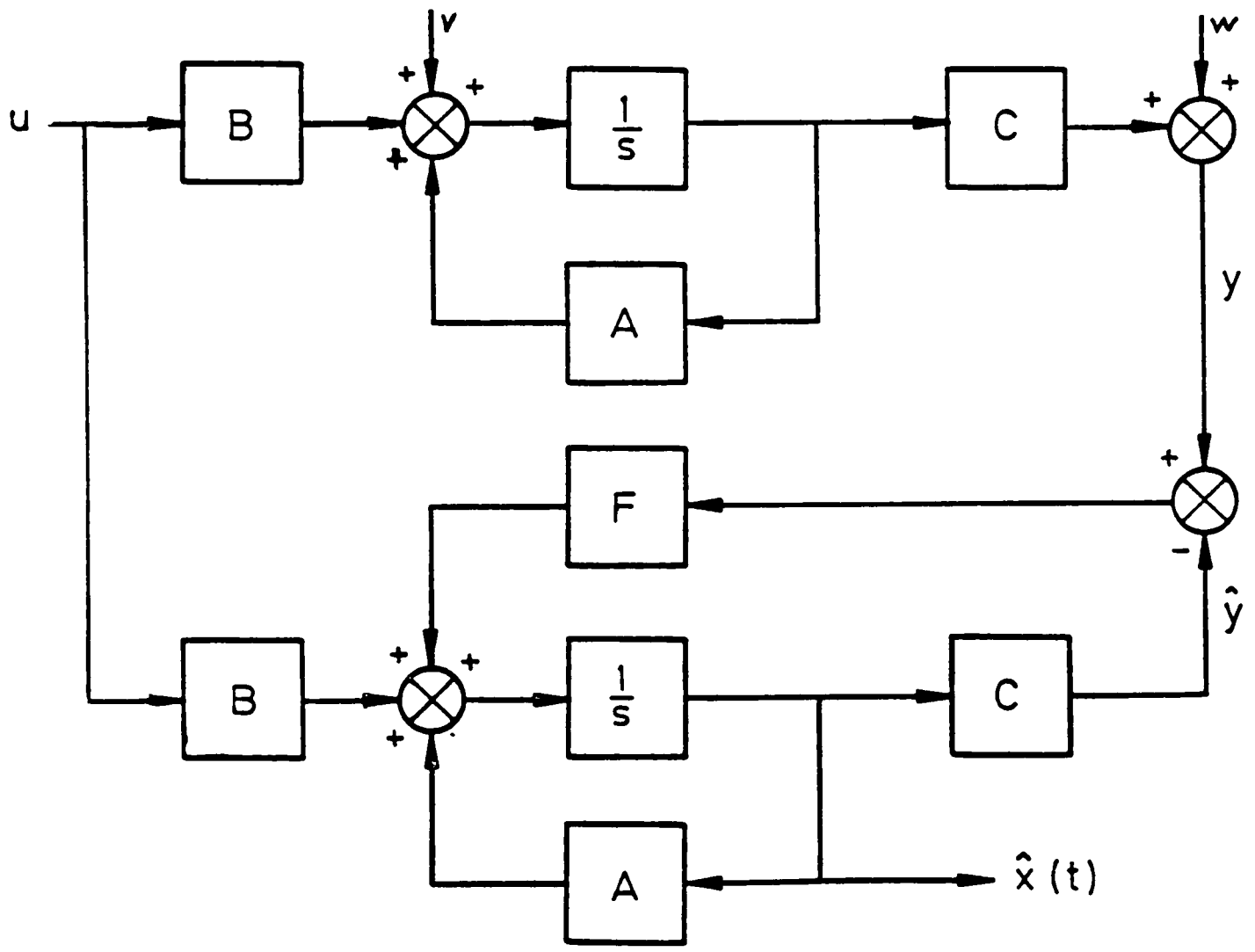


Figure 7.5 Kalman filter structure

7.4-5 Kalman filter properties

(i) Stability

If the input noise power spectral density matrix V is factored as

$$V = L^T L \tag{7.34}$$

and the system formed by (A,L,C) is both stabilizable and detectable, then the filter will be stable. That is

$$\text{Re } \lambda_i \, (A-FC) < 0 \quad \text{for all } i=1,n \tag{7.35}$$

(ii) Frequency domain properties

The Kalman filter loop transfer function CØF can be shown to have analogous properties to the LQR loop transfer function KØB. Important for the LQG/LTR method are the following equations, assuming W is diagonal = μI, s=jω,

$$(I + K\emptyset B)(I + K\emptyset B)^{*} = I + \frac{1}{\mu}(C\emptyset L)^{*}(C\emptyset L) \qquad (7.36)$$

$$\underline{\sigma}\,[I + K\emptyset B] \geq 1 \qquad \text{for all } \omega \qquad (7.37)$$

$$\underline{\sigma}\,[I + (K\emptyset B)^{-1}] \geq \frac{1}{2} \quad \text{for all } \omega \qquad (7.38)$$

7.4-6 Kalman filter loop shaping

Ignoring the physical significance of the noise power spectral density matrices, it is possible to indirectly manipulate CØF by suitable choice of $V = L^{T}L$ and W = μI. As for the LQR, a number of techniques are available to approximately match the singular values of CØF at frequencies far away from cross-over.

By modelling the noise processes as coloured white noise, extra dynamics can be included in the loop transfer function. This can be implemented by augmenting the system model with the additional dynamics, as before.

7.4-7 Problems and restrictions.

(i) The optimal observer contains a linear model of the system and will therefore always have the same number of states. In conventional observer design there are a number of techniques to design sub-optimal reduced order observers.

(ii) The same criticisms apply to Kalman filter loop shaping as to LQR loop shaping.

7.5 The linear quadratic Gaussian control problem

7.5-1 Problem description

With the specific assumptions on the system model as in the Kalman filter problem, the LQG control problem is that of finding a control u to minimize the cost function:

$$J = E\left[\lim_{T\to\infty} \frac{1}{T}\int_0^T (x^T(t)\, Qx(t) + u^T(t)\, Ru(t)\, dt\right] \qquad (7.39)$$

with Q and R as for the LQR problem, section 7.2-2. The system is assumed to have an initial position $x(t_o) = x_o$, where x_o is a stochastic vector.

7.5-2 Problem solution

A powerful result known as the Separation Theorem states that the LQG controller is a combination of the optimal observer and the optimal controller. Thus, the LQG compensator consists of a Kalman filter and a linear quadratic controller.

7.5-3 Feedback configuration

The LQG compensator is optimal only as a regulator, with equations:

$$\dot{\hat{x}} = A\hat{x} + Bu + F\,(y - C\hat{x}) \qquad (7.40)$$

$$u = -K\,\hat{x} \qquad (7.41)$$

In order to implement this controller in a servo form, it is necessary to inject a reference signal at some point, as for LQR in section 7.3.

In order to retain the physical significance of the Kalman filter states, the compensator should be implemented with the summing junction

after the filter, in a similar manner to Figure 7.4, with x_d and x_y replaced by their estimates.

An alternative is to implement the controller as a forward loop compensator, replacing y in equation (7.40) by y-r. The compensator then becomes a multivariable controller, K_{LQR} with transfer function given by

$$K_{LQG}(s) = K(sI - A + BK + CF)^{-1}F \qquad (7.42)$$

and

$$u = K_{LQG}(r-y) \qquad (7.43)$$

It will be this form of the LQG controller that will be used later in this chapter.

7.5-4 Robustness properties

With full state feedback the LQR has certain guaranteed robustness properties at input to the plant (section 7.2-5). These are obtained with only a few restrictions on the choice of weights. Unfortunately, the addition of the observer causes these guarantees to be lost. Doyle [DOY1] demonstrated this by an example which could have arbitrarily poor robustness margins.

This does not mean that LQG compensators are not robust, but simply that the final design must be checked by examination of the closed-loop singular values.

7.5-5 Robustness recovery

For minimum phase plants it is possible to asymptotically obtain the robustness properties of either the LQR or Kalman filter loop transfer function, at either input or output of the plant. This procedure is known as Loop Transfer Recovery (LTR), and the resulting design procedure, as LQG/LTR. The mathematical results concerning the asymptotic properties of

the LQG compensator were derived by Kwakernaak in 1972 [KWA1] and the LQG/LTR methodology was popularized by Doyle and Stein in 1981 [DOY3].

(i) Sensitivity recovery procedure

In this procedure the robustness properties of the Kalman filter loop transfer function are recovered at output of the plant. This procedure is applicable to plants with the number of outputs less than or equal to the number of inputs.

Step 1

Design the filter gain by suitable choice of weights, such that CØF is a desired loop transfer function.

Step 2

Design the LQR with weights

$$Q = N^T N + qC^T C$$

$$R = \rho I \qquad (7.44)$$

Then as $q \to \infty$ the loop transfer function

$$G(s)K_{LQG} \to C\emptyset F \qquad (7.45)$$

Note that in this procedure additional dynamics should be added to the plant input to retain the significance of the plant output.

(ii) Robustness recovery procedure

In this procedure the robustness properties of the LQR are recovered at plant input. This is applicable to plants with the number of outputs greater than or equal to the number of inputs.

Step 1

Design the LQR, such that KØB has desirable properties.

Step 2

Design the Kalman filter with modified noise intensity matrices.

$$V = L^T L + q\, BB^T \qquad (7.46)$$

$$W = \mu I$$

Then as $q \to \infty$ the loop transfer function

$$K_{LQG} G(s) \to K\text{Ø}B \qquad (7.47)$$

This will be the procedure used for the example in section 7.6.

7.5-6 Problems and restrictions

The LQG compensator with separate state estimation and state feedback control has proved to be a useful design tool, especially in the aerospace industry. Such controllers are usually implemented sub-optimally, using reduced order observers and with only a subset of the states being fed back. When the physical significance of the weights and controller states becomes lost in a procedure such as LQG/LTR, the controller is less attractive.

In addition to the problems inherent in implementing a truly multivariable compensator, the following criticisms apply to LQG/LTR.

(i) Controller dimension

Since the controller contains a copy of the design model, the state dimension of the controller is equal to the size of the nominal model plus

twice the number of augmented states. This means that controller size reduction will generally be necessary.

(ii) Controller pole locations

The asymptotic behaviour in the recovery procedures leads to high gains and fast poles in the LQG compensator. This is highly undesirable for implementation and time response simulation, and requires frequency weighted model reduction to remove them. Note that although the compensator has a large bandwidth, the bandwidth of the loop transfer function is determined by that of the plant.

(iii) Non-minimum phase systems

Non-minimum phase systems cannot be directly handled by the LQG/LTR procedure. The target loop transfer function KØB or CØF is always minimum phase and can still be shaped as required. The problem is that $K_{LQG}(s)G(s)$ or $G(s)K_{LQG}(s)$ must still be non-minimum phase and the recovery procedure fails at frequencies near those of the right-half plane zero. That large gains and good sensitivity cannot be achieved at these frequencies is a fundamental constraint on the system, and not on the design procedure.

The main criticism then, is that Step 1 of the LQG/LTR design does not highlight the difficulties associated with non-minimum phase systems.

7.6 Example of LQG/LTR

For this example the same helicopter model used in the previous chapter was considered. The scalings that were found necessary in the H^{∞}-design were also retained. Since the design model has 4 inputs and 6

outputs it is only possible (without disregarding outputs) to attempt to follow the robustness recovery procedures.

Step 1

Design of KØB.

The aim of this step is to design the LQR loop transfer function that will be recovered by Step 2. Figure 7.6 shows a singular value plot of the function KØB for Q = diag (1,0.1,0.1,1,1,1) and R = 0.5I.

An undesirable feature of this response is the low gain in some directions and the spread of the singular values. In an attempt to reduce this spread Figure 7.7 shows the result of choosing Q to align the singular values at DC and Figure 7.8 at 1 rads^{-1}, both with R = 0.5 I. These plots show that it is necessary to increase the low frequency gains by suitably augmenting the system.

Integral action was added by augmenting the state and output vectors with states corresponding to the integrals of the controlled outputs. Figure 7.9 shows the effect of attempting to align the singular values of this augmented system at 1 rads^{-1}, with R = 0.5I.

Although this is not ideal, particularly the low gain in one direction, Figure 7.9 was the 'best' candidate for the transfer function achieved.

Step 2

Recovery of KØB by $K_{LQG}(s)G(s)$.

Figure 7.10 shows $K_{LQG}(s)G(s)$ for q=1 in equation (7.46) with L=0 and μ=1. Figure 7.11 shows $K_{LQG}(s)G(s)$ for q=10. The recovery was terminated at this point because the controller then had a pole at s=-29, and this was increasing with increasing q.

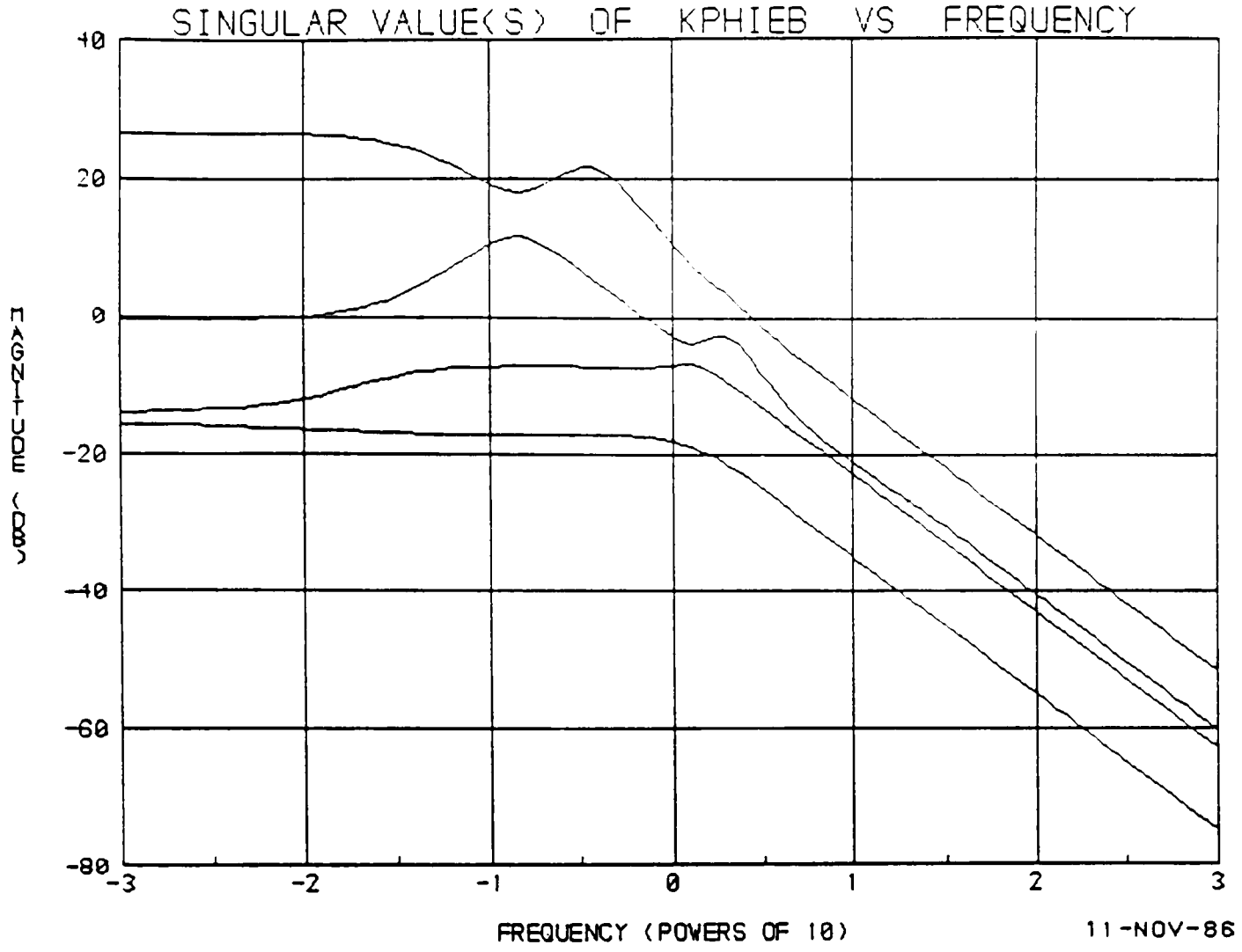


Figure 7.6 First frequency response of KΦB

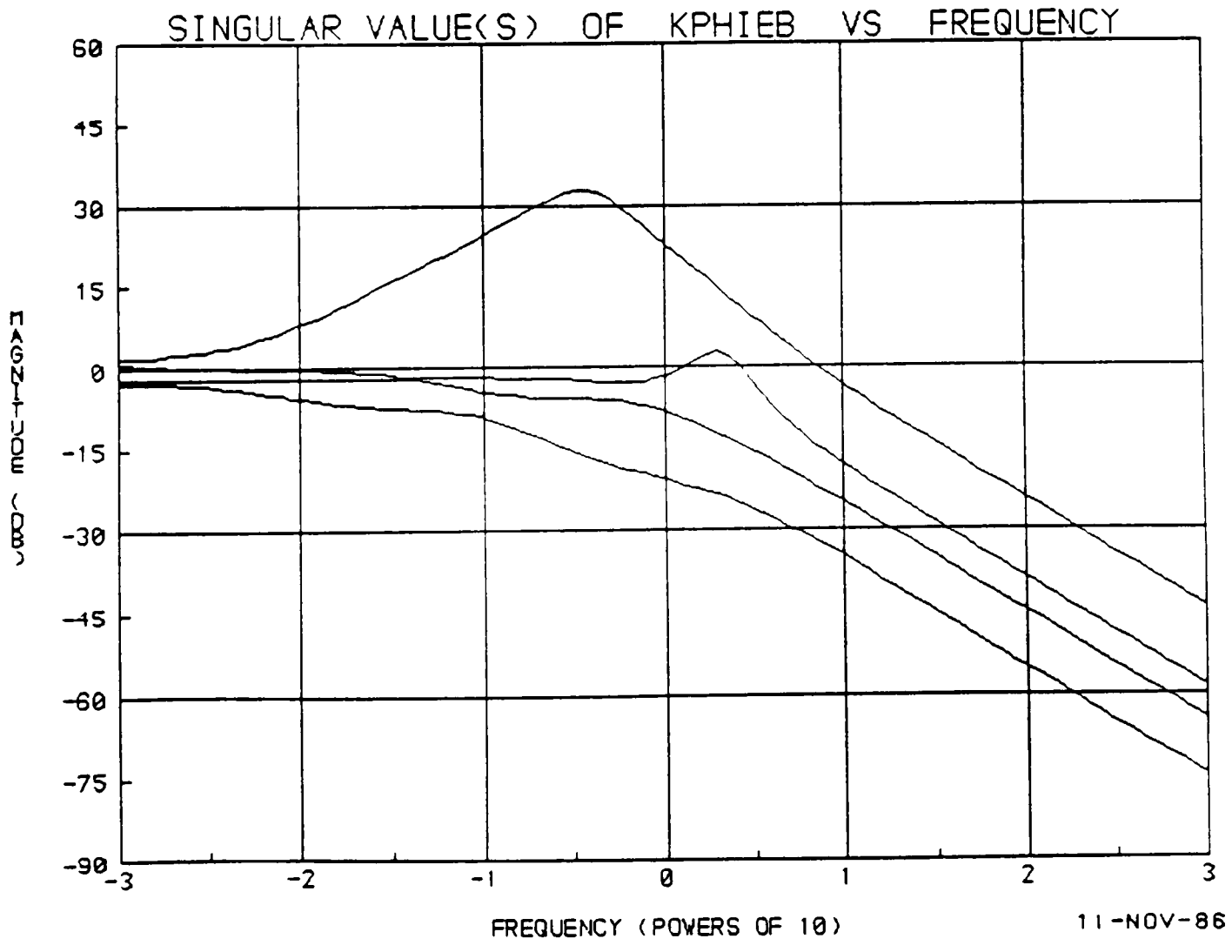


Figure 7.7 KΦB after aligning at ω=0

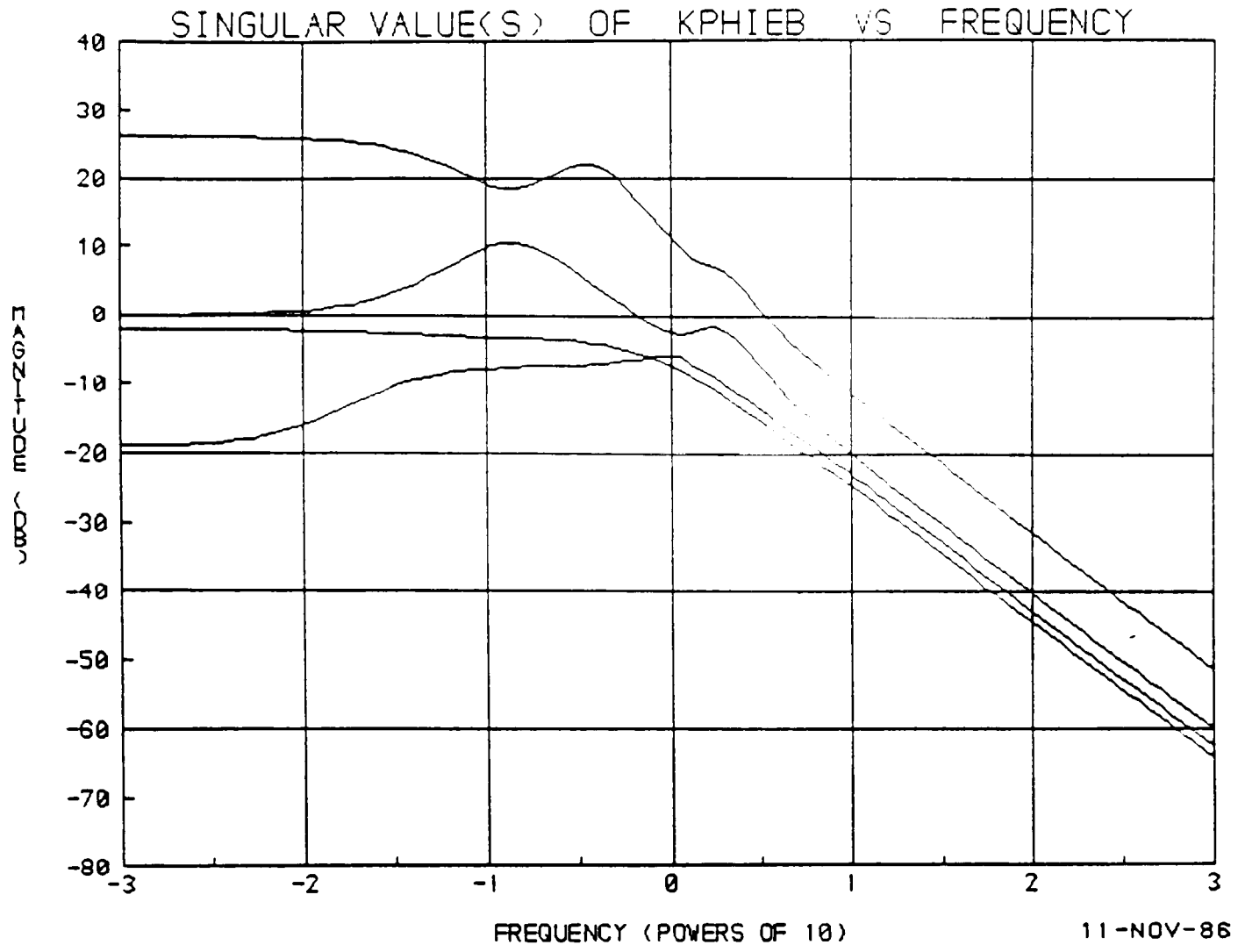


Figure 7.8 KΦB after aligning at ω=1

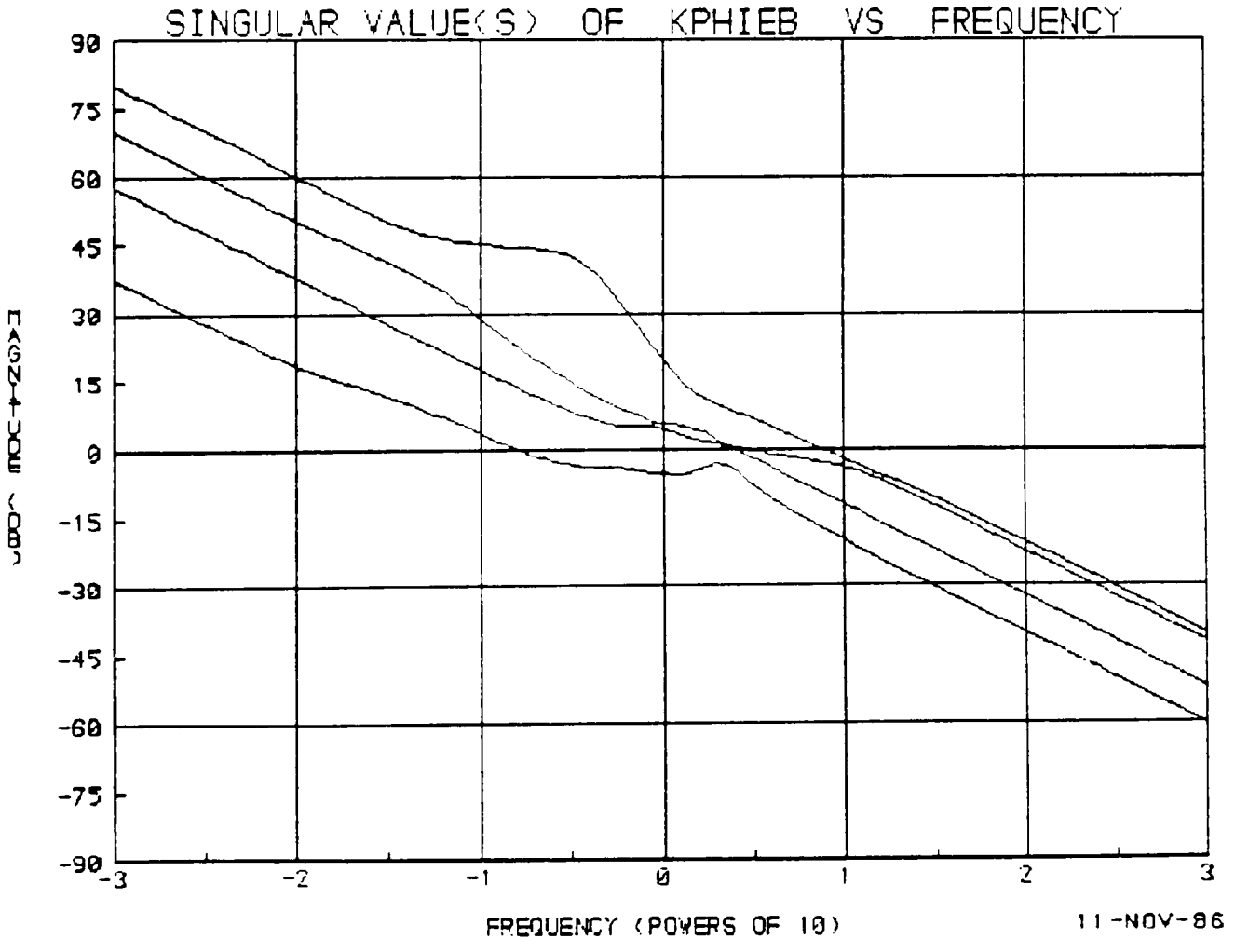


Figure 7.9 Final design KΦB

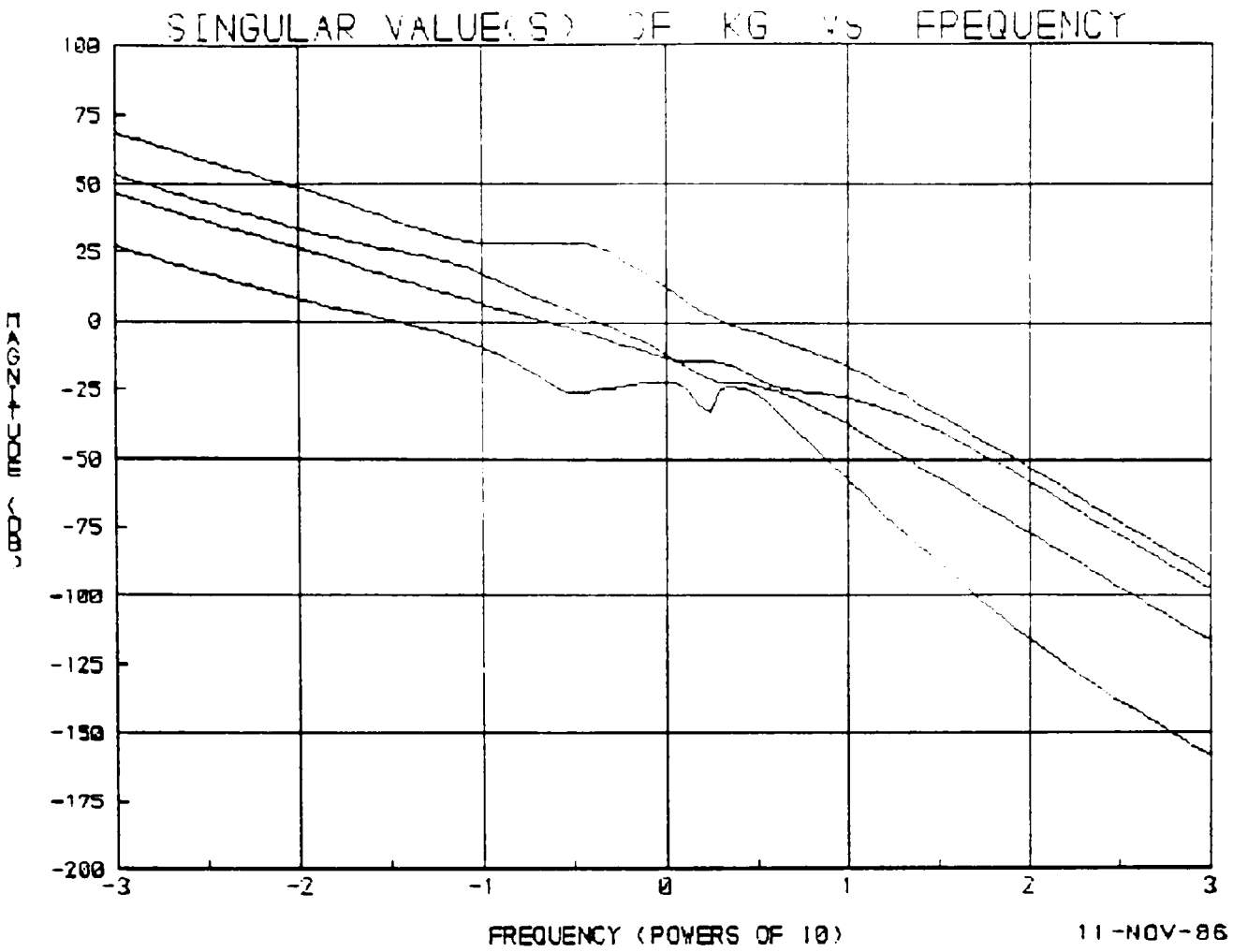


Figure 7.10 KG recovery with q=1

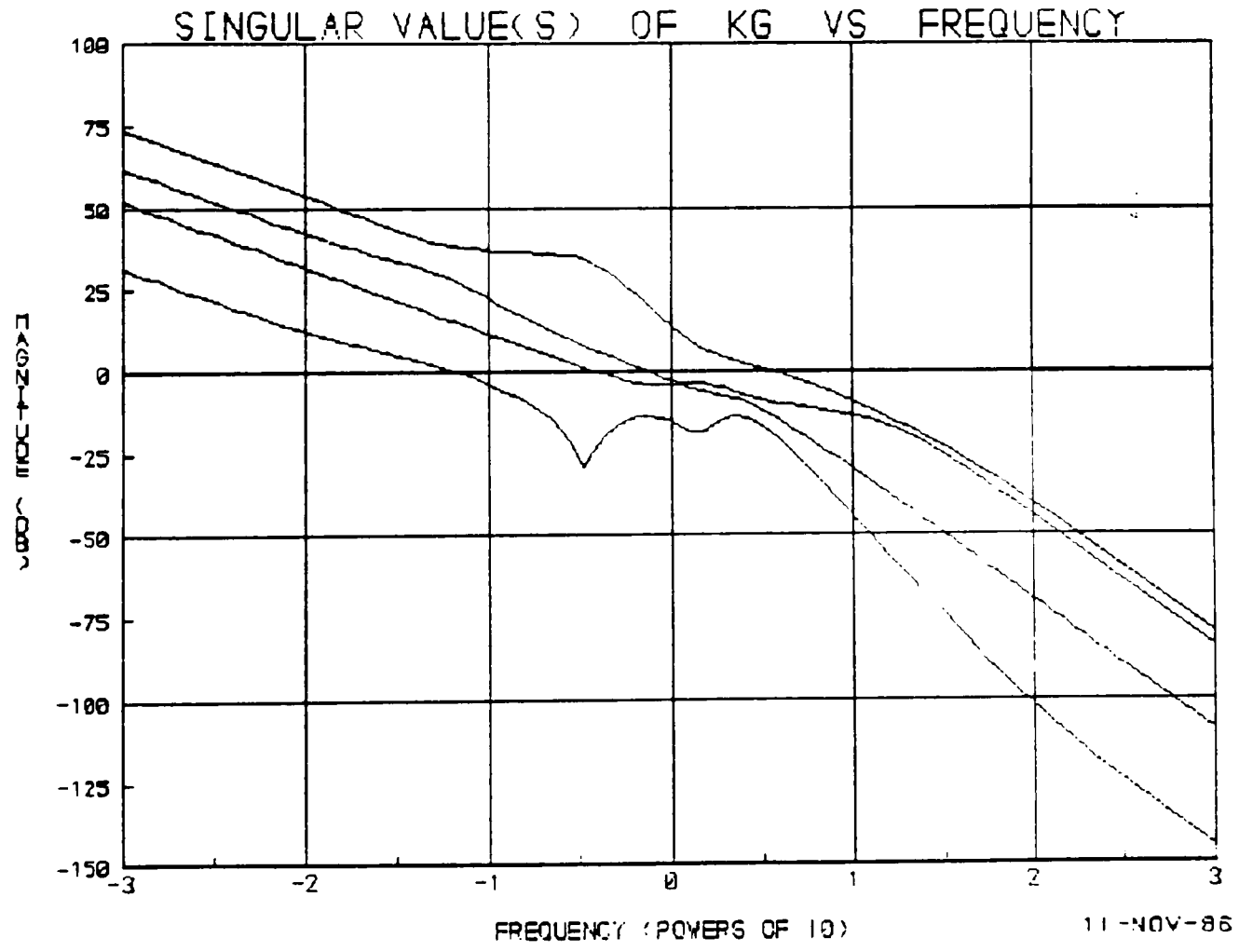


Figure 7.11 KG recovery with q=10

When the integrator states included in the design model were included in the controller, the state dimension of the controller was 16. The pole locations of this controller are given in Table 7.1.

	Open-Loop Poles:	
No.	Real	Imag.
1	-29.7	
2	-17.0	
3	-3.47	
4	-2.09	2.72
5	-2.09	-2.72
6	-1.32	
7	-1.00	
8	-0.939	0.511
9	-0.939	-0.511
10	-0.869	0.459
11	-0.869	-0.459
12	-0.017	
13	0.000	
14	0.000	
15	0.000	
16	0.000	

Table 7.1 LQG controller pole locations

The singular value magnitude plots for the closed-loop transfer function T(s) and the sensitivity function are given in Figures 7.12 and 7.13. These show that the robustness criterion of bandwidth less than 10 $rads^{-1}$ and the sensitivity requirement of zero d.c., error have been met by this design. It is clear that better control over these functions at intermediate frequencies would be desirable.

The closed-loop linear time responses for this controller are given in Figures 7.14 to 7.21. These were not considered good enough to proceed with non-linear simulation. This controller appears to have little control over pitch attitude (Output 5), and the design process should start again, penalizing errors in this direction with particular care.

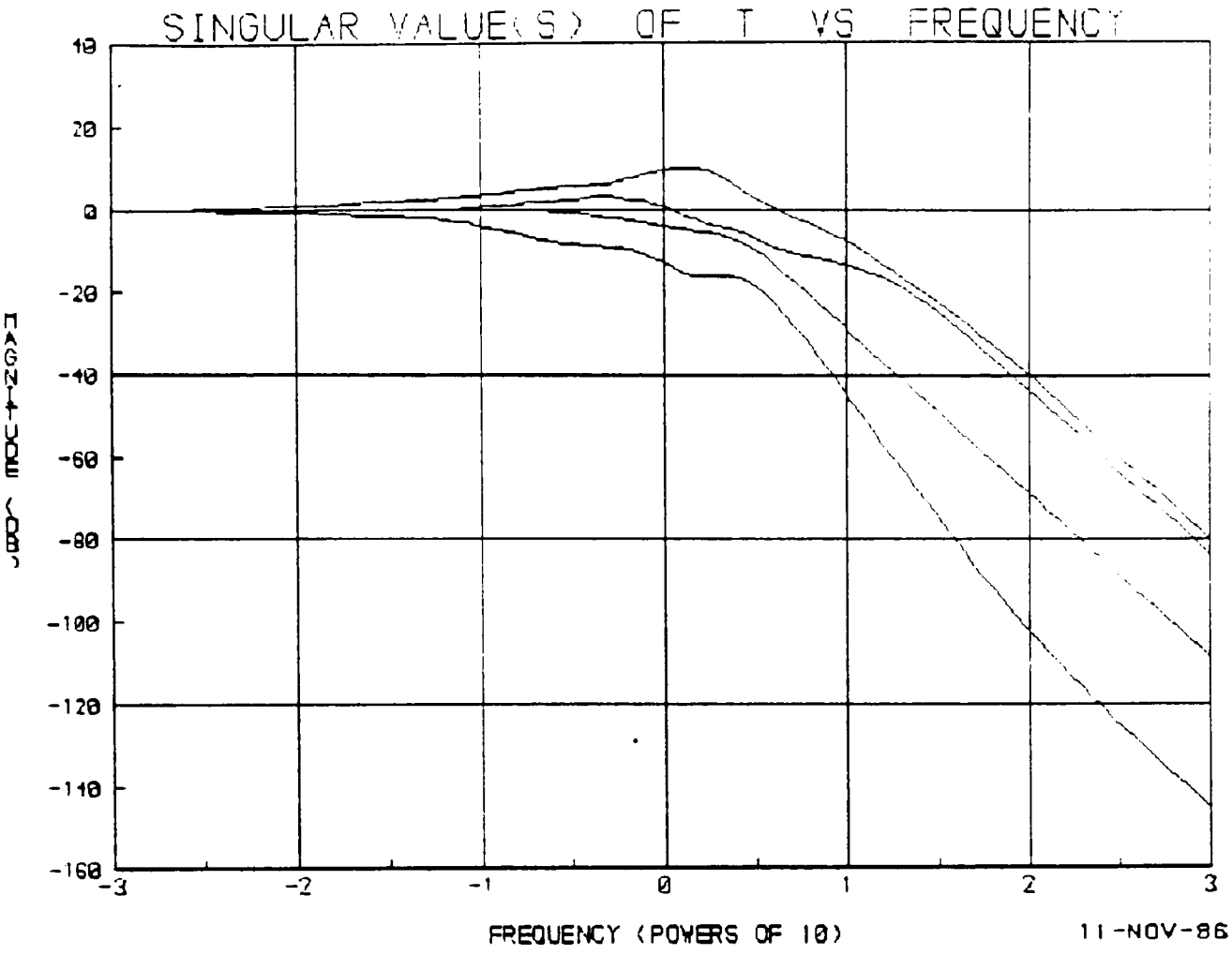


Figure 7.12

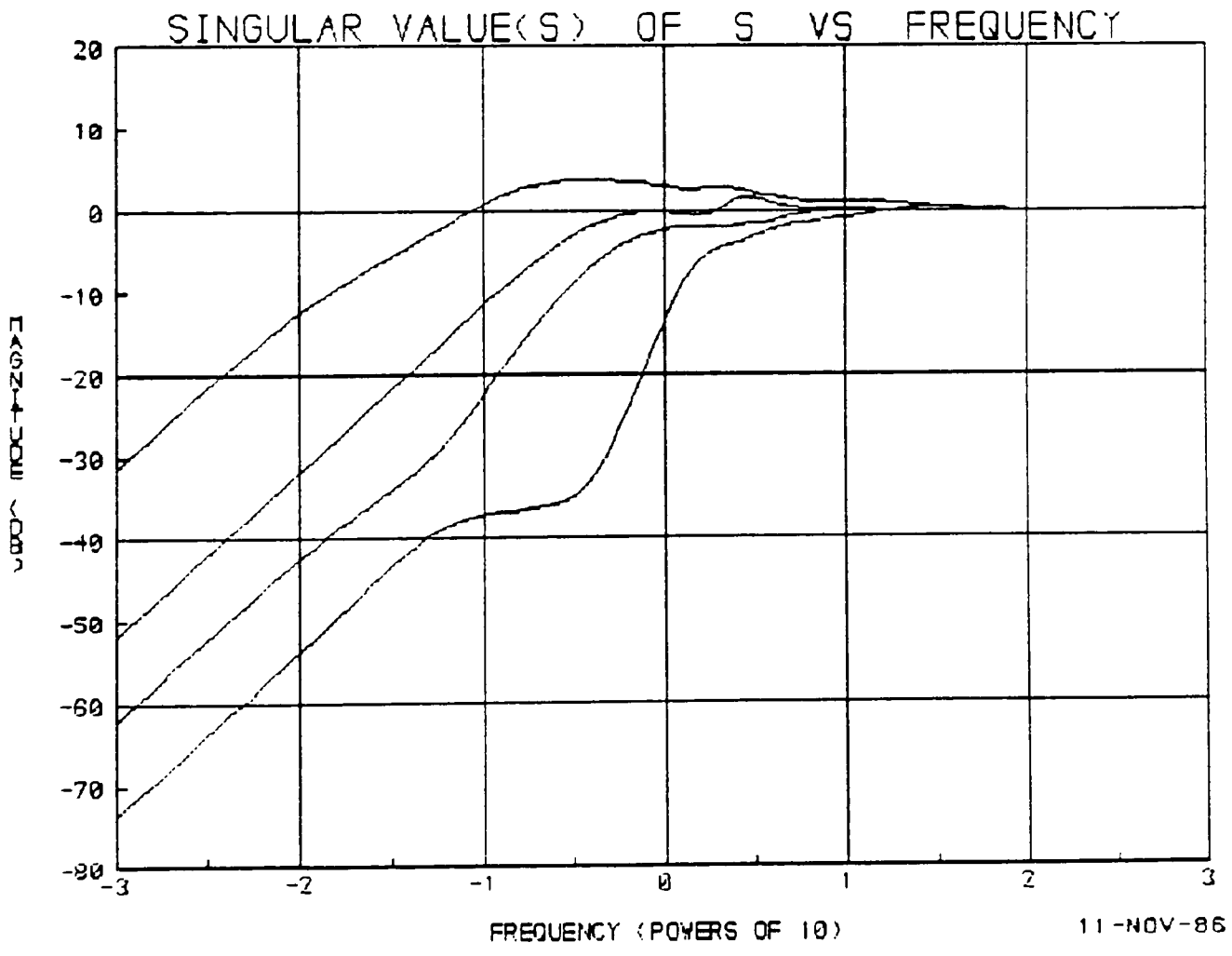


Figure 7.13

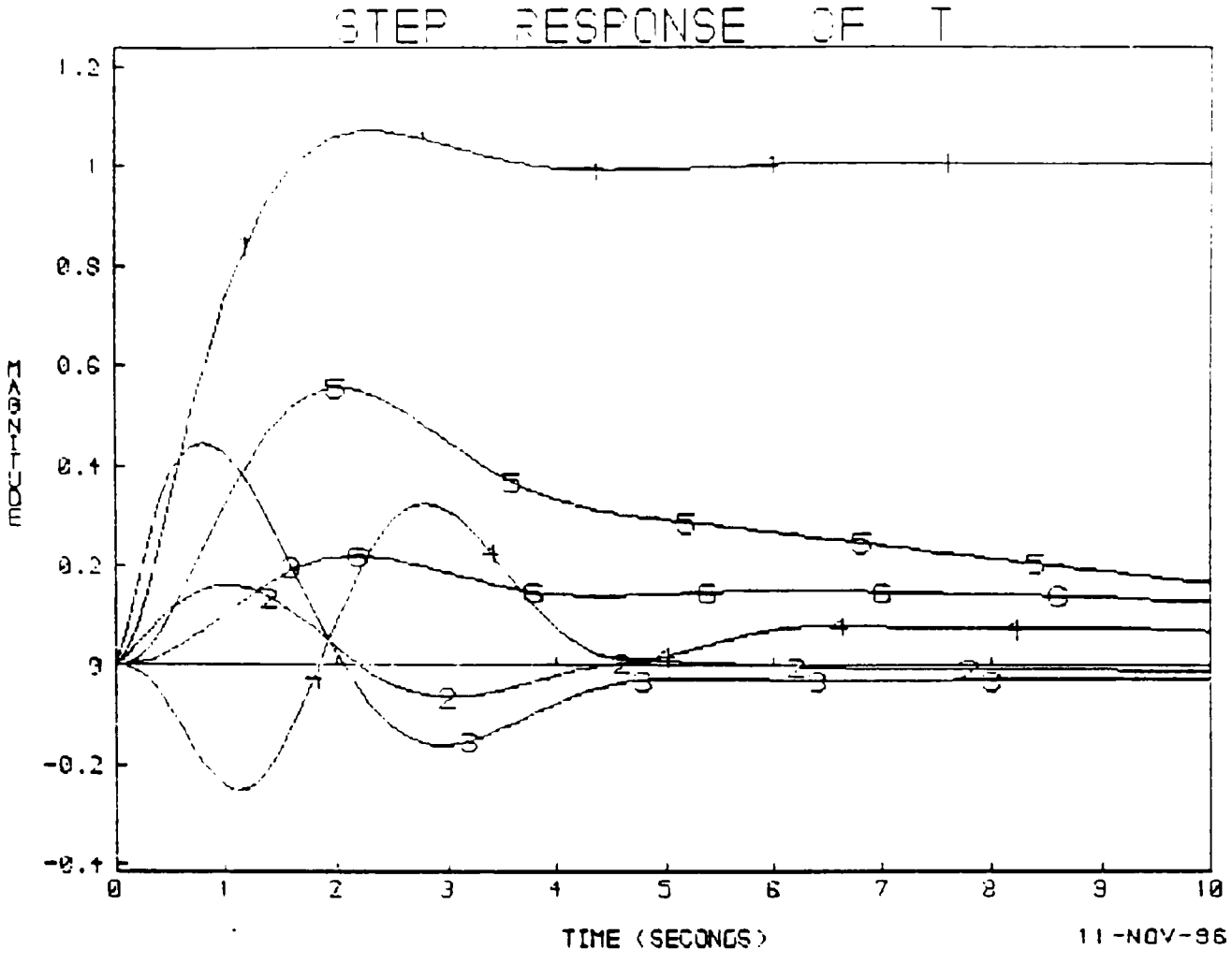


Figure 7.14 Output response to a step demand in channel 1

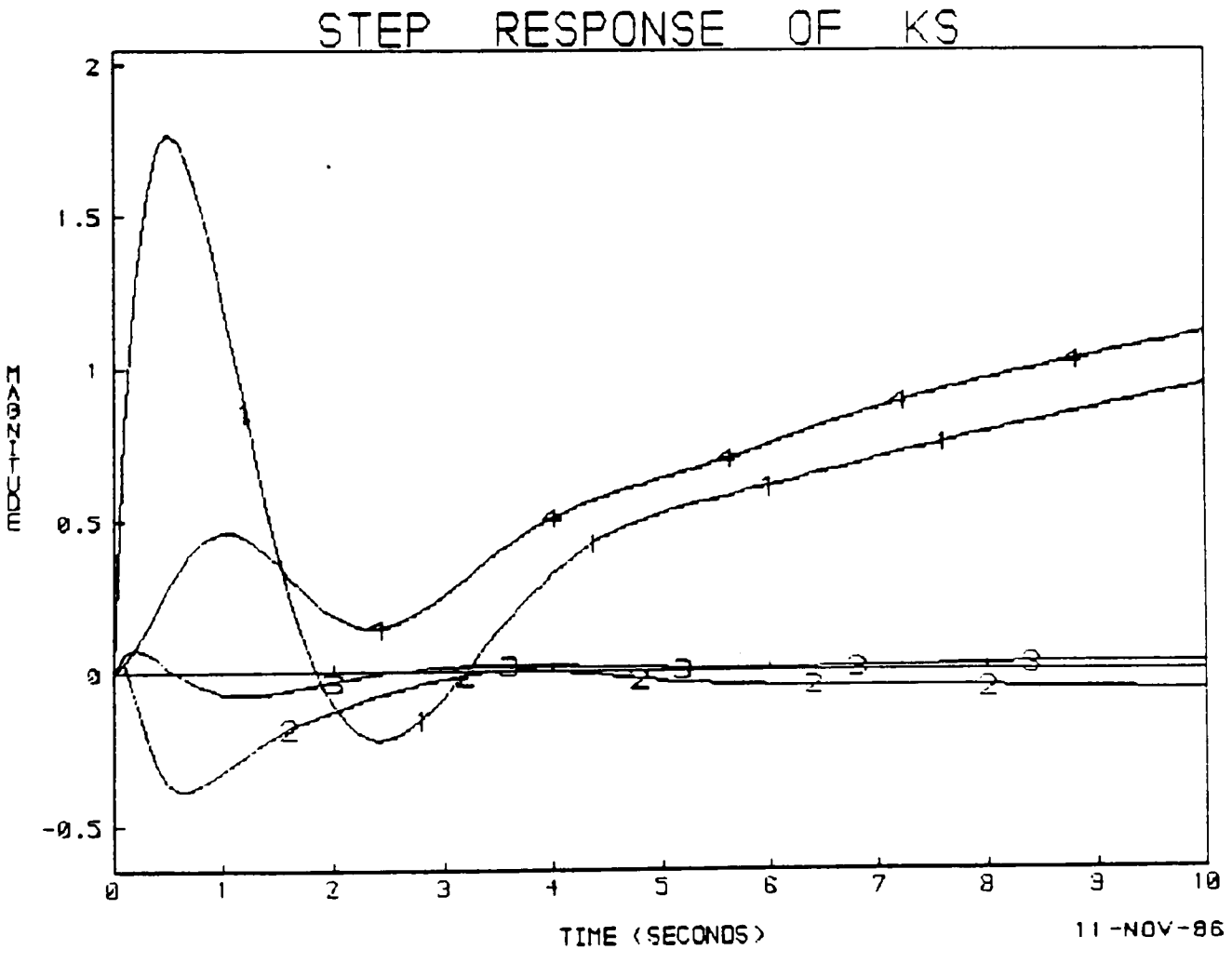


Figure 7.15 Control signal response to a step demand in channel 1

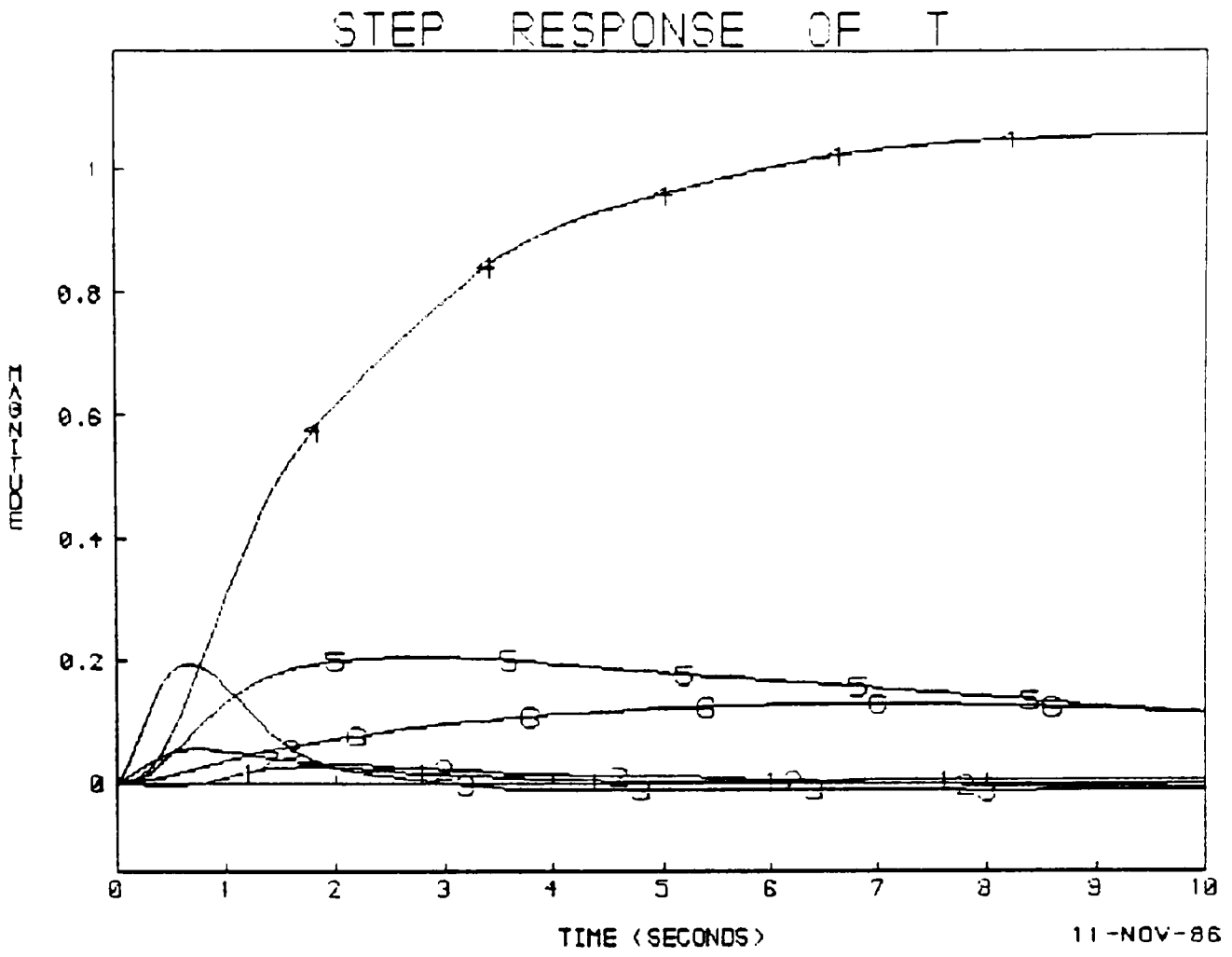


Figure 7.16 Output response to a step demand in channel 4

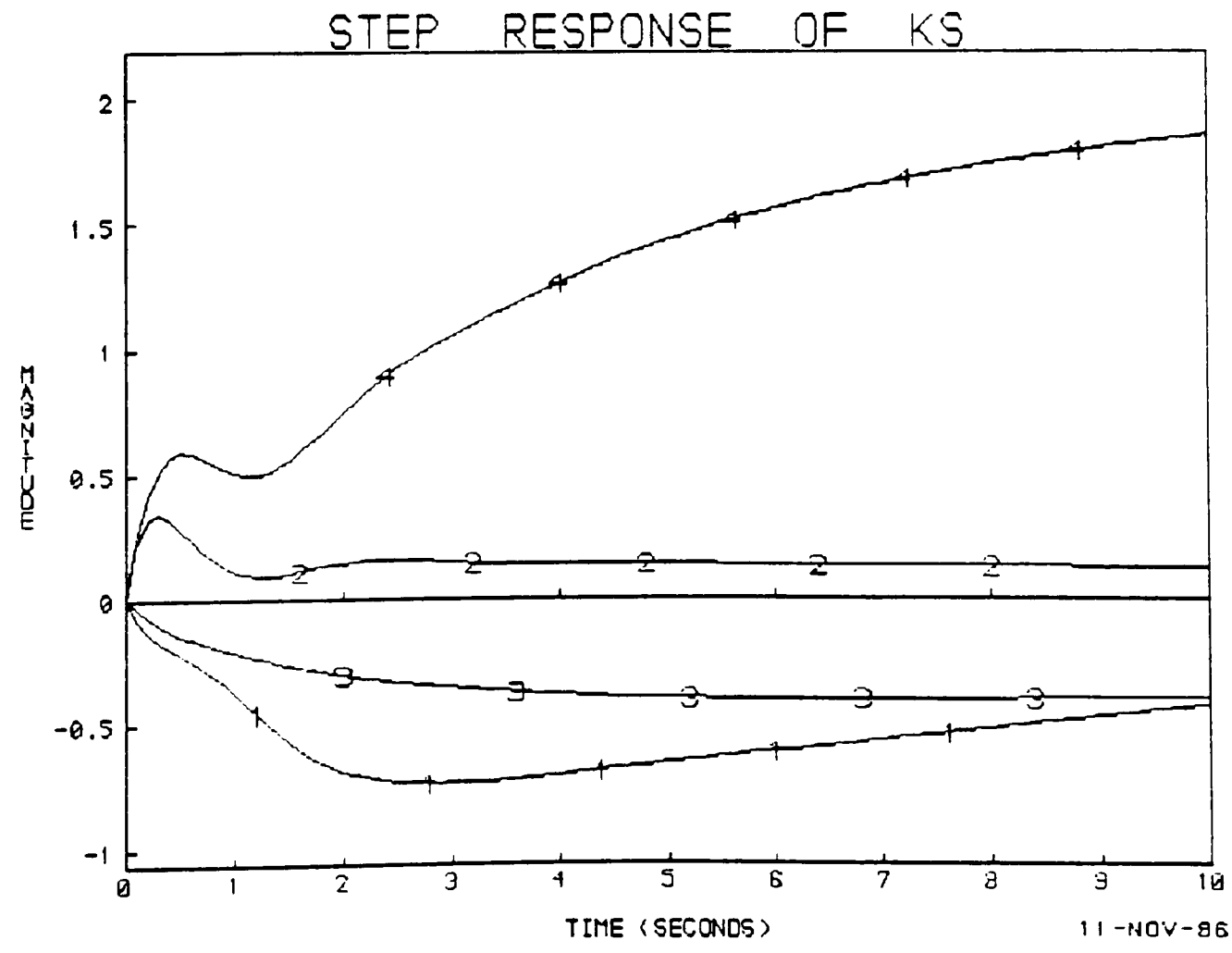


Figure 7.17 Control signal response to a step demand in channel 4

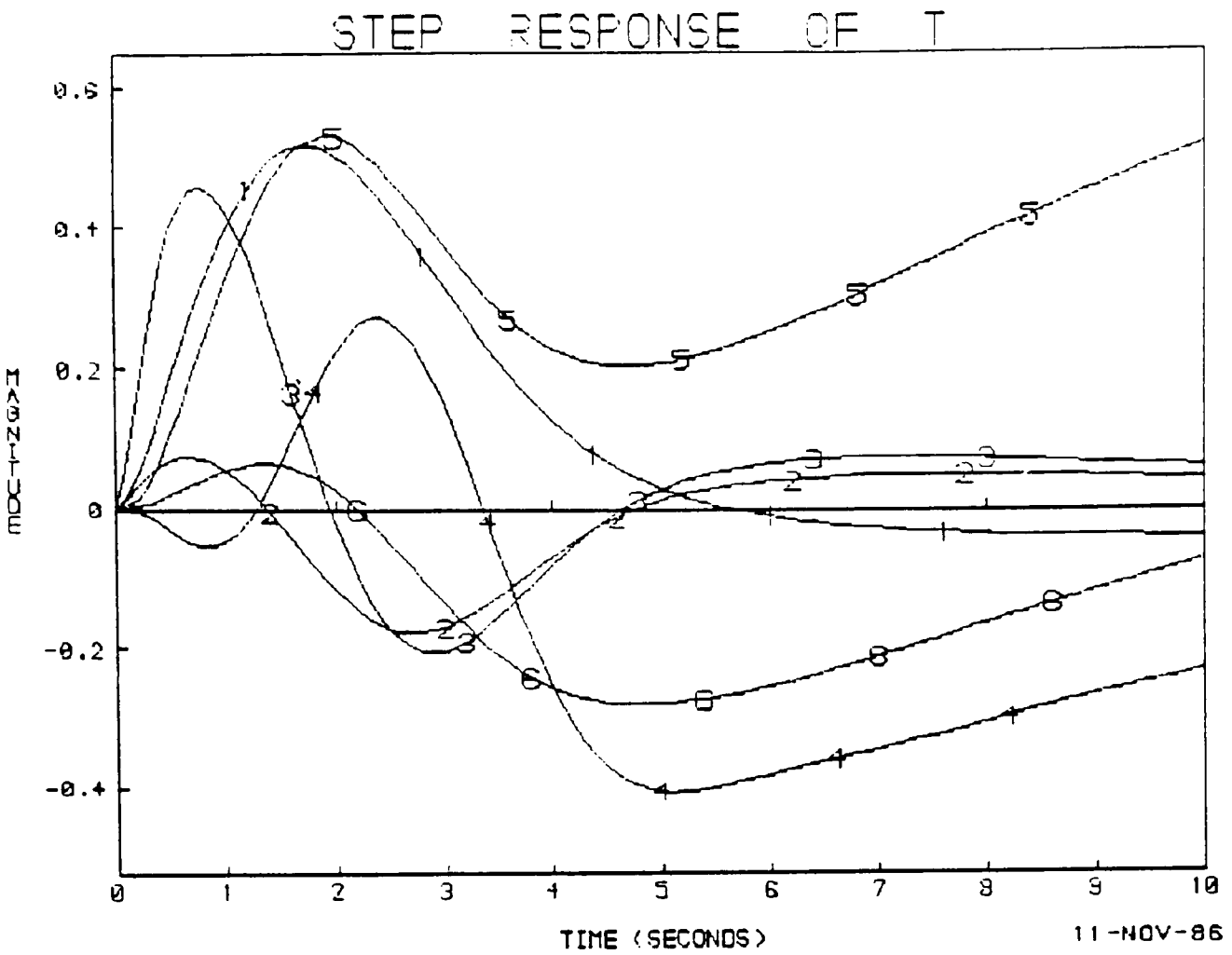


Figure 7.18 Output response to a step demand in channel 5

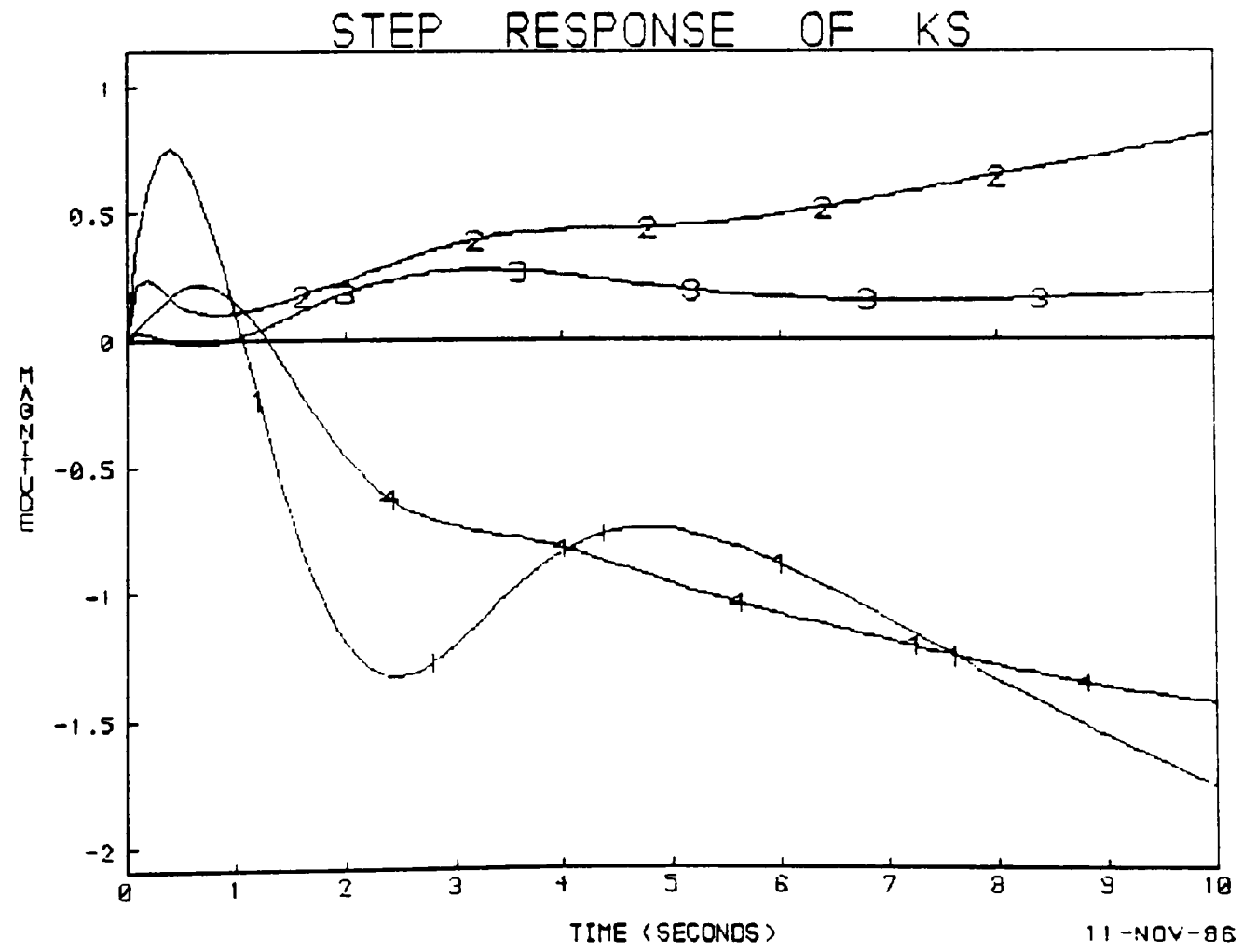


Figure 7.19 Control signal response to a step demand in channel 5

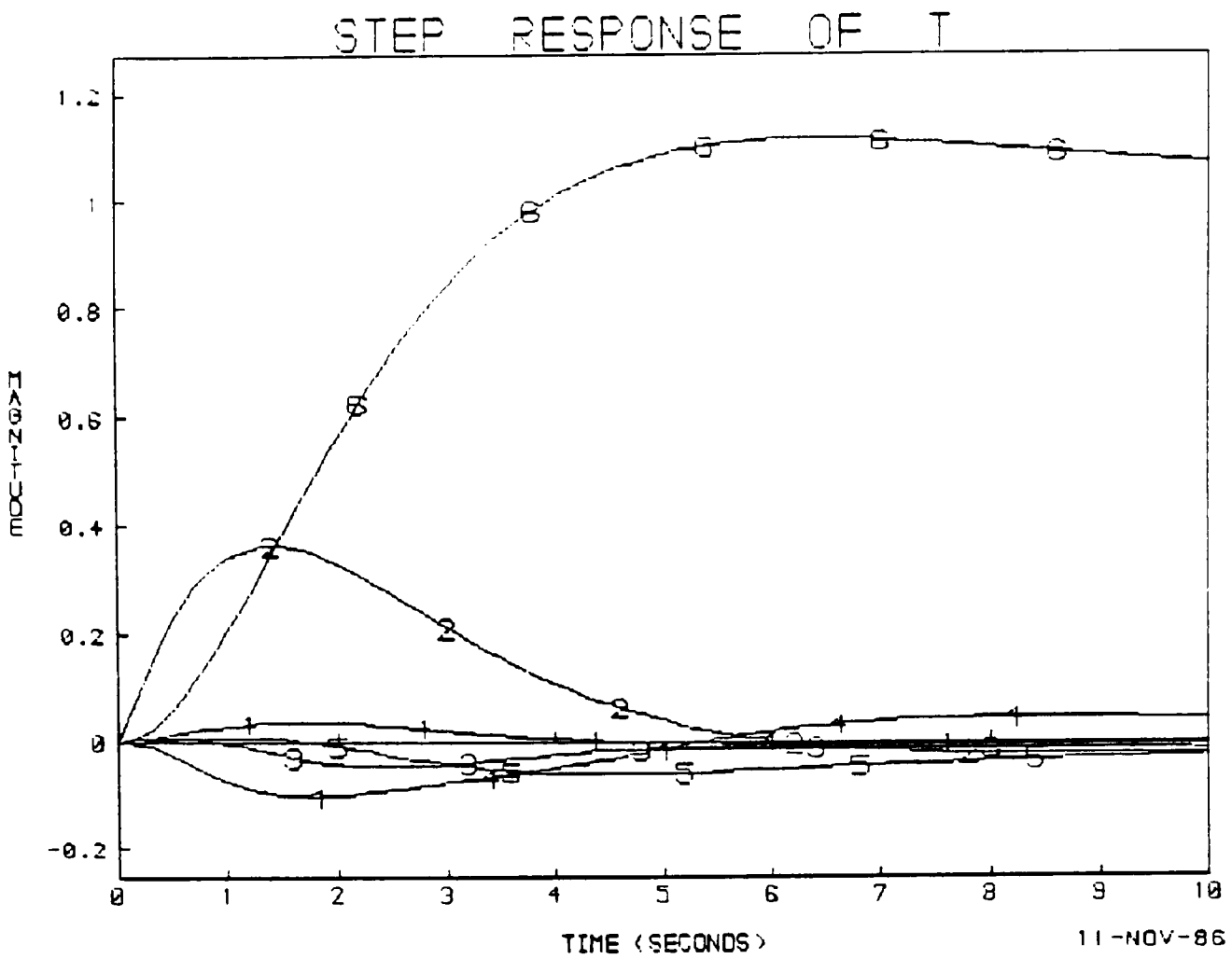


Figure 7.20 Output response to a step demand in channel 6

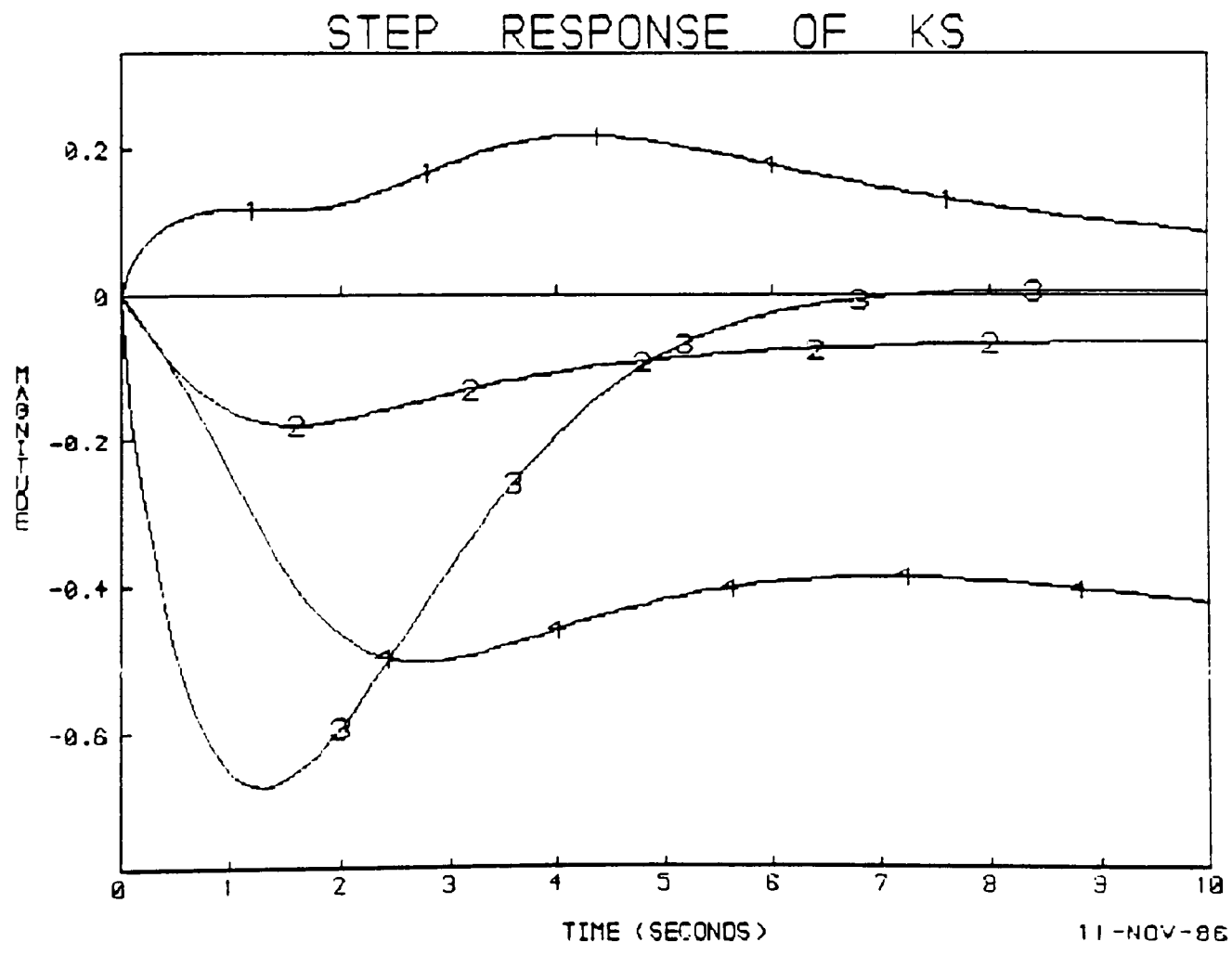


Figure 7.21 Control signal response to a step demand in channel 6

For comparison purposes the loop transfer function achieved by the H^{∞} controller, described in the previous chapter is given in Figure 7.22. It is not clear how this could be achieved via LQG/LTR or why it should generate such superior closed-loop time responses.

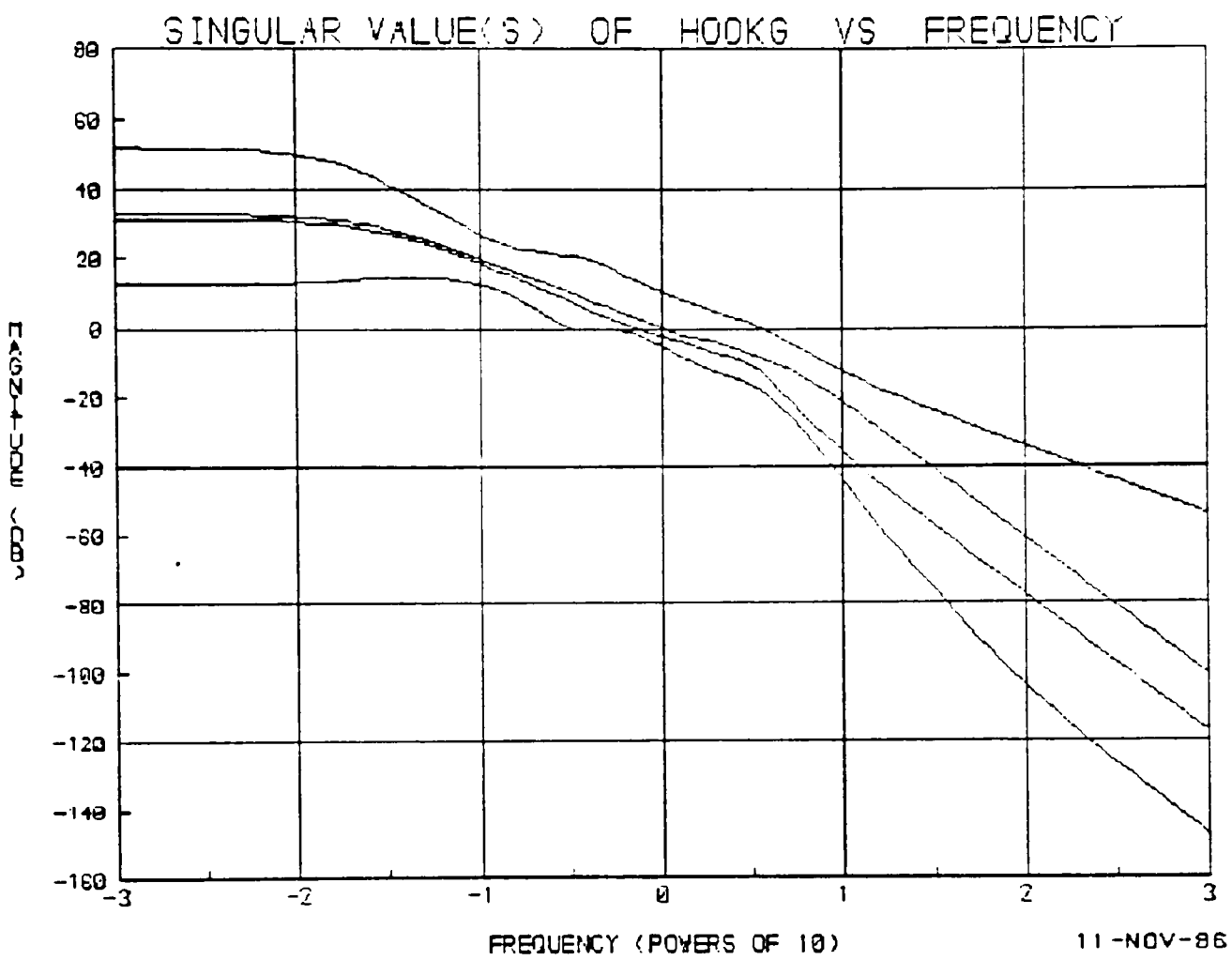


Figure 7.22 KG for the H^{∞}-controller from Chapter VI

7.7 Concluding remarks

It has been emphasized that the LQG controller is an elegant solution to a time-domain optimization problem. The optimal controller is a feedback regulator, and although various techniques can be used to implement it as a servo controller, the optimality may well be lost. When LQG/LTR is used to define the weighting matrices, the physical significance of the cost function is lost, and it is not clear in what sense the controller is optimal.

A major problem with the LQG/LTR was that the techniques used to choose the weighting functions, in order to shape the loop transfer function, depend on a number of assumptions. These assumptions were found to be invalid for the helicopter example. It is not claimed that it is impossible to obtain good results with LQG/LTR, but merely that we were unable to do so with this example.

The H^{∞}-optimization procedure presented in the previous chapter proved to be much easier to use in shaping the closed-loop transfer functions. One topic not addressed in this thesis is the standard problem approach to H^2-optimization [CHU1], which minimizes the 2-norm of a frequency domain cost function. It is expected that this may be a more efficient method for performing frequency-weighted quadratic optimization. The cost functions and assumptions on signals are not the same as in this chapter, however.

CHAPTER VIII

TRUNCATED BALANCED REALIZATION OF A STABLE NON-MINIMAL STATE-SPACE SYSTEM +

8.1 Introduction

This chapter presents a numerically reliable algorithm to compute the balanced realization of a stable state-space system that may be arbitrarily close to being unobservable and/or uncontrollable. The resulting realization, which is known to be a good approximation of the original system, must be minimal and therefore may contain a reduced number of states. Depending on the choice of partitioning of the Hankel singular values, this algorithm can be used either as a form of minimal realization or of model reduction. This illustrates that in finite precision arithmetic these two procedures are closely related.

The motivation for this work was the application of the Hankel-norm approximation theory [GL01] to systems within, and resulting from an H^{∞}-optimization design package recently developed at Oxford University [POS7], [POS8], [POS9]. The first stage in the Hankel-norm approximation theory is the computation of a balanced realization previously considered by Moore [M001] and Laub [LAU2]. Their algorithms require the original system to be completely observable and controllable and are consequently ill-conditioned when the system is close to being non-minimal. In particular, our implementation of Laub's algorithm can even return

+The contents of this chapter also appears in [TOM3].

negative Hankel singular values, because it uses an eigenvalue/eigenvector decomposition. It is stressed that this situation does not occur only in pathological cases, because model-reduction can be most successfully applied to systems that are close to being non-minimal.

One attempt to overcome these difficulties is to perform a 'minimal realization' on the original system, using routines found, for example, in SLICE [WIL1] or CTRL-C [SCT1]. These routines check separately the controllability and observability indices of the system and have been found to be very sensitive to the choice of zero-tolerance. By contrast, the Hankel singular values of a system give a much better indication of the true 'minimal' dimension of a system, by considering the combined controllability and observability properties of the system. Furthermore, the algorithm in this chapter also gives the transformations required to retain only the 'dominant sub-system'.

This problem has also been considered theoretically by Glover ([GLO1], Theorem 4.3 and Appendix B); but this work does not address the numerical difficulties that result when systems are close to being non-minimal, and it is therefore not practically implementable.

There are many similarities between this work and that of Moore [MOO1]. However, we are fortunate in using the algorithm of Hammarling [HAM1] to solve the Lyapunov equations; this avoids the need to factor or invert a non-negative definite matrix. The algorithm thus uses only real matrix multiplication and one singular value decomposition of an upper-triangular matrix. The theoretical algorithm is presented in section 8.2, implementation details are given in section 8.3, numerical examples are given in section 8.4 and conclusions are presented in section 8.5.

In a recent publication Laub et al [LAU3] have proposed a new algorithm to perform the balancing transformations. Their algorithm is very similar to the the one presented in this chapter. Appendix 8.1 compares the two independently developed techniques.

8.2 Theoretical algorithm

We consider a stable state-space system of n states described in the usual way by the matrices (A,B,C,D) and begin with some definitions.

The observability gramian Q is the solution to the Lyapunov equation:

$$A^T Q + QA = -C^T C \tag{8.1}$$

Q is symmetric, positive semi-definite, and (8.1) may be solved for R, a factor of Q such that

$$Q = R^T R \tag{8.2}$$

Similarly, the controllability gramian P is the solution to

$$AP + PA^T = -BB^T \tag{8.3}$$

and

$$P = S^T S, \; P \geq 0 \tag{8.4}$$

The Hankel singular values σ_{hi} of the system (A,B,C,D) are defined to be the positive square-roots of the eigenvalues λ_i of the product PQ (or equivalently QP), i.e.

$$\sigma_{hi} = \left(\lambda_i \, (\, PQ \,) \right)^{1/2} \tag{8.5}$$

A state-space realization of a system is said to be 'balanced' when the observability and controllability gramians are both equal to the diagonal matrix of the Hankel singular values.

We now derive an expression for the Hankel singular values, in terms of R and S. Substituting for P and Q in (8.5) from (8.2) and (8.4), the set of Hankel singular values is given by:

$$\left\{ \sigma_{hi} \right\} = \left\{ \left(\lambda_i(S^T S\ R^T R) \right)^{1/2} \right\} \tag{8.6}$$

$$= \left\{ \left(\lambda_i\ (RS^T SR^T) \right)^{1/2} \right\} \tag{8.7}$$

$$= \left\{ \sigma_i(SR^T) \right\}, \text{ by definition,} \tag{8.8}$$

where $\left\{ \sigma_i(SR^T) \right\}$ is the set of singular values of the product SR^T.

Define U and V to be the singular vectors of the singular value decomposition of SR^T. Then

$$SR^T = U\ \Sigma\ V^T \tag{8.9}$$

where Σ is the diagonal matrix of the Hankel singular values of the system (A,B,C,D), which have been conveniently arranged in order of decreasing magnitude down the diagonal.

Now assume Σ, U and V are partitioned at a given dimension, say k, such that $\Sigma_1 > 0$ where

$$SR^T = \begin{bmatrix} U_1 & U_2 \end{bmatrix} \begin{bmatrix} \Sigma_1 & 0 \\ 0 & \Sigma_2 \end{bmatrix} \begin{bmatrix} V_1^T \\ V_2^T \end{bmatrix} \tag{8.10}$$

The dimensions of U_1, V_1^T and Σ_1 are n x k, k x n, and k x k respectively. We will now use these matrices to define a new system $(\tilde{A},\tilde{B},\tilde{C},\tilde{D})$ of k states, which will be the subject of two theorems.

Let $\quad T = \Sigma_1^{-1/2} V_1^T R, \qquad T^+ = S^T U_1 \Sigma_1^{-1/2}$

then $\quad \tilde{A} = TAT^+, \qquad \tilde{B} = TB, \qquad (8.11)$

$\quad \tilde{C} = CT^+, \qquad \tilde{D} = D.$

Note that T^+ has the property that $TT^+ = I_k$, the identity matrix of dimension k, but is not a Moore-Penrose pseudo-inverse.

Theorem 8.1

The system $(\tilde{A},\tilde{B},\tilde{C},\tilde{D})$ is a balanced realization, truncated to k states, of the system (A,B,C,D).

Proof:

(i) Consider the special case when the system is minimal and k=n. The transformation is then a similarity transformation,

$$TT^+ = I_n, \; T^+T = I_n \qquad (8.12)$$

and we use the result that the observability and controllability gramians $\tilde{P}$ and $\tilde{Q}$ of $(\tilde{A},\tilde{B},\tilde{C},\tilde{D})$ are given by:

$$\tilde{P} = \quad TPT^T \quad = \Sigma^{-1/2} V^T R \; (S^T S) \; R^T V \Sigma^{-1/2} = \Sigma \qquad (8.13)$$

$$\tilde{Q} = (T^T)^{-1} Q T^{-1} = \Sigma^{-1/2} U^T S \; (R^T R) \; S^T U \Sigma^{-1/2} = \Sigma \qquad (8.14)$$

This proves that the resulting system is in balanced form.

(ii) For the general case, when $\Sigma_2 \geq 0$, we will first 'balance' the Lyapunov equations (8.1) and (8.3) by pre- and post-multiplication.

Consider (8.1), substitute for Q from (8.2), pre-multiply by $U^T S$ and post-multiply by $S^T U$ to obtain:

$$U^T S A^T R^T R S^T U + U^T S R^T R A S^T U = -U^T S C^T C S^T U \tag{8.15}$$

Now substitute for SR^T and RS^T from (8.10) to give

$$\begin{bmatrix} U_1^T \\ U_2^T \end{bmatrix} SA^T R^T \begin{bmatrix} V_1 & V_2 \end{bmatrix} \begin{bmatrix} \Sigma_1 & 0 \\ 0 & \Sigma_2 \end{bmatrix} + \begin{bmatrix} \Sigma_1 & 0 \\ 0 & \Sigma_2 \end{bmatrix} \begin{bmatrix} V_1^T \\ V_2^T \end{bmatrix} RAS^T \begin{bmatrix} U_1 & U_2 \end{bmatrix}$$

$$= - \begin{bmatrix} U_1^T \\ U_2^T \end{bmatrix} SC^T CS^T \begin{bmatrix} U_1 & U_2 \end{bmatrix} \tag{8.16}$$

We now see that the Lyapunov equation may be split into four equations, one a Lyapunov equation with solution Σ_1:

$$U_1^T S A^T R^T V_1 \Sigma_1 + \Sigma_1 V_1^T R A S^T U_1 = - U_1^T S C^T C S^T U_1 \tag{8.17}$$

Proceeding in a similar manner for equation (8.3) we obtain:

$$V_1^T R A S^T U_1 \Sigma_1 + \Sigma_1 U_1^T S A^T R^T V_1 = - V_1^T R B B^T R^T V_1 \tag{8.18}$$

Now notice that $$\Sigma_1^{1/2} \tilde{A} \Sigma_1^{1/2} = V_1^T R A S^T U_1 \tag{8.19}$$

$$\Sigma_1^{1/2} \tilde{B} = V_1^T R B \tag{8.20}$$

$$\tilde{C} \Sigma_1^{1/2} = C S^T U_1 \tag{8.21}$$

Substitution of these into (8.17) and (8.18), followed by pre- and post-multiplication by $\Sigma_1^{-1/2}$ gives

$$\tilde{A}^T \Sigma_1 + \Sigma_1 \tilde{A} = - \tilde{C}^T \tilde{C} \tag{8.22}$$

$$\tilde{A} \Sigma_1 + \Sigma_1 \tilde{A}^T = - \tilde{B} \tilde{B}^T \tag{8.23}$$

We have therefore shown that the system transformed by T and T^+ given in equation (8.11) is in balanced form with gramians equal to Σ_1.

Q.E.D.

Theorem 8.2

If the parameter k is chosen such that $\Sigma_2 = 0$ and $\Sigma_1 > 0$, then the reduced order system $(\tilde{A},\tilde{B},\tilde{C},\tilde{D})$ is a minimal realization of the system (A,B,C,D). That is, it is completely observable and controllable and has a transfer function model identical to that of the original system.

Proof:

Consider the error function E(s), the difference between the transfer function model of the original system G(s) and the reduced order system $\tilde{G}(s)$:

$$E(s) = G(s) - \tilde{G}(s) \tag{8.24}$$

A state-space model of E(s), (Ae,Be,Ce,De), is given by

$$\left[\begin{array}{c|c} Ae & Be \\ \hline Ce & De \end{array}\right] = \left[\begin{array}{cc|c} A & 0 & B \\ 0 & \tilde{A} & \tilde{B} \\ \hline C & -\tilde{C} & 0 \end{array}\right] \tag{8.25}$$

The controllability gramian P_e of this error system, appropriately partitioned, is given by:

$$\left[\begin{array}{cc} A & 0 \\ 0 & \tilde{A} \end{array}\right]\left[\begin{array}{cc} P_{11} & P_{12} \\ P_{12}^T & P_{22} \end{array}\right] + \left[\begin{array}{cc} P_{11} & P_{12} \\ P_{12}^T & P_{22} \end{array}\right]\left[\begin{array}{cc} A^T & 0 \\ 0 & \tilde{A}^T \end{array}\right] = - \left[\begin{array}{c} B \\ \tilde{B} \end{array}\right]\left[\begin{array}{cc} B^T & \tilde{B}^T \end{array}\right] \tag{8.26}$$

Clearly $P_{11} = S^T S$ (from (8.3) and (8.4))

$P_{22} = \Sigma_1$ (from (8.23))

and P_{12} is the solution of the Sylvester equation

$$AP_{12} + P_{12}\tilde{A}^T = -B\tilde{B}^T \tag{8.27}$$

Such an equation has a unique solution provided that

$$\lambda_i(A) + \lambda_j(\tilde{A}^T) \neq 0 \text{ for all } i \text{ and } j \tag{8.28}$$

and this is guaranteed in this case, since $Re[\lambda_i(A)] < 0$, by assumption, and $Re[\lambda_j(\tilde{A})] \leq 0$, by the properties of the Lyapunov equations (8.22) and (8.23).

Substituting for $\tilde{A}$ and $\tilde{B}$ from (8.11) we obtain

$$AP_{12} + P_{12}(TAT^+)^T = -BB^T T^T \tag{8.29}$$

and then substituting for BB^T from (8.3) and (8.4), for T and T^+ from (8.11), and rearranging

$$A(P_{12} - S^T S R^T V_1 \Sigma_1^{-1/2}) + (P_{12}\Sigma_1^{-1/2}U_1^T - S^T)SA^T R^T V_1 \Sigma_1^{-1/2} = 0 \tag{8.30}$$

Notice that

$$SR^T V_1 = U_1 \Sigma_1 V_1^T V_1 = U_1 \Sigma_1 \tag{8.31}$$

$$S^T = S^T(U_1 U_1^T + U_2 U_2^T) \tag{8.32}$$

and also

$$S^T U_2 U_2^T SA^T R^T V_1 \Sigma_1^{-1/2} = 0 \tag{8.33}$$

since $U_2^T SA^T R^T V_1 = 0$, from equation (8.16) with $\Sigma_2 = 0$. Equation (8.30) may now be rearranged to give

$$A(P_{12} - S^T U_1 \Sigma_1^{1/2}) + (P_{12} - S^T U_1 \Sigma_1^{1/2})\Sigma_1^{-1/2} U_1^T SA^T R^T V_1 \Sigma_1^{-1/2} = 0 \tag{8.34}$$

Therefore $P_{12} = S^T U_1 \Sigma_1^{1/2}$ and the controllability gramian is given by

$$P_e = \begin{bmatrix} S^T S & S^T U_1 \Sigma_1^{1/2} \\ \Sigma_1^{1/2} U_1^T S & \Sigma_1 \end{bmatrix} \tag{8.35}$$

Similarly we find that the observability gramian is given by

$$Q_e = \begin{bmatrix} R^T R & -R^T V_1 \Sigma_1^{1/2} \\ -\Sigma_1^{1/2} V_1^T R & \Sigma_1 \end{bmatrix} \tag{8.36}$$

We next form the product $P_e Q_e$ in order to examine the Hankel singular values of the error system.

$$P_e Q_e = \begin{bmatrix} S^T S R^T R - S^T U_1 \Sigma_1 V_1^T R & -S^T S R^T V_1 \Sigma_1^{1/2} + S^T U_1 \Sigma_1^{3/2} \\ \Sigma_1^{1/2} U_1^T S R^T R - \Sigma_1^{3/2} V_1^T R & -\Sigma_1^{1/2} U_1^T S R^T V_1 \Sigma_1^{1/2} + \Sigma_1^2 \end{bmatrix} \tag{8.37}$$

$$= \begin{bmatrix} S^T (S R^T - U_1 \Sigma_1 V_1^T) R & S^T (-S R^T V_1 + U_1 \Sigma_1) \Sigma_1^{1/2} \\ \Sigma_1^{1/2} (U_1^T S R^T - \Sigma_1 V_1^T) R & \Sigma_1^{1/2} (-U_1^T S R^T V_1 + \Sigma_1) \Sigma_1^{1/2} \end{bmatrix} \tag{8.38}$$

$$= \begin{bmatrix} 0 & 0 \\ 0 & 0 \end{bmatrix} \tag{8.39}$$

Hence $$\sigma_{hi}\left\{ E(s) \right\} = 0 \text{ for all } i. \tag{8.40}$$

Now the Hankel norm of E(s), which gives the L_2-gain from past inputs to future outputs [GL01], is equal to the maximum Hankel singular value of E(s), and is therefore zero. Therefore no input can affect any output and E(s) must be zero. The reduced order system $(\tilde{A},\tilde{B},\tilde{C},\tilde{D})$ is both controllable and observable by construction, and therefore we have shown that it is a minimal realization of the original system. **Q.E.D.**

Corollary:

A bound on the difference in frequency response between that of the original system G(s) and the truncated balanced realization $\tilde{G}_k(s)$, is given by

$$|| G(s) - \tilde{G}_k(s) ||_\infty \leq 2 \sum_{i=k+1,n} \sigma_{hi} \qquad (8.41)$$

Proof:

Glover [GL01] Theorem 9.6 gives the above result when G(s) is a minimal realization. Theorem 8.2 above allows us to extend this result to non-minimal systems, when the construction of equation 8.11 is used to construct the truncated balanced realization.

This result enables the truncated balanced realization to be used to perform minimal realization with a guaranteed error bound. A possible definition of a minimal realization is as a state-space model with the minimum number of states such that the error given by equation 8.41 is less than the uncertainty in the frequency response of the original model. If this uncertainty is known, the required minimal number of states may be obtained by examination of the Hankel singular values. A major advantage of this technique over other forms of minimal realization is that this 'tolerance' need not be defined before the computation, and the effect of different tolerances is clearly visible without further calculations.

8.3 Implementation details

Hammarling [HAM1] gives an algorithm to solve the stable non-negative definite Lyapunov equation - such as in (8.1) and (8.3) - for the Cholesky factor of the solution, without the need to compute the product on the right-hand side of the equation. In our application we do not need the

Cholesky factor, so we omit the final reduction of the solution and solve for the components of the factor R of the solution, as illustrated below.

Step 1

Solve (8.1) for the factor R, which may be rank deficient. R is composed of an upper-triangular matrix R_u, and an orthogonal matrix W such that

$$R = R_u W^T \tag{8.42}$$

where R_u is the solution of (8.1) suitably transformed to canonical form (see [HAM1]), and W is defined by the real upper Schur factorization of the system A-matrix:

$$A = W A_{us} W^T \tag{8.43}$$

where A_{us} is an n x n block upper triangular matrix with one by one and two by two blocks on the diagonal.

Step 2

Solve (8.3) for the factor S, which may also be rank deficient. By defining a permutation matrix Z with the structure $\begin{bmatrix} 0 & 1 \\ 1 & 0 \end{bmatrix}$, we can use the Schur factorization of A in (8.42) to obtain the real upper Schur factorization of A^T [BAR1], [LAU2]:

$$A^T = W \ (A_{us})^T \ W^T \tag{8.44}$$

$$= WZZ(A_{us})^T ZZW^T \tag{8.45}$$

$$= WZ \ (A^T)_{us} (WZ)^T \tag{8.46}$$

Hence we solve for

$$S = S_u Z W^T \tag{8.47}$$

where S_u is the upper triangular solution of (8.3) after suitably transforming it to canonical form [HAM1].

Step 3

Form the product SR^T. Substituting from (8.43) and (8.47), we obtain:

$$SR^T = S_u Z W^T W R_u^T \tag{8.48}$$

$$= S_u Z R_u \tag{8.49}$$

By inspection, this product is triangular, of the form $\begin{bmatrix} x & x \\ x & 0 \end{bmatrix}$. Unfortunately this appears to be a pathological structure for standard singular value decompositions as implemented in e.g., NAG [NAG1] or LINPACK [DON1], which tend to fail with 'floating point overflow'. For this reason we find the singular value decomposition of SR^TZ, which is upper triangular, and then post-multiply again by Z.

$$SR^TZ = U \Sigma V^T \tag{8.50}$$

$$SR^T = U \Sigma V^TZ \tag{8.51}$$

It is not necessary ever to form the matrix Z; its use is merely to re-order the rows and/or columns of a matrix, which is easily performed in a manner similar to the taking of a transpose.

Step 4

Before we apply the transformations of equation (8.11), it is necessary to determine the partitioning of the Hankel singular values. Of particular importance in making this choice are the ratios of consecutive singular values, and the condition number with respect to inversion of Σ_1

$$c(\Sigma_1) = \frac{\sigma_{h1}}{\sigma_{hk}}$$

which defines the numerical conditioning of the subsequent transformations. If the algorithm is to be used simply to obtain a minimal, balanced realization, then a sensible criterion for the choice of k is a maximum finite value for this condition number. That is, find the maximum k such that $c(\Sigma_1) < \frac{1}{\delta}$ where δ is a small number, e.g. $(\text{eps})^{1/2}$, where eps is the usual precision of floating point arithmetic (the smallest value such that the logical expression (1.0 + eps .GT. 1.0) is true). To use the algorithm as a form of model reduction, a sensible criterion is to look for a large value of the ratio $\frac{\sigma_{hk}}{\sigma_{hk+1}}$ indicating a natural division of the states. This selection process will be illustrated by example in the next section.

Step 5

The transformations given in equation (8.11) are then applied to the original system data. If several truncations are to be considered we need only compute a realization for the maximum number of states; then, since the others are given by partitioning this realization, there is no need to repeat the whole calculation.

8.4 Numerical examples

We will present two examples of the application of the truncated balanced realization algorithm presented in this chapter. All calculations were performed using DOUBLE PRECISION FORTRAN on a VAX 11/780 computer. The first example is intended to be reproducible, based on the system considered by Glover ([GL01], Section 10.2). The second arises

from the design of a controller for an unstable helicopter, using H^{∞}-optimization.

8.4-1 Example 1

The state matrices for this example are given in [HUN1], and describe a system with 2 inputs, 2 outputs and 12 states. Although the system itself is very close to being non-minimal, we make it definitely non-minimal in the following manner to illustrate the power of our algorithm.

$$\text{Define } G(s) = C(sI-A)^{-1}B + D := \left[\begin{array}{c|c} A & B \\ \hline C & D \end{array}\right] \tag{8.52}$$

and for this example

$$G_{ex}(s) = 0.5 \left(G(s) + G(s) \right) \tag{8.53}$$

which, because the addition is performed in state-space, has the non-minimal state-space description

$$G_{ex}(s) = \left[\begin{array}{cc|c} A & 0 & B \\ 0 & A & B \\ \hline 0.5C & 0.5C & D \end{array}\right] \tag{8.54}$$

The computed Hankel singular values are given in Table 8.1. The first 12 are in fact identical to the ones we compute for the original system. Clearly a 'good' place to truncate this model is at 8 states, which we do with the transformations given in equation (8.11). The singular values of the error function $E(s) = G(s) - G_8(s)$ are plotted in Figure 8.1.; the maximum value of this function is 0.00109. For this example, because we have introduced exact non-minimality into this problem, the 12 unwanted states for minimality could easily have been removed by a 'standard' minimal realization routine.

1	7.183D+00	11	1.412D-06	21	0.000D+00
2	1.490D+00	12	3.434D-08	22	0.000D+00
3	9.279D-01	13	4.539D-34	23	0.000D+00
4	5.876D-01	14	2.768D-34	24	0.000D+00
5	4.633D-01	15	9.391D-35		
6	2.368D-01	16	6.379D-35		
7	1.613D-01	17	4.234D-35		
8	9.358D-02	18	1.163D-35		
9	5.660D-04	19	4.187D-36		
10	2.061D-05	20	1.208D-38		

Table 8.1 Hankel singular values for Example 1

8.4-2 Example 2

This example is the controller designed in Chapter VI for the 4-input, 8-state, 6-output helicopter model. The 'standard problem', consisting of the plant augmented with weights, had a state dimension of 20. The 'raw' output from the H^{∞}-design procedure was a controller with 59 states. (Computational improvements in [POS6] should help to reduce the 'size' of the controller.) The Hankel singular values of this 6-input, 4-output stable state-space system are given in Table 8.2.

1	1.911D+02	16	6.217D-02	31	2.588D-08	46	1.872D-17
2	6.809D+01	17	1.296D-02	32	1.671D-08	47	1.204D-17
3	2.382D+01	18	8.971D-03	33	7.604D-09	48	1.094D-17
4	2.087D+01	19	1.981D-05	34	6.142D-09	49	6.328D-18
5	1.456D+00	20	1.332D-05	35	3.970D-09	50	2.546D-18
6	9.785D-01	21	1.097D-05	36	2.124D-09	51	1.734D-18
7	7.682D-01	22	8.929D-06	37	1.194D-09	52	1.548D-18
8	5.424D-01	23	4.493D-06	38	4.616D-11	53	5.193D-19
9	4.735D-01	24	1.870D-06	39	1.978D-13	54	1.865D-19
10	4.263D-01	25	1.325D-06	40	1.852D-15	55	7.492D-20
11	2.230D-01	26	6.370D-07	41	8.763D-17	56	3.278D-20
12	1.523D-01	27	3.517D-07	42	7.666D-17	57	2.109D-20
13	1.254D-01	28	2.649D-07	43	5.310D-17	58	1.042D-20
14	1.190D-01	29	1.282D-07	44	2.505D-17	59	1.341D-23
15	8.273D-02	30	5.225D-08	45	2.047D-17		

Table 8.2 Hankel singular values for Example 2

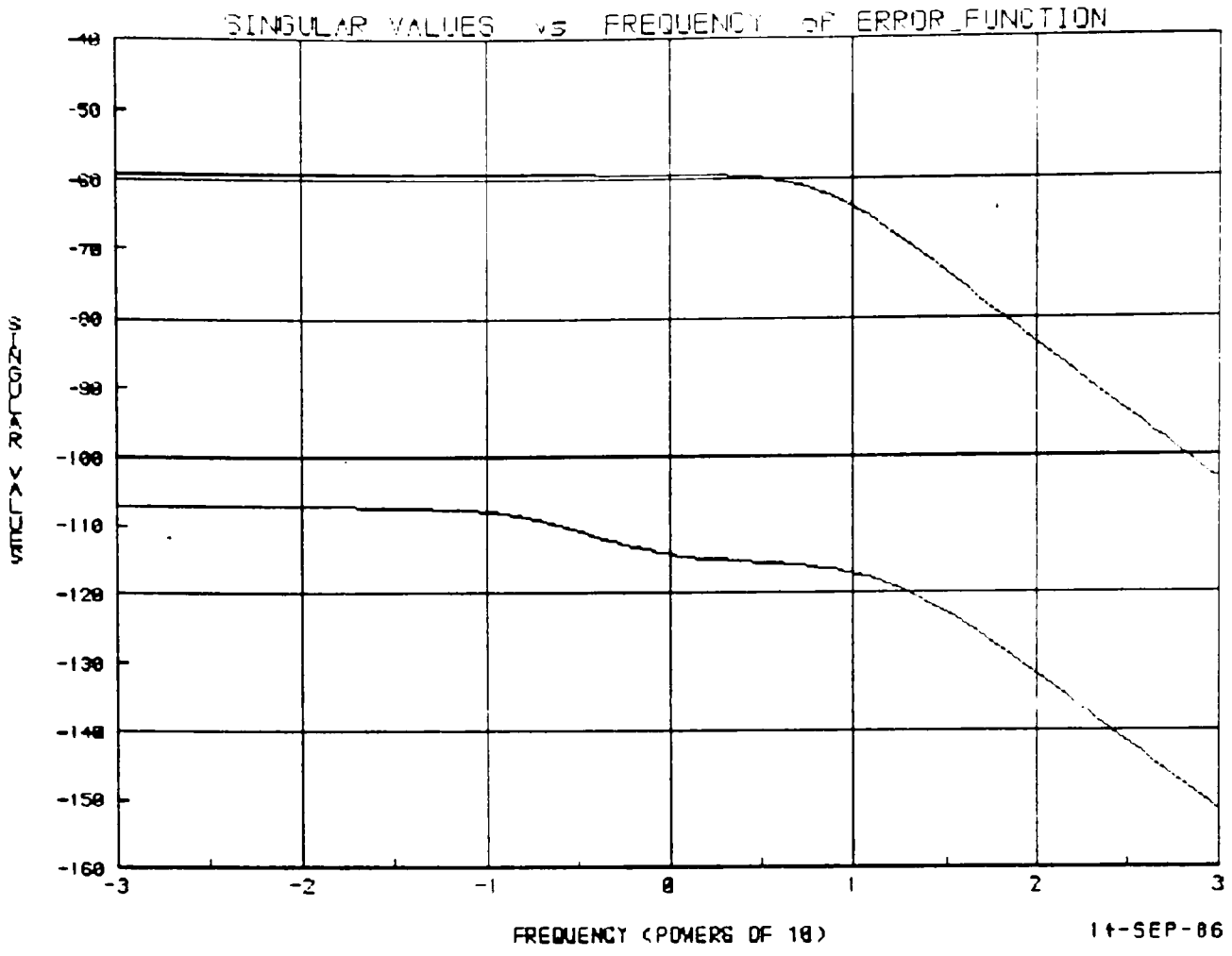


Figure 8.1 Magnitude of the error function for Example 1

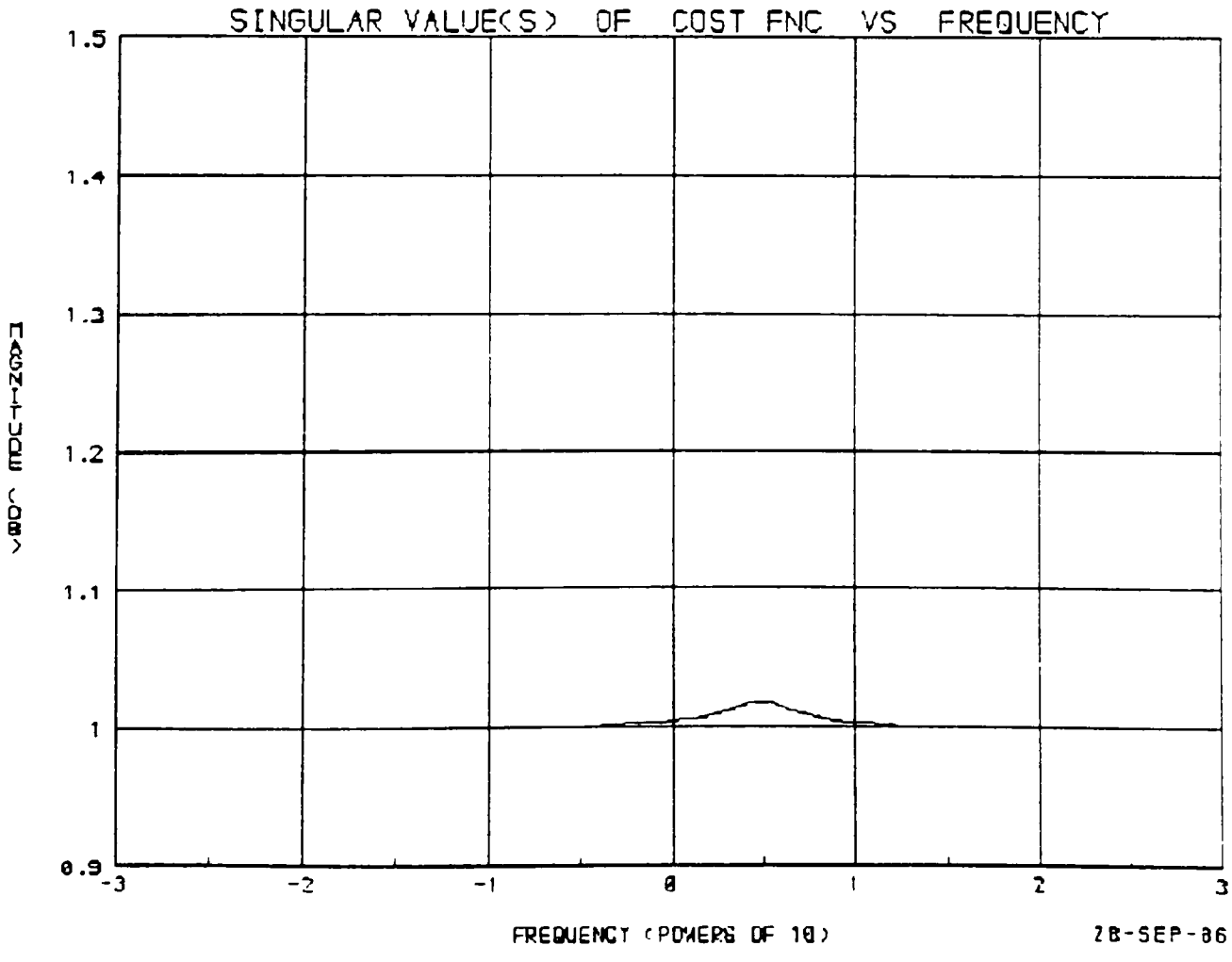


Figure 8.2 Max. value of the cost function for Example 2 with 59 state K

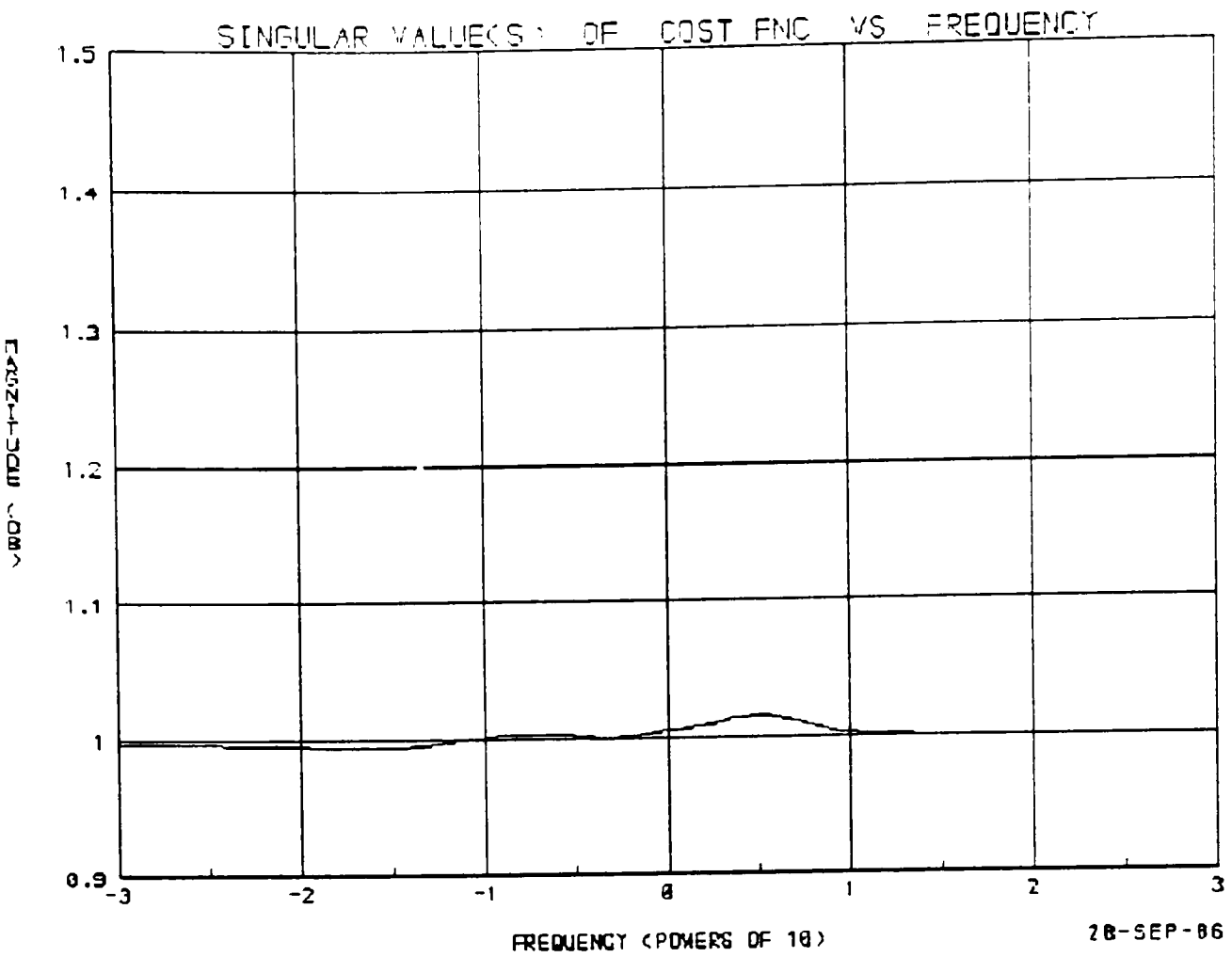


Figure 8.3 Max. value of the cost function for Example 2 with 18 state K

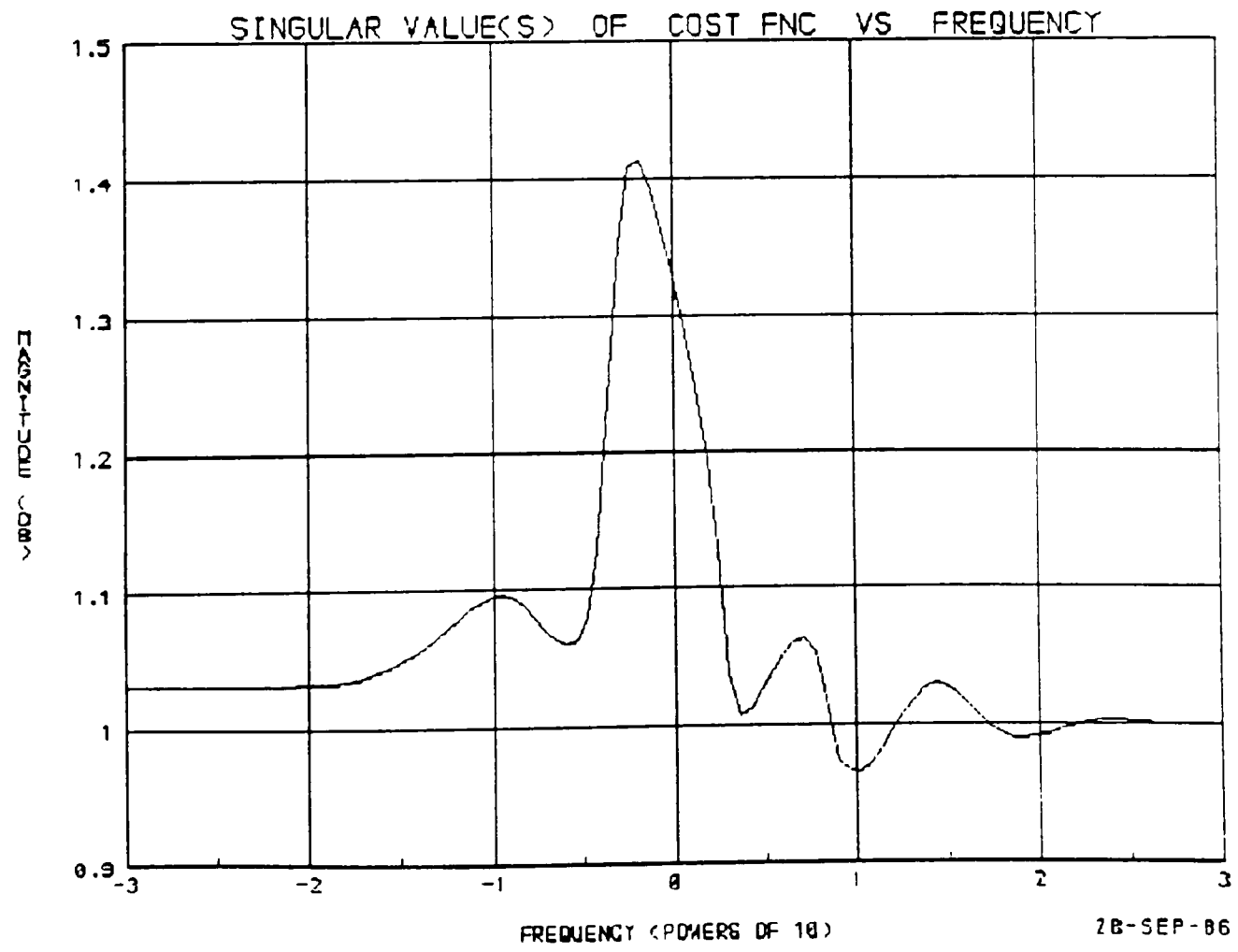


Figure 8.4 Max. value of the cost function for Example 2 with 16 state K

Two important properties of a controller that minimizes an H^∞-optimization problem are that the closed-loop system is stable and that the maximum singular value of the cost function is constant over all frequencies. These provide us with an excellent test of the validity of a reduced order controller. The maximum singular value of the cost function with the 59-state controller is given in Figure 8.2. Figures 8.3 and 8.4 show the maximum singular value of the cost function, evaluated with truncated balanced realizations of the controller, of dimensions 18 and 16. Both controllers are stabilizing, and we can clearly accept the 18-state controller as an H^∞-'optimal' controller.

8.5 Concluding remarks

The algorithm proposed in this chapter has proved to be very useful in its application to H^∞-design procedures (Chapter V). One shortcoming is that it is not directly applicable to unstable systems. This is because an unstable mode, however weakly observable or controllable, would tend eventually to dominate the time response. Therefore any model with a reduced number of unstable poles is unlikely to be regarded as a good approximation. Numerical procedures, such as H^∞-design or conversion of transfer function models to state space, can generate systems with non-minimal unstable poles. If the system is completely unstable the algorithm in this chapter can be applied to $G(-s)$; if the system is partly unstable it must first be decomposed into its stable and unstable parts. This decomposition can be performed via a Schur decomposition and the solution of a Sylvester equation, assuming no poles on the imaginary axis, and has been successfully applied in H^∞-design. When systems have poles on (or arbitrarily close to) the $j\omega$-axis, some form of $j\omega$-axis shifting could be attempted. The frequency response bound of equation

(8.41) would then apply for $s=\alpha+j\omega$, where α is the distance that the $j\omega$-axis is moved.

We make the following remarks concerning the advantages of our algorithm over those previously available:

1) We solve for the Hankel singular values directly, whereas Moore [MOO1] and Laub [LAU2] find Σ^2. Therefore we can compute small values more accurately. (For example $10^{-9} \times 10^{-9} = 10^{-18}$ which may be less than eps).

2) The algorithm makes no assumptions about the controllability or observability of the original system and has a pleasing symmetry in its use of the controllability and observability gramians.

3) The algorithm uses orthogonal transformations wherever possible, and the user has control over the conditioning of the non-orthogonal transformations given in equation (8.11). This is not the case if an eigenvalue/eigenvector decomposition is used to compute the Hankel singular values. The Lyapunov equations may be ill-conditioned, however, if the system is close to being unstable.

The truncated balanced realization has the following properties:

1) The truncated balanced realization is completely observable, controllable and stable [MOO1], [PER2], and [GLO1].

2) A bound on the difference in frequency response between that of the original system G(s) and the truncated balanced realization $\tilde{G}_k(s)$ is given by equation (8.41). Furthermore this error function is low pass in nature, tending to zero as $s \to \infty$, because the constant term D is not changed.

Finally, although the algorithm presented in this chapter was developed for use in H^{∞}-design, it can be used to provide the balanced realization required as a starting point for much recent research. For example, [GL01] gives a procedure for computing $\tilde{G}_k(s)$ such that the L_{∞} error is approximately $\sum_{i=k+1,\ n} \sigma_{hi}$, and [LAT1], [HUN2] and [AND2] consider frequency-weighted Hankel norm approximations.

Appendix 8.1 Comparison of balancing algorithms

In [LAU3] it is proposed to use for minimal systems similar transformations to those presented in this chapter. That is, they do not consider finding a truncated balanced realization in the case of non-minimal systems. Their justification for this is that systems are generically minimal, and that by performing the calculations more accurately the system gramians will not be singular. This implies that problems with the earlier algorithms are caused by the errors in 'squaring-up', in forming C^TC for example, before solving the Lyapunov equations. Thus [LAU3] proposes to solve the Lyapunov equations using Hammarling's algorithm and to perform the balancing with transformations similar to those in equation (8.11) with k=n. To avoid the potential numerical errors introduced by finding the SVD of the product SR^T (in our terminology) a new algorithm was developed to find the SVD of the product without actually forming the product [HEA1].

On implementation, [LAU3] uses R as the (upper triangular) Cholesky factor of the observability gramian and S as a lower triangular modified Cholesky factor. This is because the SVD algorithm [HEA1] requires both input matrices to be upper triangular. As mentioned in section 8.3, it is not necessary to find the Cholesky factors, and in fact S_u and ZR_u^TZ in equations (8.49-51) are both upper triangular in a suitable form for the new SVD algorithm. This means that Laub's new algorithm can be improved by removing one QR and one QL transformation.

The use of the new SVD routine would clearly improve the theoretical performance of the algorithm in this chapter. The major improvement would be in the accuracy of the smallest Hankel singular values. Since these are not important when finding a truncated balanced realization, however, this would not be expected to significantly affect the numerical results.

CHAPTER IX

CONCLUSIONS AND RECOMMENDATIONS FOR FURTHER RESEARCH

9.1 Summary

This thesis has presented one of the first applications of H^{∞}-optimization to a practical example; the design of a full authority flight control system for a high performance helicopter. The design was based on a linear model obtained from a non-linear simulation, neglecting rotor dynamics, provided by the Royal Aircraft Establishment, Bedford. This model and simulation were used exclusively during the design stage. The robustness of the final design was clearly demonstrated by its successful implementation in a new non-linear simulation which incorporated higher order rotor dynamics. The addition of these higher order dynamics had severely degraded earlier control systems designed using conventional techniques.

Particular emphasis was placed on obtaining a clear understanding of the physical system, and the resulting responses were verified to be realistic by engineers working on related problems.

The development of a new algorithm to perform minimal realization greatly improved the numerical reliability of an H^{∞}-design package being developed at Oxford. Experimentation with this software package led to the observation that the minimal dimension of the H^{∞}-optimal controller

was much smaller than had been predicted. It is conjectured that all H^∞-optimal controllers will have at most as many states as the defining standard problem.

This thesis has demonstrated that, compared with LQG/LTR, the H^∞-design procedure is a superior technique for manipulating singular values of the closed-loop frequency responses. It was not possible to obtain a design for the helicopter with satisfactory time and frequency responses using LQG/LTR.

9.2 Suggestions for future research

Despite the success of this first phase in the application of H^∞-optimization to the helicopter problem, much research is required before H^∞-optimization can be considered an attractive design tool for practising control engineers.

On the theoretical side, an important subject of research must be to precisely quantify the state dimension of the controller that results from the solution to H^∞-optimization problems. This should lead to new and more efficient techniques for finding the minimal controller. An essential part of this work is to examine the pole-zero cancellations which occur during the the current solution process [LTM1], [LTM2], [POS6]. However, this will only remove the need to perform minimal realization during the solution and will not therefore reduce the present controller size unless a dramatically new approach is developed. A further area of research is the state-space computation of the unique 'super-optimal' solution to the H^∞-design problem [YOU3], [YOU4], [FOO3]. Recent advances in this direction are reported in [TSA1].

It seems likely that the maximum dimension of the controller will be equal to that of the defining problem. However, for many situations this

will still be excessive, and an important research topic is therefore that of controller size reduction. With the current H^{∞} solution process it appears that this is best performed either on the initial P(s) or on the resultant controller - the computation should be performed as accurately as possible.

Since the H^{∞}-optimal controller has a truly 'black-box' state-space representation, new techniques are required to enable the design engineer to examine the dominant loops and interactions of the controller. This is necessary before such a system can be approved for actual implementation. This problem is not, of course, specific to H^{∞}-optimization but applies to any multivariable design procedure. An advantage of LQG in this respect is that the controller can clearly be split into state estimator and state feedback functions.

An approach not considered in this thesis, but worthy of further investigation, is that of 2 degree-of-freedom controller design. This can be integrated into H^{∞}-design as part of a 4-Block problem, or the 2-stage approach given by [MOO2] can be followed.

A future goal is the implementation of an H^{∞}-optimal controller on a piloted simulation facility at the RAE, Bedford, and eventually in flying helicopters. For further progress to be made, however, the control system design objectives must be more clearly defined. These are currently given in a combination of time-domain and frequency domain specifications defining desired handling qualities criteria, in a form unsuitable for immediate use in an H^{∞}-optimization problem. Such controllers will be digitally implemented. and it is therefore desirable to be able to design discrete-time controllers and to include selection of the sample rate in the design process. It is hoped that further research along the lines of that presented in Chapter III may prove useful in this context.

Finally, although a major thrust of recent research has been into the use of the infinity-, rather than the two-norm, for control system design, recent results enable design to be performed on the l_1-norm [DAH1]. These minimize, for example, the maximum amplitude of an error response to bounded disturbances, and could have a number of applications.

REFERENCES

[AND1] B.D.O. Anderson and J.B. Moore (1971). Linear optimal control, Prentice-Hall, Englewood Cliffs, New Jersey.

[AND2] B.D.O. Anderson (1986). 'Weighted Hankel-norm approximations: calculation of bounds', Syst and Control Lett, 7, pp.247-55.

[ATH1] M. Athans and P.L. Falb (1966). Optimal control, McGraw-Hill, New York.

[ATH2] M. Athans (1971). 'The role and use of the stochastic linear-quadratic-Gaussian problem in control system design', IEEE Trans Aut Control, AC-16, 6, p.529.

[BAB1] A.W. Babister (1961). Aircraft stability and control, Pergamon Press, Oxford.

[BAR1] R.H. Bartels and G.W. Stewart (1972). 'Solution of the matrix equation AX + XB = C', Comm ACM, 15, pp.820-26.

[BEN1] S. Bennet (1979). A history of control engineering 1800-1930, IEE Control Engineering series 8, London.

[BIR1] J.S. Bird and B.A. Francis (1986). 'On the robust disturbance attenuation problem', Proc IEEE CDC, Athens, Greece.

[BLA1] H.S. Black (1934). 'Stabilized feedback amplifiers', US Patent No. 2, 102, 671.

[BOD1] H.W. Bode (1945). Network analysis and feedback amplifier design, Van Nostrand, New York.

[BOY1] J.-M. Boyle and K.H. Pang (1986). 'The implementation of an expert system for use in control system design', Workshop on computer-aided control system design, Salford.

[BRA1] A.R.S. Bramwell (1976). Helicopter dynamics, Arnold, London.

[BRO1] J.R. Broussard, P.W. Berry and R.F. Stengel (1979). 'Modern digital flight control system design for VTOL aircraft', NASA CR 159019.

[BRO2] P. Brotherhood and M.T. Charlton (1984). 'An assessment of helicopter turning performance during Nap-of-earth flight', RAE Tech Memo FS(B) 534.

[BUC1] S.L. Buckingham (1984). 'Exploratory piloted simulation studies of advanced helicopter control systems', 38th Symposium of the AGARD Guidance and Control panel.

[CHA1] P.R. Chandler and D.W. Potts (1983). 'Shortcomings of modern control as applied to fighter flight control design', Proc IEEE CDC.

[CHA2] S.M. Chan and M. Athans (1984). 'Applications of robustness theory to power system models', IEEE Trans Aut Control, AC-29, pp.2-8.

[CHE1] R.T. Chen and J.A. Jeske (1983). 'Influence of sideslip on the flight dynamics of rotorcraft in steep turns at low speeds', Proc 39th Annual Forum, American Helicopter Society.

[CHE2] R.T.N. Chen and W.S. Hindson (1985). 'The influence of high order dynamics on helicopter flight-control system bandwidth', Proc 11th European Rotorcraft Forum, London.

[CHU1] C.C. Chu (1985). 'H^{∞}-optimization and robust multivariable control', PhD Thesis, Dept Elec Eng, Univ. of Minneapolis.

[COL1] L. Collier (1979). How to fly helicopters, Tab Books, Blue Ridge Summit, Pa.

[CRU1] J.B. Cruz and W.R. Perkins (1964). 'A new approach to the sensitivity problem in multivariable feedback system design', IEEE Trans Aut Control, AC-9, 3, pp.216-22.

[CRU2] J.B. Cruz, J.S. Freudenberg and D.P. Looze (1981). 'A relationship between sensitivity and stability of multivariable feedback feedback systems', IEEE Trans Aut Control, AC-26, pp.75-92.

[DAH1] M.A. Dahleh and J.B. Pearson (1986). 'l^1-optimal compensators for continuous-time systems', Proc IEEE CDC, Athens, Greece.

[DAN1] R. Daniel and B. Kouvaritakis (1983). 'A new robust stability criterion for linear and non-linear multivariable feedback systems', OUEL report no. 1479/83.

[DAN2] R. Daniel, B. Kouvaritakis and H. Latchman (1985). 'Principal direction alignment, a geometric framework for the complete solution to the μ-problem', OUEL report no. 1595/85.

[DAV1] E.J. Davison (1976). 'The robust control of a servomechanism problem for linear time-invariant systems', IEEE Trans Aut Control, AC-21, p.25. First presented at the Allerton conference, 1973.

[DES1] C.A. Desoer and M. Vidyasagar (1975). Feedback systems : Input - output properties, Academic Press, New York.

[DES2] C.A. Desoer, R.W. Liu, J. Murray and R. Saeks (1980). 'Feedback system design : the fractional representation approach to analysis and synthesis,' IEEE Trans Aut Control, AC-25, pp.399-412.

[DON1] J.J. Dongara, C.B. Moler, J.R. Bunch and G.W. Stewart (1979). Linpack user's guide. SIAM, Philadephia, Pa.

[DOR1] P. Dorato (1986). 'Robust control: a historical review', Proc IEEE CDC, Athens, Greece.

[DOY1] J.C. Doyle (1978). 'Guaranteed margins for LQG regulators', IEEE Trans Aut Control, AC-23, pp.756-57.

[DOY2] J.C. Doyle and G. Stein (1979). 'Robustness with observers', IEEE Trans Aut Control, AC-24, pp.607-11.

[DOY3] J.C. Doyle and G. Stein (1981). 'Multivariable feedback design: concepts for a classical/modern synthesis', IEEE Trans Aut Control, AC-26, pp.4-16.

[DOY4] J.C. Doyle (1982). 'Analysis of feedback systems with structured uncertainties', Proc IEE, part D, 129, pp.242-51.

[DOY5] J.C. Doyle, J. Wall and G. Stein (1982). 'Performance and robustness analysis for structured uncertainty', Proc 21st IEEE CDC, pp.629-36.

[DOY6] J.C. Doyle (1983). 'Synthesis of robust controllers and filters with structured plant uncertainties', Proc IEEE CDC, San Antonio, Texas.

[DOY7] J.C. Doyle (1984). 'Lecture notes in advances in multivariable control', ONR/Honeywell workshop, Minneapolis, MN.

[DOY8] J.C. Doyle, K. Lenz and A. Packard (1986). 'Design examples using μ-synthesis: space shuttle lateral axis FCS during re-entry', Proc IEEE CDC, Athens, Greece.

[EDM1] J.M. Edmunds (1984). 'Confidence limits on identified frequency responses', Control Systems Centre report no. 602, UMIST, Manchester.

[EDM2] J.M. Edmunds, S.E. Jeanes and J.M. Maciejowski (1983). 'The Cambridge linear analysis and design programs, user reference manual', 4th issue. Draft issue May 1984.

[EVA1] W.R. Evans (1953). Control system dynamics, McGraw-Hill, New York.

[FAN1] M.K.H. Fan and A.L. Tits (1986). 'Characterization and efficient computation of the structured singular value', IEEE Trans Aut Control, AC-31, pp.734-43.

[FOO1] Y.K. Foo and I. Postlethwaite (1983). 'Adequate/inadequate representations of uncertainty and their implications for robustness analysis', Oxford University Engineering Laboratory (OUEL) report no. 1498/83.

[FOO2] Y.K. Foo and I. Postlethwaite (1983). 'Extensions of the small-μ test for robust stability', OUEL report no. 1518/84. To appear in IEEE Trans Aut Control.

[FOO3] Y.K. Foo and I. Postlethwaite (1984). 'An H^∞ minimax approach to the design of robust control systems', Syst and Control Lett, 5, pp.81-88.

[FOO4] Y.K. Foo and I. Postlethwaite (1985). 'An H^∞ minimax approach to the design of robust control systems - part 2 : all solutions, all-pass form solution and the 'best' solution', OUEL report no. 1585/85.

[FOO5] Y.K. Foo (1985). 'Robustness of multivariable feedback systems: analysis and optimal design'. D.Phil Thesis, University of Oxford.

[FRA1] B.A. Francis, J.W. Helton and G. Zames (1984). 'H^∞- optimal feedback controllers for linear multivariable systems', IEEE Trans Aut Control, AC-29, pp.888-900.

[FRA2] B.A. Francis and G. Zames (1984). 'On H^∞- optimal theory for SISO feedback systems', IEEE Trans Aut Control, AC-29, pp.9-16.

[FRA3] B.A. Francis and J.C Doyle (1985). 'Linear control theory with an H_∞ - optimality criterion', Univerity of Toronto systems control group report no 8501. To appear in SIAM J Control Opt.

[FRA4] B.A. Francis (1987). 'A course in H^∞ control theory', Springer, New York.

[FRE1] J.S. Freudenberg, D.P. Looze and J.B. Cruz (1982). 'Robustness analysis using singular value sensitivities', Int J Control, pp.95-116.

[FRE2] J.S. Freudenberg and D.P. Looze (1985). 'Right half-plane poles and zeros and design trade-offs in feedback systems', IEEE Trans Aut Control, AC-30, pp.555-65.

[GES1] A. Gessow and G.C. Myers (1952). Aerodynamics of the helicopter, Ungar, New York.

[GLO1] K. Glover (1984). 'All optimal Hankel-norm approximations of linear multivariable systems and their L_∞- error bounds', Int J Control, 39, pp.1115-94.

[GLO2] K. Glover (1986). 'Robust stabilization of linear multivariable systems ; relations to approximations', Int J Control, vol. 43, no.3, pp.741-66.

[HAM1] S.J. Hammarling (1982). 'Numerical solution of the stable non-negative definite Lyapunov equation', IMA J of Num Anal, 2, pp.303-23.

[HEA1] M.T. Heath, A.J. Laub, C.C. Paige and R.C. Ward (1986). 'Computing the singular value decomposition of a product of two matrices', SIAM J Sci Stat Comp, 7, pp.1147-59.

[HEL1] J.W. Helton (1976). 'Operator theory and broadband matching', Proc Allerton Conf.

[HEL2] J.W. Helton (1983). 'Worst case analysis in the frequency domain : the H^∞ approach to control,' Proc IEEE CDC, San Antonio, Texas.

[HOR1] I.M. Horowitz (1963). Synthesis of feedback systems. Academic Press, New York.

[HOU1] S.S. Houston (1984). 'On the benefit of an active horizontal tailplane to the single main and tail-rotor helicopter'. PhD Thesis, University of Glasgow.

[HUN1] Y.S. Hung and A.G.J. MacFarlane (1982). Multivariable feedback: a quasi-classical approach, Springer-Verlag.

[HUN2] Y.S. Hung and K. Glover (1986). 'Optimal Hankel-norm approximation of stable systems with first order weighting functions'. Syst and Control Lett, 7, pp.165-72.

[JAM1] H.M. James, N.B. Nichols and R.S. Phillips (1947). Theory of servomechanisms, McGraw-Hill, New York.

[JOH1] W. Johnson (1980). Helicopter theory, Princeton, New Jersey.

[JON1] E.A. Jonckheere and J.C. Juang (1986). 'Toeplitz and Hankel structures in H^{∞}-design and the avoidance of the ε-iteration', Proc ACC, Seattle, WA.

[KAL1] R.E. Kalman and R.S. Bucy (1961). 'New results in linear filtering and predictor theory', ASME J Basic Eng, 83, pp.95-108.

[KAL2] R.E. Kalman (1964). 'When is a linear control system optimal?' ASME J Basic Eng, 86, pp.51-60.

[KOU1] B. Kouvaritakis and I. Postlethwaite (1982). 'Principal gains and phases : insensitive robustness measures for assessing the closed-loop stability property', Proc IEE, Part D, 129, pp.233-41.

[KOU2] B. Kouvaritakis and H. Latchman (1984). 'Necessary and sufficient stability criterion for systems with structured uncertainties : the major principal direction alignment property', OUEL report no. 1552/84.

[KOU3] B. Kouvaritakis and H. Latchman (1984). 'Block structured perturbations, necessary and sufficient conditions : the exact solution to the μ-problem,' OUEL report no. 1560/84.

[KWA1] H. Kwakernaak and R. Sivan (1972). Linear optimal control systems, Wiley Interscience, New York.

[KWA2] H. Kwakernaak (1985). 'Minimax frequency domain performance and robustness optimization of linear feedback systems', IEEE Trans Aut Control, AC-30, pp.994-1004.

[KWA3] H. Kwakernaak (1986). 'A polynomial approach to minimax frequency domain optimization of multivariable systems', Int J Control, 44, pp.117-56.

[LAT1] G. Latham and B.D.O. Anderson (1985). 'Frequency-weighted optimal Hankel-norm approximation of stable transfer functions', Syst Control Lett, 5, pp.229-36.

[LAU1] A.J. Laub and B.C. Moore (1978). 'Calculation of transmission zeros using QZ techniques'. Automatica, 14, pp.557-66.

[LAU2] A.J. Laub (1980). 'On computing balancing transformations'. Proc JACC, San Francisco, California.

[LAU3] A.J. Laub, M.T. Heath, C.C. Paige and R.C. Ward (1986). 'Computation of system balancing transformations', IEEE Proc CDC, Athens, pp.548-53.

[LEH1] N.A. Lehtomaki (1981). Practical robustness measures in multivariable control system analysis, PhD Thesis, MIT, Cambridge, Mass.

[LEH2] N.A. Lehtomaki, N.R. Sandell and M. Athans (1981). 'Robustness results in linear quadratic Gaussian based multivariable control designs', IEEE Trans Aut Control, AC-26, pp.75-92.

[LEH3] N.A. Lehtomaki, D.A. Castanon, B.C. Levy, G. Stein, N.R. Sandell, Jr., and M. Athans (1984). 'Robustness and modelling error characterization', IEEE Trans Aut Control, AC-29, pp.212-20.

[LEW1] M.S. Lewis (1985). 'A piloted simulation of one-on-one helicopter air combat at NOE flight levels', Proc 11th European Rotorcraft Forum, London.

[LIM1] D.J.N. Limebeer and Y.S. Hung (1986). 'An analysis of the pole-zero cancellations in H_∞-optimal control problems of the first kind', Internal report, Dept Elec Eng, Imperial College, London.

[LIM2] D.J.N. Limebeer and G. Halikias (1986). 'A controller degree bound for H_∞-optimal control problems of the second kind', Proc IEEE CDC, Athens, Greece.

[LIM3] D.J.N. Limebeer and E. Kasenally (1986). 'H^∞-optimal control of a synchronous turbo-generator', Proc IEEE CDC, Athens, Greece.

[LOH1] A.P. Loh and I. Postlethwaite (1985). 'Uncertainty estimation from system identification,' OUEL report no. 1510/85.

[LUE1] D.G. Luenberger (1966). 'Observers for multivariable systems', IEEE Trans Aut Control, AC-11, no.2, pp.190-97.

[LY1] U.-L. Ly (1983). 'Robustness analysis of a multiloop flight control system', Proc AIAA.

[MAC1] A.G.J. MacFarlane, ed., (1980). Complex variable methods for linear multivariable feedback systems, Taylor and Francis Ltd, London.

[MAC2] A.G.J. MacFarlane and B. Kouvaritakis (1977). 'A design technique for linear multivariable feedback systems', Int J Control, 25, pp.837-74.

[MAC3] A.G.J. MacFarlane (1970). 'Return-difference and return-ratio matrices and their use in analysis and design of multivariable feedback control systems', Proc IEE, 117, p.2037.

[MAC4] A.G.J. MacFarlane and J.J. Belletrutti (1973). 'The characteristic locus design method', Automatica, 9, p.575.

[MAC5] A.G.J. MacFarlane, editor, (1979). Frequency response methods in control systems, IEEE Reprint Series, IEEE, New York.

[MAC6] A.G.J. MacFarlane and Y.S. Hung (1985). 'Indicators for multivariable feedback systems', Proc IEE Conf, Cambridge, UK.

[MEE1] A.I. Mees (1981). Dynamics of feedback systems, Wiley Interscience, New York.

[MOO1] B.C. Moore (1981). 'Principal component analysis in linear systems: controllability, observability and model reduction', IEEE Trans Aut Control, AC-26, pp.17-32.

[MOO2] J.B. Moore, L. Xia and K. Glover (1986). 'On improving control-loop robustness of model-matching controllers', Syst and Control Lett, 7, p.83.

[MOR1] B.G. Morton R.M. Afoos (1985). 'New applications of μ to real parameter variation problems', Proc IEEE CDC, Fort Lauderdale, FL.

[NAG1] Numerical Algorithms Group (1984). NAG Mark II library manual.

[NET1] C.N. Nett, C.A. Jacobson and M.J. Balas (1984). 'A connection between state-space and doubly coprime fractional representations', IEEE Trans Aut Control, AC-29, pp.831-32.

[NEW1] G.C. Newton, L.A. Gould and J.F. Kaiser (1957). Analytic design of linear feedback controls, John Wiley & Sons, New York.

[NYQ1] H. Nyquist (1932). 'Regeneration theory', Bell Syst Tech J, January.

[OYO1] S.D. O'Young and B.A. Francis (1985). 'Sensitivity trade-offs for multivariable plants,' IEEE Trans Aut Control, AC-30, pp.625-32.

[OYO2] S.D. O'Young and B.A. Francis (1986). 'Optimal performance and robust stabilization,' Automatica, 22, pp.171-83.

[OYO3] S.D. O'Young, I. Postlethwaite and D.-W. Gu (1987). 'A treatment of $j\omega$-axis model-matching transformation zeros in the optimal H and H $_\infty$-control designs', OUEL report no. 1673/87.

[PAD1] G.D. Padfield (1981). 'A theoretical model of helicopter flight mechanics for application to piloted simulation', RAE Tech Report no. 81048.

[PAL1] E.H.J. Pallett (1983). Automatic flight control, Granada,

[PAR1] D.L.K. Parry and D.J. Murray-Smith (1985). 'The application of modal control theory to the single rotor helicopter', Proc 11th European Rotorcraft Forum, London.

[PAU1] H.J. Pausder (1985). 'A study of roll response required in a low altitude slalom task', Ibid.

[PEA1] J.B. Pearson and P.W. Staats Jr (1974). 'Robust controllers for linear regulators', IEEE Trans Aut Control, AC-19, pp.231-34.

[PER1] L. Pernebo (1981). 'An algebraic theory for the design of controllers for linear multivariable systems', parts 1 and 2, IEEE Trans Aut Control, AC-26, pp.171-93.

[PER2] L. Pernebo and L.M. Silverman (1982). 'Model reduction via balanced state space representations', IEEE Trans Aut Control, 27, pp.382-87.

[POS1] I. Postlethwaite and A.G.J. MacFarlane (1979). A complex variable approach to the analysis of linear multivariable feedback systems, Springer-Verlag.

[POS2] I. Postlethwaite (1982). 'Sensitivity of the characteristic gain loci', Automatica, 18, pp.709-12.

[POS3] I. Postlethwaite, J.M. Edmunds and A.G.J. MacFarlane (1981). 'Principal gains and principal phases in the analysis of linear multivariable feedback systems', IEEE Trans Aut Control, AC-26, pp.32-46.

[POS4] I. Postlethwaite and Y.K.Foo (1983). 'Robustness with simultaneous pole and zero movement across the jω-axis', OUEL report 1505/83 (revised), and Automatica, July '85, pp.433-44.

[POS5] I. Postlethwaite, M.S. Tombs, Y.K. Foo and A.P. Loh (1985). 'On the relationship between Lehtomaki's robustness test and inverse Nyquist based test', IEEE Trans Aut Control, AC-30 pp.927-28.

[POS6] I. Postlethwaite, D.-W. Gu and S.D. O'Young (1986). 'Some computational results on size reduction in H^{∞}-design', OUEL report no. 1648/86.

[POS7] I. Postlethwaite, D.-W. Gu and S.D. O'Young (1986). 'An H^{∞}-control system design package', Workshop on computer-aided design, Salford.

[POS8] I. Postlethwaite, D.-W. Gu, S.D. O'Young and M.S. Tombs (1986). 'Industrial control system design using H^{∞}-optimization', Proc IEEE CDC, Athens, Greece.

[POS9] I. Postlethwaite, S.D. O'Young and D.-W. Gu (1987). 'Stable-H user's guide', OUEL report no. 1687/87.

[ROS1] H.H. Rosenbrock (1966). 'On the design of linear multivariable control systems', Proc 3rd IFAC Congress, London.

[ROS2] H.H. Rosenbrock (1969). 'Design of multivariable control systems using the inverse Nyquist array', Proc IEE, 116, p.1929.

[ROS3] H.H. Rosenbrock (1970). State-space and multivariable theory, Nelson, London.

[ROS4] H.H. Rosenbrock (1974). Computer-aided control systems design, Academic Press, London.

[SAF1] M.G. Safonov (1977). Robustness and stability aspects of stochastic multivariable feedback system design, PhD Thesis, MIT, Cambridge, Mass. Also MIT Press, 1980.

[SAF2] M.G. Safonov and M. Athans (1977). 'Gain and phase margin for multiloop regulators', IEEE Trans Aut Control, AC-22, pp.173-79.

[SAF3] M.G. Safonov, A.J.Laub and G. Hartmann (1981). 'Feedback properties of multivariable systems: the role and use of the return difference matrix', IEEE Trans Aut Control, AC-26, pp.47-65.

[SAF4] M.G. Safonov and M. Athans (1981). 'A multiloop generalization of the circle criterion for stability margin analysis', IEEE Trans Aut control, AC-26, pp.415-22.

[SAF5] M.G. Safonov and M.S. Verma (1983). 'Multivariable L^{∞} sensitivity optimization and Hankel-norm approximaton', Proc Amer Control Conf, San Francisco, California.

[SAF6] [AG. Safonov (1984). 'Exact calculation of the multivariable structured singular-value stability margin', Proc IEEE CDC, Las Vegas.

[SAF7] M.G. Safonov (1986). 'Optimal diagonal scaling for infinity-norm optimization', Syst and Control Lett, 7, pp.257-60.

[SAF8] M.G. Safonov and R.Y. Chiang (1986). 'CACSD using state-space L^∞ theory - A design example', Proc IEEE CACSD workshop, Washington DC.

[SAF9] M.G. Safonov (1986). 'Optimal H^∞-synthesis of robust controllers for systems with structured uncertainty', Proc IEEE CDC, Athens, Greece.

[SAN1] N.R. Sandell, S.W. Gully, W.H. Lee and N.A. Lehtomaki (1981). 'Multivariable stability margins for vehicle flight control systems', Proc IEEE CDC, pp.1479-83.

[SAU1] G.H. Saunders (1975). Dynamics of helicopter flight, Wiley Interscience, New York.

[SCT1] Systems Control Technology (1986). CTRL-C user's guide.

[SMI1] M.C. Smith (1982). A generalized Nyquist/root-locus theory for multi-loop feedback systems, PhD Thesis, University of Cambridge.

[SMI2] J. Smith (1984). 'An analysis of helicopter flight mechanics. Part I : Users' guide to the software package Helistab', RAE Tech Memo FS(B) 569.

[STE1] G.Stein, G.L.Hartmann and R.C. Hendrick (1977). 'Adaptive control laws for F-8C flight test', IEEE Trans Aut Control, AC-22, pp.758-67.

[STE2] G. Stein (1981). 'LQG-based multivariable design: frequency domain interpretation', AGARD-LS, 117, 5.

[STE3] G. Stein and S. Pratt (1981). 'LQG multivariable design tools', AGARD-LS, 117, 6.

[THO1] P.M. Thompson (1982). 'Conic sector analysis of hybrid control systems', PhD Thesis, MIT, Cambridge, Mass.

[THO2] P.M. Thompson, R.L. Dailey and J.C. Doyle (1986). 'New conic sectors for sampled-data feedback systems', Syst and Control Lett, 7, pp.395-404.

[TOM1] B.N. Tomlinson and G.D. Padfield (1980). 'Piloted simulation studies of helicopter agility', Vertica, 4, pp.79-106.

[TOM2] M.S. Tombs and I. Postlethwaite (1982). 'On the relationship between robustness tests and their application to helicopter control system designs', Proc IEE Conf, pp.464-68.

[TSA1] M.C. Tsai, D.-W. Gu and I. Postlethwaite (1987). 'A state-space approach to super-optimal H^∞-control problems', OUEL report no. 1690/87.

[TYL1] D.J. Tyler and P.R.Brinson (1985). 'Flight control system philosophy for active control of a helicopter', 11th European Rotorcraft Forum.

[TOM3] M.S. Tombs and I. Postlethwaite (1987). 'Truncated balanced realization of a stable non-minimal state-space system',

[VID1] M. Vidyasagar, H. Schneider and B. Francis (1982). 'Algebraic and topological aspects of feedback stabilization', IEEE Trans Aut Control, AC-27, pp.880-94.

[VID2] M. Vidyasagar (1978). Non-linear systems analysis, Prentice-Hall, London.

[WAL1] J.E. Wall, J.C. Doyle, G.L. Hartmann, N.A. Lehtomaki and G. Stein (c.1983). 'Performance and robustness aspects of digital control systems', Honeywell Systems Inc.

[WIE1] N. Wiener (1949). Extrapolation, interpolation and smoothing of stationary time series, John Wiley & Sons, New York.

[WIL1] T.W.C. Williams (1986). 'Numerically reliable software for control : the SLICE library', IEE Proc, vol. 133, part D, no.2, pp.73-82.

[WIN1] J.S. Winter, M.J. Corbin and L.M.Murphy (1983). 'Description of TSIM2 : a software package for computer-aided design of flight control systems', RAE Tech Report 83007.

[WIN2] J.S. Winter, G.D. Padfield and S.L. Buckingham (1984). 'The evolution of ACS for helicopters: conceptual simulation studies to preliminary design', AGARD CP, no. 384.

[YOU1] D.C. Youla, H. Jabr and J.J. Bongiorno (1976). 'Modern Wiener-Hopf design of optimal controllers - part 2: the multivariable case', IEEE Trans Aut Control, AC-21, p.319.

[YOU2] D.C. Youla, J.J. Bongiorno and C.N. Lu (1974). 'Single-loop feedback stabilization of linear multivariable dynamic plants', Automatica, 10, pp.159-73.

[YOU3] N.J. Young (1984). 'Interpolation by analytic matrix functions', Operators and Function Theory : Proc NATO Advanced Study Institute, Lancaster.

[YOU4] N.J. Young (1986). 'The Nevanlinna-Pick problem for matrix-valued functions', J Operator Theory.

[YUE1] A. Yue (1986). 'Pilot handling qualities design criteria for robust control system design in high performance helicopters', 1st year research report, University of Oxford.

[ZAM1] G. Zames (1966). 'On the input-output stability of time-varying nonlinear feedback systems', parts 1 and 2, IEEE Trans Aut Control, AC-11, pp.228-38, pp.465-76.

[ZAM2] G. Zames (1981). 'Feedback and optimal sensitivity: model reference transformations, multiplicative seminorms, and approximate inverses', IEEE Trans Aut Control, AC-26, pp.301-20.

[ZAM3] G. Zames and B.A. Francis (1983). 'Feedback, minimax sensitivity and optimal robustness', IEEE Trans Aut Control, AC-28, pp.585-601.